



## Durham E-Theses

---

### *Infinite-Centre Gibbons-Hawking Metrics, Applied to Gravitational Instantons and Monopoles*

RUTLIDGE, KATIE

#### How to cite:

---

RUTLIDGE, KATIE (2010) *Infinite-Centre Gibbons-Hawking Metrics, Applied to Gravitational Instantons and Monopoles*, Durham theses, Durham University. Available at Durham E-Theses Online:  
<http://etheses.dur.ac.uk/383/>

#### Use policy

---

The full-text may be used and/or reproduced, and given to third parties in any format or medium, without prior permission or charge, for personal research or study, educational, or not-for-profit purposes provided that:

- a full bibliographic reference is made to the original source
- a [link](#) is made to the metadata record in Durham E-Theses
- the full-text is not changed in any way

The full-text must not be sold in any format or medium without the formal permission of the copyright holders.

Please consult the [full Durham E-Theses policy](#) for further details.

---

Academic Support Office, Durham University, University Office, Old Elvet, Durham DH1 3HP  
e-mail: [e-theses.admin@dur.ac.uk](mailto:e-theses.admin@dur.ac.uk) Tel: +44 0191 334 6107  
<http://etheses.dur.ac.uk>

# Infinite-Centre Gibbons-Hawking Metrics, Applied to Gravitational Instantons and Monopoles.

**Katie Rutledge**

Abstract

We investigate the convergence of infinite-centre Gibbons-Hawking metrics, in the contexts of: four-dimensional gravitational instantons and their applications, Kaluza-Klein monopoles and vortices, gravitational calorons, analytical extensions of Majumdar-Papapetrou metrics to form extreme Reissner-Nordström black holes, and Kaluza-Klein black holes. We find that, in most cases, periodic arrangements of the sources give rise to divergent potentials. We investigate the consequences of various methods of ensuring convergence, particularly in terms of the appearance of naked singularities, and construct several new solutions of Einstein's equations.

# Infinite-Centre Gibbons-Hawking Metrics, Applied to Gravitational Instantons and Monopoles.



By  
**Katie Arlene Rutledge**  
Department of Mathematical Sciences

March 2010

A DISSERTATION SUBMITTED TO THE UNIVERSITY OF DURHAM  
IN ACCORDANCE WITH THE REQUIREMENTS OF THE DEGREE  
OF DOCTOR OF PHILOSOPHY IN THE FACULTY OF SCIENCE

# Contents

<b>1</b>	<b>Introduction</b>	<b>12</b>
<b>2</b>	<b>Setting the Scene</b>	<b>18</b>
2.1	Introduction . . . . .	18
2.2	General Relativity . . . . .	19
2.3	Gravitational Instantons . . . . .	20
2.3.1	Nuts and Bolts . . . . .	21
2.3.2	Euclidean Taub-NUT Metric . . . . .	22
2.3.3	Multi Taub-NUT Metric . . . . .	23
2.3.4	Eguchi-Hanson Metric . . . . .	23
2.3.5	Schwarzschild Metric . . . . .	24
2.3.6	Topological Invariants . . . . .	24
2.3.7	Topology and Asymptotic Behaviour . . . . .	25
2.4	Hyperkähler Metrics and the Gibbons-Hawking Form . . . . .	25
2.4.1	Some Useful Definitions . . . . .	26
2.4.2	Complex Structures on Manifolds . . . . .	27
2.4.3	Kähler Manifolds . . . . .	28
2.4.4	Hyperkähler Manifolds . . . . .	29
2.4.5	Holonomy Groups of Different Manifolds . . . . .	30
2.4.6	Kähler and Hyperkähler Potentials . . . . .	30
2.4.7	Gibbons-Hawking Form . . . . .	31
2.5	Solitons in Kaluza-Klein Theory . . . . .	32
2.5.1	Magnetic Monopole . . . . .	32
2.5.2	Gravitational Properties . . . . .	33
2.5.3	Curvature Tensor . . . . .	34
2.6	Black Holes . . . . .	34
2.6.1	Event Horizons and Singularities . . . . .	35

2.6.2	Some Further Definitions . . . . .	36
<b>3</b>	<b>Solutions with Periodic Sources</b>	<b>38</b>
3.1	Introduction . . . . .	38
3.2	Considering Convergence . . . . .	40
3.2.1	Convergence of the Infinite Constant Solution . . . . .	40
3.2.2	Rate of Convergence . . . . .	41
3.2.3	Approximating the Infinite Series . . . . .	43
3.3	Zero Regions . . . . .	46
3.3.1	Case 1: Zero Strips . . . . .	46
3.3.2	Case 2: Zero Curves . . . . .	47
3.4	Convergence of $\vec{\omega} \cdot d\vec{r}$ . . . . .	48
3.5	Approximating $V$ . . . . .	50
3.6	Exterior and Interior Spacetimes . . . . .	51
3.6.1	The Exterior Spacetime . . . . .	51
3.6.2	The Interior Spacetime . . . . .	52
3.7	Higher-Dimensional Case . . . . .	53
<b>4</b>	<b>Examples of Periodic Solutions</b>	<b>55</b>
4.1	Introduction . . . . .	55
4.2	Kaluza-Klein Vortices and AdS Spacetime . . . . .	56
4.2.1	Kaluza-Klein Vortices . . . . .	56
4.2.2	Kaluza-Klein Monopoles in AdS Spacetime . . . . .	59
4.3	Dirichlet Instantons . . . . .	60
4.3.1	A Single Hypermultiplet . . . . .	61
4.3.2	Multiple Hypermultiplets . . . . .	62
4.4	Gravitational Calorons . . . . .	65
4.4.1	The Gibbons-Hawking Caloron Solution . . . . .	65
4.4.2	Euclidean Schwarzschild Solution . . . . .	69
<b>5</b>	<b>Surveying the Landscape</b>	<b>76</b>
5.1	Introduction . . . . .	76
5.2	Incompleteness of the Infinite Constant Solution . . . . .	77
5.2.1	The Two-Monopole Moduli Space on $\mathbb{R}^3$ . . . . .	77
5.2.2	The Two-Monopole Moduli Space on $\mathbb{R}^2 \times \mathbb{S}^1$ . . . . .	80
5.3	Extensions and Applications . . . . .	83

5.3.1	Stitching Together Ooguri-Vafa Metrics . . . . .	83
5.3.2	Seven-Dimensional Holonomy Spaces . . . . .	84
5.3.3	Hyperbolic Monopoles . . . . .	86
5.4	Olbers' and Seeliger's Paradoxes . . . . .	90
5.4.1	Seeliger's Paradox . . . . .	90
5.4.2	Olbers' Paradox . . . . .	91
5.4.3	Relation to Periodic Instantons . . . . .	92
<b>6</b>	<b>Alternative Approaches to Convergence</b>	<b>93</b>
6.1	Introduction . . . . .	93
6.2	Non-Periodic Instantons . . . . .	94
6.2.1	Example . . . . .	94
6.2.2	The Periodic Limit . . . . .	95
6.2.3	Multiplying the Metric by a Constant . . . . .	97
6.2.4	Rescaling $r$ . . . . .	98
6.3	Quasi-Periodic Instantons . . . . .	99
6.3.1	Rows of Instantons . . . . .	102
6.3.2	Grids of Instantons . . . . .	103
6.3.3	Cubes of Instantons . . . . .	105
6.4	Reciprocal Infinite Constant . . . . .	106
6.4.1	The Case $\rho_2 = 0$ . . . . .	107
6.4.2	The Case $\rho_2 > 0$ . . . . .	111
6.4.3	Investigating the Spacetime . . . . .	112
<b>7</b>	<b>Extreme Reissner-Nordström Black Holes</b>	<b>113</b>
7.1	Introduction . . . . .	113
7.2	Finitely Many Black Holes . . . . .	114
7.2.1	What is an Extreme Reissner-Nordström Black Hole? . . . . .	115
7.2.2	Multiple Black Holes in $(3 + 1)$ Dimensions . . . . .	117
7.2.3	Multiple Black Holes in $(D + 1)$ Dimensions . . . . .	118
7.2.4	Sources Other Than Monopoles? . . . . .	120
7.3	Infinitely Many Black Holes . . . . .	120
7.3.1	Periodic Distribution of Black Holes . . . . .	121
7.3.2	Black Hole Lattices . . . . .	125
7.3.3	Non-Periodic Distributions of Black Holes . . . . .	128
7.4	Smoothness of Event Horizons . . . . .	131

7.4.1	Gaussian Null Coordinates . . . . .	132
7.4.2	Smoothness of Horizons for $D = 4$ . . . . .	133
7.4.3	Reflection-Symmetric Solutions . . . . .	134
7.4.4	Consequences . . . . .	135
7.5	Einstein-Maxwell-Dilaton Theory . . . . .	135
7.5.1	Finitely Many Black Holes . . . . .	136
7.5.2	Infinitely Many Black Holes . . . . .	138
7.5.3	Cosmological Black Holes . . . . .	143
7.5.4	Lattice Solution . . . . .	146
7.5.5	Non-Periodic Distribution . . . . .	146
<b>8</b>	<b>Kaluza-Klein Black Holes</b>	<b>147</b>
8.1	Introduction . . . . .	147
8.2	Special Cases . . . . .	150
8.3	Useful Metrics . . . . .	151
8.3.1	Eguchi-Hanson Metric . . . . .	151
8.3.2	The Klemm-Sabra Metric . . . . .	152
8.3.3	The Reissner-Nordström de-Sitter Metric . . . . .	152
8.3.4	Stationary Solutions . . . . .	153
8.4	Regularity at the Event Horizons . . . . .	154
8.4.1	Non-Cosmological Black Holes . . . . .	154
8.4.2	Cosmological Black Holes . . . . .	156
8.4.3	The Case $\beta = -1$ . . . . .	156
8.4.4	The Case $\beta = 1$ . . . . .	157
8.4.5	The SC Case . . . . .	158
8.5	Asymptotic Behaviour . . . . .	158
8.5.1	Asymptotic Behaviour for $\epsilon = 0$ . . . . .	159
8.5.2	Asymptotic behaviour for $\epsilon = 1$ . . . . .	161
8.5.3	Conclusion . . . . .	162
8.6	Periodic Distributions . . . . .	162
8.6.1	The Case of $\beta = -1$ . . . . .	163
8.6.2	The Case of $\beta = 1$ . . . . .	164
8.6.3	Values of the Parameter $\alpha$ . . . . .	165
8.6.4	Useful Examples . . . . .	166
8.7	Periodic Solutions - Singularity Properties . . . . .	167



8.7.1	Non-Cosmological Black Holes . . . . .	168
8.7.2	Cosmological Black Holes . . . . .	170
8.8	Non-Periodic and Lattice Distributions . . . . .	170
8.8.1	Non-Periodic Distributions of Black Holes . . . . .	170
8.8.2	The Case $\beta = -1$ . . . . .	171
8.8.3	The Case $\beta = 1$ . . . . .	172
8.8.4	Values of the Parameter $\alpha$ . . . . .	173
8.8.5	Useful Example . . . . .	173
8.8.6	Lattices of Black Holes . . . . .	174
8.9	Static and Non-Cosmological Black Holes . . . . .	174
8.9.1	Periodic Solutions - Curvature . . . . .	174
8.9.2	Non-Periodic Solutions . . . . .	175
8.10	Rotating, Non-Cosmological Black Holes . . . . .	176
8.10.1	Periodic Solutions - Curvature . . . . .	176
8.10.2	Periodic Solutions - Ergoregions . . . . .	177
8.10.3	Periodic Solutions - Closed Timelike Curves . . . . .	178
8.10.4	Non-Periodic Solutions . . . . .	179
8.11	Static, Cosmological Black Holes . . . . .	181
8.11.1	Periodic Solutions - Curvature . . . . .	182
8.11.2	Periodic Solutions - Closed Timelike Curves . . . . .	182
8.11.3	Non-Periodic Solutions . . . . .	183

**9 Conclusion and Bibliography** **185**

# List of Figures

3.1	Quadratic convergence of the periodic instanton potential minus an infinite constant, using (3.24), (3.25), (3.28) with $\rho_2 = 1 = x_3$ . . . . .	44
3.2	Periodic potential (3.5) with a zero strip . . . . .	46
3.3	Periodic potential (3.5) with zero curves around each singularity . . . . .	47
3.4	Variation in behaviour of $\vec{\omega} \cdot d\vec{r}$ for small $\rho_2$ , using (3.41) with $V_c = 1$ . . . . .	49
4.1	The potential $V$ for a Kaluza-Klein vortex using (4.2) with $\rho_2 \in [0, 1]$ , $x_3 \in [0, 2\pi]$	57
4.2	The zero region around the origin for a Kaluza-Klein vortex, using values from table in section 4.2.1 . . . . .	58
4.3	Comparison of $V$ (from (4.2)) and $V_{appx}$ (from (4.8)) near the zero for the Kaluza-Klein vortex solution for $\rho := \rho_2 \in [0, 1]$ . . . . .	59
4.4	The potential $V$ for a single matter hypermultiplet using (4.18) with $\rho_2 \in [0, 2]$ , $x_3 \in [0, 1]$ . . . . .	62
4.5	Comparison of $V$ (from (4.18)) and $V_{appx}$ (from (4.23)) near the zero for the Ooguri-Vafa solution with $\rho := \rho_2 \in [0, 1]$ . . . . .	63
4.6	Potential for the Gibbons-Hawking caloron solution, using (4.40) with $\rho_2 \in [0, 1]$ and $x_3 \in [0, 1]$ . . . . .	66
4.7	Approximation of the zero region for the gravitational caloron solution (4.40) using (4.53) and table in section 4.4.1 . . . . .	68
4.8	Comparison of $V$ (from (4.40)) and $V_{appx}$ (from (4.56)) near the zero for the Sanchez solution for $x_3 = 0.5$ and $\rho := \rho_2$ . . . . .	69
4.9	Comparison of the exact sum (from (4.42)) with the Taylor series approximation (from (4.78)) for an example of the Euclidean Schwarzschild metric with $x_4 = 0.5$ . . . . .	73
4.10	Snapshots of potential $V$ for the Euclidean Schwarzschild metric, using (4.40) for various choices of $x_4$ . . . . .	74

4.11	Comparison of two-variable Taylor series approximation around $(\rho_2, x_4) = (0, 0, 5)$ (from (4.80)) with exact potential (from (4.40)) for the Euclidean Schwarzschild metric . . . . .	75
5.1	Plot of $\coth(x)$ for $x > 0$ . . . . .	89
6.1	The Riemann curvature scalar (6.15) for the simplest non-periodic instanton distribution . . . . .	96
6.2	A section of the Euclidean lattice for the quasi-periodic instanton solution . .	101
6.3	2D representation of $V$ (using (6.41) and (6.42)) between two members of a row of quasi-periodic instantons, with $x := x_1 \in [11, 12]$ . . . . .	103
6.4	3D representation of $V$ (using (6.41) and (6.42)) between two members of a row of quasi-periodic instantons, with $x := x_1 \in [11, 12]$ and $y := x_2 \in [0, 2]$ .	104
6.5	Behaviour of $V$ (using (6.45) and (6.45)) between members of a grid of quasi-periodic instantons, with $x := x_1 \in [5, 6]$ and $y := x_2 \in [5, 6]$ . . . . .	105
6.6	Plot illustrating the choice of upper bound for $\phi$ in (6.70) for $n = 1$ and $x_3 \in [0, 1]$	110
7.1	The most general extension of the two black hole Majumdar-Papapetrou metric	118
7.2	The periodic potential with an infinite constant (7.38) for ERN black holes in $D = 3$ with $\rho := \rho_2 \in [0, 1]$ and $x_3 \in [0, 1]$ . . . . .	123
7.3	Plot of (7.58) - (7.57) for various $\rho := \rho_3$ , with $j_2 \in [-10, 10]$ . . . . .	127
7.4	Non-periodic distribution (7.67) of black holes along $x_D$ -axis . . . . .	129
7.5	Non-periodic distribution (7.70) of black holes in two-dimensions . . . . .	131
8.1	Presence of CTCs for non-cosmological black hole examples ((8.90), (8.91) and (8.92) are examples one, two and three respectively) and $\beta = -1$ , with $\rho := \rho_2 \in [1.3, 2.3]$ . . . . .	166
8.2	The interior and exterior regions for a Kaluza-Klein black hole . . . . .	167
8.3	The Riemann curvature scalar (8.136) for non-periodic SN black holes using (8.126) with $m = n = 1$ and $\rho := \rho_2 \in [0, 10]$ . . . . .	176
8.4	The regions of CTCs for three examples ((8.90), (8.91) and (8.92) are examples one, two and three respectively) of RN black holes with $\rho := \rho_2 \in [1, 3]$ . . . .	179
8.5	The Riemann curvature scalar (8.149) and (8.151) for non-periodic RN black holes using example (8.126) for $m = n = 1$ , with $\rho := \rho_2 \in [0, 3]$ and various $\alpha, \beta$ . . . . .	181
8.6	The Riemann curvature scalar (8.157) for non-periodic SC black holes using example (8.126) with $\lambda = 1$ , $\rho := \rho_2 \in [0, 1]$ , $t \in [0, 1]$ . . . . .	184

The copyright of this thesis rests with the author. No quotation from it should be published without the prior written consent and information derived from it should be acknowledged.

# Acknowledgements

I'd like to thank the following people who have helped and supported me along the way:

My supervisor, Professor Richard Ward, for lots of helpful ideas and suggestions, putting up with my aversion to departmental paperwork and several gentle but necessary kicks up the backside!

EPSRC for generously providing funding for me to produce this thesis.

My parents, Barry and Yvonne, for much support and encouragement down the years.

Jinny Matters, without whose love, care, hospitality and cake I may never have made it to Durham in the first place, and Julie Lunn, without whose love, care, patience and hugs I may never have made it to the end of my time in Durham with some grains of sanity still intact!

It'd be a huge list if I mentioned all the friends who have been invaluable along the way, but those who particularly spring to mind are Stuart Abram, Laura Baker, Matthew Barnard, Liam Beadle, Kate Boardman, Anne Cameron, Laura Campbell, Jen Carson, Liz Evershed, Jon Fryer, David Grieve, Ceri Hendy, Richard Hilton, Sara Huxley, Lesley Jones, Teresa Layborne, Jon Lawson, Charlotte Mulliner, Kirsty Pepper, Chris Phillips, Ali Stacey-Chapman, David Sudron, Miranda Threlfall-Holmes and all my fellow loiterers in Durham Cathedral and North Road Methodist Church.

Finally, I'd like to thank Sally Rush, the love of my life, who makes me complete.

# Chapter 1

## Introduction

Albert Einstein finished formulating his general theory of relativity in 1915, ten years after completing the special theory. He was not initially involved in the movement seeking to unite his theories with electromagnetism in a classical field theory, but in 1920 during his inaugural lecture in Leyden he remarked,

*“It would be a great step forward to unify in a single picture the gravitational and electromagnetic fields. Then there would be a worthy completion of the epoch of theoretical physics begun by Faraday and Maxwell...”*

In 1921, he presented a paper by Theodor Kaluza [41] which united gravity with electromagnetism by postulating the existence of a fifth dimension of spacetime. According to [10], “Maxwell’s theory of electromagnetism is an inevitable consequence of Einstein’s general theory of relativity, given that one is willing to buy the idea of an extra dimension.”

There are several problems with Kaluza’s ideas. Firstly, for no obvious reason the fifth dimension is suppressed [61]. Secondly, “Einstein and Grommer found that Kaluza’s vacuum field equations cannot produce non-singular rotation symmetric particle solutions” such as a singularity-free electron [10]. Thirdly and perhaps most obviously: if there is an extra dimension, why don’t we see it?

In 1926, Oskar Klein revisited Kaluza’s ideas, which had been temporarily ignored by Einstein because of the above problems, and wrote two influential papers [44], [45]. He assumed that the fifth dimension had circular topology and hence the coordinate is periodic; the extra dimension is taken to be compact. He proceeded by “taking as a fact the quantized nature

---

of the electric charge” [61] and found that if the fundamental unit of charge is identified with the charge on the electron then the radius of the extra dimension is  $r \approx 10^{-35}$  metres, the Planck size, which explains why we don’t experience it in everyday life [10].

Einstein studied this five-dimensional Kaluza-Klein theory extensively between 1938-43. He hoped to undercut quantum theory which he had objected to from the beginning, famously remarking, “God does not play dice!” However, it became clear to him that it was going nowhere: “In 1943 he argued, together with Pauli, that in Kaluza’s theory it would principally be impossible to find a non-singular particle. Einstein never worked in five dimensions again” [61]. That wasn’t the end of the story, however, as the quest to unite general relativity with quantum mechanics gave rise to various attempts to construct a ‘quantum theory of gravity’ with extra compact dimensions.

In 1978, Gary Gibbons and Stephen Hawking introduced a particular self-dual gravitational instanton and showed that its metric could be written in a very specific form, the Gibbons-Hawking form [16]. It was later proven that any hyperkähler four-metric with a triholomorphic Killing vector can be written in this way for some choice of coordinate system [13], [22]. Consequently, metrics in this form, of which the principle examples are Eguchi-Hanson [12] and Taub-NUT solutions [32], [21], can be found in a variety of settings, such as gravitational instantons, Kaluza-Klein monopoles (such as the Dirac monopole) and vortices and black holes.

The examples given by Gibbons and Hawking involved four-dimensional gravitational instantons with a finite number of centres. Hawking defines a gravitational instanton as “a solution of the classical field equations which is non-singular on some section of complexified spacetime and in which the curvature tensor dies away at large distances” [61]. The potential  $V$  is of the form

$$V = \epsilon + \sum_{j=-N}^N m_j |\vec{r} - \vec{r}_j|^{-1}, \quad (1.1)$$

where the instantons were positioned at the points  $\vec{r}_j$  with mass  $m_j$ . For the Eguchi-Hanson case,  $\epsilon$  is zero and for the Taub-NUT case,  $\epsilon$  is one. It was noted, as we shall see, that the singularities that arise at the points where  $\vec{r} = \vec{r}_j$  can be removed by taking all of the  $m_j$  to be equal and imposing periodicity on one of the coordinates, the fourth dimension  $x_4$ .

---

Infinite centre Gibbons-Hawking metrics arise in various contexts such as periodic monopoles. The problem with the potential given above is that when we let  $N$  go to infinity, it is no longer convergent. We will study four methods of trying to ensure the potential does converge through the course of this work, noting their respective advantages and disadvantages in the contexts in which they occur. The structure of this thesis is as follows:

**Chapter Two - Setting the Scene:** We outline the key definitions and concepts that will be employed throughout this work. We introduce some of the maths involved in Kaluza-Klein theory and the basic general relativistic ideas we will need. Four types of gravitational instantons, Taub-NUT, multi-Taub-NUT, Eguchi-Hanson and Euclidian Schwarzschild [16], are then introduced and some of their properties discussed. We see, having defined the necessary concepts along the way, that any hyperkähler four-metric with a triholomorphic Killing vector can be written in Gibbons-Hawking form for some coordinates. Solitons are introduced which incorporate our instantons into five-dimensional Kaluza-Klein theory, and finally we introduce some useful ideas concerning black holes.

Chapters three and four explore attempts to ensure the convergence of the infinite centre periodic potential  $V$  by subtracting an infinite constant. The difficulty with this approach is that  $V$  is then zero at some points and it turns out that such points are in fact curvature singularities. Moreover, if we incorporate the infinite multi-Taub-NUT and Eguchi-Hanson metrics into a five-dimensional gravitational context as such Kaluza-Klein monopoles, these singularities turn out to be naked singularities. We will outline the theory behind this in chapter three and explore examples of its occurrence in different contexts in chapter four. The work in these chapters (apart from the outlining of the solutions) is entirely original.

**Chapter Three - Solutions with Periodic Sources:** We begin by proving that subtracting an infinite constant does result in a convergent potential, and moreover, one that can be sufficiently well approximated by a finite sum and whose behaviour can be explored by graphical methods. We see both graphically and analytically that  $V$  does become zero at given points. The gauge field  $\vec{\omega}$  is shown to be convergent when we have infinitely many sources, and we develop a logarithmic approximation to  $V$  near to where it becomes zero. Incorporating this instanton potential into a five-dimensional setting, we show that such points are naked singularities. Finally, we show that higher-dimensional versions of this potential converge without the need to subtract an infinite constant.



---

**Chapter Four - Examples of Periodic Solutions:** We investigate examples of the above theory for Kaluza-Klein vortices [53], Dirichlet instantons [55] and gravitational calorons [58]. In each of the three cases, we use graphical methods to see that  $V$  does become zero in some regions and our logarithmic approximation to show that these regions are singular. Additionally, we study Kaluza-Klein monopoles in AdS spacetime [54], which also have naked singularities, the problem with Ketov et al's attempt [42] to generalise the work in [55] to a solution with multiple hypermultiplets, and the difficulties with the Euclidean Schwarzschild solution given by Sanchez in [58].

The next chapter seeks to set this work in context:

**Chapter Five - Surveying the Landscape:** We survey the literature to see awareness of the problem of the incompleteness of the infinite constant solutions, looking at the deviations of the Atiyah-Hitchin metric [2] and ALG metrics [7] from their asymptotic forms. These metrics parallel the Taub-NUT solutions. We then consider three papers in which Gibbons-Hawking metrics with infinite centre potentials have been incorporated into different contexts [9], [26], [28], and the problems resulting from the previously unnoted presence of naked singularities. Finally, we note the parallel between the infinite constant convergence problem and Olbers' and Seeliger's paradoxes.

In chapter six, we explore three other possible methods of ensuring the convergence of the infinite centre potential. Again, apart from outlining the ideas in the papers of others, the work in this chapter is entirely original.

**Chapter Six - Alternative Approaches to Convergence:** We study the work of Anderson et al [1] in which the instantons are positioned non-periodically along one of the axes, and explore the problems that arise in the periodic limit. Next, we look at a lattice solution [52] and see that these quasi-periodic instantons also have points at which  $V$  is zero and the metric is singular. Finally, we explore what happens if we take the infinite constant to be a quotient rather than subtracting it. The resulting potential behaves like a series of delta functions along one of the axes and is otherwise constant, and the metric is everywhere flat.

In the final two chapters, we explore black hole solutions in which issues arise due to the need to ensure the potential(s) converge. In chapter seven, we study Majumdar-Papapetrou metrics and their analytical extensions to multiple Extreme Reissner-Nordström metrics, which

---

are essentially modifications of the Euclidean metrics. In chapter eight, we study Kaluza-Klein black holes, which are essentially modifications of the Gibbons-Hawking metrics.

**Chapter Seven - Extreme Reissner-Nordström Black Holes:** An ERN black hole is one with both charge and mass, which are equal to each other in this extreme case. We first outline the constructions of Hartle and Hawking [30] and Myers [50] for finitely many ERN black holes in  $(D + 1)$ -dimensions for  $D \geq 3$ , noting that the metrics are regular at the event horizons, whose positions correspond to the positions of the monopole sources.

We then turn to the situation with infinitely many black holes. If they are arranged periodically along one of the axes, we show that if  $D = 3$  then naked singularities arise. If  $D \geq 4$ , the potentials are known to be convergent and we show that the curvature is then well-behaved and no unwanted singularities arise. We follow Myers' construction of a lattice solution, demonstrating that the potential he suggests does converge. We show that the construction of Anderson et al [1] for a non-periodic distribution can be modified to work for black holes (which as far as one is aware has not been previously done), calculate the curvature (which is well-behaved) and construct some examples.

We explore the work of Candlish and Reall [4] on the smoothness of the event horizons to our three constructions. Finally, we look at dilaton solutions [60], [59], outlining the work done for finitely many black holes and then moving to infinitely many black holes (which as far as one is aware has not been explored before). We show that for  $D = 3$ , periodic solutions give rise to naked singularities, whilst for  $D \geq 4$ , the curvature is well-behaved. We see that London's work on ERN black holes with a cosmological constant [48] can be extended to explore infinitely many black holes with a dilaton term. Finally, we see that we can bring our lattice and non-periodic solutions into this context and have well-behaved curvature.

**Chapter Eight - Kaluza-Klein Black Holes:** In this chapter we study the behaviour of five dimensional Kaluza-Klein black holes, with and without a cosmological constant and rotating or static. We begin by looking at some special cases of these black holes that link back to earlier work and act as checks for calculations. We then introduce the Eguchi-Hanson [39], Klemm-Sabra [46] and Reissner-Nordström de-Sitter metrics and show that these are stationary, before exploring the behaviour at the event horizons and asymptotic behaviour of our black holes. This work is a mixture of a summary of other authors' work and application of their ideas to new situations.

---

We then explore the behaviour of periodic solutions with infinitely many black holes, which as far as one is aware has not been considered before, demonstrating the presence of naked singularities when one of the potentials  $U$  and  $V$  becomes zero. We give some useful examples and explore the appearance of closed timelike curves in our solutions. We construct non-periodic solutions, seeing that the curvature is well-behaved and looking for the presence of closed timelike curves. We show that little is gained from trying to construct a lattice solution. Finally, we explore the behaviour of the curvature and the presence of closed timelike curves for three special cases, and in the case of rotating black holes we study the ergoregions.

**Conclusion:** Finally, we summarise our results, set our research in the wider context and outline some open questions for further work. The bibliography follows at the end.

### Notation

Throughout this work, we use the following conventions:

The metric is taken to be mostly positive,  $(-, +, \dots, +)$ .

For the Gibbons-Hawking metrics in  $(D + 1)$ -dimensions, we take

$$t := x_0 \quad \text{and} \quad \vec{r} = (x_1, \dots, x_{D-1}), \quad \text{where} \quad \tau := x_4. \quad (1.2)$$

We will often use

$$\rho_n := \sqrt{x_1^2 + \dots + x_n^2}, \quad (1.3)$$

and denote the Riemann curvature scalar by

$$[R]^2 := R_{\mu\nu\rho\sigma} R^{\mu\nu\rho\sigma}. \quad (1.4)$$

The coordinate systems we use, in three dimensions and extended in the obvious way for other cases, are

- Euclidian coordinates:  $d\vec{r}^2 = dx_1^2 + dx_2^2 + dx_3^2$ ,
- Cylindrical coordinates:  $d\vec{r}^2 = d\rho_2^2 + \rho_2^2 d\theta^2 + dx_3^2$ ,
- Spherical coordinates:  $d\vec{r}^2 = dr^2 + r^2 d\theta^2 + r^2 \sin^2 \theta d\phi^2$ .

We have used Maple 10 and 12 to produce graphs and for curvature calculations in this thesis.

## Chapter 2

# Setting the Scene

### 2.1 Introduction

In this chapter we introduce useful definitions and ideas that will be employed throughout the rest of this thesis. The structure of this chapter is therefore as follows:

**General relativity:** We introduce the fundamental ideas from general relativity that we need throughout this thesis: geodesics, connection coefficients, affine parameters, the Riemann curvature tensor, Killing vectors and static and stationary metrics.

**Gravitational instantons:** We introduce the main varieties of gravitational instantons that we will be studying. These metrics admit certain symmetries and so to begin with, we define nuts and bolts and (anti)self-dual metrics. We then introduce the Euclidean Taub-NUT, the multi-Taub-NUT and Eguchi-Hanson metrics as examples of nut solutions and the Schwarzschild solution as an example of a bolt solution. There are two topologically invariant quantities associated with these solutions, the signature and the Euler number. We define these and show how they relate to the number of nuts and bolts that a particular solution admits. Finally, we discuss the asymptotic behaviour of the Taub-NUT metrics.

**Hyperkähler metrics and the Gibbons-Hawking form:** We work towards the main result to note in this chapter: that any hyperkähler four-metric with a triholomorphic Killing vector can be written in Gibbons-Hawking form. To accomplish this, we introduce complex structures, Kähler and hyperkähler manifolds and potentials, and triholomorphic Killing vectors. We then discuss the form the potential must take in order to yield a complete solution.

**Solitons in Kaluza-Klein theory:** We introduce the magnetic monopole as an example of

how gravitational instantons can be incorporated into Kaluza-Klein theory by the addition of a time component to the metric. We discuss the gravitational properties of the resulting soliton and note that the curvature scalar in the instanton and soliton cases will be the same. Finally, in calculating the curvature, we see what goes wrong with the asymptotic approximation to the Atiyah-Hitchin metric, which will be discussed in a later chapter.

**Black holes:** We introduce the basic ideas behind the theory of black holes, which we will make use of in the final two chapters. We define an event horizon rigorously by looking at hypersurfaces. We present the Riemann curvature scalar as a method for checking for the presence of singularities. Finally, we introduce the useful ideas of Killing horizons, surface gravity and stationary limit surfaces.

## 2.2 General Relativity

In this section we introduce some basic ideas from general relativity that will be of use throughout this thesis. We follow the treatment in [5].

A **geodesic** is a generalisation of the definition of a straight line from Euclidean geometry; that is, it is the path of shortest distance between two points. Alternatively, it is the path that parallel-transport its own tangent vector. Given a path  $x^\mu(\lambda)$ , where  $\lambda$  is an affine parameter, the condition that its tangent vector  $\frac{dx^\mu}{d\lambda}$  be parallel-transported is given by the **geodesic equation**

$$\frac{d^2x^\mu}{d\lambda^2} + \Gamma_{\rho\sigma}^\mu \frac{dx^\rho}{d\lambda} \frac{dx^\sigma}{d\lambda} = 0, \quad (2.1)$$

where the **connection coefficients** (sometimes called the **Christoffel symbols**) are defined by

$$\Gamma_{\mu\nu}^\sigma = \frac{1}{2} g^{\sigma\rho} (\partial_\mu g_{\nu\rho} + \partial_\nu g_{\rho\mu} - \partial_\rho g_{\mu\nu}). \quad (2.2)$$

An **affine parameter** is such that the transformation of the proper time  $\tau$  given by

$$\tau \rightarrow \lambda = a\tau + b, \quad (2.3)$$

where  $a$  and  $b$  are constants, leaves the geodesic equation unchanged. The curvature of the metric is embodied in the **Riemann curvature tensor**, which is given by

$$R_{\sigma\mu\nu}^\rho = \partial_\mu \Gamma_{\nu\sigma}^\rho - \partial_\nu \Gamma_{\mu\sigma}^\rho + \Gamma_{\mu\lambda}^\rho \Gamma_{\nu\sigma}^\lambda - \Gamma_{\nu\lambda}^\rho \Gamma_{\mu\sigma}^\lambda, \quad (2.4)$$

which can be written as

$$R_{\rho\sigma\mu\nu} = g_{\rho\lambda} R_{\sigma\mu\nu}^{\lambda}. \quad (2.5)$$

In order to have workable metrics, we require that they possess a certain amount of symmetry. If  $x^{\sigma}$  is a coordinate that the components of the metric,  $g_{\mu\nu}$ , are independent of then the vector

$$K^{\mu} = (\partial_{\sigma})^{\mu} = \delta_{\sigma}^{\mu} \quad (2.6)$$

generates an isometry, meaning that the transformation under which the geometry is invariant is expressed infinitesimally as a motion in the direction of  $K^{\mu}$ . Such a vector is called a **Killing vector**, and a given vector is a Killing vector if and only if it satisfies the **Killing equation**,

$$\nabla_{\mu} K_{\nu} + \nabla_{\nu} K_{\mu} = 0. \quad (2.7)$$

A metric is said to be **stationary** if it has a Killing vector that is timelike near infinity, and is **static** if it possesses a timelike Killing vector that is orthogonal to a family of hypersurfaces, given by  $t = \text{const}$ . In practice, this means there will be no 'cross terms' in the metric.

## 2.3 Gravitational Instantons

There has been much work done over the years on instantons in four-dimensional Euclidean gravity. Many of these have been described by Hawking and Gibbons [32], [16], [17]. We outline, following their descriptions, the structure of some types of gravitational instantons that will be of use later.

We first give some of the background theory, introducing the notions of nuts and bolts and (anti) self-dual metrics. Next, we discuss some nut solutions: the Taub-NUT solution, multi-Taub-NUT solutions and the Eguchi-Hanson metric. We also discuss a bolt solution, the Schwarzschild metric. Finally, we look at topological invariants for our different solutions and at the asymptotic behaviour of the Taub-NUT metric.

### 2.3.1 Nuts and Bolts

Let  $M$  be an oriented four-dimensional manifold with a positive definite metric  $g_{\mu\nu}$ . Suppose it admits at least a one-parameter isometry group  $G$  with action

$$\phi_\tau : M \rightarrow M,$$

where  $\tau$  is the parameter and  $K = K^\alpha \frac{\partial}{\partial x^\alpha} = \frac{\partial}{\partial \tau}$  is the Killing vector. At a fixed point  $p$  (which is a point where  $K = 0$ ) the action of  $\phi_\tau$  on  $M$  gives rise to an isometry

$$\phi_\tau^* : T_p(M) \rightarrow T_p(M),$$

where  $T_p(M)$  is the tangent space at  $p$ . This isometry is generated by an antisymmetric matrix  $K_{\mu;\nu}$  which can have rank 0, 2 or 4.

Rank zero is uninteresting because  $\phi_\tau^*$  will be the identity matrix,  $K = 0$ , and the action of  $G$  is trivial.

If  $K_{\mu;\nu}$  has rank two,  $\phi_\tau^*$  will have the canonical form

$$\phi_\tau^* = \begin{pmatrix} 1 & 0 & 0 & 0 \\ 0 & 1 & 0 & 0 \\ 0 & 0 & \cos \kappa\tau & \sin \kappa\tau \\ 0 & 0 & -\sin \kappa\tau & \cos \kappa\tau \end{pmatrix}, \quad (2.8)$$

and thus leave a two-dimensional subspace  $T_1$  of  $T_p(M)$  unchanged and rotate its orthogonal complement  $T_2$  about itself. Here,  $\kappa$  is the surface gravity (defined in (2.46)).

A **bolt** is a two-dimensional totally geodesic sub-manifold of fixed points. As “the image of  $T_1$  under the exponential map will not be moved” by  $\phi_\tau$ , it is a two-dimensional fixed point set and therefore a bolt.

If  $K_{\mu;\nu}$  has rank four,  $\phi_\tau^*$  will have the canonical form

$$\phi_\tau^* = \begin{pmatrix} \cos \kappa_1\tau & \sin \kappa_1\tau & 0 & 0 \\ -\sin \kappa_1\tau & \cos \kappa_1\tau & 0 & 0 \\ 0 & 0 & \cos \kappa_2\tau & \sin \kappa_2\tau \\ 0 & 0 & -\sin \kappa_2\tau & \cos \kappa_2\tau \end{pmatrix}, \quad (2.9)$$

where  $\kappa_1$  and  $\kappa_2$  are the skew eigenvalues of  $K_{\mu;\nu}$ . This means there are no directions which  $\phi_\tau^*$  will leave invariant at  $p$ , meaning that it is an isolated fixed point, a **nut**.

We can have **nuts** (where  $\kappa_1\kappa_2 > 0$ ) and **antinuts** (where  $\kappa_1\kappa_2 < 0$ ). A further distinction we can make is to say that if  $p$  and  $q$  are relatively prime integers and  $\kappa_1\kappa_2^{-1} = pq^{-1}$  then the action of  $\phi_\tau$  will be periodic with period  $\beta = 2\pi p\kappa_1^{-1} = 2\pi q\kappa_2^{-1}$ . We call this a **nut of type**  $(p, q)$ . A nut is **self-dual** if its antisymmetric part is 0, giving  $p = q = \pm 1$ . If the curvature is self dual,

$$R_{abcd} = \frac{1}{2}\epsilon_{abef}R_{cd}^{ef}, \quad (2.10)$$

then the nut will be self-dual everywhere if it is self-dual at one point. The corresponding result applies for **anti-self-dual** nuts, for which  $p = -q = \pm 1$ .

### 2.3.2 Euclidean Taub-NUT Metric

We follow the treatment in ref. [61]. The four-dimensional **Euclidean Taub-NUT metric** can be written in the form

$$\begin{aligned} ds^2 &= V^{-1}(d\tau + \vec{\omega} \cdot d\vec{r})^2 + Vd\vec{r}^2, \\ V &= 1 + \frac{4m}{r}, \end{aligned} \quad (2.11)$$

where  $m$  is the mass. The potential  $V$  and the one-form  $\omega$ , the gauge field, are related by

$$\vec{\nabla}V = \pm\vec{\nabla} \times \vec{\omega}. \quad (2.12)$$

Note that in this case (and in the multi-Taub-NUT case), the metric is

- self-dual if  $\vec{\nabla}V = \vec{\nabla} \times \vec{\omega}$ ;
- anti-self-dual if  $\vec{\nabla}V = -\vec{\nabla} \times \vec{\omega}$ .

In spherical coordinates,  $\omega_r = 0 = \omega_\theta$  and  $\omega_\phi = 4m(1 - \cos\theta)(r \sin\theta)^{-1}$ , giving

$$\vec{\omega} \cdot d\vec{r} = 4m(1 - \cos\theta)d\phi. \quad (2.13)$$

This metric is singular when  $\theta = \pi$ , as then  $g_{\tau\phi} = V^{-1}\omega_\phi$ . This singularity can be removed using a coordinate patch. We take  $\tau_N = \tau_S - 8m\phi$ , giving



$$\omega_\phi^N = V g_{\phi\tau_N} \text{ and } \omega_\phi^S = -\frac{4m(1 + \cos \theta)}{r \sin \theta}. \quad (2.14)$$

This is singular at  $\theta = 0$ . Both of these singularities are coordinate singularities and we can employ

- $(\tau_N, \omega_\phi^N)$  in the northern hemisphere i.e. except when  $\theta = \pi$ ;
- $(\tau_S, \omega_\phi^S)$  in the southern hemisphere i.e. except when  $\theta = 0$ .

This gives us a non-singular description of the (Euclidean) Taub-NUT spacetime. This construction explains the periodicity of  $\tau$ :  $\phi$  has a period of  $2\pi$  and hence  $\tau$  has a period of  $16\pi m$ .

We can see from examining the potential  $V$  that there is an apparent singularity at  $r$  is zero. This can be removed using the coordinate transformation  $r = (16m)^{-1}\rho^2$ , which results from  $\tau$  being periodic. This fixed point of  $\partial_\tau$  defines a nut with surface gravity  $\kappa_1 = \kappa_2 = (8m)^{-1}$ .

### 2.3.3 Multi Taub-NUT Metric

We have the following self-dual metric [53]:

$$ds^2 = V^{-1}(d\tau + \vec{\omega} \cdot d\vec{r})^2 + V d\vec{r}^2, \quad \vec{\nabla}V = \vec{\nabla} \times \vec{\omega}, \quad (2.15)$$

with the potential being given by

$$V = 1 + \sum_{j=1}^N 4m_j |\vec{r} - \vec{r}_j|^{-1}. \quad (2.16)$$

This is sometimes known as the ***N*-instanton Taub-NUT metric** with nuts positioned at  $\vec{r}_j$  with mass  $m_j$ . If all the  $m_j$  are equal then we can remove the apparent singularities by taking  $\tau$  to have a period of  $16\pi m$ .

### 2.3.4 Eguchi-Hanson Metric

Another useful gravitational instanton is given by the same metric (2.15) but without the constant term in the potential [16]. This metric has the same isometry group as the above but is **asymptotically locally Euclidean (ALE)**, meaning that it is ‘‘asymptotic to Euclidean space identified under a discrete sub group of  $SO(4)$ ’’.

In this case, we still need the  $m_j$  to be equal in order for the metric to be regular but we can achieve this by rescaling the coordinates. If  $N = 1$  we have flat space and  $N = 2$  gives the **Eguchi-Hanson metric**:

$$ds^2 = \left(1 - \frac{a^4}{r^4}\right)^{-1} dr^2 + \left(1 - \frac{a^4}{r^4}\right) \frac{r^2}{4} (d\tau + \cos\theta d\phi)^2 + \frac{r^2}{4} (d\theta^2 + \sin^2\theta d\phi^2). \quad (2.17)$$

In order to remove the apparent singularity, we take  $\tau$  to have period  $2\pi$ . For large values of  $r$ , the metric tends towards Euclidean flat space. For surfaces of constant  $r > a$ , the topology is that of  $\mathbb{R}P^3$ . The surface at  $r = a$  is a 2-sphere.

### 2.3.5 Schwarzschild Metric

The **Euclidean Schwarzschild metric** takes the following form [17]:

$$ds^2 = V d\tau^2 + V^{-1} dr^2 + r^2 (d\theta^2 + \sin^2\theta d\phi^2),$$

$$V = 1 - \frac{2m}{r}. \quad (2.18)$$

There is an apparent singularity at  $r = 2m$  which can be removed by taking  $\tau$  to have a period of  $8\pi m$ . We see that the radial coordinate  $r$  has a range of  $2m \leq r < \infty$  and the topology is  $\mathbb{R}^2 \times \mathbb{S}^2$ .

### 2.3.6 Topological Invariants

According to Hawking and Gibbons [17], “There are two topological invariants which can be expressed as integrals of the curvature of a 4-dimensional metric.” These are the **Euler number**

$$\chi := (128\pi^2)^{-1} \int_M \epsilon_{ab}^{\epsilon f} R_{efgh} \epsilon_{cd}^{\epsilon gh} R^{abcd} \sqrt{g} d^4x, \quad (2.19)$$

and the **signature**

$$\tau := (96\pi^2)^{-1} \int_M R_{abcd} \epsilon^{cdef} R_{ef}^{ab} \sqrt{g} d^4x. \quad (2.20)$$

On a compact manifold, we have

$$\chi[M] = N_+ + N_- + \sum_j \chi_j \quad (2.21)$$

and

$$\tau = - \sum_{\text{nuts}} \cotan p\theta \cotan q\theta + \sum_{\text{bolts}} Y \operatorname{cosec}^2\theta, \quad (2.22)$$

where  $N_+$  is the number of nuts,  $N_-$  is the number of antinuts,  $\chi_j$  is the Euler number of the  $j$ -th bolt,  $Y$  is the self intersection number of a bolt and  $2\theta$  is the group parameter.

We therefore have

Schwarzschild	$\chi = 2$	$\tau = 0$
Taub-NUT	$\chi = 1$	$\tau = 0$
Multi Taub-NUT	$\chi = n$	$\tau = n - 1$
Eguchi-Hanson	$\chi = 2$	$\tau = 1$

### 2.3.7 Topology and Asymptotic Behaviour

An **asymptotically Euclidean** metric is one that approaches the normal Euclidean metric on  $\mathbb{R}^4$  outside of a compact region with potentially different topology than that of  $\mathbb{R}^4$ . Any such metric will, according to Gibbons and Hawking [16], have zero action.

The **Positive Action Conjecture** states that the action of any asymptotically Euclidean metric with  $R_{\mu}^{\mu} = 0$  everywhere is zero if and only if it is flat. Thus, if this conjecture holds, there are no (anti)self-dual asymptotically Euclidean instantons.

The topology of the multi Taub-NUT solutions (of which the standard Taub-NUT solution is a particular case) is such that [17] the surface surrounding the nuts is a 3-sphere with  $n$  points identified, where  $n$  is the number of nuts as above. It is therefore not, in the usual sense, asymptotically flat.

The Eguchi-Hanson metric is, as already mentioned, asymptotically locally Euclidean and as such is asymptotic to Euclidean space modulo  $\mathbb{Z}_n$ . This identification comes from the use of coordinate patches required to remove the Dirac string type singularities in the function  $\vec{\omega}$ . This possibly is not excluded by the positive action conjecture [16].

## 2.4 Hyperkähler Metrics and the Gibbons-Hawking Form

In this section, we will see that any hyperkähler four-metric with a triholomorphic Killing vector can be written in **Gibbons-Hawking form**

$$ds^2 = V^{-1} (d\tau + \vec{\omega} \cdot d\vec{r})^2 + V d\vec{r}^2,$$

$$\vec{\nabla} V = \vec{\nabla} \times \vec{\omega}. \tag{2.23}$$

We first give the necessary definitions following the treatment in [40] and then follow [22] and [13] to obtain our result. As such, we will introduce the notions of holonomy and symplectic groups, define a complex structure and thus be in a position to define a Kähler manifold. Next, we define a generalisation of this, the hyperkähler manifold, and what it means to have a triholomorphic Killing vector. Next, we discuss Kähler and hyperkähler potentials. Having laid these foundations, we give our main result and consider some of the implications. Along the way, we will introduce Calabi-Yau manifolds and the Atiyah-Hitchin metric for later study.

### 2.4.1 Some Useful Definitions

#### Holonomy

Let  $G$  be a Lie group and  $P$  a principal  $G$ -bundle over a smooth, paracompact manifold  $M$ . Let  $\omega$  be a connection on  $P$ . For a piecewise smooth loop  $\gamma : [0, 1] \rightarrow M$  based at the point  $x \in M$  and a point  $p$  in the fibre over  $x$ , the connection defines a unique horizontal lift  $\tilde{\gamma} : [0, 1] \rightarrow P$  such that  $\tilde{\gamma}(0) = p$ .

The end-point of this lift will frequently not be  $p$ , but instead will be a point  $p \cdot g$  in the fibre over  $x$ . We define an equivalence relation on  $P$  by requiring that  $p \sim q$  if and only if they can be joined by a piecewise smooth horizontal path in  $P$ .

The **holonomy group** of  $\omega$  based at  $p$  is

$$\text{Hol}_p(\omega) = \{g \in G | p \sim p \cdot g\}. \tag{2.24}$$

Let  $(M, g)$  be a Riemannian manifold with Levi-Civita connection  $\Gamma$ . The **holonomy group**  $\text{Hol}(g)$  of  $g$  is  $\text{Hol}(\Gamma)$  on the tangent bundle to  $M$ . Thus,  $\text{Hol}(g)$  is a subgroup of  $O(n)$ , defined up to conjugation in  $O(n)$ .

#### Symplectic Groups

The **quaternions** are the associative, non-abelian real algebra

$$\mathbb{H} := \{x_0 + x_1i + x_2j + x_3k \mid x_i, x_j, x_k \in \mathbb{R}\}, \quad (2.25)$$

where  $ij = -ji = k$ ,  $jk = -kj = i$ ,  $ki = -ik = j$ ,  $i^2 = j^2 = k^2 = -1$ .

The  $m$ -th dimensional symplectic group is the group of  $m \times m$  matrices given by

$$\mathrm{Sp}(m) := \{A \in M_m(\mathbb{H}) \mid A\bar{A}^T = I\}. \quad (2.26)$$

Now,  $\dim \mathrm{Sp}(m) = 2m^2 + m$  and  $\dim \mathrm{SU}(2m) = 4m^2 - 1$ . Thus, for  $m > 1$ ,  $\mathrm{Sp}(m)$  is a proper subgroup of  $\mathrm{SU}(2m)$  and they are equivalent if  $m = 1$ .

### 2.4.2 Complex Structures on Manifolds

Let  $M$  be a real manifold of dimension  $2m$ .

An **almost complex structure**  $J$  on  $M$  is a smooth tensor  $J_a^b$  on  $M$  which satisfies the relation

$$J_a^b J_b^c = -\delta_a^c. \quad (2.27)$$

Suppose that  $v$  is a smooth vector field on  $M$ . We can define a new vector field  $J_v$  by

$$(J_v)_b = J_a^b v^a, \quad (2.28)$$

showing that  $J$  acts linearly on vector fields. Combining these two observations shows us that

$$J(J_v) = -v \quad \implies \quad J^2 = -1. \quad (2.29)$$

From this, we can see that  $J$  will give each tangent space  $T_p(M)$  the structure of a complex vector space. Now, let  $v, w$  be smooth vector fields on  $M$ . We can define a new vector field  $N_J(v, w)$  by

$$N_J(v, w) = [v, w] + J([J_v, w] + [v, J_w]) - [J_v, J_w], \quad (2.30)$$

where  $[\cdot, \cdot]$  denotes the Lie bracket. It turns out that  $N_J$  is a tensor (the **Nijenhuis tensor**) and so  $N_J(v, w)$  is pointwise bilinear in  $v$  and  $w$ .

Let  $M$  be a real manifold of dimension  $2m$  and  $J$  an almost complex structure on  $M$ . We call  $J$  a **complex structure** if  $N_J \equiv 0$  on  $M$ . A **complex manifold** is a manifold  $M$  equipped with a complex structure  $J$  and denoted  $(M, J)$ .

### 2.4.3 Kähler Manifolds

Let  $(M, J)$  be a complex manifold and  $g$  be a Riemannian metric on  $M$ .  $g$  is a **Hermitian metric** if the following (equivalent) conditions hold:

- i)  $\forall$  vector fields  $v, w$  on  $M$ ,  $g(v, w) = g(Jv, Jw)$ ;
- ii)  $g_{ab} \equiv J_a^c J_b^d g_{cd}$ .

For a Hermitian metric  $g$ , we can define a 2-form  $\omega$  on  $g$  called the **Hermitian form** in the following (equivalent) ways:

- i)  $\forall$  vector fields  $v, w$  on  $M$ ,  $\omega(v, w) = g(Jv, w)$ ;
- ii)  $\omega_{ac} = J_a^b g_{bc}$ .

Let  $M$  be a complex manifold and  $g$  a Hermitian metric on  $M$  with Hermitian form  $\omega$ . We say that  $g$  is a **Kähler metric** if  $d\omega = 0$ . We then call  $\omega$  a **Kähler form** and  $(M, J, g)$  a **Kähler manifold**. The following is a useful result:

Let  $M$  be a manifold of dimension  $2m$ ,  $J$  an almost-complex structure on  $M$  and  $g$  a Hermitian metric with Hermitian form  $\omega$ . Let  $\Gamma$  denote the Levi-Civita connection of  $g$ . Then the following are equivalent:

- i)  $J$  is a complex structure and  $g$  is Kähler;
- ii)  $\Gamma J = 0$ ;
- iii)  $\Gamma \omega = 0$ ;
- iv)  $\text{Hol}(g) \subset U(m)$  and  $J$  is associated to the corresponding  $U(m)$  structure.

Note that if  $g$  is a Hermitian matrix on a complex manifold then  $d\omega = 0$  implies that  $\Gamma J = \Gamma \omega = 0$ .

#### 2.4.4 Hyperkähler Manifolds

Let  $(M, g)$  be a Riemannian  $4m$ -manifold with  $\text{Hol}(g) \subseteq \text{Sp}(m)$ . Each  $\text{Sp}(m)$ -invariant tensor on  $\mathbb{R}^{4m}$  corresponds to a tensor on  $M$  which is constant under the Levi-Civita connection  $\Gamma$  of  $g$ . From this, it follows that there exist almost complex structures  $J_1, J_2, J_3$  and 2-forms  $\omega_1, \omega_2, \omega_3$  on  $M$ , each constant under  $\Gamma$ .

As  $\Gamma J_j = 0$ , each  $J_j$  is an integrable complex structure.  $g$  is Kähler with respect to  $J_j$ , with Kähler form  $\omega_j$ . If  $a_1, a_2, a_3 \in \mathbb{R}$  with  $a_1^2 + a_2^2 + a_3^2 = 1$  then  $a_1 J_1 + a_2 J_2 + a_3 J_3$  is also a complex structure on  $M$ .  $g$  is Kähler with respect to it, with Kähler form  $a_1 \omega_1 + a_2 \omega_2 + a_3 \omega_3$ . Therefore, we can see that  $g$  is Kähler with respect to a whole 2-sphere of complex structures. We then call  $g$  **hyperkähler**.

Let  $M$  be a  $4m$ -manifold. An **almost hyperkähler structure** on  $M$  consists of the quadruple  $(J_1, J_2, J_3, g)$ . The  $J_j$  are almost-complex structures on  $M$  satisfying the relations  $J_1 J_2 = J_3$  and cyclic permutations thereof.  $g$  is a Riemannian metric on  $M$  which is Hermitian with respect to  $J_1, J_2, J_3$ .

We call  $(J_1, J_2, J_3, g)$  a **hyperkähler structure** on  $M$  if in addition to the above, we have  $\Gamma J_j = 0 \forall j$  where  $\Gamma$  is the Levi-Civita connection of  $g$ . Thus,  $(M, J_1, J_2, J_3, g)$  is a **hyperkähler manifold** and  $g$  a **hyperkähler metric**.

Each of the  $J_j$  is integrable and  $g$  is Kähler with respect to them. The Kähler forms  $\omega_1, \omega_2, \omega_3$  are called the **hyperkähler 2-forms** of  $M$ . The following is a useful result:

Let  $M$  be a manifold of dimension  $4m$ ,  $(J_1, J_2, J_3, g)$  an almost-hyperkähler structure on  $M$ . Let  $\omega_1, \omega_2, \omega_3$  be the Hermitian forms of  $J_1, J_2, J_3$ . Then the following are equivalent:

- i)  $(J_1, J_2, J_3, g)$  a hyperkähler structure;
- ii)  $d\omega_1 = d\omega_2 = d\omega_3 = 0$ ;
- iii)  $\Gamma\omega_1 = \Gamma\omega_2 = \Gamma\omega_3 = 0$ ;
- iv)  $\text{Hol}(g) \subset \text{Sp}(m)$  and  $J_1, J_2, J_3$  are the induced complex structures.

All hyperkähler metrics are Ricci-flat.

If our hyperkähler metric possesses a Killing vector  $K$  which is holomorphic with respect to each of the complex structures, so that

$$\mathcal{L}_K J_1 = \mathcal{L}_K J_2 = \mathcal{L}_K J_3 = 0, \quad (2.31)$$

then the Killing vector is called **triholomorphic**.

### Calabi-Yau Manifolds

We can generalise the notion of a hyperkähler manifold:

A **Calabi-Yau manifold** is a compact Kähler manifold  $(M, J, g)$  of dimension  $m \geq 2$  with  $\text{Hol}(g) = \text{SU}(m)$ . Such manifolds are Ricci-flat. These objects crop up in string theory and will be of interest later on.

#### 2.4.5 Holonomy Groups of Different Manifolds

Berger [3] classified the different holonomy groups as follows:

$\text{Hol}(g)$	$\dim(M)$	Manifold Type	Properties
$\text{SO}(n)$	$n$	oriented	-
$\text{U}(n)$	$2n$	Kähler manifold	Kähler
$\text{SU}(n)$	$2n$	Calabi-Yau manifold	Ricci-flat, Kähler
$\text{Sp}(n)$	$4n$	hyperkähler manifold	Ricci-flat, Kähler

Note that  $\text{Sp}(n) \subset \text{SU}(2n) \subset \text{U}(2n) \subset \text{SO}(4n)$ , so every hyperkähler manifold is a Calabi-Yau manifold, every Calabi-Yau manifold is a Kähler manifold, and every Kähler manifold is orientable.

#### 2.4.6 Kähler and Hyperkähler Potentials

Let  $M$  be a hyperkähler manifold with complex structures  $J_1, J_2, J_3$  and corresponding Hermitian forms  $\omega_1, \omega_2, \omega_3$ . A function  $V : M \rightarrow \mathbb{R}$  is called a **Kähler potential** for the complex structure  $J_i$  if

$$\omega_i = -i\partial_{J_1}\bar{\partial}_{\bar{J}_1}V = -\frac{1}{2}dJ_1dV. \quad (2.32)$$

The function  $V$  is a **hyperkähler potential** if it is simultaneously a Kähler potential for each of  $J_1, J_2$  and  $J_3$ .



### 2.4.7 Gibbons-Hawking Form

In 1987, Hitchin et al [34] proved the following result, which is further discussed and clarified in [13]:

**Theorem 2.1** Any hyperkähler 4-metric with triholomorphic Killing vector must be of Gibbons-Hawking form (2.23).

There is another useful theorem from Gibbons and Ruback [22]:

**Theorem 2.2** Let  $g_{\alpha\beta}$  be hyperkähler with 2 commuting Killing vectors. Then there exists a linear combination which is triholomorphic and hence the metric can be written in Gibbons-Hawking form.

The hyperkähler structures are given by

$$\begin{aligned} J_1 &= (d\tau + \vec{\omega} \cdot d\vec{r}) \wedge dx_1 - V dx_2 \wedge dx_3, \\ J_2 &= (d\tau + \vec{\omega} \cdot d\vec{r}) \wedge dx_2 - V dx_3 \wedge dx_1, \\ J_3 &= (d\tau + \vec{\omega} \cdot d\vec{r}) \wedge dx_3 - V dx_1 \wedge dx_2. \end{aligned} \tag{2.33}$$

To obtain complete metrics, we must take  $V$  to be of the form

$$V = V_0 + \sum_{j=1}^N 4m |\vec{r} - \vec{r}_j|^{-1}, \tag{2.34}$$

where  $m > 0$  and as before,  $\tau \in [0, 16\pi m)$ .

If  $V_0 = 0$  then the metrics are **asymptotically locally Euclidean** (ALE) and if  $V_0 = 1$  the metrics are **asymptotically locally flat** (ALF).

Finally, we note that the only  $SO(3)$  complete non-singular invariant half-flat 4-metrics with 3-dimensional orbits are

- i) the Atiyah-Hitchin metric ( $V_0 = 1 = N$ ,  $m < 0$ );
- ii) the Taub-NUT metric ( $V_0 = 1 = N$ ,  $m > 0$ );
- iii) the Eguchi-Hanson metric ( $V_0 = 0$ ,  $N = 2$ ,  $m > 0$ ).

Note that the Atiyah-Hitchin metric (whose asymptotic form is the Taub-NUT metric with a negative mass) does not have a tri-holomorphic Killing vector and so cannot be written in Gibbons-Hawking form.

## 2.5 Solitons in Kaluza-Klein Theory

We can construct solitons in Kaluza-Klein theory from existing gravitational instanton solutions. We will discuss their gravitational properties and note a useful result concerning the curvature.

A **soliton** is a “non-singular solution of the classical field equations which represents spatially localized lumps that are topologically stable” [27]. We are aiming for solutions of our five-dimensional field equations that approach the vacuum solution  $g_{AB} \approx \eta_{AB}$  at spatial infinity, meaning that  $V = 1$ ,  $A_\mu = 0$  and  $g_{\mu\nu}^4 = \eta_{\mu\nu}^4$  (note that  $\mu, \nu = 0, 1, 2, 3$  and  $A, B = 0, 1, 2, 3, 5$ ).

In order to obtain such soliton solutions, we assume the following:

- The metric is *static*, with  $\partial_\tau$  as a Killing vector and  $\partial_\tau g_{AB} = 0$ ;
- In analogy with Yang-Mills theory,  $g_{0A} = \delta_{0A}$ .

These conditions mean that the “four-dimensional, wholly spacelike, manifold at each fixed  $t$  has vanishing Ricci tensor” [27]. This means that, “This reduces the field equations to the equations of Euclidean gravity on surfaces of constant time, and the fifth dimension now plays the same role as the Euclidean time in the four dimensional theory” [61]. Thus, we can incorporate gravitational instantons into Kaluza-Klein theory by simply adding a time coordinate to the metric in a “topologically trivial” way.

### 2.5.1 Magnetic Monopole

A Kaluza-Klein monopole is a spacetime of the form

$$\begin{aligned} ds^2 &= -dt^2 + V^{-1}(d\tau + \vec{\omega} \cdot d\vec{r})^2 + V d\vec{r}^2, \\ \vec{\nabla} \times \vec{\omega} &= \vec{\nabla} V, \\ V &= 1 + \frac{4m}{r}. \end{aligned} \tag{2.35}$$

Here, the Taub-NUT gravitational instanton has been generalised to give the magnetic monopole. The apparent singularity at  $r = 0$  can be removed by taking  $\tau$  to have a period of  $16\pi m$ , using the same argument as for the instanton case. The magnetic field is given by

$$\vec{B} = \vec{\nabla} \times \vec{\omega} = \frac{4m\vec{r}}{r^3}. \quad (2.36)$$

The magnetic charge is given by  $(2e)^{-1}$  which is one unit of Dirac charge. The mass of the monopole is given by  $\sqrt{\frac{m_P^2}{\alpha}}$  where  $\alpha = e^2(4\pi\hbar c)^{-1}$  and  $m_P$  is the Planck mass.

Multimonopole solutions can also be constructed with the same metric and potential

$$V = 1 + \sum_{j=1}^N 4m_j |\vec{r} - \vec{r}_j|^{-1}. \quad (2.37)$$

The singularities at each of the  $\vec{r}_j$  can be removed by making all the  $m_j$  the same and taking  $\tau$  to be periodic with period  $16\pi m$  as usual. As Gross and Perry note, “a remarkable property of Kaluza-Klein monopoles that they do not interact” which allows us to construct such solutions. They state that

*“One might have thought that the reason that they were non-interacting was their gravitational attraction was cancelled by their electromagnetic repulsion. However the situation is quite different, since the gravitational attraction is cancelled by the interaction with the scalar field. The electromagnetic interaction of the monopoles in fact vanishes”.*

We can perform a similar exercise for the Schwarzschild metric ([61], [27]) and by the regularity condition see that it also must have a periodic fifth dimension.

### 2.5.2 Gravitational Properties

One of the peculiar features of the solitons we have studied thus far is that they have inertial mass but no gravitational mass, so an observer at a fixed point in space cannot tell if the soliton is there or not! As we have incorporated the instantons into Kaluza-Klein theory by adding a topologically trivial time dimension, the resulting solitons are ‘flat’ in the time dimension. In these spaces, there exist time-like geodesics that correspond to a particle sitting at rest relative to the soliton [61]. The Newtonian force that a test particle experiences is proportional to  $\frac{1}{2}\nabla g_{00}$  and this vanishes. Thus, the solitons have zero gravitational mass. This might be thought to violate the five-dimensional principle of equivalence but actually

violates the four-dimensional version of Birkhoff's theorem, as the Schwarzschild solution isn't the only possible choice for the  $g_{\mu\nu}^{(4)}$  part of a rotation symmetric  $5 \times 5$  metric at large distances. These unusual properties mean that classical Kaluza-Klein theory is unlikely to be physically realistic!

### 2.5.3 Curvature Tensor

We note the following for later use. Consider the magnetic monopole in spherical coordinates  $(r, \theta, \phi)$ :

$$ds^2 = -dt^2 + V^{-1} (d\tau + 4m(1 - \cos\theta)d\phi)^2 + V (dr^2 + r^2(d\theta^2 + \sin\theta d\phi^2)),$$

$$V = 1 + \frac{4m}{r}. \tag{2.38}$$

Looking at the metric, we can see that if  $V$  is zero, so in this case if  $r = -4m$ , then we will run into problems. If we calculate the Riemann curvature, we see that we obtain the same result as if we ignored the  $-dt^2$  term and just considered the Euclidean Taub-NUT metric, as  $R_{\mu\nu\rho\sigma} = 0$  if any of  $\mu, \nu, \rho, \sigma$  are  $t$ . We have

$$[R]^2 = \frac{384m^2}{r^6V^6} = \frac{384m^2}{(r + 4m)^6}. \tag{2.39}$$

If  $r = -4m$  then  $V$  is zero and the curvature scalar goes to infinity. Consequently, we have a singularity (see the section below for an explanation of this). Moreover, using Cartan's formula for a general Gibbons-Hawking metric (2.23) yields the formula [28]

$$[R]^2 = \frac{V^{-1}\Delta\Delta(V^{-1})}{2}, \tag{2.40}$$

which means that whenever  $V$  is zero there will be a singularity.

As has been briefly mentioned, the Atiyah-Hitchin metric has for its asymptotic form the Taub-NUT metric with negative mass. It is clear from the above that, as the Atiyah-Hitchin metric is complete, it must deviate from its asymptotic form for small values of  $r$ . We will utilise this fact later. Finally, we note that adding the  $-dt^2$  term does not alter the curvature. This is something we can see will be generally true and thus a result we can use for different choices of  $V$  in subsequent chapters.

## 2.6 Black Holes

A black hole is the result of the gravitational collapse of a massive star, and is essentially a singularity hidden behind an event horizon. We will define event horizons, discuss the

singularity theorems of Hawking and Penrose and introduce the Riemann curvature scalar that we will use to check for the presence of curvature (as opposed to simply coordinate) singularities in our later work. Finally, we introduce the further concepts of Killing horizons, surface gravity and stationary limit surfaces. In this we follow the treatment in [5].

### 2.6.1 Event Horizons and Singularities

We outline the formal definition of an event horizon and of a singularity, explaining how we will look for the latter objects in our later calculations. When a star collapses a considerable amount of information, such the chemical composition of the star, is lost and so a black hole can be completely defined by relatively few parameters, such as the mass, electric and magnetic charge, and angular momentum. This is an example of a 'no hair theorem'.

Black holes are characterised by the fact that one can enter but never exit. Thus, their most important future is not the singularity so much as the **event horizon**. We denote the **future null infinity** by  $\mathcal{I}^+$  and the **causal past** by  $J^-$ . The event horizon is then the boundary of the closure of  $J^- (\mathcal{I}^+)$ , and is a null hypersurface.

A **hypersurface** is an  $(n - 1)$ -dimensional submanifold  $\Sigma$  of an  $n$ -dimensional manifold  $M$ . It can be defined by  $f(x) = \text{const}$  for some function  $f$ . The vector field

$$\zeta^\mu = g^{\mu\nu} \nabla_\nu f \tag{2.41}$$

will be normal to the surface, which is a **null hypersurface** if  $\zeta^\mu$  is null. It turns out that  $\zeta^\mu$  is tangent to  $\Sigma$  as well, as null vectors are orthogonal to themselves. Therefore the integral curves  $x^\mu(\lambda)$  (which turn out to be necessarily geodesics, so  $\lambda$  is an affine parameter) satisfying

$$\zeta^\mu = \frac{dx^\mu}{d\lambda} \tag{2.42}$$

are null curves contained in the hypersurface. Thus, the union of the geodesics  $x^\mu(\lambda)$  is the hypersurface  $\Sigma$  and they are called the **generators** of  $\Sigma$ . If we write the metric in **Gaussian normal coordinates**, then the event horizon  $r_H$  will be located at the points where

$$g^{rr}(r_H) = 0. \tag{2.43}$$

Inside the event horizon, we would expect to find a singularity as, by the **singularity theorems** of Hawking and Penrose, once the gravitational collapse of a star has progressed

beyond a certain point, their formation is inevitable. We know this point has been reached when we observe the formation of a **trapped surface**, which is a compact, spacelike, two dimensional submanifold with the property that outgoing future-directed light rays converge in both directions everywhere on the submanifold.

One way to test if a singularity is merely a coordinate singularity (and thus can be removed by a coordinate transformation) or actually a curvature singularity is to compute scalar quantities such as the **Riemann curvature scalar**

$$[R]^2 = R_{\mu\nu\rho\sigma}R^{\mu\nu\rho\sigma}, \quad (2.44)$$

and see if they are infinite. If they are, this indicates that something has gone wrong with the metric that cannot be remedied by changing the coordinates. The **cosmic censorship conjecture** tells us that we should not expect to see **naked singularities**, ones from which  $\mathcal{I}^+$  can be reached in a finite time and for a finite value of the affine parameter, in any physically realistic theory.

### 2.6.2 Some Further Definitions

In this section, we will define the following useful notions for our later work: Killing horizons, surface gravity and stationary limit surfaces.

#### Killing Horizons

If a Killing vector field  $K^\mu$  is null along some null hypersurface  $\Sigma$ , we say that  $\Sigma$  is a **Killing horizon** of  $K^\mu$ . Killing horizons are closely related to event horizons:

- Every event horizon  $\Sigma$  in a stationary, asymptotically flat spacetime is a Killing horizon for some Killing vector field  $K^\mu$ ;
- If the spacetime is static,  $K^\mu$  will be the Killing vector field  $K^\mu = (\partial_t)^\mu$  representing time translations at infinity;
- If the spacetime is stationary but not static, it will be axisymmetric with a rotational Killing vector field  $R^\mu = (\partial_\phi)^\mu$ .

#### Surface Gravity

Consider a Killing vector  $K^\mu$  with Killing horizon  $\Sigma$ ; as  $K^\mu$  is normal to  $\Sigma$ , along the Killing horizon it obeys the geodesic equation given by

$$K^\nu \nabla_\nu K^\mu = -\kappa K^\mu, \quad (2.45)$$

where the constant  $\kappa$  is called the **surface gravity**. It can be found from the formula

$$\kappa^2 = -\frac{1}{2} (\nabla_\mu K_\nu) (\nabla^\mu K^\nu). \quad (2.46)$$

In a static, asymptotically flat spacetime, the surface gravity is the acceleration of a static observer near the horizon, as measured by a static observer at infinity.

### Stationary Limit Surfaces

In the above, suppose that the metric is stationary but not static. The Killing vector  $K^\mu$  will not become null at a Killing horizon but generally at some timelike surface outside the horizon. The place where

$$K^\mu K_\mu = g_{tt} = g_{00} = 0 \quad (2.47)$$

is called the **stationary limit surface** or **ergosurface**. Inside this surface,  $K^\mu$  is spacelike and so no observer can remain stationary, even if they still outside the event horizon, but has to move with respect to the Killing field. In the region between the event horizon and the stationary limit surface, known as the **ergoregion**, timelike paths are inevitably dragged along with the rotation of the black hole.

Having laid these foundations, we now investigate infinite-centre gravitational instantons with periodic potentials.

## Chapter 3

# Solutions with Periodic Sources

### 3.1 Introduction

Throughout the course of this work we will need to consider metrics with potentials that have sources periodically distributed along one of the axes. In this chapter we will look at some of the theory about them that we will utilise in later chapters. As an example of when these occur, consider self-dual metrics in the Gibbons-Hawking form:

$$ds_{GH}^2 = V^{-1}(d\tau + \vec{\omega} \cdot d\vec{r})^2 + V d\vec{r}^2, \quad (3.1)$$

$$\vec{\nabla}V = \vec{\nabla} \times \vec{\omega}. \quad (3.2)$$

Suppose we have a  $(2N + 1)$ -instanton solution for the potential  $V$  on  $\mathbb{R}^3$ :

$$V = V_0 + V_c \sum_{j=-N}^N |\vec{r} - \vec{r}_j|^{-1}, \quad (3.3)$$

where  $V_0$  and  $V_c$  are constants. We have assumed that each instanton has the same mass  $m$  and thus we can remove the singularities at the  $\vec{r}_j$  by taking  $\tau$  to have period  $4\pi V_c$ . In order to obtain a finite chain of instantons on  $\mathbb{R}^2 \times \mathbb{S}^1$ , we can take the instantons to be evenly distributed along the  $x_3$ -axis, with period  $P$ , yielding:

$$V = V_0 + V_c \sum_{j=-N}^N (x_1^2 + x_2^2 + (x_3 - Pj)^2)^{-\frac{1}{2}}. \quad (3.4)$$

At this point, one may ask what happens if we allow  $N$  to tend to infinity and thus obtain a chain of infinitely many instantons. Well, we cannot simply do this because it is well-known that the sum does not converge (see, for example, papers by Ward [62], Dunne and Khemani [11] or Cherkis and Kapustin [6]).



One possible remedy for this is to subtract an infinite constant in order to ensure convergence.

We would then have the **periodic potential**

$$V(\rho_2, x_3) = V_0 + V_c \left( \sum_{j=-\infty}^{\infty} (\rho_2^2 + (x_3 - Pj)^2)^{-\frac{1}{2}} - 2 \sum_{j=1}^{\infty} (Pj)^{-1} \right). \quad (3.5)$$

This choice of potential is to some extent arbitrary, but this is allowed for by the flexibility we have in the choice of  $V_0$  and  $V_c$ . The difficulty with using this approach to ensure convergence is that  $V$  will become zero for some values of  $\rho_2$  and  $x_3$ . This behaviour will give rise to naked singularities. Later, we consider a higher-dimensional variation on this potential,

$$V = V_0 + V_c \sum_{j=-\infty}^{\infty} (\rho_2^2 + (x_3 - Pj)^2)^{(1-\frac{D}{2})} \quad (3.6)$$

for  $D \geq 4$  which converges (here,  $\rho_2 := \sqrt{x_1^2 + x_2^2}$ ). The structure of this chapter is as follows:

**Considering Convergence:** We study the work of Gross and Wilson [28] and their demonstration of the convergence of the potential formed by subtracting an infinite constant using the Harnack Convergence Theorem. Next, we consider the rate of convergence of  $V$  in order to verify that an approximation using a finite sum is sufficiently accurate to be of use. We develop such an approximation which then allows us use graphical methods to investigate the behaviour of  $V$ .

**Zero regions:** We use graphical methods to see that the potential is indeed zero at some points and use the Intermediate Value Theorem to confirm that this has to be the case.

**Convergence of  $\vec{\omega}$ :** We will see that the components of the vector  $\vec{\omega}$  are convergent for infinitely many sources.

**Approximating  $V$ :** We consider a useful approximation for  $V$  that will allow us to calculate the curvature easily, and show that if  $V$  is zero then there is indeed a curvature singularity.

**Exterior and interior spacetimes:** We show that for a Kaluza-Klein monopole constructed from a gravitational instanton in Gibbons-Hawking form, such a singularity can be reached in finite time, indicating that the singularity is naked.

**Higher-dimensional case:** We demonstrate that the higher-dimensional version of our periodic potential does converge.

## 3.2 Considering Convergence

We will show that the infinite constant solution does converge and that we can approximate  $V$  using finitely many terms. We first show that each additional term in the series becomes small very quickly. This will indicate that a finite approximation is sensible. We then note that the convergence is quadratic and use this to form an approximation to  $V$ , which we will see from estimating the error gives sufficiently accurate results as to be useful later on.

### 3.2.1 Convergence of the Infinite Constant Solution

In this section we will outline the argument of Gross and Wilson [28] that demonstrates the convergence of a potential of the form of (3.5). First we state a useful theorem [25]:

**Harnack Convergence Theorem** If a monotone sequence of harmonic functions in a bounded region  $G$  converges at some point in  $G$  then it converges at all points of  $G$  to a harmonic function, and this convergence is uniform on any closed subdomain of  $G$ .

Now, let  $D \subset \mathbb{R}^3$  be an open disk centred at the origin. Define the potential  $V$  to be given by

$$V := \sum_{j=-\infty}^{\infty} ((x_3 + j\varepsilon)^2 + \rho_2^2)^{-\frac{1}{2}} - \sum_{j=-\infty}^{\infty} a_{|j|}, \quad (3.7)$$

with

$$a_j := \begin{cases} (j\varepsilon)^{-1} & \text{if } j \neq 0, \\ \frac{2(-\gamma + \log(2\varepsilon))}{\varepsilon} & \text{if } j = 0, \end{cases} \quad (3.8)$$

where  $\gamma$  is Euler's constant and  $\varepsilon$  is the period of the instantons that are distributed along the  $x_3$ -axis.  $V$  is a harmonic function, as it satisfies Laplace's equation  $\Delta V = \nabla^2 V = 0$ .

**Theorem 3.1** Consider the sequence

$$T_N := \sum_{j=-N}^N ((x_3 + j\varepsilon)^2 + \rho_2^2)^{-\frac{1}{2}} - \sum_{j=-N}^N a_{|j|}, \quad (3.9)$$

where  $a_j$  is defined as above. Then  $\{T_N\}$  converges uniformly on  $D \times \mathbb{R} - (\{0\} \times \varepsilon\mathbb{Z})$  to a harmonic function  $V$ .

**Proof** Let  $p$  be the smallest integer greater than  $\varepsilon^{-1}\sqrt{1 + \varepsilon^2}$ . Then for any  $x_3 \in [0, \varepsilon]$ ,  $\rho_2 \leq 1$ , we have

$$\left((x_3 + j\varepsilon)^2 + \rho_2^2\right)^{-\frac{1}{2}} > a_{|j|+p} \quad \forall j. \quad (3.10)$$

Define

$$R_N := \sum_{j=-N}^N \left((x_3 + j\varepsilon)^2 + \rho_2^2\right)^{-\frac{1}{2}} - \sum_{j=-N}^N a_{|j|+p}. \quad (3.11)$$

Then, we can see that for  $N > 2p$ ,

$$T_N - R_N = -a_p - a_0 - 2 \sum_{j=1}^{p-1} a_j + 2 \sum_{j=N-p+1}^N a_{j+p}. \quad (3.12)$$

Define

$$C(\varepsilon) := -a_p - a_0 - 2 \sum_{j=1}^{p-1} a_j, \quad (3.13)$$

and note that

$$\sum_{j=N-p+1}^N a_{j+p} \rightarrow 0 \text{ as } N \rightarrow \infty. \quad (3.14)$$

Thus, if  $R_N$  converges uniformly to  $R$ , say, then  $T_N$  converges to  $R + C(\varepsilon)$ , which is also harmonic. Now for any  $x_3 \in (0, \varepsilon)$ ,  $\rho_2 < 1$ ,  $R_N$  is a monotonically increasing sequence of harmonic functions, since each term is positive. The sequence is also bounded at  $x_3 = \frac{\varepsilon}{2}$ ,  $x_1 = x_2 = 0$  and therefore by the Harnack Convergence Theorem, the  $R_N$  converge to a harmonic function  $R$  and  $V = R + C(\varepsilon)$ .

□

### 3.2.2 Rate of Convergence

In what follows, we need to study the behaviour of the periodic potential for  $x_3 \in [0, P)$  because if we know how it behaves in that region we know how it will behave throughout by virtue of the periodicity in  $x_3$ . We consider the infinite sum

$$\phi(\rho_2, x_3) := \sum_{j=-\infty}^{\infty} \left(\rho_2^2 + (x_3 - Pj)^2\right)^{-\frac{1}{2}} - 2 \sum_{j=1}^{\infty} (Pj)^{-1}. \quad (3.15)$$

This can be written as

$$\phi = \left(\rho_2^2 + x_3^2\right)^{-\frac{1}{2}} + \alpha(\rho_2, x_3) + \beta(\rho_2, x_3), \quad (3.16)$$

where

$$\alpha(\rho_2, x_3) := \sum_{j=1}^{\infty} \left( \left( \rho_2^2 + (x_3 - Pj)^2 \right)^{-\frac{1}{2}} - (Pj)^{-1} \right) \quad (3.17)$$

and

$$\beta(\rho_2, x_3) := \sum_{j=1}^{\infty} \left( \left( \rho_2^2 + (x_3 + Pj)^2 \right)^{-\frac{1}{2}} - (Pj)^{-1} \right). \quad (3.18)$$

Both  $\alpha$  and  $\beta$  converge and therefore the sequences of partial sums  $\{\alpha_m\}_{m \in \mathbb{N}}$  and  $\{\beta_n\}_{n \in \mathbb{N}}$ , where

$$\alpha_m := \sum_{j=1}^m \left( \left( \rho_2^2 + (x_3 - Pj)^2 \right)^{-\frac{1}{2}} - (Pj)^{-1} \right) \quad (3.19)$$

and

$$\beta_n := \sum_{j=1}^n \left( \left( \rho_2^2 + (x_3 + Pj)^2 \right)^{-\frac{1}{2}} - (Pj)^{-1} \right) \quad (3.20)$$

are Cauchy sequences. In particular, for a fixed  $\epsilon > 0$  there exist  $N_\alpha, N_\beta \in \mathbb{N}$  such that  $\forall m \geq N_\alpha$  and  $\forall n \geq N_\beta$ ,

$$|\alpha_m - \alpha_{m-1}| < \epsilon, \quad |\beta_n - \beta_{n-1}| < \epsilon. \quad (3.21)$$

For a real function  $f$ , define  $Q_f(\epsilon)$  to be the smallest  $N \in \mathbb{N}$  such that  $|f_N - f_{N-1}| < \epsilon$ . The smaller  $Q_f(\epsilon)$  is, the faster the series converges. For the above series, we have

$$Q_\alpha(\epsilon) \text{ is the smallest } N \in \mathbb{N} \text{ such that } \left\| \left( \rho_2^2 + (x_3 - PN)^2 \right)^{-\frac{1}{2}} - (PN)^{-1} \right\| < \epsilon \quad (3.22)$$

and

$$Q_\beta(\epsilon) \text{ is the smallest } N \in \mathbb{N} \text{ such that } \left\| \left( \rho_2^2 + (x_3 + PN)^2 \right)^{-\frac{1}{2}} - (PN)^{-1} \right\| < \epsilon. \quad (3.23)$$

For example, for  $P = 1$ ,  $\rho_2 = 1$  and  $x_3 = 0.5$  we have the following results:

- $Q_\alpha(10^{-5}) = 224 = Q_\beta(10^{-5})$ ,  $Q_{\alpha+\beta}(10^{-5}) = 37$ ;
- $Q_\alpha(10^{-8}) = 7071$ ,  $Q_\beta(10^{-8}) = 7072$ ,  $Q_{\alpha+\beta}(10^{-8}) = 369$ ;
- $Q_{\alpha+\beta}(10^{-10}) = 1710$ .

If  $P = 2\pi$ ,  $\rho_2 = 1$  and  $x_3 = \pi$  we have:

- $Q_\alpha(10^{-5}) = 90$ ;  $Q_\beta(10^{-5}) = 89$ ,  $Q_{\alpha+\beta}(10^{-5}) = 20$ ;
- $Q_\alpha(10^{-8}) = 2822$ ,  $Q_\beta(10^{-8}) = 2821$ ,  $Q_{\alpha+\beta}(10^{-8}) = 197$ ;
- $Q_{\alpha+\beta}(10^{-10}) = 912$ .

This data does suggest that approximating the infinite series by a finite one is feasible. In order to explore this further one can look at *how* the series converges.

### 3.2.3 Approximating the Infinite Series

We now study an approximation for the infinite series that will provide us with a sound approximation using a finite number of terms. We will discover that the rate of convergence is quadratic and will use this fact to obtain our approximation. Define

$$\alpha_j := (\rho_2^2 + (x_3 - Pj)^2)^{-\frac{1}{2}} - (Pj)^{-1} \quad (3.24)$$

and

$$\beta_j := (\rho_2^2 + (x_3 + Pj)^2)^{-\frac{1}{2}} - (Pj)^{-1}. \quad (3.25)$$

Note that

$$\alpha_j = (\rho_2^2 + (\tilde{x}_3 + Pj)^2)^{-\frac{1}{2}} - (Pj)^{-1} \quad (3.26)$$

for some  $\tilde{x}_3 \in \mathbb{R}$  (if  $x_3 \in [0, P)$  then  $\tilde{x}_3 = -x_3$ ) and, for small  $\rho_2$ ,

$$\begin{aligned} (\rho_2^2 + (x_3 + Pj)^2)^{-\frac{1}{2}} - (Pj)^{-1} &\leq (x_3 + Pj)^{-1} - (Pj)^{-1} \\ &= -x_3(Pj)^{-1}(x_3 + Pj)^{-1} \\ &\approx cj^{-2}, \end{aligned} \quad (3.27)$$

where  $c$  is a constant. Thus, we should expect quadratic convergence. If we plot the first few values of  $\alpha_j$  and  $\beta_j$ , say from  $j = 1$  to  $j = 10$ , we see that for sufficiently large  $N$  and  $M$ , both  $\alpha_j$  and  $\beta_j$  quickly settle down and do indeed appear to behave like  $j^{-2}$ . We therefore consider the following approximations:

$$\alpha_j \approx \alpha_{appx} := N^2 \alpha_N j^{-2} \quad \text{and} \quad \beta_j \approx \beta_{appx} := M^2 \beta_M j^{-2}, \quad (3.28)$$

where we would take  $N$  and  $M$  to be reasonably large (at least 1000, as in the diagram below).

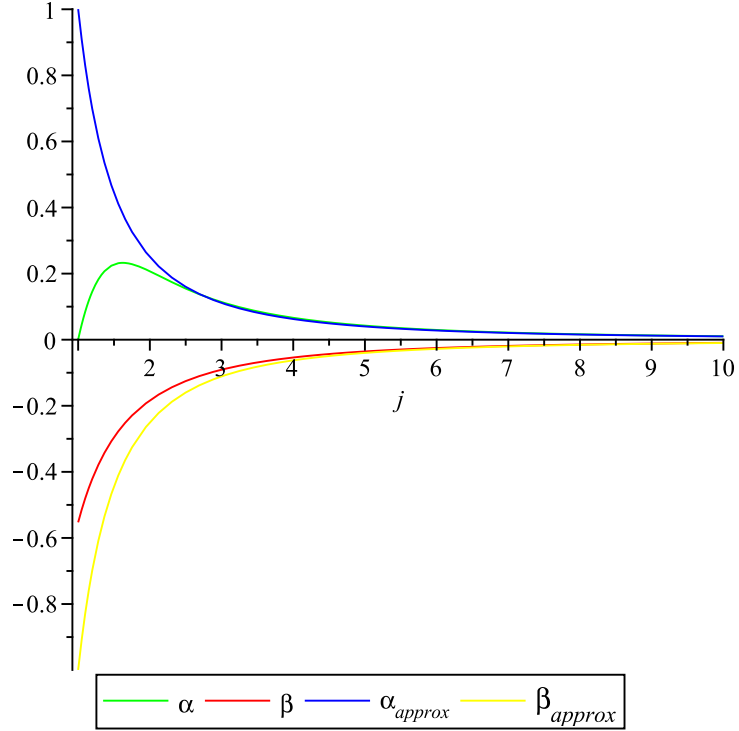


Figure 3.1: Quadratic convergence of the periodic instanton potential minus an infinite constant, using (3.24), (3.25), (3.28) with  $\rho_2 = 1 = x_3$

If we look at the error

$$\left| \alpha_j - N^2 \alpha_N j^{-2} \right| \quad (3.29)$$

over a range of values of  $\rho_2$  and  $x_3$ , we see that it is very small.

$\rho_2/x_3$	0	0.5	1
$\underline{P = 1}$			
0.5	$1.15 \times 10^{-12}$	$1.15 \times 10^{-12}$	$7.86 \times 10^{-12}$
1	$4.5 \times 10^{-12}$	$2.21 \times 10^{-12}$	$4.5 \times 10^{-12}$
3	$4.0499 \times 10^{-11}$	$3.827 \times 10^{-11}$	$3.162 \times 10^{-11}$
5	$1.12497 \times 10^{-10}$	$1.1038 \times 10^{-10}$	$1.0387 \times 10^{-10}$

$\rho_2/x_3$	0	0.5	1
$\underline{P = 2\pi}$			
0.5	$1.4 \times 10^{-14}$	$3.48 \times 10^{-13}$	$1.428 \times 10^{-12}$
1	$2 \times 10^{-14}$	$3.33 \times 10^{-13}$	$1.413 \times 10^{-12}$
3	$1.71 \times 10^{-13}$	$1.92 \times 10^{-13}$	$1.271 \times 10^{-12}$
5	$4.54 \times 10^{-13}$	$1.01 \times 10^{-13}$	$9.78 \times 10^{-13}$

We have taken  $N = 1000$  and  $j = 10000$  here and we note that the error decreases as we increase  $j$  and/or  $N$ . Similar results are obtained for

$$\left| \beta_j - M^2 \beta_M j^{-2} \right|, \quad (3.30)$$

for  $M = 1000$ . Consequently, we can use these approximations for  $\alpha$  and  $\beta$ , yielding

$$\begin{aligned} \alpha &= \sum_{j=1}^{\infty} \alpha_j = \sum_{j=1}^N \alpha_j + \sum_{j=N+1}^{\infty} \alpha_j \\ &\approx \sum_{j=1}^N \alpha_j + (N+1)^2 \alpha_{N+1} \sum_{j=N+1}^{\infty} j^{-2} \\ &= \sum_{j=1}^N \alpha_j + (N+1)^2 \alpha_{N+1} \left( \frac{\pi^2}{6} - \sum_{j=1}^N j^{-2} \right), \end{aligned} \quad (3.31)$$

and similarly

$$\beta \approx \sum_{j=1}^M \beta_j + (M+1)^2 \beta_{M+1} \left( \frac{\pi^2}{6} - \sum_{j=1}^M j^{-2} \right). \quad (3.32)$$

If we take  $N = M$  and look what happens to  $\phi(\rho_2, x_3)$ , we see that

$$\begin{aligned} \phi(\rho_2, x_3) &= (\rho_2^2 + x_3^2)^{-\frac{1}{2}} + \sum_{j=1}^{\infty} \alpha_j + \sum_{j=1}^{\infty} \beta_j \\ &\approx (\rho_2^2 + x_3^2)^{-\frac{1}{2}} + \sum_{j=1}^N (\alpha_j + \beta_j) + (N+1)^2 \left( \frac{\pi^2}{6} - \sum_{j=1}^N j^{-2} \right) (\alpha_{N+1} + \beta_{N+1}) \\ &= (\rho_2^2 + x_3^2)^{-\frac{1}{2}} + \sum_{j=1}^N (\alpha_j + \beta_j) + \kappa_N (\alpha_{N+1} + \beta_{N+1}), \end{aligned} \quad (3.33)$$

where

$$\kappa_N := (N+1)^2 \left( \frac{\pi^2}{6} - \sum_{j=1}^N j^{-2} \right). \quad (3.34)$$

In our examples with  $N = 1000$ , we have  $\kappa_{1000} = 1001.500167$ .

## Conclusion

From both of the above perspectives, we see that  $\phi(\rho_2, x_3)$  will converge fairly rapidly and that the errors involved in taking a finite approximation of the infinite series are very small. Therefore, in the examples that follow we can use graphical methods to see if the potential  $V$  has a zero. Furthermore, as  $V$  is periodic in  $x_3$ , it was sufficient to obtain a good approximation for  $V$  in the region  $x_3 \in [0, P)$ , which we have done.

### 3.3 Zero Regions

We will see that the periodic potential (3.5) is zero for various values of  $\rho_2$  and  $x_3$ . There are two types of ‘zero-region’ that can occur. We will use graphical methods to illustrate these and will use the Intermediate Value Theorem to prove that such regions always exist as specified. We will assume that  $V_c > 0$  but similar arguments apply if  $V_c < 0$ . Note that  $V$  is continuous for  $(\rho_2, x_3) \neq (0, Pj)$  for  $j \in \mathbb{Z}$ . We have two cases to consider:

#### 3.3.1 Case 1: Zero Strips

In this case,  $V(\rho_2, x_3)$  has the shape shown in the diagram below.

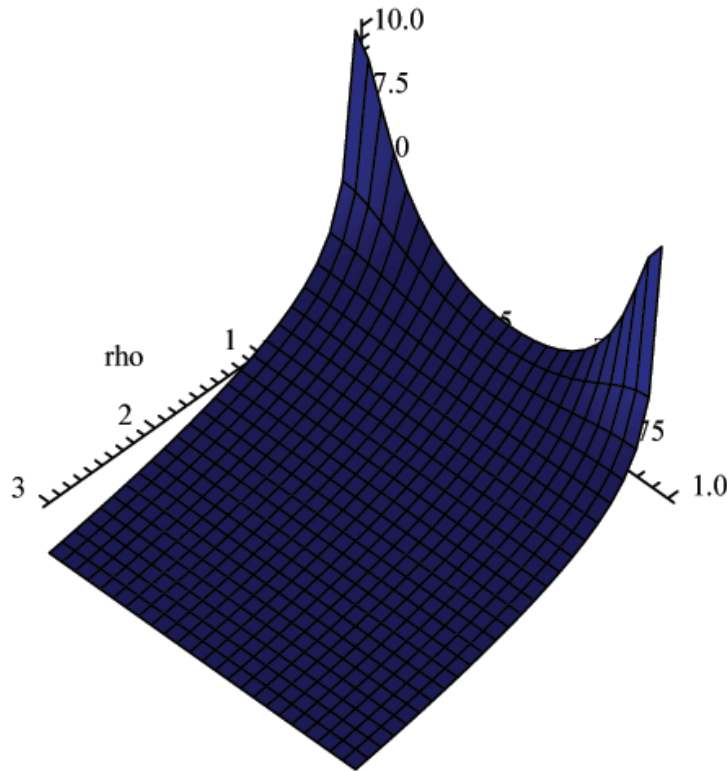


Figure 3.2: Periodic potential (3.5) with a zero strip

**Lemma 3.2** Let  $V$  be a periodic potential of the form (3.5) with  $V_c > 0$  and  $V(0, x_3) > 0$  for all  $x_3 \in [0, P)$ . Then for any  $x_3 \in [0, P)$  there exists a  $\rho_2 > 0$  such that  $V(\rho_2, x_3) = 0$ .

**Proof** Fix  $x_3 \in [0, P)$ . The choice of  $V_c$  is such that  $V(0, x_3) > 0$ . As  $V \rightarrow -c \ln \rho_2$  as  $\rho_2 \rightarrow \infty$  [62] where  $c$  is a constant, we know that for a sufficiently large choice of  $\rho_2$ , say



$\tilde{\rho}$ , we will have  $V(\tilde{\rho}, x_3) < 0$ . Consequently, by the Intermediate Value Theorem for each  $x_3$  there exists a  $\rho_0 \in (0, \tilde{\rho})$  such that  $V(\rho_0, x_3) = 0$ .

□

### 3.3.2 Case 2: Zero Curves

In this case,  $V(\rho_2, x_3)$  has the following shape, where  $V$  is the red surface and the blue surface is the  $(\rho_2, x_3, 0)$ -plane. The choice of  $V_c$  is such that there are zero regions around each of the points  $(0, Px_3)$  for  $x_3 \in \mathbb{Z}$ , as we can see in the diagram below. We restrict our attention to  $x_3 \in [0, P)$ .

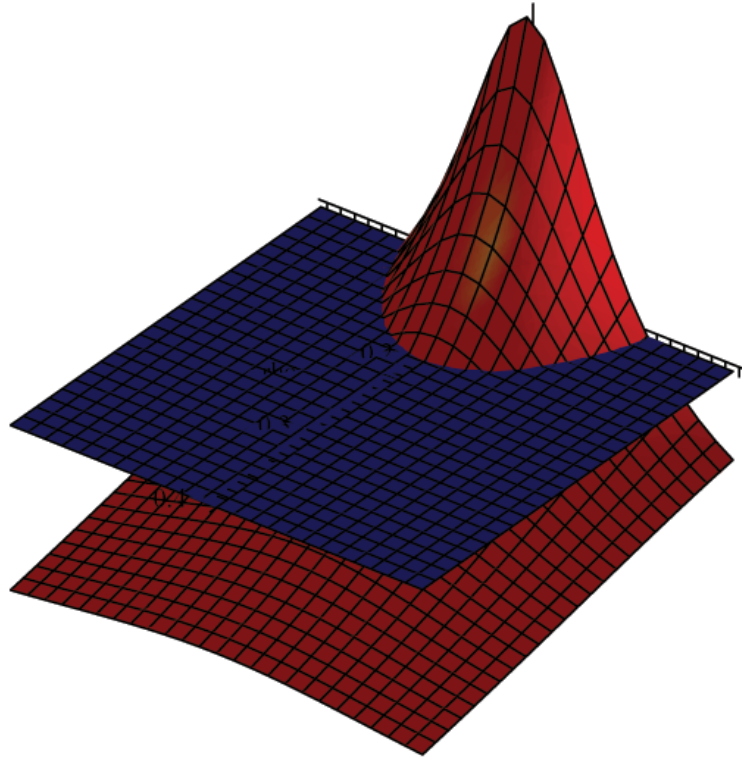


Figure 3.3: Periodic potential (3.5) with zero curves around each singularity

**Lemma 3.3** Let  $V$  be a periodic potential of the form (3.5) with  $V_c > 0$  and  $V(0, \frac{P}{2}) < 0$ . Define  $\rho_0$  to be the value of  $\rho_2$  such that  $V(\rho_0, 0) = 0$ . Then for any  $\rho_2 \in [0, \rho_0]$  there exists a  $x_3 \in (0, \frac{P}{2})$  such that  $V(\rho_2, x_3) = 0$ .

**Proof** We have the following derivative:

$$\begin{aligned}
 \left( \frac{\partial}{\partial x_3} \sum_{j=-n}^n (\rho_2^2 + (x_3 - Pj)^2)^{-\frac{1}{2}} \right) \Big|_{x_3=0} &= \left( \sum_{j=-n}^n (Pj - x_3) (\rho_2^2 + (x_3 - Pj)^2)^{-\frac{3}{2}} \right) \Big|_{x_3=0} \\
 &= \sum_{j=-n}^n (Pj) (\rho_2^2 + P^2 j^2)^{-\frac{3}{2}} = 0.
 \end{aligned} \tag{3.35}$$

for  $\rho_2 \neq 0$ . Thus, for a given value of  $\rho_2 > 0$ ,  $V(\rho_2, x_3)$  has a maximum point at  $x_3 = 0$ .

Now, note that for a fixed  $x_3$ ,  $V$  is clearly monotonically decreasing in  $\rho_2$ . If  $0 < \rho_2 \leq \rho_0$ , we can see that

- $V(\rho_2, 0) \geq 0$ , as  $V$  is monotonically decreasing from  $V(0, 0) \rightarrow \infty$  yet by assumption is not negative;
- $V(\rho_2, \frac{P}{2}) < 0$ , as  $V$  is monotonically decreasing and we assumed that  $V(0, \frac{P}{2}) < 0$ .

Consequently, for  $\rho_2 \in [0, \rho_0]$  there exists an  $x_3 \in (0, \frac{P}{2})$  such that  $V(\rho_2, x_3) = 0$ , by the Intermediate Value Theorem.

Conversely, if  $\rho_2 > \rho_0$  then  $V(\rho_2, 0) < 0$ . As this is the maximum point,  $V(\rho_2, x_3) < 0$  for  $x_3 \in [0, P)$ .

□

As  $V$  is periodic in  $x_3$ , we would expect to see identical zero-regions centred at  $(0, Px_3)$  for all  $x_3 \in \mathbb{Z}$ .

### 3.4 Convergence of $\vec{\omega} \cdot d\vec{r}$

In this section, we will demonstrate that  $\vec{\omega} \cdot d\vec{r}$  converges as we let the number of identical sources  $N$  go to infinity. If we have

$$V = V_0 + V_c \sum_{j=-N}^N |\vec{r} - \vec{r}_j|^{-1}, \tag{3.36}$$

then, as we require that

$$\vec{\nabla} V = \vec{\nabla} \times \vec{\omega}, \tag{3.37}$$

we have

$$\vec{\omega} \cdot d\vec{r} = V_c \sum_{j=-N}^N \frac{x_3 - x_{3j} (x_1 - x_{1j}) dx_2 - (x_2 - x_{2j}) dx_1}{|\vec{r} - \vec{r}_j| \left( (x_1 - x_{1j})^2 + (x_2 - x_{2j})^2 \right)^{\frac{1}{2}}}, \quad (3.38)$$

where  $\vec{r}_j = (x_{1j}, x_{2j}, x_{3j})$  denotes the position of the  $j$ -th instanton [63]. If the instantons are identical and periodically distributed along the  $x_3$ -axis with period  $P$ , then  $\vec{r}_j = (0, 0, Pj)$  for  $j \in \mathbb{Z}$  and so, in cylindrical coordinates

$$x_1 = \rho_2 \cos \theta, \quad x_2 = \rho_2 \sin \theta, \quad x_3 = x_3, \quad (3.39)$$

we have

$$\vec{\omega} \cdot d\vec{r} = V_c \sum_{j=-\infty}^{\infty} \frac{x_3 - Pj}{(\rho_2^2 + (x_3 - Pj)^2)^{\frac{1}{2}}} d\theta, \quad (3.40)$$

which for small  $\rho_2$  becomes

$$\vec{\omega} \cdot d\vec{r} \approx V_c \sum_{j=-\infty}^{\infty} \frac{x_3 - Pj}{|x_3 - Pj|} d\theta \approx V_c \left( \left\lfloor \frac{x_3}{P} \right\rfloor + \left\lceil \frac{x_3}{P} \right\rceil \right) d\theta. \quad (3.41)$$

This is illustrated in the diagram below. Similar results can be found for non-periodic distributions as we shall see in chapter six.

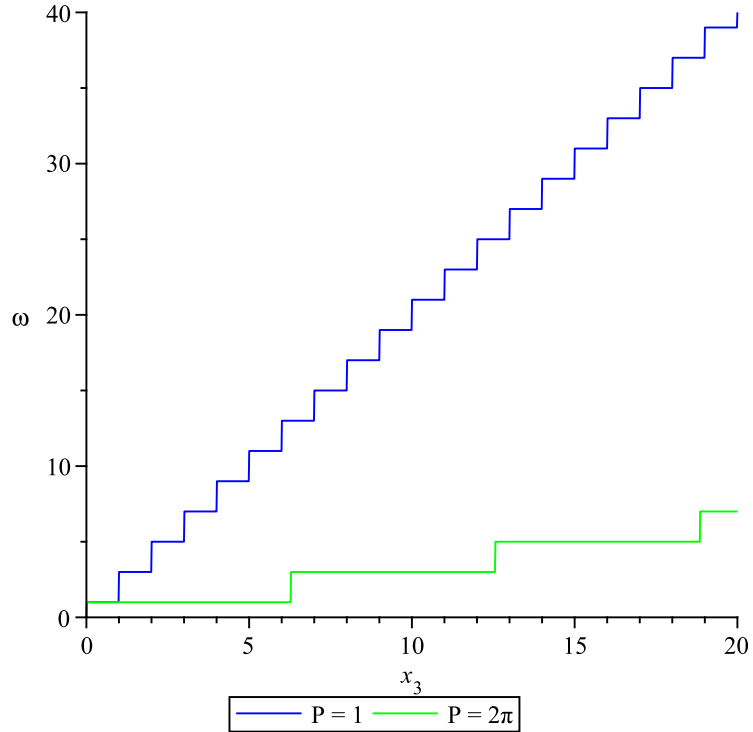


Figure 3.4: Variation in behaviour of  $\vec{\omega} \cdot d\vec{r}$  for small  $\rho_2$ , using (3.41) with  $V_c = 1$

### 3.5 Approximating $V$

An approximation for  $V$  is formulated that will allow us to compute the Riemann scalar with relative ease, which is necessary as even with the above result, the computation is still rather complex. The metric is taken to be that of the Kaluza-Klein monopole solution (2.35) which, as before, is formed by taking the Gibbons-Hawking metric (3.1) and adding a  $-dt^2$  term. Note that, as mentioned earlier, the curvature in the two cases will be the same. In order to study the spacetime at  $V = 0$ , we can approximate  $V$  for a given value of  $x_3$  by

$$V_{approx} = c - 2k \ln \rho_2. \quad (3.42)$$

Take  $V_0 := V_0(\rho_2)$  and for a given  $x_3$  define  $\rho_{x_3}$  to be the value of  $\rho_2$  such that  $V(\rho_{x_3}, x_3) = 0$ . We have

$$\frac{\partial V}{\partial \rho_2} = \frac{\partial V_0}{\partial \rho} - V_c \sum_{j=-\infty}^{\infty} \rho_2 (\rho_2^2 + (x_3 - Pj)^2)^{-\frac{3}{2}}, \quad (3.43)$$

which must equal

$$\frac{\partial V_{approx}}{\partial \rho_2} = -\frac{2k}{\rho_2} \quad (3.44)$$

for  $\rho_2 = \rho_{x_3}$ . Thus, we have

$$k = -\frac{\rho_{x_3}}{2} \left. \frac{\partial V}{\partial \rho_2} \right|_{\rho_{x_3}} ; \quad c = -\rho_{x_3} \ln(\rho_{x_3}) \left. \frac{\partial V}{\partial \rho_2} \right|_{\rho_{x_3}}. \quad (3.45)$$

This yields

$$\vec{\omega} = (0, 0, -2k\theta), \quad (3.46)$$

where  $\theta = \arg(x_1 + ix_2)$ . The metric then becomes

$$ds^2 = -dt^2 + V dx_1^2 + V dx_2^2 + (V + 4k^2\theta^2 V^{-1}) dx_3^2 - 4k\theta V^{-1} dx_3 d\tau + V^{-1} d\tau^2. \quad (3.47)$$

If we compute the scalar  $R_{\mu\nu\rho\sigma} R^{\mu\nu\rho\sigma}$  we get

$$[R]^2 = \frac{32k^2(V^2 + 6k(2k - V))}{V^6 \rho_2^4}. \quad (3.48)$$

When  $V = 0$ , we see the above tends to infinity, indicating the presence of a singularity at  $V = 0$ . We therefore need to ensure two conditions are satisfied to have a singularity:

- The potential  $V$  must have a point at which it equals zero;
- $V$  must be able to be reasonably approximated by  $V_{approx} = c - 2k \ln \rho_2$  at that point.

## 3.6 Exterior and Interior Spacetimes

Many of the spacetimes we will encounter will have singularities that occur when the potential is zero and can be approximated in the above manner. The following argument demonstrates that such singularities are naked and is the simplest such argument in this work. We will adapt the method developed here in other contexts later on.

### 3.6.1 The Exterior Spacetime

Here, the metric is the Kaluza-Klein metric (2.35). The following results will therefore apply to the Kaluza-Klein vortex case and the Gibbons-Hawking gravitational instanton of Sanchez (as we can simply add a  $-dt^2$  term). Consider radial geodesics, taking

$$x_1 = x(s), t = t(s), x_2 = x_3 = \tau = 0. \quad (3.49)$$

The metric becomes

$$ds^2 = -dt^2 + V^{-1}(x)(\omega_x dx)^2 + V(x)dx^2, \quad (3.50)$$

as  $V$  is positive and the metric is therefore Lorentzian. The corresponding Lagrangian is

$$\mathcal{L} = -\dot{t}^2 + V^{-1}(x)(\omega_x \dot{x})^2 + V(x)\dot{x}^2 \quad (3.51)$$

and the geodesics are given by the Euler-Lagrange equations

$$\frac{d}{ds} \left( \frac{\partial \mathcal{L}}{\partial \dot{q}_i} \right) - \frac{\partial \mathcal{L}}{\partial q_i} = 0, \quad (3.52)$$

yielding

$$\frac{d}{ds}(-2\dot{t}) = 0; \quad \frac{d}{ds} (2\dot{x}(V^{-1}\omega_x^2 + V)) - \omega_x^2 \dot{x}^2 \frac{d}{dx}(V^{-1}) - \dot{x}^2 \frac{d}{dx}(V) = 0. \quad (3.53)$$

We then have  $t = \alpha s$  where  $\alpha$  is some positive constant. If we again use our approximation  $V_{appx} = c - 2k \ln x$  for  $V$ ,  $\omega_x = 0$  and thus we have

$$\{-1, 0, 1\} = \mathcal{L} = -\alpha^2 + V(x)\dot{x}^2 \quad (3.54)$$

for spacelike, null and timelike geodesics respectively. If we look at the null case, we have

$$\dot{x}^2 = \frac{\alpha^2}{V} \quad \Rightarrow \quad x = \pm \int \frac{\alpha}{\sqrt{V}} ds \quad (3.55)$$

and

$$t = \alpha s = \pm \int_{x_0}^{x_1} \sqrt{V} dx, \quad (3.56)$$

where  $x_0 = e^{\frac{c}{2k}}$  is the point where  $V_{appx}$  is zero and hence where the singularity lies, and  $x_1$  is far away from  $x_0$ . We take the positive values of  $x$  and  $t$  for outgoing geodesics and the negative values for incoming geodesics. If, in both cases,  $t$  is finite, it means that a photon can reach a large distance away from the singularity in a finite time for a finite value of the parameter  $s$  and hence the singularity is naked. For the approximation used above, we have

$$t = \pm \int_{x_0}^{x_1} \sqrt{c - 2k \ln x} dx, \quad (3.57)$$

which is finite for large values of  $x_1$ .

### 3.6.2 The Interior Spacetime

If we think about the interior spacetime, the metric becomes

$$ds^2 = dt^2 + V^{-1}(x)(\omega_x dx)^2 + V(x)dx^2, \quad (3.58)$$

as we require that the metric is Lorentzian and  $V < 0$ . The corresponding Lagrangian is

$$\mathcal{L} = \dot{t}^2 + V^{-1}(x)(\omega_x \dot{x})^2 + V(x)\dot{x}^2, \quad (3.59)$$

and the geodesics are given by

$$\frac{d}{ds}(2\dot{t}) = 0; \quad \frac{d}{ds}(2\dot{x}(V^{-1}\omega_x^2 + V)) - \omega_x^2 \dot{x}^2 \frac{d}{dx}(V^{-1}) + \dot{x}^2 \frac{d}{dx}(V) = 0. \quad (3.60)$$

As before, we have  $t = \beta s$  where  $\beta$  is some positive constant. Approximating  $V$  by  $V_{appx}$  gives  $\omega_x = 0$  and thus we have

$$\{-1, 0, 1\} = \mathcal{L} = \beta^2 + V(x)\dot{x}^2 \quad (3.61)$$

for spacelike, null and timelike geodesics respectively. If we look at the null case once again and use  $V_{appx} = c - 2k \ln x < 0$ , we have

$$\dot{x}^2 = \frac{-\beta^2}{V} \quad \Rightarrow \quad x = \pm \int \frac{\beta}{\sqrt{-V}} ds, \quad (3.62)$$

and

$$t = \pm \int_{x_1}^{x_0} \sqrt{-(c - 2k \ln x)} dx, \quad (3.63)$$

which is finite for large values of  $x_1$ . These results mean that photons can move towards or out from the singularity.

### 3.7 Higher-Dimensional Case

Consider the  $D$ -dimensional potential

$$V = 1 + \sum_{j=-\infty}^{\infty} \frac{m_j}{|\vec{r} - \vec{r}_j|^{D-2}}, \quad (3.64)$$

where  $\vec{r} = (x_1, \dots, x_D)$ . Suppose that the point sources in this case are identical and periodically distributed along the  $x_D$ -axis with period  $P$ , yielding

$$V = 1 + \sum_{j=-\infty}^{\infty} m (\rho_{D-1}^2 + (x_D - Pj)^2)^{(1-\frac{D}{2})}. \quad (3.65)$$

We will demonstrate that this sum also is convergent for all  $D \geq 4$ .

**Theorem 3.4**      The potential (3.65) converges for  $D \geq 4$ .

**Proof**      We first note that as  $V$  is periodic in  $x_D$  with period  $P$ , we can assume in what follows that  $x_D \in [0, P)$ . If  $x_D = 0$ , we have

$$V = 1 + m\rho_{D-1}^{(2-D)} + 2m \sum_{j=1}^{\infty} (\rho_{D-1}^2 + P^2j^2)^{(1-\frac{D}{2})}. \quad (3.66)$$

If  $x_D \in (0, P)$ , the situation is slightly more complicated and we have

$$\begin{aligned} V &= 1 + m (\rho_{D-1}^2 + x_D^2)^{(1-\frac{D}{2})} + m (\rho_{D-1}^2 + (P - x_D)^2)^{(1-\frac{D}{2})} \\ &\quad + m \sum_{j=1}^{\infty} (\rho_{D-1}^2 + (x_D + Pj)^2)^{(1-\frac{D}{2})} \\ &\quad + m \sum_{j=1}^{\infty} (\rho_{D-1}^2 + ((P - x_D) + Pj)^2)^{(1-\frac{D}{2})}. \end{aligned} \quad (3.67)$$

Having written the potential in this form, we now note that

$$c_1 + (c_2 + Pj)^2 \geq (Pj)^2 \quad \forall j \in \mathbb{N}, \quad (3.68)$$

where  $c_1, c_2 \geq 0$  are constants. We therefore have

$$\begin{aligned}\sum_{j=1}^{\infty} (c_1 + (c_2 + Pj)^2)^{(1-\frac{D}{2})} &\leq P^{(2-D)} \sum_{j=1}^{\infty} (j^2)^{(1-\frac{D}{2})} \\ &\leq P^{(2-D)} \sum_{j=1}^{\infty} j^{-2} \\ &= \frac{\pi^2}{6} P^{(2-D)},\end{aligned}\tag{3.69}$$

for  $D \geq 4$ . Therefore,  $V$  converges for  $D \geq 4$  by the comparison test.

□



## Chapter 4

# Examples of Periodic Solutions

### 4.1 Introduction

In this chapter, we will investigate various scenarios where instanton or monopole solutions in different contexts can be written in Gibbons-Hawking form and have an infinite centre periodic potential. When  $V$  becomes zero, curvature singularities arise that can be reached in finite time. The structure of the chapter is as follows:

**Kaluza-Klein vortices:** We study the work of Onemli and Tekin [53] on Kaluza-Klein vortices. We use the machinery developed previously to demonstrate the presence of naked singular regions where  $V$  is zero. We then consider a subsequent paper of theirs [54] which looks at Kaluza-Klein monopoles in AdS spacetime and show that these solutions are also singular when  $V$  is zero.

**Dirichlet instantons:** We next study the work of Ooguri and Vafa [55] as they apply D-instanton corrections to a Calabi-Yau manifold. The modified potential they use is of Gibbons-Hawking form and has singular regions when  $V$  is zero. We demonstrate this but note that it does not make sense to talk about the singularity being naked as we are not working in the gravitational context. We then examine the paper of Ketov, Santillan and Zorin [42] as they try to develop this work to consider multiple hypermultiplets as opposed to the single hypermultiplet solution of Ooguri and Vafa. We show that, as  $V$  is zero at some points, their analysis is incorrect.

**Gravitational calorons:** Finally in this chapter we examine the work of Sanchez [58]. She constructs several gravitational instanton solutions, including one in Gibbons-Hawking form and a Euclidean Schwarzschild solution, each of which contains errors.

## 4.2 Kaluza-Klein Vortices and AdS Spacetime

We study the work of Onemli and Tekin, firstly on Kaluza-Klein vortices [53] and secondly on Kaluza-Klein monopoles in AdS spacetime [54]. We show that in all these cases, when the hyperkähler potential is zero, there is a curvature singularity.

### 4.2.1 Kaluza-Klein Vortices

A Kaluza-Klein monopole in M-theory is a spacetime of the form

$$ds^2 = -dt^2 + \sum_{j=5}^{10} dx_j dx_j + V^{-1}(d\tau + \vec{\omega} \cdot d\vec{r})^2 + V d\vec{r}^2. \quad (4.1)$$

Here, we have a  $D6$  brane where  $(\tau, \vec{r} = \{x_1, x_2, x_3\})$  are the spatial transverse coordinates and  $\{x_5, \dots, x_{10}\}$  are the longitudinal coordinates. We look for vortex type soliton solutions to pure gravity.

If we suppress the longitudinal coordinates, we are left with  $4 + 1$  dimensional gravity and hence the metric is the usual Kaluza-Klein metric (2.35), with the relationship between  $V$  and  $\vec{\omega}$  given by (3.2), and  $\tau$  is taken to have a period of  $16\pi m$ .

Searching for smooth solutions of the above for periodic monopoles located at the points  $(x_3 = x_{3a}, \rho_2 = \rho_{2a})$  in  $\mathbb{R}^2 \times \mathbb{S}^1$  and  $x_3 \in \mathbb{S}^1$  yields

$$V(\rho_2, x_3) = V_0 + V_c \sum_a m_a \left( \sum_{j=-\infty}^{\infty} \left( (\rho_2 - \rho_{2a})^2 + (x_3 - x_{3a} - 2\pi j)^2 \right)^{-\frac{1}{2}} - 2 \sum_{j=1}^{\infty} (2\pi j)^{-1} \right), \quad (4.2)$$

where the period  $P$  is  $2\pi$ . We concentrate on a single periodic monopole with position  $(x_{3a} = 0, \rho_{2a} = 0)$  and  $m = 1$ . We then have the periodic potential (3.5) with

$$V_0 = 1 + \frac{\ln 4\pi - C}{2\pi}, \quad V_c = -\frac{1}{2}, \quad (4.3)$$

where  $C$  is Catalan's constant. The diagram below illustrates the behaviour of  $V$ , using our earlier numerical approximation.

If we restrict our attention to  $x_3 \in [0, 2\pi)$ , we have a zero region around the origin and can see that for all  $\rho_2 \leq \rho_0$  there exists  $x_3 \in (0, \pi)$  such that  $V(\rho_2, x_3) = 0$ . Here,  $\rho_0 = 0.3976375$ .

We can therefore (by thinking about the symmetry of the potential) expect to see these zero regions along the  $x_3$ -axis, centred around  $(0, 2\pi n)$  for  $n \in \mathbb{Z}$ . Calculating the values of  $\rho_2$  and  $x_3$  such that  $V$  is zero gives

$\rho_2$	$x_3$	$\rho_2$	$x_3$
0	0.3976	0.25	0.3095
0.05	0.3948	0.3	0.2612
0.1	0.3852	0.35	0.1888
0.15	0.3686	0.375	0.1324
0.2	0.3439	0.3976	0

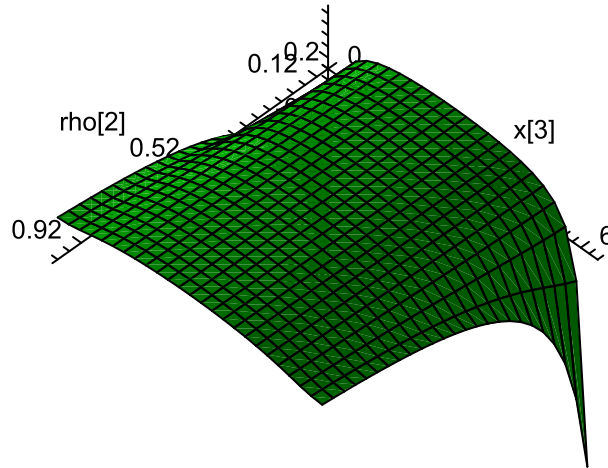


Figure 4.1: The potential  $V$  for a Kaluza-Klein vortex using (4.2) with  $\rho_2 \in [0, 1]$ ,  $x_3 \in [0, 2\pi]$

which taking account of the symmetry of the potential yields the zero-region shown in the diagram below, which can be approximated by a semi-circle of radius  $\rho_0$  centred at the origin. In order to see that these zero-regions are singular regions, we need to show that we can obtain a logarithmic approximation to  $V$  as before at the required points. Following the approach we developed earlier, we have

$$\frac{\partial V}{\partial \rho_2} = \frac{1}{2} \sum_{j=-\infty}^{\infty} \rho_2 \left( \rho_2^2 + (x_3 - 2\pi j)^2 \right)^{-\frac{3}{2}}, \quad (4.4)$$

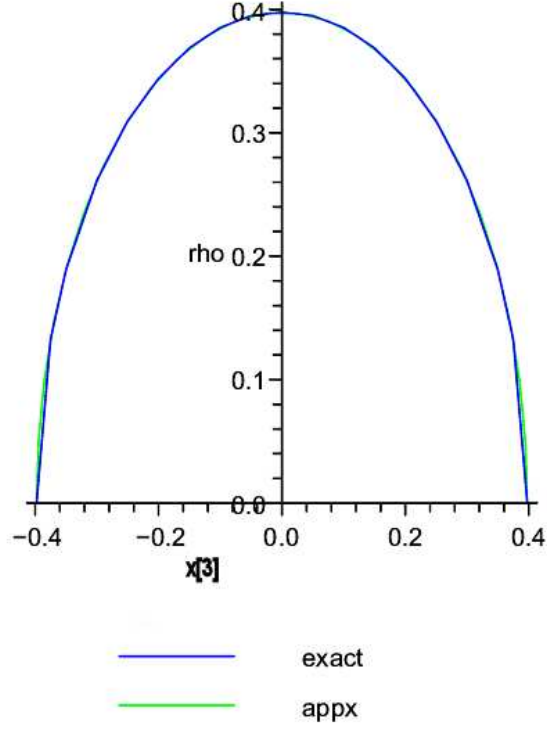


Figure 4.2: The zero region around the origin for a Kaluza-Klein vortex, using values from table in section 4.2.1

and so for  $x_3 \in [-\rho_0, \rho_0]$ , we have

$$V_{appx} = c - 2k \ln \rho_2, \quad (4.5)$$

where

$$k = \frac{x_3^2 - \rho_0^2}{4} \sum_{j=-\infty}^{\infty} (\rho_0^2 - 2\pi j x_3 + 4\pi^2 j^2)^{-\frac{3}{2}} \quad (4.6)$$

and

$$c = \frac{x_3^2 - \rho_0^2}{4} \ln(\rho_0^2 - x_3^2) \sum_{j=-\infty}^{\infty} (\rho_0^2 - 2\pi j x_3 + 4\pi^2 j^2)^{-\frac{3}{2}}. \quad (4.7)$$

One therefore finds that, for instance,

$$V_{appx} = 1.161 + 1.258 \ln \rho_2 \quad (4.8)$$

is a good approximation to  $V$  near the zero when  $x_3 = 0$ , as we can see in the diagram below.

Thus, there is a singular region when  $V$  is zero.

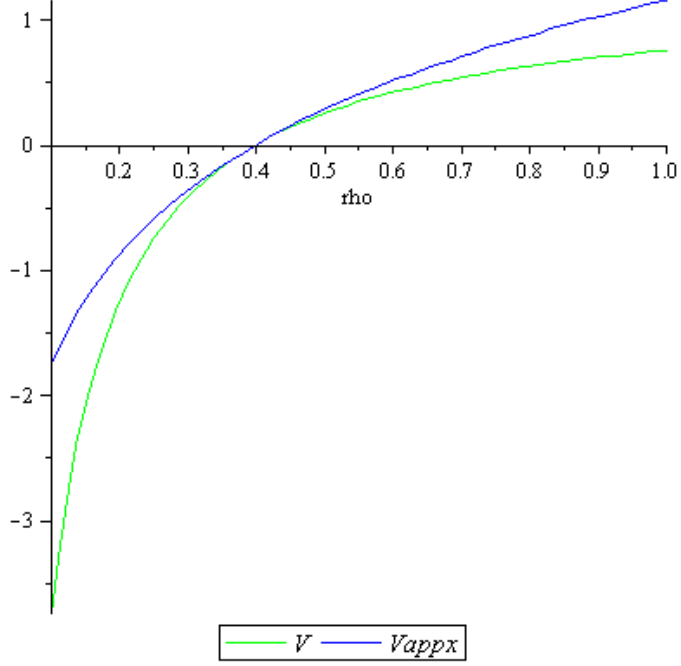


Figure 4.3: Comparison of  $V$  (from (4.2)) and  $V_{appx}$  (from (4.8)) near the zero for the Kaluza-Klein vortex solution for  $\rho := \rho_2 \in [0, 1]$

### 4.2.2 Kaluza-Klein Monopoles in AdS Spacetime

In a subsequent paper, [54], Onemli and Tekin consider analogues of the flat space Kaluza-Klein monopoles considered above, in locally anti-de Sitter (AdS) spaces for  $(D \geq 5) + 1$  dimensions. They prove that there is no five-dimensional static Kaluza-Klein monopole in AdS spacetime that smoothly reduces to the flat space solution as the cosmological constant goes to zero and thus construct a 6D AdS monopole. In the latter part of the paper they relax the requirement of having a negative cosmological constant and consider other monopoles.

#### 6D Braneworld

They construct a 6D braneworld with the following metric:

$$ds^2 = \exp(-2L|x_5|) (-dt^2 + ds_{GH}^2) + dx_5^2, \quad (4.9)$$

where  $L \in \mathbb{R}$  is defined in relation to the Ricci curvature by

$$R_{\alpha\beta} = 5L^2 g_{\alpha\beta}. \quad (4.10)$$

In order for the solution to be smooth, the  $x_4$  direction must be compact. However, the  $x_5$  direction has an infinite extent, with  $x_5 = -\infty$  as the boundary of the space and  $x_5 = +\infty$

as the Killing horizon. One can construct Kaluza-Klein monopole solutions as before, taking  $V$  to be the periodic potential given by (3.5) where  $V_0$  and  $V_c$  are constants. We take

$$V_{appx} = c - 2k \ln \rho_2 \quad (4.11)$$

and so  $\omega_{x_1} = \omega_{x_2} = 0$ ,  $\omega_{x_3} = -2k\theta$ . Calculating the Riemann curvature scalar gives, as  $V \rightarrow 0$ ,

$$[R]^2 \rightarrow 4 (96k^4 \exp(4L|x_5|) + \kappa_1 L^4) \rho_2^{-4} V^{-6}, \quad (4.12)$$

where  $\kappa_1$  is a constant. This tends to infinity as  $V \rightarrow 0$ , indicating the presence of a singularity when  $V$  is zero.

One could generalise this to  $D$  dimensions by adding more flat directions, ensuring they are multiplied by  $\exp(-2L|x_5|)$ . We could also have multiple Kaluza-Klein vortices as in [53] by modifying the potential as before (see (4.2)).

### Time-Dependent 5D Euclidian Solution

Another spacetime that is proposed in the paper [54] gives a 5D Euclidean solution which is not static. The metric is

$$ds^2 = dt^2 + \exp(-2Lt) ds_{GH}^2. \quad (4.13)$$

Calculating the Riemann curvature gives, as  $V \rightarrow 0$ ,

$$[R]^2 \rightarrow 8 (48k^4 \exp(4Lt) + \kappa_2 VL^4) \rho_2^{-4} V^{-6} \rightarrow \infty, \quad (4.14)$$

where  $\kappa_2$  is a constant. We have a singularity when  $V$  is zero once again.

## 4.3 Dirichlet Instantons

We consider the papers of Ooguri and Vafa [55] and Ketov, Santillan and Zorin [42]. Ooguri and Vafa studied D-instanton quantum corrections to the quantum moduli space metric of a matter hypermultiplet for the Calabi-Yau-compactified type IIA superstrings near a conifold singularity. The solution is the hyperkähler metric in the limit of flat four-dimensional spacetime, i.e. when  $N = 2$  supergravity decouples and the universal hypermultiplet is switched off, while five-brane instantons are suppressed. Ketov et al studied D-instanton quantum corrections to the moduli space metric of several identical hypermultiplets.

### 4.3.1 A Single Hypermultiplet

We examine the construction of a single hypermultiplet by Ooguri and Vafa. Here, the spacetime is given by the Gibbons-Hawking metric (3.1) with  $\tau$  and  $x_3$  being periodic with period 1. The potential  $V$  must satisfy the following conditions:

$$\vec{\nabla} \times \vec{\omega} = \vec{\nabla} V, \quad (4.15)$$

$$\vec{\nabla}^2 V = \left( \frac{\partial^2}{\partial x_1^2} + \frac{\partial^2}{\partial x_2^2} + \frac{\partial^2}{\partial x_3^2} \right) V = 0, \text{ almost everywhere,} \quad (4.16)$$

$$V \rightarrow V_{classical} = -\frac{1}{2\pi} \ln \rho_2 + \text{const as } \rho_2 \rightarrow \infty, \quad (4.17)$$

and there are no two charges at the same point. The unique potential satisfying these conditions is given by

$$V(\rho_2, x_3) = \frac{1}{4\pi} \left( \sum_{j=-\infty}^{\infty} (\rho_2^2 + (x_3 - j)^2)^{-\frac{1}{2}} - 2 \sum_{j=1}^{\infty} j^{-1} \right) + \text{const.} \quad (4.18)$$

This function has a zero region, as we can see in the diagram below. We can then make use of the approximation

$$V_{approx} = c - 2k \ln \rho_2. \quad (4.19)$$

We therefore have

$$\frac{\partial V}{\partial \rho_2} = -(4\pi)^{-1} \sum_{j=-\infty}^{\infty} \rho_2 (\rho_2^2 + (x_3 - j)^2)^{-\frac{3}{2}}, \quad (4.20)$$

and consequently find that

$$k = \frac{1.261129}{8\pi} \sum_{j=-\infty}^{\infty} \left( 1.261129 + (x_3 - j)^2 \right)^{-\frac{3}{2}} \quad (4.21)$$

and

$$c = \frac{1.261129 \ln 1.123}{4\pi} \sum_{j=-\infty}^{\infty} \left( 1.261129 + (x_3 - j)^2 \right)^{-\frac{3}{2}}, \quad (4.22)$$

as this region is practically a straight line given approximately by  $\rho_2 = 1.123$  and thus  $V$  can be approximated by, for instance when  $x_3 = 0$ ,

$$V_{approx} = 0.0196 - 0.1601 \ln \rho_2. \quad (4.23)$$

By the same argument as before, there is a singular region when  $V$  is zero.

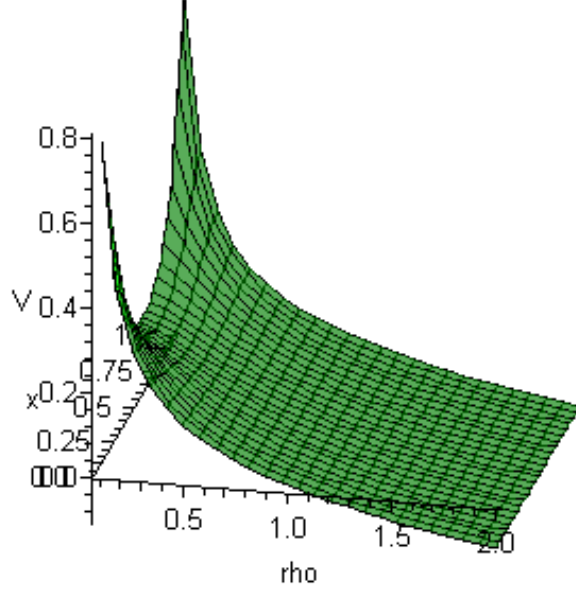


Figure 4.4: The potential  $V$  for a single matter hypermultiplet using (4.18) with  $\rho_2 \in [0, 2]$ ,  $x_3 \in [0, 1]$

### 4.3.2 Multiple Hypermultiplets

Here, we consider the case of  $n > 1$  hypermultiplets, and the argument of Ketov et al [42]. Each hypermultiplet has its own set of coordinates  $(x_1^i, x_2^i, x_3^i, t_i)$  and there are  $n$  sets of these. Thus, the total  $4n$ -dimensional hyper-Kähler space has coordinates  $(x_1^i, x_2^i, x_3^i, t_i)$ ,  $i = 1, \dots, n$ . The hyper-Kähler metric (also known as the Pedersen-Poon (PP) metric) takes the following form:

$$ds^2 = U_{ij} dx^i \cdot dx^j + U^{ij} (dt_i + A_i)(dt_j + A_j). \quad (4.24)$$

This is a generalisation of the Gibbons-Hawking metric and contains  $n$  commuting triholomorphic isometries. In order to reflect the  $n$  isometries, all of the metric components are supposed to be independent from all the  $t_i$ . We have  $U^{ij} = U_{ij}^{-1}$ , so we require that  $U$  be everywhere invertible. The  $A_i$  terms relate to the gauge fields  $A$ . The PP metric is completely specified by its (real) PP potential  $F(x, w, \bar{w})$ , which in turn depends on  $3n$  variables:

$$x^j = x_3^j, \quad w^j = \frac{x_1^j + ix_2^j}{2}, \quad \bar{w}^j = \frac{x_1^j - ix_2^j}{2}, \quad (4.25)$$

where

$$U_{ij} = F_{x^i x^j}, \quad F_{x^i x^j} + F_{w^i \bar{w}^j} = 0. \quad (4.26)$$



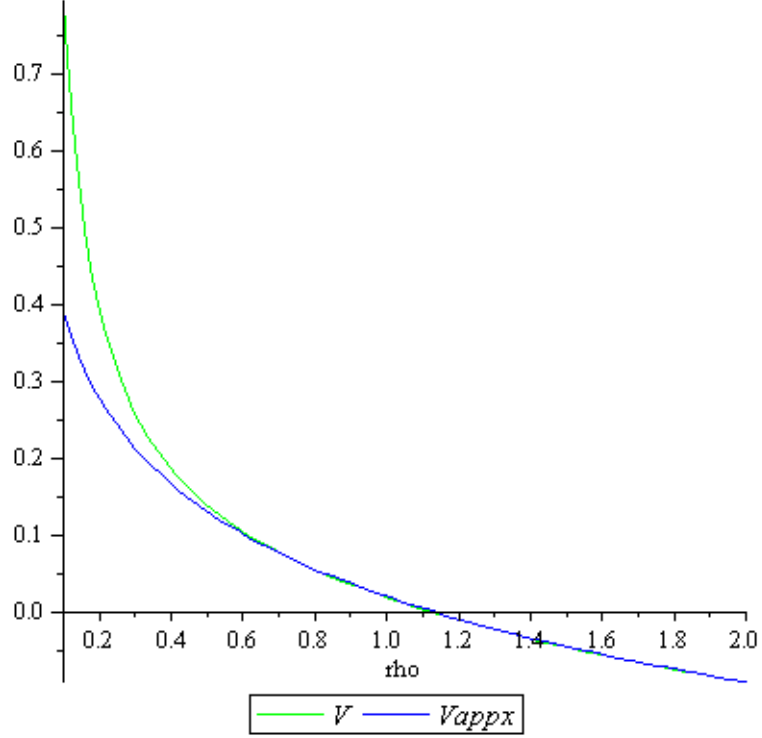


Figure 4.5: Comparison of  $V$  (from (4.18)) and  $V_{appx}$  (from (4.23)) near the zero for the Ooguri-Vafa solution with  $\rho := \rho_2 \in [0, 1]$

We now make the following assumptions:

- All the  $x_i$  are periodic with period 1;
- The classical potential  $F$  near a CY conifold singularity should have a logarithmic behaviour and be independent from all  $x_i$  (when all  $w_i \rightarrow \infty$ );
- The classical singularity of the metric should be removable;
- The metric is symmetric under the permutation group of  $n$  sets of hypermultiplet coordinates  $(x^j, w^j, \bar{w}^j)$ , where  $j = 1, 2, \dots, n$ .

For the case of  $n = 2$ , where we are considering two identical hypermultiplets, we can define a new function  $F(x, w)$  in terms of the Ooguri-Vafa solution by

$$F_{xx} = -F_{w\bar{w}} = V_{OV}(x, w). \tag{4.27}$$

The first multiplet has coordinates  $(x_1^1, x_2^1, x_3^1, t_1)$  and the second has coordinates  $(x_1^2, x_2^2, x_3^2, t_2)$ . There exists a trivial solution given by the PP potential

$$F_0 = c_0(F(x_1, w_1) + F(x_2, w_2)) \quad (4.28)$$

where  $c_0$  is a real constant. Here,

$$x_1 = x_3^1, w_1 = \frac{x_1^1 + ix_2^1}{2} \text{ and } x_2 = x_3^2, w_2 = \frac{x_1^2 + ix_2^2}{2}. \quad (4.29)$$

We have a particular non-trivial solution given by

$$F_{PS} = c_+ F(x_1 + x_2, w_1 + w_2) + c_- F(x_1 - x_2, w_1 - w_2) \quad (4.30)$$

with  $c_+$  and  $c_-$  constants, yielding the general solution

$$F = F_0 + F_{PS}. \quad (4.31)$$

Using the second partial derivatives of the above, we obtain the following components for the matrix  $U$ :

$$U_{11} = \frac{1}{4\pi}(A_+ + A_- + A_0^1), \quad U_{22} = \frac{1}{4\pi}(A_+ + A_- + A_0^2), \quad U_{12} = U_{21} = \frac{1}{4\pi}(A_+ + A_-), \quad (4.32)$$

where

$$A_+ = c_+ \left( \sum_{j=-\infty}^{\infty} ((x_1 + x_2 - j)^2 + |w_1 + w_2|^2)^{-\frac{1}{2}} - 2 \sum_{j=1}^{\infty} j^{-1} \right), \quad (4.33)$$

$$A_- = c_- \left( \sum_{j=-\infty}^{\infty} ((x_1 - x_2 - j)^2 + |w_1 - w_2|^2)^{-\frac{1}{2}} - 2 \sum_{j=1}^{\infty} j^{-1} \right), \quad (4.34)$$

$$A_0^1 = c_0 \left( \sum_{j=-\infty}^{\infty} ((x_1 - j)^2 + |w_1|^2)^{-\frac{1}{2}} - 2 \sum_{j=1}^{\infty} j^{-1} \right), \quad (4.35)$$

and

$$A_0^2 = c_0 \left( \sum_{j=-\infty}^{\infty} ((x_2 - j)^2 + |w_2|^2)^{-\frac{1}{2}} - 2 \sum_{j=1}^{\infty} j^{-1} \right), \quad (4.36)$$

with the modulus parameter  $\lambda$  set to 1. A short calculation shows that the determinant of  $U$  is given by

$$\det U = \frac{1}{16\pi^2}(A_+ + A_-)(A_0^1 + A_0^2) + A_0^1 A_0^2. \quad (4.37)$$

Now we know that for every  $(x_1, x_2)$  there exist  $(w_1, w_2)$  such that  $A_0^1 = 0$  and  $A_0^2 = 0$  respectively. Consequently, there exist points where  $\det U = 0$ , which contradicts our assumption that  $U$  is everywhere invertible.

## 4.4 Gravitational Calorons

We now consider the paper of Sanchez [58]. There are two solutions we will investigate here: the Gibbons-Hawking caloron solution and the Euclidean Schwarzschild solution.

### 4.4.1 The Gibbons-Hawking Caloron Solution

A **caloron** is a finite temperature instanton. Caloron solutions satisfy

$$V(\vec{r}, \tau) = V(\vec{r}, \tau + \beta), \quad \beta = (k_B T)^{-1} \quad (4.38)$$

where  $T$  is the temperature of the theory. We consider caloron solutions obtained from the known multi-centre metrics of Taub-NUT type [17]. After eliminating horizon and string type singularities, the spacetime is given by the Gibbons-Hawking metric (3.1). Here, the potential is given by

$$V(\rho_2, x_3) = 1 + \frac{8m}{\beta} \sum_{j=1}^{\infty} K_0 \left( \frac{2\pi j \rho_2}{\beta} \right) \cos \left( \frac{2\pi j x_3}{\beta} \right). \quad (4.39)$$

Here,  $\beta$  is the period of  $V$ , so  $V(\rho_2, x_3) = V(\rho_2, x_3 + \beta)$ , and  $K_0$  is the modified Bessel function of the second kind. When we take  $m = 1 = \beta$ , this is equivalent to

$$V(\rho_2, x_3) = 1 + 4\gamma + 4 \ln \left( \frac{\rho_2}{2} \right) + 2 \left( \sum_{j=-\infty}^{\infty} (\rho_2^2 + (x_3 - j)^2)^{-\frac{1}{2}} - 2 \sum_{j=1}^{\infty} j^{-1} \right). \quad (4.40)$$

The function has a zero, as we can see from the diagram below. Now, for which values of  $x_3 \in [0, 1]$  does there exist a  $\rho_2 > 0$  such that  $V$  is zero?

**Lemma 4.1**      The potential  $V$  given in (4.40) does not have a zero for  $x_3 = 0$  (and thus for all  $x_3 \in \mathbb{Z}$ ).

**Proof**      If  $x_3 = 0$ , we have

$$V(\rho_2, x_3) = 1 + 4\gamma + 4 \ln \left( \frac{\rho_2}{2} \right) + 2\phi(\rho_2, 0), \quad (4.41)$$

where

$$\phi(\rho_2, x_3) := \sum_{j=-\infty}^{\infty} (\rho_2^2 + (x_3 - j)^2)^{-\frac{1}{2}} - 2 \sum_{j=1}^{\infty} j^{-1}. \quad (4.42)$$

We can see that

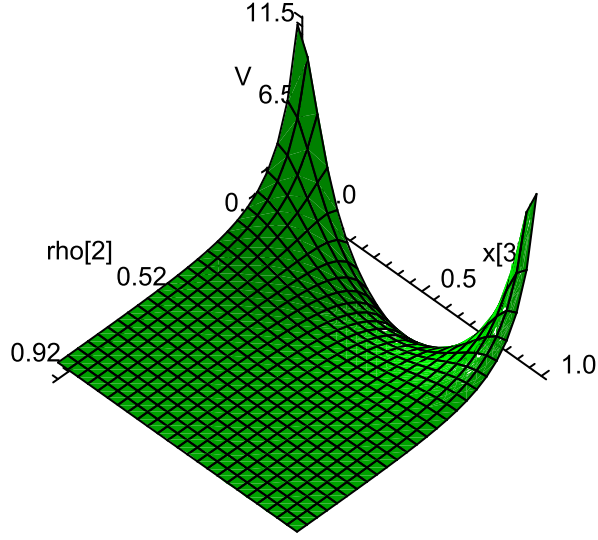


Figure 4.6: Potential for the Gibbons-Hawking caloron solution, using (4.40) with  $\rho_2 \in [0, 1]$  and  $x_3 \in [0, 1]$

$$\phi(\rho, 0) = \rho_2^{-1} + 2 \sum_{j=1}^{\infty} (\rho_2^2 + j^2)^{-\frac{1}{2}} - 2 \sum_{j=1}^{\infty} j^{-1}. \quad (4.43)$$

Differentiating  $V$  gives us

$$\frac{dV}{d\rho_2} = 4 \left( \rho_2^{-1} - 2\rho_2^{-2} - \sum_{j=1}^{\infty} \rho_2 (\rho_2^2 + j^2)^{-\frac{3}{2}} \right) < 0 \quad (4.44)$$

for all  $\rho_2 > 0$ , meaning that  $V$  decreases as  $\rho_2$  increases. We show that when  $\rho_2$  is zero,  $V$  goes to infinity and when  $\rho_2$  goes to infinity,  $V$  takes a finite and positive value, meaning that it can never be zero.

Now,  $\phi(\rho_2, 0) \rightarrow \rho_2^{-1}$  as  $\rho_2 \rightarrow 0$ , which means that

$$V(\rho_2, 0) \rightarrow 1 + 4\gamma + 4 \ln \left( \frac{\rho_2}{2} \right) + 2\rho_2^{-1}. \quad (4.45)$$

As  $\ln \rho_2$  shrinks more slowly than  $\rho_2^{-1}$  grows,

$$\frac{dV}{d\rho_2} = \frac{2}{\rho_2^2} (2\rho_2 - 1) < 0 \text{ for } \rho_2 < \frac{1}{2}, \quad (4.46)$$

we have  $V \rightarrow \infty$  as  $\rho_2 \rightarrow 0$ . For large values of  $\rho_2$ , we have  $\frac{dV}{d\rho_2} \rightarrow 0$  as  $\rho_2 \rightarrow \infty$ , as

$$\sum_{j=1}^{\infty} \rho_2 (\rho_2^2 + j^2)^{-\frac{3}{2}} \approx \rho_2^{-1}. \quad (4.47)$$

Thus,  $V \rightarrow 1 + 4\gamma$ , and  $V$  does not have a zero if  $x_3 \in \mathbb{Z}$ .

□

**Lemma 4.2**      The potential  $V$  given in (4.40) has a zero for  $x_3 \in (0, 1)$  (and thus for all  $x_3 \in \mathbb{R}/\mathbb{Z}$ ).

**Proof**      Let  $\epsilon > 0$  and fix a  $x_3 \in (0, 1)$ . As

$$\lim_{\rho_2 \rightarrow 0} (\rho_2^2 + (x_3 - j)^2)^{-\frac{1}{2}} = |x_3 - j|^{-1}, \quad (4.48)$$

there exists  $\rho_a > 0$  such that, for  $\rho_2 < \rho_a$ ,

$$\left| \sum_{j=-\infty}^{\infty} (\rho_2^2 + (x_3 - j)^2)^{-\frac{1}{2}} - \sum_{j=-\infty}^{\infty} |x_3 - j|^{-1} \right| < \epsilon. \quad (4.49)$$

We have

$$0 = 1 + 4\gamma + 4 \ln \left( \frac{\rho_2}{2} \right) + 2\phi(0, x_3) - 2\epsilon < 0 \quad (4.50)$$

for  $\rho_2 < \rho_b$ , where

$$\rho_b = 2 \exp \left( \frac{-(1 + 4\gamma + 2\phi(0, x_3) - 2\epsilon)}{4} \right) > 0. \quad (4.51)$$

Let  $\rho_0 := \min\{\rho_a, \rho_b\}$ . Then for  $\rho_2 \in (0, \rho_0)$ , we have  $V < 0$ . By a similar argument to that in Lemma 4.1, we have  $V \rightarrow 1 + 4\gamma$  as  $\rho_2 \rightarrow \infty$  for a fixed  $x_3 \in (0, 1)$ . Thus, for a large value of  $\rho_2$ , say  $\rho_c$ , we have  $V > 0$ . Fixing  $\alpha_{x_3} \in (0, \rho_0)$  we can apply the Intermediate Value Theorem and thus conclude that for each  $x_3 \in (0, 1)$  there exists some  $\rho_{x_3} \in (\alpha_{x_3}, \rho_c)$  such that  $V$  is zero.

□

If use the approximation near  $\rho_2 = 0$ ,  $\phi(\rho_2, x_3) \approx \phi(0, x_3)$ , we obtain

$$\rho_2 \approx 2 \exp \left( \kappa - \frac{\phi(0, x_3)}{2} \right), \quad (4.52)$$

where  $\kappa := -\frac{1}{4} - \gamma$ . We have, remembering that  $V$  is symmetrical about  $x_3 = 0.5$ , the following data about the zero region:

$x_3$	$\rho_2$	$x_3$	$\rho_2$	$x_3$	$\rho_2$
0.1	0.005822	0.225	0.1143	0.35	0.2470
0.125	0.01625	0.25	0.1462	0.375	0.2600
0.15	0.03280	0.275	0.1764	0.4	0.2721
0.175	0.05537	0.3	0.2031	0.45	0.2875
0.2	0.08313	0.325	0.2258	0.5	0.2924

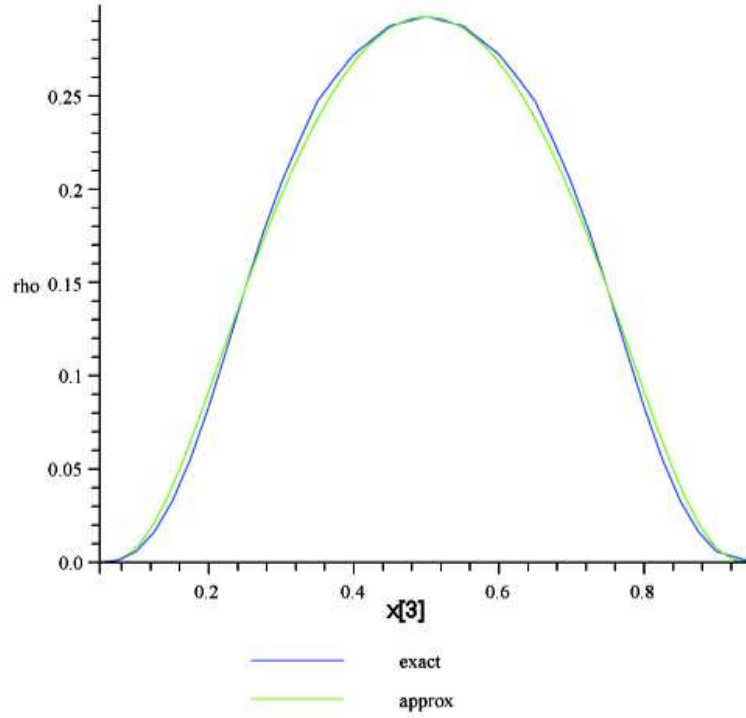


Figure 4.7: Approximation of the zero region for the gravitational caloron solution (4.40) using (4.53) and table in section 4.4.1

It turns out that a good approximation to this curve is

$$\rho_2 = \frac{0.2924}{\exp\left(\kappa - \frac{\phi(0,0.5)}{2}\right)} \exp\left(\kappa - \frac{\phi(0, x_3)}{2}\right) \approx 1.3374 \exp\left(\kappa - \frac{\phi(0, x_3)}{2}\right). \quad (4.53)$$

Thus, for each  $x_3 \in (0, 1)$  (and in every other interval  $(n, n+1)$  where  $n \in \mathbb{Z}$ ) there exists a  $\rho_2 > 0$  such that  $V$  is zero.

Finally, we need to find a logarithmic approximation to  $V$ . As usual,

$$V_{appx} = c - 2k \ln \rho_2. \quad (4.54)$$

We have

$$\frac{\partial V}{\partial \rho_2} = \frac{4}{\rho_2} - 2 \sum_{j=-\infty}^{\infty} \frac{\rho_2}{4\pi (\rho_2^2 + (x_3 - j)^2)^{\frac{3}{2}}}. \quad (4.55)$$

Using the approximation above we get, for instance at  $x_3 = 0.5$ ,

$$V_{approx} = 2.588 + 2.104 \ln \rho_2, \quad (4.56)$$

which is shown in the graph. Therefore, for all  $x_3 \in (0, 1)$  (and thus in  $\mathbb{R}/\mathbb{Z}$ ), we can see that there is a curvature singularity.

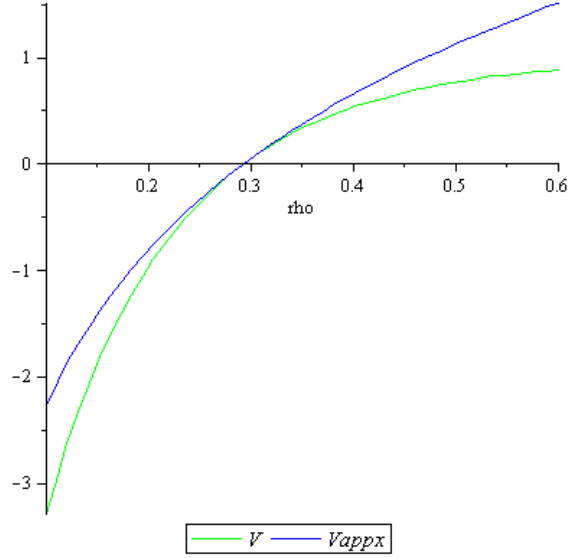


Figure 4.8: Comparison of  $V$  (from (4.40)) and  $V_{approx}$  (from (4.56)) near the zero for the Sanchez solution for  $x_3 = 0.5$  and  $\rho := \rho_2$

#### 4.4.2 Euclidean Schwarzschild Solution

Sanchez produces another solution in addition to the caloron solution discussed earlier, with the same self-dual potential  $V$  as in (4.40), satisfying  $V(\rho_2, x_4) = V(\rho_2, x_4 + \beta)$ , where  $\rho_2 := \sqrt{x_2^2 + x_3^2}$ . Here, we take  $\beta = 1$ . This solution is obtained from the superposition of  $n$  Schwarzschild sources with equal masses  $m$  in the Euclidean regime. The metric in this case is

$$ds^2 = V dx_1^2 + (V^{-1} - 1) dr^2 + d\vec{r}^2, \quad (4.57)$$

where  $\vec{r} = (x_2, x_3, x_4)$  and  $r = \sqrt{x_2^2 + x_3^2 + x_4^2}$ . Obviously,  $r$  is one of the spherical coordinates  $(r, \theta, \phi)$ . If we apply this coordinate transformation throughout, setting

$$\begin{aligned}
 x_2 &= r \sin \theta \cos \phi, \\
 x_3 &= r \sin \theta \sin \phi, \\
 x_4 &= r \cos \theta,
 \end{aligned} \tag{4.58}$$

we see that  $\rho_2 = r \sin \theta$  and  $x_4 = r \cos \theta$ , so

$$V \rightarrow V(r, \theta) = 1 + 4\gamma + 4 \ln \left( \frac{r \sin \theta}{2} \right) + 2 \left( \sum_{j=-\infty}^{\infty} (r^2 + j^2 - 2jr \cos \theta)^{-\frac{1}{2}} - 2 \sum_{j=1}^{\infty} j^{-1} \right), \tag{4.59}$$

and the metric becomes

$$ds^2 = V dx_1^2 + V^{-1} dr^2 + r^2 d\theta^2 + r^2 \sin^2 \theta d\phi^2. \tag{4.60}$$

Calculating the Riemann curvature scalar gives

$$[R]^2 = \frac{D(r, \theta) + 8V^2(\partial_\theta V)^2 \cot^2 \theta}{4V^4 r^4}, \tag{4.61}$$

where

$$\begin{aligned}
 D(r, \theta) &:= 11(\partial_\theta V)^4 - 16V \partial_{\theta\theta} V (\partial_\theta V)^2 \\
 &\quad + 4V^2 (2r \partial_r V (\partial_\theta V)^2 + 2(\partial_{\theta\theta} V)^2 - r^2 \partial_{rr} V (\partial_\theta V)^2) \\
 &\quad + 4V^3 (-4r \partial_\theta V \partial_{r\theta} V + 4(\partial_\theta V)^2 + 2r^2 (\partial_{\theta r} V)^2) \\
 &\quad + 4V^4 (4r^2 (\partial_r V)^2 + r^4 (\partial_{rr} V)^2 + 4) - 32V^5 + 16V^6.
 \end{aligned} \tag{4.62}$$

Now, there remains the question of whether  $D$  cancels out the factor of  $V^4$  in the denominator. We therefore need to look at the following expression, of terms where  $V^4$  is not automatically cancelled out:

$$\begin{aligned}
 K(r, \theta) &:= 2.75(\partial_\theta V)^4 V^{-4} - 4V^{-3} \partial_{\theta\theta} V (\partial_\theta V)^2 \\
 &\quad + V^{-2} (2r \partial_r V (\partial_\theta V)^2 + 2(\partial_{\theta\theta} V)^2 - r^2 \partial_{rr} V (\partial_\theta V)^2) \\
 &\quad + V^{-1} (-4r \partial_\theta V \partial_{r\theta} V + 4(\partial_\theta V)^2 + 2r^2 (\partial_{\theta r} V)^2).
 \end{aligned} \tag{4.63}$$



### Outlining the Theory

As  $V$  is periodic in  $x_4$  with period 1, we will consider values of  $x_4$  in  $[0, 1)$ , and begin by fixing  $x_4 \in (0, 1)$ , taking  $\phi$  to be as in (4.42). Near  $\rho_2 = 0$ , we have the following Taylor expansion:

$$\phi(\rho_2, x_4) = \sum_{n=0}^{\infty} \frac{\phi(\rho_2, x_4)^{(n)} \Big|_{\rho_2=0}}{n!} \rho_2^n. \quad (4.64)$$

Firstly, for  $\rho_2 = 0$ , we have

$$\begin{aligned} \phi(0, x_4) &= \sum_{j=-\infty}^{\infty} |x_4 - j|^{-1} - 2 \sum_{j=1}^{\infty} j^{-1} \\ &= x_4^{-1} + \sum_{j=1}^{\infty} |x_4 - j|^{-1} + \sum_{j=1}^{\infty} (x_4 + j)^{-1} - 2 \sum_{j=1}^{\infty} j^{-1} \\ &= x_4^{-1} (1 - x_4)^{-1} + \sum_{j=1}^{\infty} (x_4 + j)^{-1} + \sum_{j=1}^{\infty} ((1 - x_4) + j)^{-1} - 2 \sum_{j=1}^{\infty} j^{-1} \\ &= x_4^{-1} (1 - x_4)^{-1} - \sum_{j=1}^{\infty} x_4 j^{-1} (x_4 + j)^{-1} - \sum_{j=1}^{\infty} (1 - x_4) j^{-1} ((1 - x_4) + j)^{-1}. \end{aligned} \quad (4.65)$$

Next, we calculate the  $n$ th derivative of  $\phi(\rho_2, x_4)$  with respect to  $\rho_2$ . By inspection we can see that, for  $n \in \mathbb{N}$ ,

$$\phi(\rho_2, x_4)^{(n)} = \sum_{j=-\infty}^{\infty} \sum_{k=1}^{\lfloor n/2 \rfloor + 1} (-1)^{\lfloor \frac{n}{2} \rfloor + k - r} c_n^k \sigma^{n+2k-r} \rho_2^{2k-1-r}, \quad (4.66)$$

where  $\sigma := (\rho_2^2 + (x_4 - j)^2)^{-\frac{1}{2}}$  and  $r = 0$  if  $n$  is odd,  $r = 1$  if  $n$  is even. The  $c_n^k$  are real constants.

Thus, when  $n$  is odd,  $\phi^{(n)}(\rho_2, x_4) \Big|_{\rho_2=0} = 0$ . For  $n$  is even,

$$\phi(0, x_4)^{(n)} = \sum_{j=-\infty}^{\infty} (-1)^{\frac{n}{2}} c_n \sigma^{n+1} \Big|_{\rho_2=0} = (-1)^{\frac{n}{2}} c_n \sum_{j=-\infty}^{\infty} |x_4 - j|^{-(n+1)}, \quad (4.67)$$

where the  $c_n := c_n^1$  are given by

$$c_n = \prod_{l=1}^{\frac{n}{2}} (2l - 1)^2. \quad (4.68)$$

Thus, for  $n$  even,

$$\phi(0, x_4)^{(n)} = (-1)^{\frac{n}{2}} c_n \left( x_4^{-(n+1)} (1-x_4)^{-(n+1)} + \sum_{j=1}^{\infty} (x_4 + j)^{-(n+1)} + \sum_{j=1}^{\infty} ((1-x_4) + j)^{-(n+1)} \right). \quad (4.69)$$

Finally we can use the change of coordinates  $\rho_2 = r \sin \theta$  to calculate  $K$ . We calculate the relevant derivatives, taking  $V$  to be

$$V(r, \theta) = 1 + 4\gamma + 4 \ln \left( \frac{r \sin \theta}{2} \right) + 2 \sum_{j=0}^{\infty} C_{2j} r^{2j} \sin^{2j} \theta, \quad (4.70)$$

where the  $C_j$  are the constants in the Taylor series. We have

$$\partial_{\theta} V = 4 \cot \theta + 4 \sum_{j=1}^{\infty} j C_{2j} r^{2j} \sin^{2j-1} \theta \cos \theta, \quad (4.71)$$

$$\partial_{\theta\theta} V = -4 \sin^{-2} \theta + 4 \sum_{j=1}^{\infty} j C_{2j} r^{2j} \left( (2j-1) \sin^{2j-2} \theta \cos^2 \theta - \sin^{2j} \theta \right), \quad (4.72)$$

$$\partial_r V = 4r^{-1} + 4 \sum_{j=1}^{\infty} j C_{2j} r^{2j-1} \sin^{2j} \theta, \quad (4.73)$$

$$\partial_{rr} V = -4r^{-2} + 4 \sum_{j=1}^{\infty} j(2j-1) C_{2j} r^{2j-2} \sin^{2j} \theta, \quad (4.74)$$

$$\partial_{r\theta} V = 8 \sum_{j=1}^{\infty} j^2 C_{2j} r^{2j-1} \sin^{2j-1} \theta \cos \theta. \quad (4.75)$$

We can see from these results that the factors of  $V$  in  $K$  do not get cancelled out, so whenever  $V$  has a zero, there is a singularity. As the potential  $V$  is the same as the first of the Sanchez solutions, we know that there are bell-shaped zero-regions all along the  $x_4$ -axis. Therefore there are singular regions in this Euclidean Schwarzschild space.

#### A Specific Example: $x_4 = 0.5$

We examine a specific case, that of  $x_4 = 0.5$ . Firstly, we construct a Taylor series following the method above. We have

$$\phi\left(0, \frac{1}{2}\right) = 4 - \sum_{j=1}^{\infty} j^{-1} \left(\frac{1}{2} + j\right)^{-1} = \ln 16 \approx 2.773, \quad (4.76)$$

and

$$\phi\left(0, \frac{1}{2}\right)^{(n)} = (-1)^{\frac{n}{2}} \left( \prod_{l=1}^{\frac{n}{2}} (2l-1)^2 \right) \left( 2^{n+2} + 2 \sum_{j=1}^{\infty} \left(\frac{1}{2} + j\right)^{-(n+1)} \right). \quad (4.77)$$

Therefore near  $\rho_2 = 0$  we have

$$\begin{aligned}
 \phi\left(\rho_2, \frac{1}{2}\right) &\approx 2.773 - 8.414\rho_2^2 + 24.109\rho_2^4 - 80.038\rho_2^6 \\
 &+ 280.014\rho_2^8 - 1008.006\rho_2^{10} + 3696.00\rho_2^{12} - 13728.001\rho_2^{14} \\
 &+ 51480\rho_2^{16} - 194480\rho_2^{18} + 739024\rho_2^{20} - 2822172.8\rho_2^{22} \\
 &+ 10816624\rho_2^{24} - 41602399.98\rho_2^{26}.
 \end{aligned}
 \tag{4.78}$$

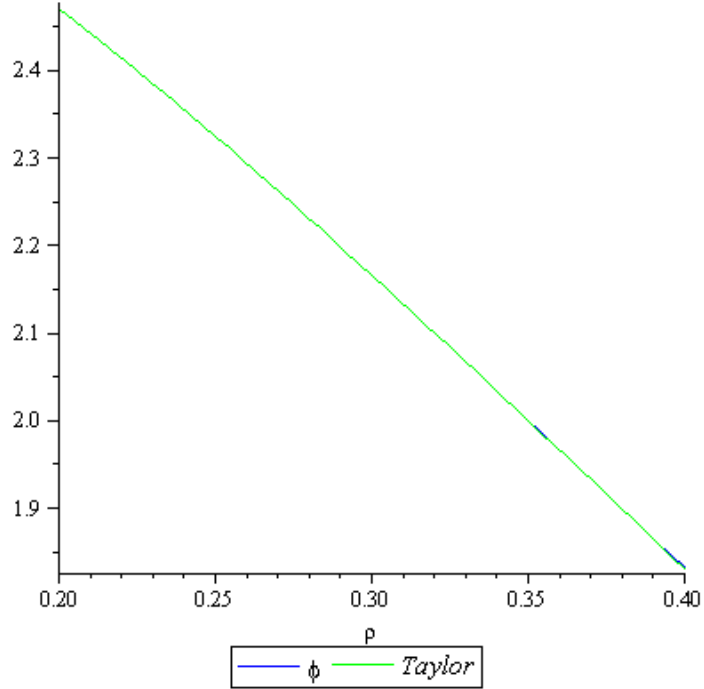


Figure 4.9: Comparison of the exact sum (from (4.42)) with the Taylor series approximation (from (4.78)) for an example of the Euclidean Schwarzschild metric with  $x_4 = 0.5$

Next, we calculate the factor  $K(r, \theta)$ . For  $x_4 = 0.5$  and  $\rho_2 = 0.292481$ , we have  $r = 0.579262$  and  $\theta = 0.529288$ , giving

$$K(r, \theta) = 460.0965289V^{-4} + 795.0545068V^{-3} + 585.3928936V^{-2} + 146.2501545V^{-1}. \tag{4.79}$$

Thus, there is a curvature singularity, in contrast to the normal Schwarzschild configuration, for  $x_4 = 0.5$ .

**More Generally:**  $x_4 \in (0, 1)$

We can apply the same method for other vales of  $x_4$ . The following diagram illustrates a range of values of  $x_4$  such that  $V$  has a zero for some  $\rho_2$ . We have produced graphs of  $V$  for  $x_4 = \{0.1, 0.2, 0.3, 0.4, 0.5\}$ .

The red curve corresponds to  $x_4 = 0.1$ , the green to  $x_4 = 0.2$ , the yellow to  $x_4 = 0.3$ , the blue to  $x_4 = 0.4$  and the purple to  $x_4 = 0.5$ .

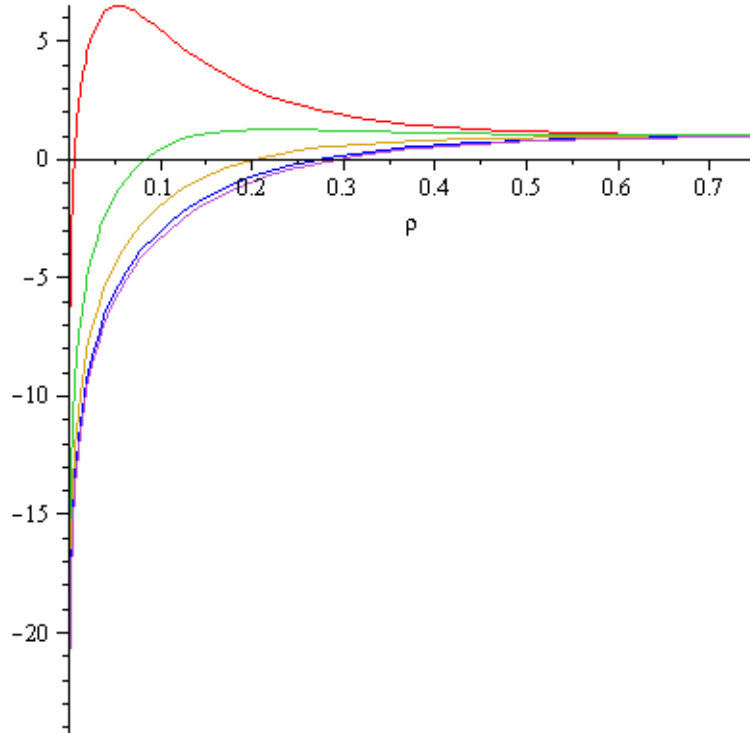


Figure 4.10: Snapshots of potential  $V$  for the Euclidean Schwarzschild metric, using (4.40) for various choices of  $x_4$

We calculate the factor  $K(r, \theta)$  and the results are illustrated in the table below:

$x_4$	$\rho_2$	$K(r, \theta)$
0.5	0.29248	$460.0965V^{-4} + 795.0545V^{-3} + 585.3929V^{-2} + 146.2502V^{-1}$
0.4	0.27207	$228.6159V^{-4} + 424.7961V^{-3} + 349.2504V^{-2} + 103.3927V^{-1}$
0.3	0.20307	$201.2258V^{-4} + 391.2047V^{-3} + 332.3595V^{-2} + 99.0038V^{-1}$
0.2	0.083133	$4205.0407V^{-4} + 4750.6242V^{-3} + 2235.8263V^{-2} + 344.7403V^{-1}$
0.1	0.00587192	$55248730.4V^{-4} + 21224023.57V^{-3} + 2856170.417V^{-2} + 18563.934V^{-1}$

Thus, we can see that for a range of different values of  $x_4$ , there is a curvature singularity.

Finally, we allow  $x_4$  to vary. Using the Taylor expansion again, we have, near  $(\rho_2, x_4) = (0, 0.5)$ ,

$$\phi(\rho_2, x_4) = \sum_{t=0}^{\infty} \sum_{n=0}^t \left( \frac{\phi^{(n,t-n)}(\rho_2, x_4)}{n!(t-n)!} \right) \rho_2^n (x_4 - 0.5)^{t-n}, \quad (4.80)$$

where

$$\phi^{(p,q)}(\rho_2, x_4) := \left( \frac{\partial^p}{\partial \rho_2^p} \frac{\partial^q}{\partial x_4^q} \phi(\rho_2, x_4) \right) \Big|_{\rho_2=0, x_4=0.5}. \quad (4.81)$$

Approximating this to the eighteenth order gives  $V_{approx}$ , which we compare with  $V$  in the diagram below. To check that the factors of  $V$  in  $K$  do not cancel out, we compute the derivatives of  $V$ , in spherical coordinates:

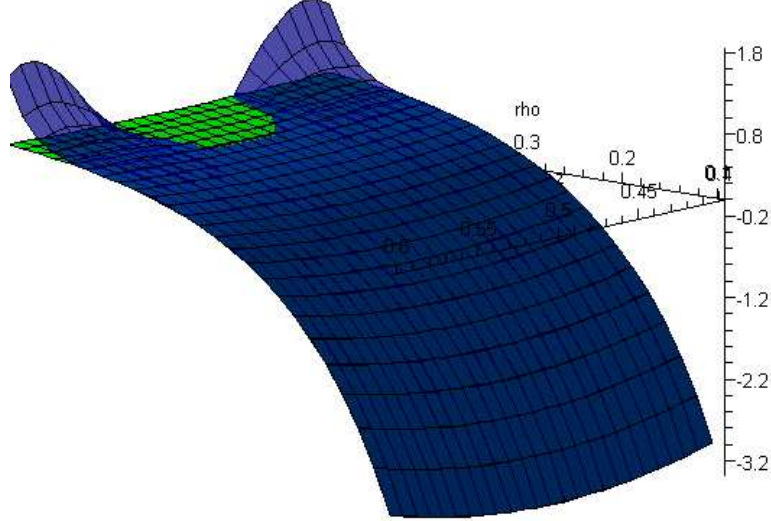


Figure 4.11: Comparison of two-variable Taylor series approximation around  $(\rho_2, x_4) = (0, 0.5)$  (from (4.80)) with exact potential (from (4.40)) for the Euclidean Schwarzschild metric

$$\partial_r V = 4r^{-1} + 2 \sum_{t=1}^{\infty} \sum_{n=0}^t \frac{(rt \cos \theta - 0.5n) r^n \sin^n \theta (r \cos \theta - 0.5)^{t-n}}{(r \cos \theta - 0.5) r}, \quad (4.82)$$

$$\partial_\theta V = 4 \cot \theta + 2 \sum_{t=1}^{\infty} \sum_{n=0}^t \frac{(rt \sin^2 \theta + 0.5n \cos \theta - nr) r^n \sin^n \theta (r \cos \theta - 0.5)^{t-n}}{(r \cos \theta - 0.5) \sin \theta}. \quad (4.83)$$

It is clear from these (and the even messier second derivatives!) that the factors do not vanish and thus there are curvature singularities where  $V$  is zero.

## Chapter 5

# Surveying the Landscape

### 5.1 Introduction

In the previous chapter, we studied periodic instantons in Gibbons-Hawking form. We therefore had the following metric:

$$\begin{aligned} ds_{GH}^2 &= V^{-1}(d\tau + \vec{\omega} \cdot d\vec{r})^2 + V d\vec{r}^2, \\ \vec{\nabla}V &= \vec{\nabla} \times \vec{\omega}. \end{aligned} \tag{5.1}$$

In cylindrical coordinates, the potential is given by

$$V = V_0 + V_c \sum_{j=-\infty}^{\infty} (\rho_2^2 + (x_3 - Pj)^2)^{-\frac{1}{2}}. \tag{5.2}$$

As already noted, this series does not converge. Various methods have been adopted in order to ensure the convergence of the series by different authors. In chapters three and four, the method employed was the subtracting of an infinite constant, yielding a potential given by

$$V = V_0 + V_c \left( \sum_{j=-\infty}^{\infty} (\rho_2^2 + (x_3 - Pj)^2)^{-\frac{1}{2}} - 2 \sum_{j=1}^{\infty} (Pj)^{-1} \right). \tag{5.3}$$

However, as has been demonstrated, when  $V$  is zero, curvature singularities arise. In this chapter, we will consider the implications of this in a range of contexts. As such, the structure of the chapter is as follows:

**Incompleteness of infinite constant solution:** We demonstrate an awareness of the incompleteness of the infinite constant solution in the literature. We firstly investigate the construction of the Atiyah-Hitchin [2] metric and note how it deviates from its asymptotic form, the Taub-NUT metric. We then explore the work of Cherkis and Kapustin [7] and the

ALG metrics they formulate, which behave in an analogous manner to the Atiyah-Hitchin metric. We see the parallels between this work on the two-monopole moduli space on  $\mathbb{R}^2 \times \mathbb{S}^1$  and the Ooguri-Vafa metric [55] and briefly look at the discussion of this incompleteness in the literature.

**Extensions and applications:** We consider three papers where the authors have tried to extend the infinite constant solution in different contexts. Firstly we study the paper of Gross and Wilson [28], who construct a new metric by stitching together twenty-four Ooguri-Vafa metrics, and note that they have failed to address the incompleteness of the said metric, which is carried into their new solution. Secondly, we investigate the work of Giribet and Santillan [26], who attempt to take four-dimensional hyperkähler metrics and extend them to seven-dimensional metrics with  $G_2$  holonomy using the Apostolov-Salamon Theorem, again resulting in incomplete solutions. Finally, we look at the work of Gibbons and Warnick [24] on extending solutions in flat space to solutions in hyperbolic spaces. Their solutions are parallel to the Atiyah-Hitchin solution, in the sense of deviating from their asymptotic forms.

**Olbers' and Seeliger's paradoxes:** The problem of the potential given by an infinite periodic array of instantons is a similar problem in its context to Olbers' and Seeliger's paradoxes. We therefore outline the nature of these two paradoxes, both being concerned with the consequences of postulating an infinite, eternal universe with an even distribution of matter (in particular of stars) within. We then note the parallel with our situation.

## 5.2 Incompleteness of the Infinite Constant Solution

In this section we consider the nature of the external and internal spaces of the Ooguri-Vafa (OV) [55] metric. We look at the Atiyah-Hitchin (AH) metric and how its asymptotic form deviates from the Taub-NUT metric. Next, we look at the construction of periodic strings of BPS monopoles in  $\mathbb{R}^2 \times \mathbb{S}^1$ , the reduced moduli space of which forms an ALG instanton. This deviates from its asymptotic form in the interior as well and has the same logarithmic behaviour as the external Ooguri-Vafa solution. We note how this has been alluded to in the literature.

### 5.2.1 The Two-Monopole Moduli Space on $\mathbb{R}^3$

The **two-monopole moduli space** takes the form

$$M = \mathbb{R}^3 \times \frac{\mathbb{S}^1 \times M_0}{\mathbb{Z}_2}, \quad (5.4)$$

where  $M_0$  is a four-dimensional manifold on which  $\text{SO}(3)$  acts (the AH metric) and the  $\mathbb{Z}_2$  is present as the monopoles cannot be distinguished. We will outline the construction of the Atiyah-Hitchin (AH) metric on this space, following references [2], [64], [20]. The metric on  $\mathbb{R}^3 \times \mathbb{S}^1$  is flat, being given by

$$ds^2 = 4(d\vec{r} \cdot d\vec{r} + d\chi^2), \quad (5.5)$$

where  $\chi \in \mathbb{S}^1$  with  $0 \leq \chi \leq 2\pi$  and  $\vec{r} = (x_1, x_2, x_3) \in \mathbb{R}^3$ .

The metric on  $M_0$  is independent of  $(\vec{r}, \chi)$ , is  $\text{SO}(3)$  symmetric, and is thus given by

$$ds^2 = f(r)^2 dr^2 + a(r)^2 \sigma_1^2 + b(r)^2 \sigma_2^2 + c(r)^2 \sigma_3^2, \quad (5.6)$$

where the metric functions obey

$$\frac{2bc}{f} \frac{da}{dr} = b^2 + c^2 - a^2 - 2bc \quad (5.7)$$

(and cyclic permutations thereof), with the one-forms  $(\theta, \phi \in [0, \pi], \psi \in [0, 2\pi])$ ,

$$\begin{aligned} \sigma_1 &= -\sin \psi d\theta + \cos \psi \sin \theta d\phi, \\ \sigma_2 &= \cos \psi d\theta + \sin \psi \sin \theta d\phi, \\ \sigma_3 &= d\psi + \cos \theta d\phi, \end{aligned} \quad (5.8)$$

satisfying

$$d\sigma_i = \frac{1}{2} \epsilon_{ijk} \sigma_j \wedge \sigma_k. \quad (5.9)$$

Here,  $r$  is a radial coordinate,  $\theta$  and  $\phi$  are spherical coordinates and  $\psi$  is a  $U(1)$  angle. We then have two forms for the asymptotic metric:

$$ds^2 = \left(1 + \frac{2m}{r}\right) d\vec{r}^2 + 4m^2 \left(1 + \frac{2m}{r}\right)^{-1} (d\psi + \vec{\omega}(r) \cdot d\vec{r})^2. \quad (5.10)$$

If  $m > 0$  this is the asymptotic form for the Taub-NUT manifold, which happens to be exact for the Taub-NUT geometry. On the other hand, if  $m < 0$  we have the asymptotic form for the AH manifold. Clearly when  $r = 2m$  there is a singularity, so the AH metric must deviate from the asymptotic form as  $r$  approaches  $2m$ .



To find the general form of the AH metric, one could follow Atiyah and Hitchin's original choice [2] and take  $f = abc$  but it is easier to follow [64], [20] and choose  $f = -\frac{b}{r}$ . We parameterise  $r$  by  $\beta$  so that

$$r = 2K(\sin \beta/2), \quad (5.11)$$

where

$$K(x) = \int_0^{\pi/2} (1 - x^2 \sin^2(t))^{-1/2} dt \quad (5.12)$$

is the elliptic integral. Here,  $\beta \in [0, \pi]$ , so  $r \in [\pi, \infty)$ . The AH solution is given by

$$\begin{aligned} ab &= -r(\sin \beta) \frac{dr}{d\beta} + \frac{1}{2}(1 - \cos \beta)r^2, \\ bc &= -r(\sin \beta) \frac{dr}{d\beta} - \frac{1}{2}(1 + \cos \beta)r^2, \\ ca &= -r(\sin \beta) \frac{dr}{d\beta}. \end{aligned} \quad (5.13)$$

To understand how this metric deviates from the asymptotic form of the metric, following references [20] and [64], we need to look at what happens when  $r$  draws near to  $\pi$ .

Using the series expansion for the elliptical integral  $K$ , we see that there is a bolt where  $r = \pi$ . Near the bolt, the metric becomes

$$ds^2 = dr^2 + 4(r - \pi)^2 (d\bar{\psi} + \cos \bar{\theta} d\bar{\phi})^2 + \pi^2 (d\bar{\theta}^2 + \sin^2 \bar{\theta} d\bar{\phi}^2), \quad (5.14)$$

where we use the new Euler angles

$$\begin{aligned} \sigma_1 &= d\bar{\psi} + \cos \bar{\theta} d\bar{\phi}, \\ \sigma_2 &= -\sin \bar{\psi} d\bar{\theta} + \cos \bar{\psi} \sin \bar{\theta} d\bar{\phi} \\ \sigma_3 &= \cos \bar{\psi} d\bar{\theta} + \sin \bar{\psi} \sin \bar{\theta} d\bar{\phi} \end{aligned} \quad (5.15)$$

and impose the identification

$$I : \bar{\psi} \rightarrow \bar{\psi} + \pi$$

which is, in terms of the original Euler angles,

$$I : \quad \theta \rightarrow \pi - \theta, \quad \phi \rightarrow \phi + \pi, \quad \psi \rightarrow -\psi. \quad (5.16)$$

This means that  $\psi \in [0, \pi]$  and so the metric gives a smooth manifold near  $r = \pi$ , which is known as the double-cover of the AH manifold [2]. From [64] we see that this must be  $M_0$ .

### 5.2.2 The Two-Monopole Moduli Space on $\mathbb{R}^2 \times \mathbb{S}^1$

We look at the paper by Cherkis and Kapustin [7] and consider the construction of the reduced moduli space of  $SU(2)$  BPS monopoles in this context. The solution will be known for future reference as the Cherkis-Kapustin (CK) solution.

#### Background

Asymptotically, the moduli space of  $k$   $SU(2)$  monopoles on  $\mathbb{R}^3$  looks like a  $T^k$  fibration over  $(\mathbb{R}^3)^k/S_k$ , where we divide by the symmetry group  $S_k$  to reflect the indistinguishability of the monopoles. Since the electric charges are conserved, the fiberwise action of  $T^k$  is a triholomorphic isometry.

The relative moduli space, that found by fixing both the centre of mass coordinates of the monopoles and the sum of their internal degrees of freedom, turns out to be a  $4(k-1)$ -dimensional hyperkähler manifold. In the case of  $k=2$ , the relative moduli space is the Atiyah-Hitchin metric, for which the asymptotic metric has the Taub-NUT form.

Cherkis and Kapustin study the relative moduli space for two BPS monopoles on  $\mathbb{R}^2 \times \mathbb{S}^1$  with the product metric. As is argued in Cvetic et al, [9], the circle has radius  $L$ . When  $L \rightarrow \infty$ , it approaches the Atiyah-Hitchin metric.

#### ALG Instantons

An ALG instanton is defined by Cherkis and Kapustin to be an ALF gravitational instanton which asymptotically has a triholomorphic  $T^2$  action. There is as of yet no exact expression for this metric but asymptotically it takes the form

$$ds^2 = \tau_2 dz d\bar{z} + \tau_2^{-1} |dt + \tau d\chi|^2, \quad (5.17)$$

where  $\tau(z) = \tau_1(z) + i\tau_2(z)$  is a (anti)holomorphic function, and  $t$  and  $\chi$  are periodic. This asymptotic form is not valid in the interior. We now review their construction of ALF hyperkähler manifolds of dimension  $4(k-1)$  which asymptotically have a triholomorphic  $T^{2(k-1)}$  isometry.

To begin to get down to mathematical details, consider  $k$   $SU(2)$  monopoles on  $\mathbb{R}^2 \times \mathbb{S}^1$  with a flat metric. We can identify  $\mathbb{R}^2 \times \mathbb{S}^1$  with  $\mathbb{C} \times \mathbb{S}^1$ . Let  $z \in \mathbb{C}$  and  $\chi \in \mathbb{S}^1$  where  $\chi \sim \chi + 2\pi$ .

We suppose that the monopoles are located at points  $a_j = (z_j, \chi_j)$  for  $j = 1, \dots, k$ .

The field configuration at a distant point  $x = (z, \chi)$  is given, in a suitable gauge, by

$$\phi(x) = v + \sum_{j=1}^k \phi^j(z - z_j). \quad (5.18)$$

where

$$A_\chi = b + \sum_{j=1}^k A_\chi^j(z - z_j), \quad A_z = 0. \quad (5.19)$$

When the monopoles are well-separated, we can think of them as being like particles on  $\mathbb{R}^2 \times \mathbb{S}^1$ . The moduli space coordinates parameterise the positions of the monopoles and the sum of their internal degrees of freedom in  $\mathbb{S}^1$ .

In order to avoid ending up with the kinetic energy on the moduli space being infinite (thus rendering the metric on the moduli space to be ill-defined), in terms of the universal covering space of  $\mathbb{R}^2 \times \mathbb{S}^1$ , we consider each periodic monopole to be an array of infinitely many 't Hooft-Polyakov monopoles. In order to ensure that all the masses and fields are finite, we further replace each infinite array by a finite array of  $2N + 1$  monopoles and send  $N \rightarrow \infty$ .

The Higgs field produced by one periodic monopole located at  $z = 0$ , at distances large compared to the size of the monopole, is

$$\phi^j(x) = \sum_{l=-N}^N \frac{-g}{\sqrt{|z|^2 + (\chi - 2\pi l)^2}}, \quad (5.20)$$

where  $g$  is the charge of the monopole. As we will consider what happens when  $N \rightarrow \infty$ , we can assume that  $|z| \ll N$  and so we have

$$\phi^j(x) = \frac{g}{\pi} \ln |z| - gC_N + O\left(\frac{1}{|z|}\right), \quad (5.21)$$

where  $C_N$  is a constant with  $C_N \rightarrow \infty$  logarithmically as  $N \rightarrow \infty$ , reflecting the divergence of (5.20). In this case, in a suitable gauge, we have

$$A_\chi^j = \frac{g}{\pi} \arg(z), \quad A_z^j = 0. \quad (5.22)$$

For large  $z$ , the total field  $\phi(x)$  is given by

$$\phi(x) = v - kgC_N + \frac{kg}{\pi} \ln |z|. \quad (5.23)$$

We define  $v_{ren} := v - kgC_N$  and adjust  $v$  so that  $v_{ren}$  remains fixed when  $N \rightarrow \infty$ , meaning that  $v \rightarrow \infty$  as  $N \rightarrow \infty$ , which gives us convergence in the manner of the infinite constant method.

Introducing an electric charge for each monopole and calculating the Lagrangian of the resulting dyons yields the following asymptotic metric on the moduli space:

$$\frac{1}{4\pi} ds^2 = \tau_2^{CK}(z) |dz|^2 + \tau_2^{CK}(z)^{-1} |dt + \tau^{CK}(z) d\chi|^2, \quad (5.24)$$

where

$$\tau_1^{CK}(z) = \frac{b}{2} + \frac{1}{\pi} \arg(z), \quad \tau_2^{CK}(z) = \frac{v_{ren}}{2} + \frac{\ln|z|}{\pi} \quad (5.25)$$

and

$$\tau^{CK}(z) := \tau_1^{CK}(z) + i\tau_2^{CK}(z) = \frac{i}{2} (v_{ren} - ib) + \frac{i}{\pi} \ln \bar{z}. \quad (5.26)$$

Here,  $t$  has period 1. Since  $\partial_\chi \tau_2^{CK} = 0$ , there is a triholomorphic  $T^2$  isometry as was required. This metric is valid for large  $|z|$ , but when  $|z|$  is small, there is a singularity at the hypersurface  $\tau_2(z) = 0$ , so the metric is geodesically incomplete. This behaviour is in complete analogy with the case of the Atiyah-Hitchin metric which deviates from its asymptotic form, which we recall looks like the Taub-NUT metric but with the opposite sign in the potential, as  $|z|$  becomes small.

### Relation to the Ooguri-Vafa Solution

Finally, adopting the above notation, the OV metric for large  $|z|$  looks like the following:

$$ds^2 = \tau_2^{OV}(z) |dz|^2 + \tau_2^{OV}(z)^{-1} |dt + \tau^{OV}(z) d\chi|^2, \quad (5.27)$$

where

$$\tau^{OV}(z) := \tau_1^{OV}(z) + i\tau_2^{OV}(z) = -\frac{i}{2\pi} \ln \bar{z} \quad (5.28)$$

with

$$\tau_1^{OV}(z) = \frac{i}{4\pi} (\ln z - \ln \bar{z}), \quad \tau_2^{OV}(z) = -\frac{1}{2\pi} \ln |z|. \quad (5.29)$$

Note that this metric is also of Gibbons-Hawking form. Thus, the OV solution, having the same logarithmic form as the CK metric, deviates from its asymptotic form for small  $|z|$ .

Cherkis and Kapustin [7] comment that, “we expect that the exact metric on the relative moduli space of two periodic monopoles is smooth and complete, just like the Atiyah-Hitchin metric”. In a later paper [8] they state that, “No examples of complete hyperkähler metrics on elliptic fibrations which are locally flat at infinity were known prior to this work (a non-complete example is provided by the so-called Ooguri-Vafa metric [55])”. So they acknowledge that the exact ALG metric should be complete, and record the incompleteness of the Ooguri-Vafa solution.

## 5.3 Extensions and Applications

In this section, we consider three situations in which attempts are made to apply the Gibbons-Hawking metric with infinite potential defined in equations (5.1) and (5.3) to different contexts. We outline and comment on the work of Gross and Wilson [28] stitching together Ooguri-Vafa metrics, Giribet and Santillan [26] constructing seven-dimensional metrics with  $G_2$  holonomy and Gibbons and Warnick [24], who extend solutions in flat space to solutions in hyperbolic spaces.

### 5.3.1 Stitching Together Ooguri-Vafa Metrics

Gross and Wilson [28] aim to extend the infinite-centre Gibbons-Hawking solution by gluing several Ooguri-Vafa metrics together to form a new metric. We outline their construction and discuss its validity in the light of the singular regions present when the potential  $V$  is zero. Firstly, a couple of definitions:

Let  $X$  be a Calabi-Yau manifold. A **large complex structure limit point** is “a point in a compactified moduli space of complex structures  $MX$  on  $X$  which, in some sense, represents the ‘worst possible degeneration’ of the complex structure”.

A metric is said to be **semi-flat** if it restricts to a flat metric on each elliptic fibre. In order to define this rigorously, one needs to consider two holomorphic functions  $\tau_1$  and  $\tau_2$ , the properties of which are given in their example 2.2.

In order to study Ricci-flat metrics, Gross and Wilson look at metrics on  $K3$  surfaces which approach large complex structure limit points. Approaching such a limit can be demonstrated to be roughly the same as “fixing the complex structure on a  $K3$  elliptic fibration  $f : X \rightarrow P^1$ , and letting the Kähler form  $\omega$  on  $X$  vary in such a way that the area of the fibres approaches

zero". They take  $f$  to have twenty-four singular fibres, each of Kodaira type  $I_1$  (a pinched torus), and semi-flat metrics constitute a family of explicit Ricci-flat metrics.

The Ooguri-Vafa metric is an explicit Ricci-flat metric defined in the neighbourhood of each singular fibre; it decays exponentially to a semi-flat metric. Their plan is to glue twenty-four copies of the Ooguri-Vafa metric into the semi-flat metric, obtaining a metric such that it is bound in absolute value by  $O\left(\frac{\varepsilon^{-C}}{\varepsilon}\right)$ , and so as  $\varepsilon \rightarrow 0$  the Ricci curvature approaches zero very rapidly.

Let  $B \subseteq \mathbb{C}$  be open. We have two 1-forms on  $B$ ,  $\tau_1 dy$  and  $\tau_2 dy$ . Then we can locally replace  $y$  with a holomorphic function  $g$  on an open set  $U$  such that  $dg = \tau_1 dy$ , and thus can assume  $\tau_1 = 1$ . Then in these coordinates, the semi-flat metric coincides with the Gibbons-Hawking metric obtained by taking  $V = \frac{\Im\tau_2}{\varepsilon}$  on  $U\mathbb{R}/\varepsilon\mathbb{Z}$ ".

Using the formula

$$[R]^2 = \frac{V^{-1}\Delta\Delta(V^{-1})}{2}, \quad (5.30)$$

the Riemann curvature is then given by

$$[R]^2 = \frac{\varepsilon^2(\Im\tau_2)^{-1}\Delta\Delta(\Im\tau_2)^{-1}}{2} \rightarrow 0 \text{ as } \varepsilon \rightarrow 0. \quad (5.31)$$

However, this calculation does not allow for the possibility that  $V$  can be zero, thus giving rise to infinite curvature and singularities.

### 5.3.2 Seven-Dimensional Holonomy Spaces

The exceptional Lie group  $G_2$  can be thought of as  $\text{Aut}(\mathbb{O})$ . We explore the construction of Giribet and Santillan [26], who construct toric  $G_2$  holonomy spaces from four-dimensional hyperkähler manifolds. We demonstrate that the metrics they construct are incomplete as they do not take account of the possibility of the potential  $V$  being zero and giving rise to singular regions.

Let  $M$  be a complex four-dimensional manifold with metric

$$g_4(\mu) = \delta_{ab}e^a \otimes e^b, \quad (5.32)$$

and  $J_1$  be a complex structure on  $M$ . We can then define

$$\tilde{J}_1 := g_4(J_1, \cdot)(\mu) \quad \bar{J}_1 := g_4(J_1, \cdot). \quad (5.33)$$

Suppose  $g_4$  also admits a complex symplectic form  $\Omega := \bar{J}_2 + i\bar{J}_3$ . We can then introduce a function  $f$  which depends on  $\mu$  and the coordinates of  $M$  and satisfies

$$2\mu\tilde{J}_1(\mu) \wedge \bar{J}_1(\mu) = f\Omega \wedge \Omega. \quad (5.34)$$

We can then define a seven-dimensional metric  $g_7$  by

$$g_7 := \frac{(d\alpha + H_2)^2}{\mu^2} + \mu \left( f d\mu^2 + \frac{(d\beta + H_1)^2}{f} + g_4(\mu) \right), \quad (5.35)$$

where  $\alpha$  and  $\beta$  are new coordinates of  $g_7$  such that  $\partial_\alpha$  and  $\partial_\beta$  are Killing vectors and the one-forms  $H_1$  and  $H_2$  are defined on  $M \times \mathbb{R}_\mu$  and  $M$  respectively.

Suppose now that we have an hyperkähler four-metric  $g$  with a tri-holomorphic Killing vector  $\partial_t$ . There exists a coordinate system in which  $g$  can be written in Gibbons-Hawking form:

$$g = V^{-1} (dt + \vec{\omega})^2 + V dx_i \cdot dx_j \delta^{ij},$$

$$\vec{\nabla} V = \vec{\nabla} \times \vec{\omega} \quad (5.36)$$

which is hyperkähler with respect to the hyperkähler triplet

$$\bar{J}_1 = (dt + \vec{\omega}) \wedge dx_1 - V dx_2 \wedge dx_3,$$

$$\bar{J}_2 = (dt + \vec{\omega}) \wedge dx_2 - V dx_3 \wedge dx_1, \quad (5.37)$$

$$\bar{J}_3 = (dt + \vec{\omega}) \wedge dx_3 - V dx_1 \wedge dx_2.$$

and thus the isometry group of the  $G_2$  space is  $T^3$ .

At this stage, it is worth noting that if a hyperkähler metric possesses a non-triholomorphic isometry then there exists a coordinate system such that the metric can be written as

$$g_h = f_z \left( e^f (dx_1^2 + dx_2^2) + dx_3^2 \right) + f_{x_3}^{-1} (dt + (f_{x_1} dx_2 - f_{x_2} dx_1))^2, \quad (5.38)$$

with  $f$  satisfying the  $SU(\infty)$  Toda equation

$$\left( e^f \right)_{x_3 x_3} + f_{yy} + f_{x_1 x_1} = 0, \quad (5.39)$$

where we use the notation  $f_p + \partial_p f$ . We can see that  $\partial_t$  is a Killing vector and that it is hyperkähler with respect to the hyperkähler triplet

$$\begin{aligned}\bar{J}_1 &= e^f f_{x_3} dx_1 \wedge dx_2 + dx_3 \wedge (dt + (f_{x_1} dx_2 - f_{x_2} dx_1)), \\ \bar{J}_2 &= e^{f/2} \cos(t/2) \tilde{J}_2 + e^{f/2} \sin(t/2) \tilde{J}_3, \\ \bar{J}_3 &= e^{f/2} \sin(t/2) \tilde{J}_2 - e^{f/2} \cos(t/2) \tilde{J}_3,\end{aligned}\tag{5.40}$$

with

$$\tilde{J}_2 := -f_{x_3} dx_3 \wedge dx_2 + (dt + f_y dx_1) \wedge dx_2,\tag{5.41}$$

$$\tilde{J}_3 := f_{x_3} dx_3 \wedge dx_1 + (dt + f_{x_1} dx_2) \wedge dx_1,\tag{5.42}$$

From this, we can see that  $\partial_t$  will preserve  $\bar{J}_1$  but  $\bar{J}_2$  and  $\bar{J}_3$  are dependent on  $t$ . This means that one cannot preserve two of three  $\bar{J}_i$  without preserving the third and thus a four-dimensional  $U(1)$  isometry that preserves two of the three Kähler forms of a hyperkähler metric is triholomorphic.

Giribet and Santillan investigate various structures that satisfy these properties, including ALG and Ward metrics and extend them to seven-dimensional metrics with  $G_2$  holonomy.

In their study of the ALG metrics, they say “a particular case of such a class of metrics was shown to describe the single matter hypermultiplet target space for type IIA superstrings compactified on a Calabi-Yau threefold when supergravity and D-instanton effects are switched off” when referring to the connection between ALG and the Ooguri-Vafa metric. We also note that the ALG metrics deviate from their asymptotic form (which is due to the singularities present as already noted) and thus that their seven-dimensional extensions of this will also include unwanted singular regions. Their extensions of Ward metrics follows similar lines and the incompleteness affects their seven-dimensional metric.

### 5.3.3 Hyperbolic Monopoles

We examine the paper of Gibbons and Warnick [24], which looks at the extent to which results concerning well-separated monopoles in flat space can be applied to monopoles in hyperbolic spaces. We show that we end up in a similar situation to the Atiyah-Hitchin metric, with



the solution deviating from its asymptotic form.

We begin by introducing  $SU(2)$  monopoles on hyperbolic space. Let  $\mathbb{H}^3$  denote the hyperbolic three-space of constant curvature  $-1$  and with metric  $h$ . For a principle  $SU(2)$  bundle  $P \rightarrow \mathbb{H}^3$ , let  $A$  be a connection on  $P$  and  $\Phi$  denote the Higgs field. The pair  $(A, \Phi)$  represents a magnetic monopole of mass  $M > 0$  and charge  $k \in \mathbb{N} \cup \{0\}$  if it satisfies the following two criteria:

the **Bogomol'nyi equation**:

$$d_A \Phi = - \star_h F^A, \quad (5.43)$$

and the **Prasad-Sommerfeld boundary conditions**:

$$M = \lim_{r \rightarrow \infty} \left| \Phi(r) \right|, \quad k = \lim_{r \rightarrow \infty} \frac{1}{4\pi} \int_{S_r^2} \text{tr}(\Phi F^A), \quad (5.44)$$

where  $S_r^2$  denotes a sphere of radius  $r$  centred around some fixed point in  $\mathbb{H}^3$  and  $F^A$  is the curvature of the connection  $A$ .

The **moduli space of hyperbolic monopoles** of charge  $k$  is the space of solutions satisfying these conditions modulo gauge transformations. This is a manifold of dimension  $4k - 1$ , for  $k \geq 1$ , but can be enlarged by a circle factor to yield a moduli space with dimension  $4k$ . For well-separated BPS monopoles in flat space, treating them as point particles carrying scalar, electric and magnetic charges makes it possible to find a metric on the moduli space. We denote by  $\mathcal{M}_k$  the moduli space of  $k$ -monopoles in flat space and by  $\tilde{\mathcal{M}}_k$  the  $k$ -fold covering of  $\mathcal{M}_k$ , which can be written as

$$\tilde{\mathcal{M}}_k = \tilde{\mathcal{M}}_k^0 \times \mathbb{S}^1 \times \mathbb{E}^3, \quad (5.45)$$

where  $\mathbb{E}^3$  represents the centre of motion of the system,  $\tilde{\mathcal{M}}_k^0$  the relative motions and  $\mathbb{S}^1$  the total conserved electrical charge. (For  $k = 2$ ,  $\tilde{\mathcal{M}}_2^0$  is the Euclidean Taub-NUT metric with negative parameter) For monopoles in  $\mathbb{H}^3$ , there is no equivalent splitting of the covering space. As such, in order to simplify the problem we are then facing, we consider a simplified (and unphysical) situation where one or more of the monopoles has a fixed position, and it is to this construction that we turn next.

### Motion of a Test Monopole

We consider the motion of a monopole moving in hyperbolic space  $\mathbb{H}^3$  with  $k$  monopoles at fixed points  $P_j$ ,  $j = 1, \dots, N$  in  $\mathbb{H}^3$ . We treat these fixed monopoles as point particles with electric charge (denoted by  $q$ ), magnetic charge (denoted by  $g$ ) and resulting scalar charge  $(g^2 + q^2)^{\frac{1}{2}}$ . The metric in this case is

$$ds^2 = -dt^2 + h, \quad (5.46)$$

where, as above,  $h$  is a metric on  $\mathbb{H}^3$  and  $\star_h$  is the resulting Hodge operator on  $h$ . The Higgs field  $\Phi$  at the point  $P \in \mathbb{H}^3$  is given by

$$\Phi = \frac{(g^2 + q^2)}{4\pi} V \quad (5.47)$$

with

$$V = \sum_{j=1}^N \coth D(P, P_j) - N, \quad dV = \star_h d\omega, \quad (5.48)$$

where  $V$  satisfies the Laplace equation on  $\mathbb{H}^3$ ,  $d_{\star_h} dV = 0$  and  $D(P, P_j)$  denotes the hyperbolic distance between  $P$  and  $P_j$ .

Gibbons and Warnick go on to demonstrate that the slow motion of a monopole in this environment is equivalent to a geodesic motion on a space with metric at  $P$  given by

$$ds^2 = Vh + V^{-1} (d\tau + \omega)^2 \quad (5.49)$$

with

$$V = 1 + p \left( N - \sum_{j=1}^N \coth D(P, P_j) \right), \quad dV = \star_h d\omega, \quad (5.50)$$

where  $g = 4\pi p$ . Thus, monopole motion in  $\mathbb{H}^3$  in the presence of  $N$  fixed monopoles can be described by geodesic motion on a hyperbolic multi-centre metric given by the above construction.

### Singularities

The choice of parameter  $p$  is important in determining whether we have a singular or non-singular metric. Le Brun [47] considered the above metric with  $p = -\frac{1}{2}$ . In that case, we have

$$\begin{aligned}
V &= 1 - \frac{1}{2} \left( N - \sum_{j=1}^N \coth D(P, P_j) \right) \\
&= \left( 1 - \frac{N}{2} \right) + \frac{1}{2} \sum_{j=1}^N \coth D(P, P_j) \\
&\geq \left( 1 - \frac{N}{2} \right) + \frac{N}{2} \\
&= 1,
\end{aligned} \tag{5.51}$$

due to the behaviour of  $\coth$ . Thus, the solution is everywhere regular and the apparent singularities are nuts as with the Taub-NUT metrics.

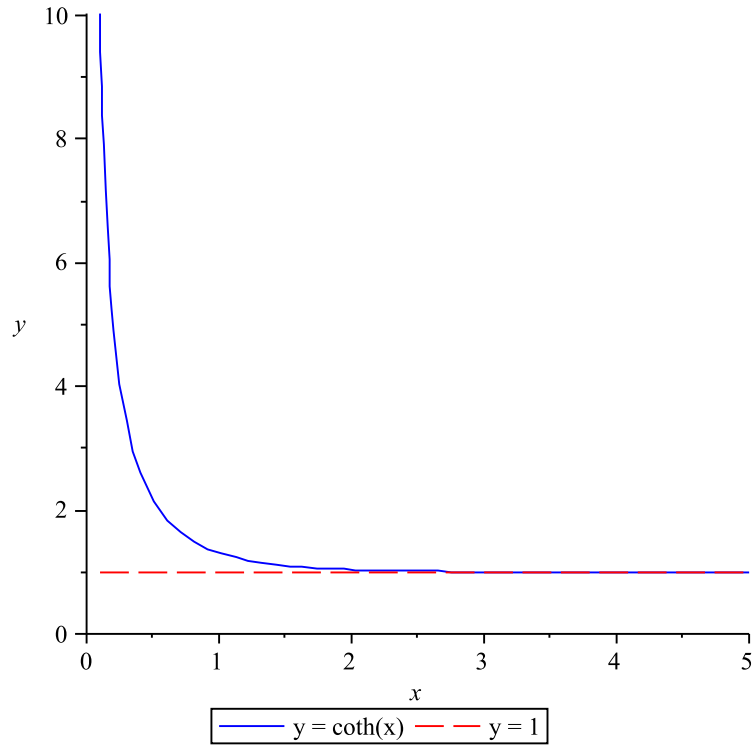


Figure 5.1: Plot of  $\coth(x)$  for  $x > 0$

In the case of  $p > 0$  which Gibbons and Warnick pursue, the situation is somewhat different. We have

$$V = 1 + p \left( N - \sum_{j=1}^N \coth D(P, P_j) \right)$$

$$\begin{aligned}
 &= 1 + pN - p \sum_{j=1}^N \coth D(P, P_j) \\
 &\leq 1 + pN - pN \\
 &= 1.
 \end{aligned}
 \tag{5.52}$$

There exists the possibility that  $V$  is zero and, as the authors acknowledge, this gives rise to singularities as in the Gibbons-Hawking case. However, they go on to say they will ignore them and that they get smoothed out in the moduli space - "This is precisely what happens in the case of monopoles in flat space, where the full Atiyah-Hitchin metric is regular, while the negative mass Taub-NUT is not."

## 5.4 Olbers' and Seeliger's Paradoxes

As a historical note, we will briefly discuss both Olbers' and Seeliger's paradoxes and how convergence of the potential given by an infinite array of periodic instantons is the equivalent problem in our context.

### 5.4.1 Seeliger's Paradox

In 1895, Hugo von Seeliger demonstrated that an infinite universe with a roughly uniform mass distribution is incompatible with Newton's theory of gravitation.

Consider a Cartesian coordinate system with a sphere of radius  $R$ , constant density  $\rho$  and volume  $V$  centred at the origin. The **Newtonian potential**  $\Phi(x_0, y_0, z_0)$  at the point  $P(x_0, y_0, z_0)$  inside the sphere is given by:

$$\Phi(x_0, y_0, z_0) = G\rho \int_V \frac{dV}{|\vec{r} - \vec{r}_0|^{\frac{1}{2}}} = 2\pi G\rho \left( R^2 - \frac{r_0^2}{3} \right), \tag{5.53}$$

where  $\vec{r} = (x, y, z)$  and  $\vec{r}_0 = (x_0, y_0, z_0)$ . If we now let  $R \rightarrow \infty$ , we see that  $\Phi \rightarrow \infty$ , corresponding to infinite matter in the sphere.

If we now calculate the **gravitational force**,  $\vec{F} = \nabla\Phi$ , it only has a radial component and we obtain

$$F_{r0} = -\frac{GM_0}{r_0^2}, \tag{5.54}$$

which does not depend on  $R$ . If we choose  $P(r_0)$  to be the origin, we have  $F_{r_0} = 0$ , even though  $\Phi = \infty$ . Thus, the gravitational force is indeterminate, depending as it does on the choice of origin. This stems from the lack of a gravitating centre in an infinite universe with evenly distributed stars throughout.

Seeliger attempted to resolve the situation by modifying Newton's theory, but this and other approaches are still left facing a puzzle: why is the sky so dark?

### 5.4.2 Olbers' Paradox

In 1823, Wilhelm Olbers described one of the difficulties with assuming the universe is homogeneous, isotropic and infinite in time and space. These assumptions mean that our location in the universe is not special in any way; the same laws of physics apply everywhere and we would expect to find the same substances anywhere. Consequently, when averaged over a sufficiently large region of space, we will see roughly the same number of stars in whatever direction we look. As the universe is infinite, we would expect to see stars wherever we look and all the night sky would be bright. Moreover, an infinite amount of energy will have reached us, making the universe impossibly bright and hot.

Let us explore this mathematically. The **flux** we receive from a single star is given by

$$f = \frac{L}{4\pi r^2}, \quad (5.55)$$

where  $L$  is the **luminosity** of the star and  $r$  is the distance away from us. The total flux we would receive from all stars,  $f_{total}$  is the flux from one star multiplied by the number density of  $N$  stars integrated over all space. In spherical polar coordinates  $\{r, \theta, \phi\}$ , we have

$$\begin{aligned} f_{total} &= \int_0^{2\pi} \int_0^\pi \int_0^\infty \frac{NL}{4\pi r^2} r^2 \sin\theta dr d\theta d\phi \\ &= \int_0^{2\pi} \int_0^\pi \frac{NL \sin\theta}{4\pi} \left( \int_0^\infty dr \right) d\theta d\phi \\ &= \int_0^{2\pi} \frac{NL}{2\pi} \left( \int_0^\infty dr \right) d\phi \\ &= NL \int_0^\infty dr \\ &= \infty. \end{aligned} \quad (5.56)$$

Why does this not occur in real life? Well, various factors are thought to come into play:

- The **age of the universe is finite** and, combined with the speed of light being finite, this means that light from the most distant stars is yet to reach us;
- There is **fractal distribution of galaxies**, meaning that there is a lot of empty space between stars and galaxies and thus the energy coming from each direction would not add up to infinity. This explanation is due to Mandelbrot;
- The **universe is expanding** and thus by the time the light reaches us from distant stars it will have been red-shifted.

### 5.4.3 Relation to Periodic Instantons

Recall that the Gibbons-Hawking metric is given by

$$ds^2 = V^{-1} (d\tau + \vec{\omega} \cdot d\vec{r})^2 + V d\vec{r}^2, \quad (5.57)$$

where the infinite centre solution for  $V$  with periodic instantons along the  $x_3$  axis is given by

$$V = \sum_{j=-\infty}^{\infty} (\rho_2^2 + (x_3 - j)^2)^{-\frac{1}{2}}. \quad (5.58)$$

Clearly this does not converge (see Gross and Wilson [28]) and represents the same problem we see in Olbers' and Seeliger's Paradoxes. To quote Cvetič et al, "one is likely to run into the problem that if all the terms are taken to be positive, then the associated expression for the potential is that of a periodic array of charges all of the same sign and the same magnitude, and this sum will not converge".

## Chapter 6

# Alternative Approaches to Convergence

### 6.1 Introduction

In the previous chapters, we have tried to ensure the convergence of the potential for a distribution of infinitely many instantons with identical sources. We have

$$\begin{aligned} ds^2 &= V^{-1} (d\tau + \vec{\omega} \cdot d\vec{r})^2 + V d\vec{r}^2, \\ V &= V_0 + V_c \sum_{j=-\infty}^{\infty} |\vec{r} - \vec{r}_j|^{-1}, \quad \vec{\nabla}V = \vec{\nabla} \times \vec{\omega}. \end{aligned} \quad (6.1)$$

The solution to the convergence problem we have employed thus far is to subtract an infinite constant, giving

$$V = V_0 + V_c \left( \sum_{j=-\infty}^{\infty} (\rho_2^2 + (x_3 - j)^2)^{-\frac{1}{2}} - 2 \sum_{j=1}^{\infty} j^{-1} \right), \quad (6.2)$$

but with a singularity occurring when  $V$  is zero. From now on,  $\rho_2 := \sqrt{x_1^2 + x_2^2}$ . In this chapter we will investigate three alternative approaches:

**Non-periodic instantons:** We study the work of Anderson et al [1] who solve the problem of convergence by supposing that instead of having a periodic array of instantons, we position them at increasing distances from each other. We outline their construction and discuss what happens if we try to force the distribution to be periodic.

**Quasi-periodic instantons:** We explore the construction of Nergiz and Saçiloğlu [52] who use a subtraction term to ensure convergence, but this time within the construction of three-

dimensional lattices of instantons. This approach gives rise to zero-regions which are singular.

**Reciprocal infinite constant:** Finally, we construct a solution with our potential divided by the infinite constant and show that it corresponds to a potential that is constant apart from along the  $x_3$ -axis, where it behaves like a row of delta functions, and that the resulting spacetime is flat but with delta singularities occurring.

## 6.2 Non-Periodic Instantons

We consider the work of Anderson, Kronheimer and LeBrun [1], who solve the problem of the divergence of the potential  $V$  in a different way to the method of subtracting an infinite constant, by using a hierarchical distribution of instantons. We will show that if we try to force the distribution to be periodic then this results in either singularities or flat metrics, even after modifying the metric.

The basis of their idea is as follows. Let  $\{\vec{r}_j\}_{j=1}^{\infty} \subset \mathbb{R}^3$  be a divergent sequence such that for some point  $\vec{r}_0 \in \mathbb{R}^3$ ,

$$U := \sum_{j=1}^{\infty} |\vec{r}_0 - \vec{r}_j|^{-1} < \infty. \quad (6.3)$$

We can then define a smooth function  $V : \mathbb{R}^3 / \{\vec{r}_j\} \rightarrow \mathbb{R}$  by

$$V(\vec{r}) := \frac{1}{2} \sum_{j=1}^{\infty} |\vec{r} - \vec{r}_j|^{-1}. \quad (6.4)$$

The metric is the standard Gibbons-Hawking metric (6.1). This construction yields a complete Ricci-flat Kähler manifold, and relies on the uneven distribution of the instantons. If we fix the value of  $x_3$ , which simplifies the form of  $\vec{\omega}$  (as it becomes a function of  $\rho := \rho_2$  only) and thus the metric, we can calculate the Riemann curvature scalar:

$$[R]^2 = \frac{27\rho^2 (\partial_\rho V)^4 + 12V^2 \left( \rho^2 (\partial_{\rho\rho} V)^2 + (\partial_\rho V)^2 \right) + 8\rho V \partial_\rho V \partial_{\rho\rho} V (V - 4\rho \partial_\rho V)}{4\rho^2 V^6}. \quad (6.5)$$

### 6.2.1 Example

Let  $\epsilon > 0$  and take  $\vec{r}_j = (0, 0, j^{1+\epsilon})$  and  $r_0 = (0, 0, 0)$ . Then

$$U = \sum_{j=1}^{\infty} j^{-(1+\epsilon)} < \infty, \quad (6.6)$$



and  $V$  is smooth on its domain. Clearly  $V$  satisfies the Laplace equation. Taking  $\epsilon = 0$  means  $U$  would diverge and  $V$  would no longer be smooth. We would have

$$V = \sum_{j=-\infty}^{\infty} (\rho_2^2 + (x_3 - j)^2)^{-\frac{1}{2}}. \quad (6.7)$$

It is then clear that this sum diverges. We pause to consider the convergence of  $\vec{\omega}$ . If we take  $\epsilon = 1$ , then we have

$$\vec{\omega} \cdot d\vec{r} = n \left( \sum_{j=-\infty}^{\infty} \frac{x_3 - j^2}{(\rho_2^2 + (x_3 - j^2)^2)^{\frac{1}{2}}} \right) d\theta \approx \lim_{N \rightarrow \infty} n \left( 2 \left( \left\lfloor x_3^{\frac{1}{2}} \right\rfloor + \left\lceil x_3^{\frac{1}{2}} \right\rceil \right) + 2N - 1 \right) d\theta \quad (6.8)$$

for small values of  $\rho$ , which clearly diverges. On the other hand, if we take  $\epsilon = 2$ , then we have

$$\vec{\omega} \cdot d\vec{r} = n \left( \sum_{j=-\infty}^{\infty} \frac{x_3 - j^3}{(\rho_2^2 + (x_3 - j^3)^2)^{\frac{1}{2}}} \right) d\theta \approx n \left( \left\lfloor x_3^{\frac{1}{3}} \right\rfloor + \left\lceil x_3^{\frac{1}{3}} \right\rceil \right) d\theta \quad (6.9)$$

for small  $\rho_2$ , which converges. For careful choices of  $\epsilon$ , then, this example works and gives a finite value for the Riemann curvature scalar (6.5), even at the positions of the instantons.

### 6.2.2 The Periodic Limit

What happens if we try to have periodically distributed instantons in this setup? Near a pole, say  $\vec{r}_1$ , we have

$$V \approx \frac{1}{2} |\vec{r} - \vec{r}_1|^{-1} + c, \quad (6.10)$$

where  $c \rightarrow \infty$  in the periodic limit. We can examine what is going on here by taking the simplest case: let

$$V = c + \frac{m}{|\vec{r} - \vec{r}_0|}, \quad (6.11)$$

near  $\vec{r}_0 = 0$ , so one point in  $\mathbb{R}^3$ . This yields

$$\vec{\nabla} V = \frac{(-mx_1, -mx_2, -mx_3)}{r^3} = -m \frac{\vec{r}}{r^3}, \quad \vec{\omega} = \frac{(mx_2, -mx_3, 0)}{r(x_3 + r)}. \quad (6.12)$$

It is easier to think of this in spherical polar coordinates. Note that

$$\vec{\nabla} V = -m \frac{\vec{r}}{r^3} \implies \vec{\omega} \cdot d\vec{r} = m \cos \theta d\phi. \quad (6.13)$$

The metric is, spherical coordinates, given by

$$ds^2 = V (dr^2 + r^2 d\theta^2 + r^2 \sin^2 \theta d\phi^2) + V^{-1} (d\tau + m \cos \theta d\phi)^2. \quad (6.14)$$

We can therefore calculate the curvature, obtaining

$$Q := [R]^2 = \frac{24m^2 c^2}{(cr + m)^6}. \quad (6.15)$$

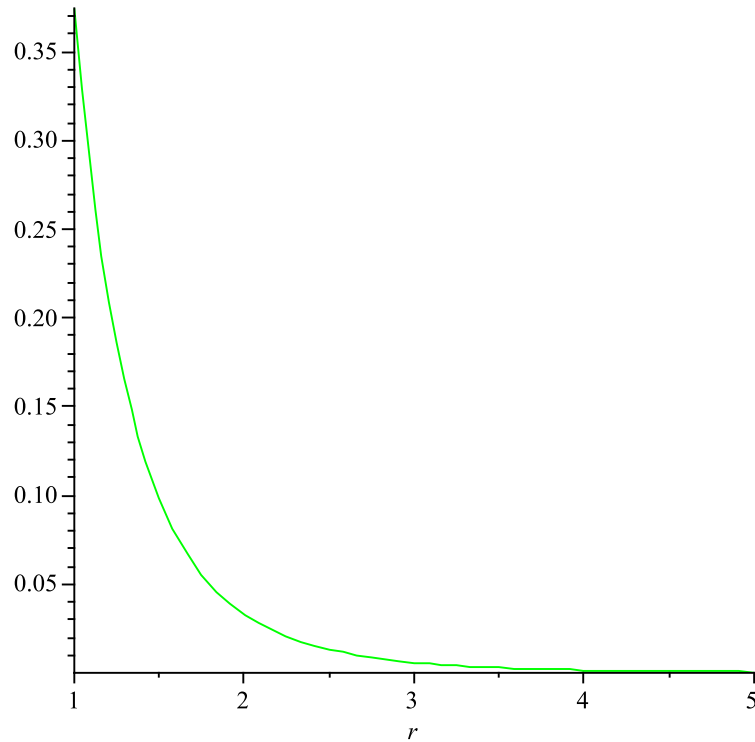


Figure 6.1: The Riemann curvature scalar (6.15) for the simplest non-periodic instanton distribution

Note that the curvature is always positive as  $m$  and  $c$  are positive. In order to investigate what happens to the curvature for different choices of the constants, we calculate some useful quantities. We have

$$\frac{dQ}{dr} = -\frac{144m^2 c^3}{(cr + m)^7}, \quad (6.16)$$

and so

$$M := \max_{r \in [0, \infty)} Q = Q|_{r=0} = \frac{24c^2}{m^4} \quad (6.17)$$

gives us the maximum curvature. The area under the curve is given by

$$A := \int_0^\infty \frac{24m^2c^2}{(cr+m)^6} dr = \frac{24}{5} \frac{c}{m^3}, \quad (6.18)$$

and the width, which is defined to be  $r_w$ , the value of  $r$  such that  $Q(r_w) = \frac{M}{2}$ , is given by

$$r_w := \frac{m}{c} \left( 2^{\frac{1}{6}} - 1 \right). \quad (6.19)$$

Now, if  $m$  is fixed, we have

- $M \rightarrow \infty$  as  $c \rightarrow \infty$ ,
- $A \rightarrow \infty$  as  $c \rightarrow \infty$ ,
- $r_w \rightarrow 0$  as  $c \rightarrow \infty$ ,

and we have a singularity at  $r = 0$ . On the other hand, we could suggest that  $m$  should also tend to infinity, and so could take  $m = c^{\frac{1}{2}}$ , giving

- $M = 24$ ,
- $A = \frac{24}{5} c^{-\frac{1}{2}} \rightarrow 0$  as  $c \rightarrow \infty$ ,
- $r_w = \left( 2^{\frac{1}{6}} - 1 \right) c^{-\frac{1}{2}} \rightarrow 0$  as  $c \rightarrow \infty$ .

We either therefore have a singularity at the origin (which we would expect from looking at the definition of  $V$ ) or an almost flat space with the exception of the origin. We might attempt to rescue the situation, aiming to have a finite maximum curvature and to prevent the width and the area under the curve from tending to zero.

### 6.2.3 Multiplying the Metric by a Constant

We could multiply the whole of the metric by a constant, say  $\alpha$ , to obtain

$$ds^2 = \alpha (V dr^2 + r^2 d\theta^2 + r^2 \sin^2 \theta d\phi^2) + \alpha V^{-1} (d\tau + m \cos \theta d\phi)^2. \quad (6.20)$$

Calculating the curvature scalar gives us

$$Q := [R]^2 = \frac{24m^2c^2}{(rc+m)^6 \alpha^2}. \quad (6.21)$$

This is equivalent to multiplying the potential  $V$  by  $\alpha$ , giving us the original metric but with

$$V(r) = \alpha \left( c + \frac{m}{r} \right). \quad (6.22)$$

Consequently we have

$$\begin{aligned}
 M &= \frac{24c^2}{m^4\alpha^2}, \\
 A &= \frac{24c}{5m^3\alpha^2}, \\
 r_w &= \frac{m}{c} \left( 2^{\frac{1}{6}} - 1 \right).
 \end{aligned} \tag{6.23}$$

In this case, if  $m$  is fixed, then we could take  $\alpha = c$ , giving

- $M = 24m^{-4}$ ,
- $A = \frac{24}{5}m^{-3}c^{-1} \rightarrow 0$  as  $c \rightarrow \infty$ ,
- $r_w \rightarrow 0$  as  $c \rightarrow \infty$ .

On the other hand, taking  $m = c$  gives us

- $M = 24c^{-2}\alpha^{-2} \rightarrow 0$  as  $c \rightarrow \infty$ ,
- $A = \frac{24}{5}c^{-2}\alpha^{-2} \rightarrow 0$  as  $c \rightarrow \infty$ ,
- $r_w = 2^{\frac{1}{6}} - 1$ .

Clearly, taking  $\alpha = c^{-1}$  gives us a potential

$$V(r) = 1 + \frac{1}{r}, \tag{6.24}$$

yielding a normal self-dual Taub-NUT metric. (Note that  $M, A$  and  $r_w$  would all be finite). However, using an infinite constant to eliminate another infinite constant rather defeats the point of the exercise!

#### 6.2.4 Rescaling $r$

We could try rescaling  $r$ , so  $r \mapsto \alpha r$ . We obtain the following metric:

$$\begin{aligned}
 ds^2 &= \alpha^2 V dr^2 + \alpha^2 r^2 d\theta^2 + \alpha^2 r^2 \sin^2 \theta d\phi^2 + \alpha V^{-1} \left( d\tau + \frac{m}{\alpha} \cos \theta d\phi \right)^2, \\
 V(r) &= c + \frac{m}{\alpha r}.
 \end{aligned} \tag{6.25}$$

Calculating the curvature in this case gives

$$Q := [R]^2 = \frac{m^2}{4} \frac{\left( 11m^2 (\alpha^2 - 1)^2 + 48\alpha^4 c^2 r^2 (\alpha^2 + 1) + 32\alpha^3 c r m (\alpha^2 - 1) \right)}{(c r \alpha + m)^6 \alpha^6 r^2}. \tag{6.26}$$

As  $Q$  is singular when  $r = 0$ , it does not make sense to talk about the maximum curvature or the width as defined above. We can however discuss the area,  $A$ . We have

$$\begin{aligned} I &= \int_0^\infty Q(r) dr \\ &= 12m^2 \alpha^{-2} c^2 (\alpha^2 + 1) I_1 + 8\alpha^{-3} cm^3 (\alpha^2 - 1) I_2 + \frac{11}{4} \alpha^{-6} m^4 (\alpha^2 - 1)^2 I_3, \end{aligned} \quad (6.27)$$

where

$$\begin{aligned} I_1 &= \int_0^\infty (r\alpha c + m)^{-6} dr = (5cm^5\alpha)^{-1}, \\ I_2 &= \int_0^\infty r^{-1} (r\alpha c + m)^{-6} dr = -\frac{137}{60m^6} - m^{-6} \left[ \ln \left( \frac{r\alpha c + m}{r} \right) \right]_0^\infty, \\ I_3 &= \int_0^\infty r^{-2} (r\alpha c + m)^{-6} dr = \frac{87c\alpha}{10m^7} - m^{-6} \left[ r^{-1} \right]_0^\infty + \frac{6c\alpha}{m^7} \left[ \ln \left( \frac{r\alpha c + m}{r} \right) \right]_0^\infty. \end{aligned} \quad (6.28)$$

Thus,

$$\begin{aligned} I &= cm^{-3} \alpha^{-5} \left( \frac{967}{120} \alpha^4 - \frac{1631}{60} \alpha^2 + \frac{957}{40} + (\alpha^2 - 1) \left( \frac{17}{2} \alpha^2 - \frac{33}{2} \right) T \right) \\ &\quad - \frac{11}{4} m^{-2} \alpha^{-6} (\alpha^2 - 1)^2 \left[ r^{-1} \right]_0^\infty, \end{aligned} \quad (6.29)$$

where

$$T := \left[ \ln \left( \frac{r\alpha c + m}{r} \right) \right]_0^\infty. \quad (6.30)$$

We can see that the only way to salvage the situation is if  $\alpha = \pm 1$ , which takes us back to where we started! We therefore have a singularity at  $r = 0$  and flat space elsewhere.

### 6.3 Quasi-Periodic Instantons

In an essay in the book ‘General Relativity: An Einstein Centenary Survey’ [33], Hawking discussed spacetime structures that have one gravitational instanton per characteristic volume, whose size is defined by a normalisation constant.

In discussing the best method of looking for a quantum theory of gravity, Hawking favours the path-integral approach suggested by Feynman. This leads to the idea that “there can be quantum fluctuations of the metric not only within each topology but from one topology

to another,” an idea first suggested by Wheeler in 1963. He thought that such spacetimes might have a ‘foam-like’ structure on the scale of the Planck length.

In order to make this rigorous, Hawking considers the “path integral over all compact metrics which have a given spacetime volume  $V$ ”. In calculating  $N(V)dV$ , the number of gravitational fields with 4-volumes between  $V$  and  $V+dV$ , he shows that the dominant contributions to  $N(V)$  come from “metrics with one gravitational instanton per volume  $h^{-1}$ ”.

The paper by Nergiz and Saçiloğlu [52] claims to give an explicit example of this spacetime foam using an infinite centre generalisation of the Gibbons-Hawking metric (see (6.1)). Hawking’s description of spacetime foam suggested that the metric should involve quasi-periodic functions of the coordinates. Through the work of Rossi [57] and Gursev and Tze [29] it is possible to envisage a solution consisting of BPS monopoles arranged on a three-dimensional lattice. We now review Nergiz and Saçiloğlu’s solution (from now on referred to as the quasi-periodic solution).

We take the  $\vec{r}_j$  to be the points  $\vec{q}$  on a three-dimensional lattice with

$$\vec{q} := n_1 \vec{q}_1 + n_2 \vec{q}_2 + n_3 \vec{q}_3, \quad (6.31)$$

where  $n_1, n_2, n_3 \in \mathbb{Z}$  and  $\{\vec{q}_1, \vec{q}_2, \vec{q}_3\}$  are the basis vectors of the lattice. In order to ensure convergence, we cannot simply take

$$V = \sum_{n_1} \sum_{n_2} \sum_{n_3} |\vec{r} - \vec{q}|^{-1}, \quad (6.32)$$

as an integral version of this has a quadratic divergence of the form

$$\int_{|\vec{q}|_{min}}^{\infty} \frac{d|\vec{q}||\vec{q}|^2}{|\vec{q}|}. \quad (6.33)$$

Instead, it turns out that the following potential  $V$ , which contains subtraction terms, does converge:

$$V(\vec{r}) = r^{-1} + \sum_{\{\vec{q}\} \neq 0} \sum \sum \psi(\vec{r}, \vec{q}), \quad (6.34)$$

where

$$\psi(\vec{r}, \vec{q}) := |\vec{r} - \vec{q}|^{-1} - |\vec{q}|^{-1} \left( 1 + \frac{\vec{q} \cdot \vec{r}}{q^2} + (2q^4)^{-1} \left( 3(\vec{q} \cdot \vec{r})^2 - q^2 r^2 \right) \right). \quad (6.35)$$

We have to calculate the whole of  $\psi$  before performing the summation otherwise the sum is meaningless. The question is: does this potential ever equal zero, and if so, does this result in a singularity?

To investigate this, let us choose the standard Euclidean basis  $\{e_1, e_2, e_3\}$  and consider the infinite lattice given by

$$V(x_1, x_2, x_3) = (x_1^2 + x_2^2 + x_3^2)^{-\frac{1}{2}} + \sum_{k=1}^{\infty} \sum_{j=1}^{\infty} \sum_{i=1}^{\infty} \psi_{ijk}(x_1, x_2, x_3), \quad (6.36)$$

where

$$\begin{aligned} \psi_{ijk}(x_1, x_2, x_3) := & ((x_1 - i)^2 + (x_2 - j)^2 + (x_3 - k)^2)^{-\frac{1}{2}} - (i^2 + j^2 + k^2)^{-\frac{1}{2}} \\ & - \frac{ix_1 + jx_2 + kx_3}{(i^2 + j^2 + k^2)^{\frac{3}{2}}} - \frac{3(ix_1 + jx_2 + kx_3)^2}{2(i^2 + j^2 + k^2)^{\frac{5}{2}}} + \frac{1}{2} \frac{x_1^2 + x_2^2 + x_3^2}{(i^2 + j^2 + k^2)^{\frac{3}{2}}}, \end{aligned} \quad (6.37)$$

with  $i, j, k \in \mathbb{N}$ . We have the following picture:

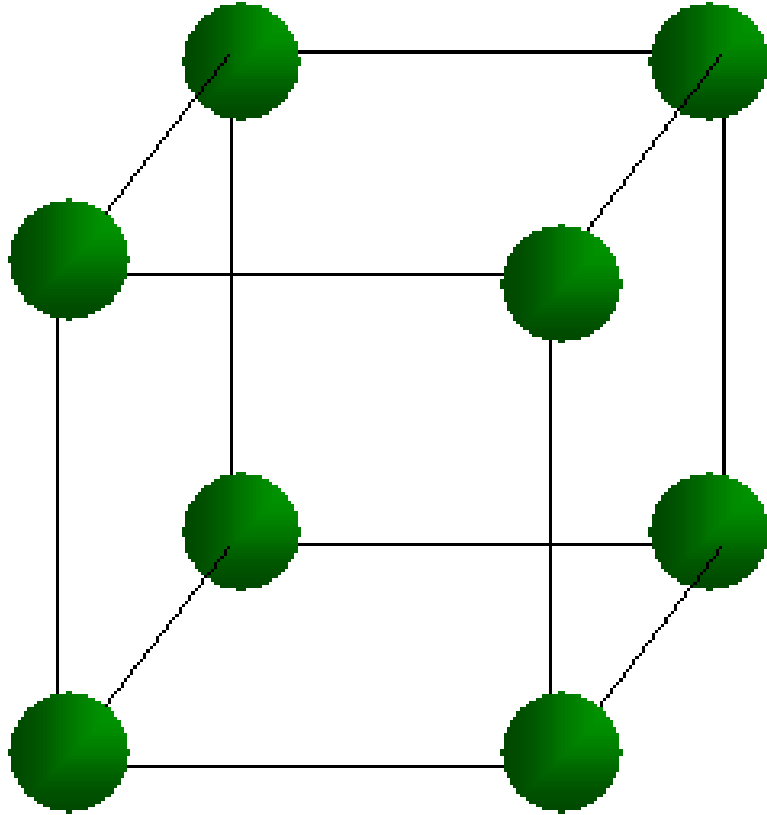


Figure 6.2: A section of the Euclidean lattice for the quasi-periodic instanton solution

The  $i$ -sum is a row of instantons, the  $j$ -sum a grid and the  $k$ -sum a cube. This is a good

choice of lattice as it is an infinite-centre lattice in a basis that is easy to work with. It also avoids the singularity at  $r = 0$ . If we calculate the value of  $\psi$  at the position of one of the instantons, so  $(x_1, x_2, x_3) = (i, j, k)$ , we have

$$\psi_{ijk}(i, j, k) = ((i - i)^2 + (j - j)^2 + (k - k)^2)^{-\frac{1}{2}} - 3(i^2 + j^2 + k^2)^{-\frac{1}{2}} \rightarrow \infty, \quad (6.38)$$

and so around each instanton there is a region such that  $V > 0$ . In order to investigate the behaviour of  $V$  between the instantons, we consider first a one-dimensional version of the problem.

### 6.3.1 Rows of Instantons

The potential  $V$  for a row of instantons is given by

$$V(x_1, x_2, x_3) = (x_1^2 + x_2^2 + x_3^2)^{-\frac{1}{2}} + \sum_{i=1}^{\infty} \psi_i(x_1, x_2, x_3), \quad (6.39)$$

where

$$\begin{aligned} \psi_i := \psi_{i11} &= ((x_1 - i)^2 + (x_2 - 1)^2 + (x_3 - 1)^2)^{-\frac{1}{2}} - (i^2 + 2)^{-\frac{1}{2}} \\ &\quad - \frac{ix_1 + x_2 + x_3}{(i^2 + 2)^{\frac{3}{2}}} - \frac{3(ix_1 + x_2 + x_3)^2}{2(i^2 + 2)^{\frac{5}{2}}} + \frac{1}{2} \frac{x_1^2 + x_2^2 + x_3^2}{(i^2 + 2)^{\frac{3}{2}}}. \end{aligned} \quad (6.40)$$

We can narrow our attention down just to the space between the instantons by choosing that  $x_2 = 1 = x_3$ , yielding the following potential:

$$V = (x_1^2 + 2)^{-\frac{1}{2}} + \sum_{i=1}^{\infty} \psi_i(x_1, 1, 1), \quad (6.41)$$

where

$$\begin{aligned} \psi_i(x_1, 1, 1) &= |x_1 - i|^{-1} - (i^2 + 2)^{-\frac{1}{2}} + (x_1^2(1 - i^2) - (8 + i^2)(1 + ix_1)) (i^2 + 2)^{-\frac{5}{2}} \\ &\approx |x_1 - i|^{-1} - (i^2 + 2)^{-\frac{1}{2}} - x_1 i^{-2}. \end{aligned} \quad (6.42)$$

We can see from the figures below that  $V$  is negative between instantons for a range of values of  $x_1$ . As  $V$  is clearly continuous away from the instantons, there will, by the Intermediate Value Theorem, be points where  $V$  is zero. In the second diagram, we take  $x_3 = 1$  and vary  $x_2$ ; we could have done the opposite and the result would be the same because of the symmetry.



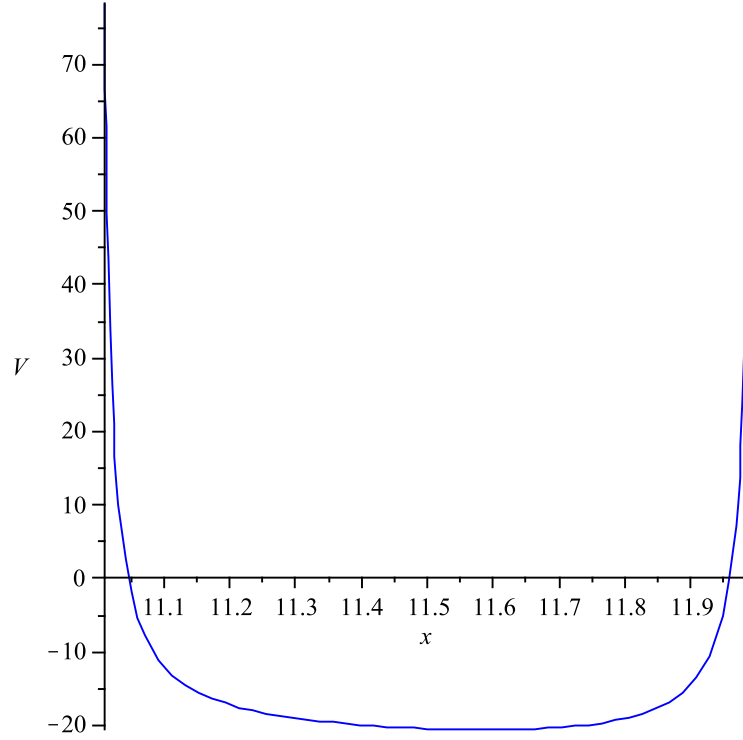


Figure 6.3: 2D representation of  $V$  (using (6.41) and (6.42)) between two members of a row of quasi-periodic instantons, with  $x := x_1 \in [11, 12]$

$x_1$	$V$	$x_1$	$V$
1.5	1.54797	9.5	-14.46200
2.5	0.45678	10.5	-17.36534
3.5	-1.01964	11.5	-20.44930
4.5	-2.75225	12.5	-23.71252
5.5	-4.70359	13.5	-27.15395
6.5	-6.85744	14.5	-30.77275
7.5	-9.20505	15.5	-34.56827
8.5	-11.74107	16.5	-38.53995

### 6.3.2 Grids of Instantons

We now consider a grid of instantons with potential given by

$$V = (x_1^2 + x_2^2 + x_3^2)^{-\frac{1}{2}} + \sum_{j=1}^{\infty} \sum_{i=1}^{\infty} \psi_{ij}(x_1, x_2, x_3), \quad (6.43)$$

where

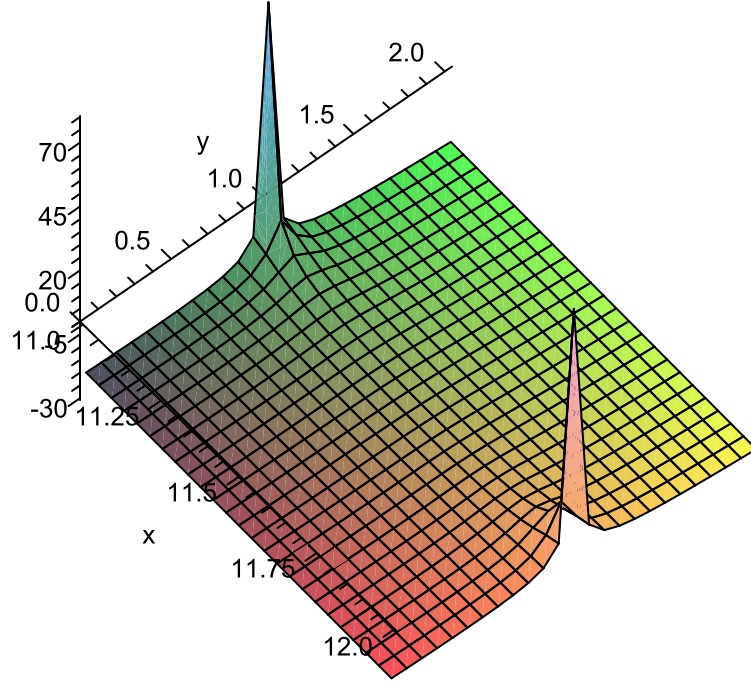


Figure 6.4: 3D representation of  $V$  (using (6.41) and (6.42)) between two members of a row of quasi-periodic instantons, with  $x := x_1 \in [11, 12]$  and  $y := x_2 \in [0, 2]$

$$\begin{aligned} \psi_{ij} := \psi_{ij1} = & \left( (x_1 - i)^2 + (x_2 - j)^2 + (x_3 - 1)^2 \right)^{-\frac{1}{2}} - (i^2 + j^2 + 1)^{-\frac{1}{2}} \\ & - \frac{ix_1 + jx_2 + x_3}{(i^2 + j^2 + 1)^{\frac{3}{2}}} - \frac{3}{2} \frac{(ix_1 + jx_2 + x_3)^2}{(i^2 + j^2 + 1)^{\frac{5}{2}}} + \frac{1}{2} \frac{x_1^2 + x_2^2 + x_3^2}{(i^2 + j^2 + 1)^{\frac{3}{2}}}. \end{aligned} \quad (6.44)$$

Again, suppose we consider just the region between the instantons, taking  $x_3 = 1$  to simplify the potential. We have

$$V = (x_1^2 + x_2^2 + 1)^{-\frac{1}{2}} + \sum_{j=1}^{\infty} \sum_{i=1}^{\infty} \psi_{ij}(x_1, x_2, 1), \quad (6.45)$$

where

$$\psi_{ij}(x_1, x_2, 1) \approx \left( (x_1 - i)^2 + (x_2 - j)^2 \right)^{-\frac{1}{2}} - (i^2 + j^2 + 1)^{-\frac{1}{2}} - x_1 x_2 i^{-2} j^{-2}. \quad (6.46)$$

We have the following figures for different parts of the grid. It is clear from this that the behaviour of the system is the same as in the case of just considering a single row and there are zero regions around the instantons.

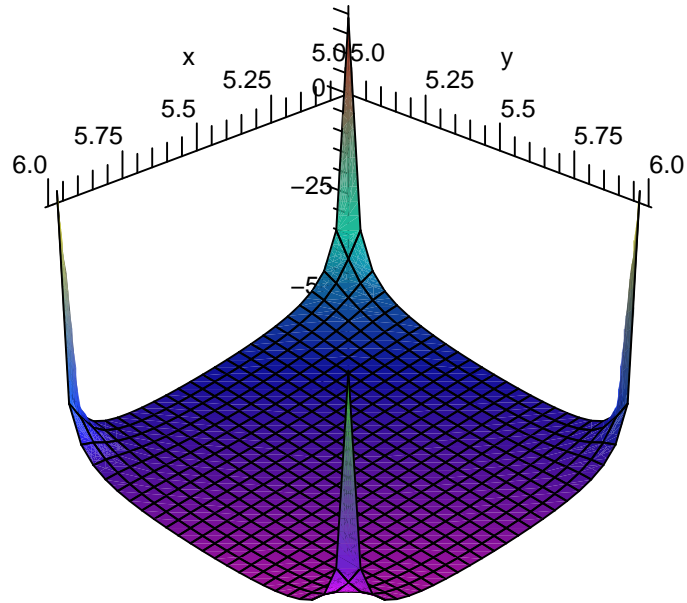


Figure 6.5: Behaviour of  $V$  (using (6.45) and (6.45)) between members of a grid of quasi-periodic instantons, with  $x := x_1 \in [5, 6]$  and  $y := x_2 \in [5, 6]$

$x_1$	$x_2 = 1$	$x_2 = 3$	$x_2 = 5$
-2.5	2.25919	-0.84682	-8.63947
-1.5	0.31359	-4.13109	-14.09088
-0.5	-0.00515	-5.07719	-16.93109
0.5	2.062382	-2.61493	-16.18125
1.5	3.41630	-0.72778	-16.00242
2.5	1.18274	-3.38381	-20.55435
3.5	-3.64472	-9.48574	-28.85445
4.5	-10.86078	-18.62906	-40.53357
5.5	-20.36554	-30.57563	-55.34708
6.5	-32.09447	-45.16796	-73.11535

### 6.3.3 Cubes of Instantons

We can now consider the full metric. Following the pattern from earlier, we can see that

$$V = (x_1^2 + x_2^2 + x_3^2)^{-\frac{1}{2}} + \sum_{k=1}^{\infty} \sum_{j=1}^{\infty} \sum_{i=1}^{\infty} \psi_{ijk}(x_1, x_2, x_3), \quad (6.47)$$

where

$$\psi_{ijk}(x_1, x_2, x_3) \approx ((x_1 - i)^2 + (x_2 - j)^2 + (x_3 - k)^2)^{-\frac{1}{2}} - (i^2 + j^2 + k^2)^{-\frac{1}{2}} - x_1 x_2 x_3 i^{-2} j^{-2} k^2. \quad (6.48)$$

The table below has data for  $x_2 = 1$  and  $x_3 = 10$ :

$x_1$	$V$
-2.5	-54.45775
-1.5	-68.34261
-0.5	-79.42547
0.5	-86.82682
1.5	-94.82779
2.5	-107.70995
3.5	-124.59506
4.5	-145.19040
5.5	-169.29930
6.5	-196.76745

It is then clear that there are zero regions around each of the instantons in our lattice, and that at these points, the metric is singular as, following Gross and Wilson [28], we see that the Riemann curvature for a Gibbons-Hawking metric is given by

$$[R]^2 = \frac{V^{-1} \Delta \Delta (V^{-1})}{2}, \quad (6.49)$$

and so when  $V$  is zero, it blows up to infinity and we have a singularity.

## 6.4 Reciprocal Infinite Constant

In this section we will construct a gravitational instanton solution in which the convergence of the potential given by a series of periodic instantons is achieved by dividing it by an infinite constant. Consider the Gibbons-Hawking metric with

$$V = \phi(\rho_2, x_3) = \lim_{n \rightarrow \infty} \phi_n(\rho_2, x_3), \quad (6.50)$$

where

$$\phi_n(\rho_2, x_3) = (2H_n)^{-1} \sum_{j=-n}^n (\rho_2^2 + (x_3 - j)^2)^{-\frac{1}{2}} \quad (6.51)$$

and

$$H_n = \sum_{j=1}^n j^{-1}. \quad (6.52)$$

is the  $n$ th **harmonic number**. This is a perfectly good instanton solution, but instead of subtracting an infinite constant, we use the fact that  $H_n \rightarrow \infty$  as  $n \rightarrow \infty$  to counter the divergence of the potential. In this section, we will demonstrate that our potential can be written as

$$\phi(\rho_2, x_3) = \begin{cases} \infty & \text{if } \rho_2 = 0, x_3 \in \mathbb{Z}, \\ 1 & \text{if otherwise.} \end{cases} \quad (6.53)$$

In other words,  $\phi$  behaves like a series of delta functions spread along the  $x_3$ -axis, and is otherwise a constant function. In order to demonstrate this, we consider the cases where  $\rho_2 = 0$  and  $\rho_2 > 0$  separately, and then will study the resulting metric.

#### 6.4.1 The Case $\rho_2 = 0$

Consider the case where  $\rho_2 = 0$ . We have

$$\phi_n(0, x_3) = H_n^{-1} \sum_{j=-n}^n |x_3 - j|^{-1}. \quad (6.54)$$

A theorem of Euler shows that

$$\sum_{j=-\infty}^{\infty} (a + dj)^{-1} = \frac{\pi}{d} \cot\left(\frac{a\pi}{d}\right), \quad (6.55)$$

and so we have

$$\sum_{j=-\infty}^{\infty} (x_3 - j)^{-1} = \pi \cot(x_3\pi) \quad (6.56)$$

as  $\cot$  is an odd function. As this is clearly singular when  $x_3 \in \mathbb{Z}$ , we would expect that, as  $n \rightarrow \infty$ ,  $\phi_n$  would tend to a series of delta functions. We make the following conjecture:

$$\phi(0, x_3) = \lim_{n \rightarrow \infty} \phi_n(0, x_3) = \begin{cases} \infty & \text{if } x_3 \in \mathbb{Z}, \\ 1 & \text{if } x_3 \notin \mathbb{Z}. \end{cases} \quad (6.57)$$

Firstly, we note that  $\phi_n(0, x_3) = \phi_n(0, -x_3) \forall x_3 \in \mathbb{R}$  and  $\phi_n$  is non-singular in the regions between integer values of  $x_3$ . As we can see by inspection,  $\phi_n(0, x_3)$  diverges for integer values of  $x_3$  and within each region has a minimum half-way between integer values. We will now prove the following results:

- **Lemma 6.1:**  $\phi\left(0, \frac{1}{2}\right) = \phi\left(0, r + \frac{1}{2}\right) \quad \forall r \in \mathbb{Z},$
- **Lemma 6.2:**  $\phi\left(0, \frac{1}{2}\right) = 1 \quad \forall r \in \mathbb{Z},$
- **Lemma 6.3:**  $\phi(0, x_3) \geq \phi\left(0, \frac{1}{2}\right) \quad \forall x_3 \in \mathbb{R}/\mathbb{Z},$
- **Lemma 6.4:**  $\phi(0, x_3) \leq 1 \quad \forall x_3 \neq \mathbb{Z}.$

We use (6.1), (6.2) and (6.3) to show that  $\phi(0, x_3) \geq 1 \quad \forall x_3 \neq \mathbb{Z}$ . Combining this with (6.4) and applying the Sandwich Theorem gives the result.

### Proof of Lemma 6.1

We can construct a suitable function  $T$  which tends to zero and thus arrive at the result. We have

$$\begin{aligned}
 T_n &:= \sum_{j=-n}^n \left| j - \frac{1}{2} \right|^{-1} - \sum_{j=-n}^n \left| j - \left( r + \frac{1}{2} \right) \right|^{-1} \quad \text{where } r \in \mathbb{Z} \\
 &= \sum_{j=-n}^n \left| j - \frac{1}{2} \right|^{-1} - \sum_{j=-n}^n \left| (j-r) - \frac{1}{2} \right|^{-1} \\
 &= \sum_{j=-n}^n \left| j - \frac{1}{2} \right|^{-1} - \sum_{j=-n-r}^{n-r} \left| j - \frac{1}{2} \right|^{-1}.
 \end{aligned} \tag{6.58}$$

Taking the limit as  $n \rightarrow \infty$  gives us

$$T = \lim_{n \rightarrow \infty} T_n = \sum_{j=-\infty}^{\infty} \left| j - \frac{1}{2} \right|^{-1} - \sum_{j=-\infty}^{\infty} \left| j - \left( r + \frac{1}{2} \right) \right|^{-1} = 0. \tag{6.59}$$

Thus,

$$\phi\left(0, \frac{1}{2}\right) = \phi\left(0, \frac{1}{2} + r\right) \quad \forall r \in \mathbb{Z}. \tag{6.60}$$

□

### Proof of Lemma 6.2

Notice that we can write

$$\phi\left(0, \frac{1}{2}\right) = \lim_{n \rightarrow \infty} \left( \frac{\left( n + \frac{1}{2} \right)^{-1} + 2 \sum_{j=1}^n \left( j - \frac{1}{2} \right)^{-1}}{2 \sum_{j=1}^n j^{-1}} \right), \tag{6.61}$$

because

$$\sum_{j=-n}^n \left| j - \frac{1}{2} \right|^{-1} = 2 + \sum_{j=1}^n \left| j - \frac{1}{2} \right|^{-1} + \sum_{j=-n}^{-1} \left| j - \frac{1}{2} \right|^{-1} \quad (6.62)$$

and

$$\sum_{j=-n}^{-1} \left| j - \frac{1}{2} \right|^{-1} = \sum_{j=2}^{n+1} \left| j - \frac{1}{2} \right|^{-1} = \sum_{j=1}^n \left| j - \frac{1}{2} \right|^{-1} + \left( n + \frac{1}{2} \right)^{-1} - 2. \quad (6.63)$$

We have

$$\sum_{j=1}^n \left( j - \frac{1}{2} \right)^{-1} = \frac{1}{2} \sum_{j=1}^n \left( j^2 - \frac{j}{2} \right)^{-1} + \sum_{j=1}^n j^{-1}. \quad (6.64)$$

Using the above gives us

$$\phi \left( 0, \frac{1}{2} \right) = 1 + \lim_{n \rightarrow \infty} \left( \frac{\left( n + \frac{1}{2} \right)^{-1} + \sum_{j=1}^n \left( j^2 - \frac{j}{2} \right)^{-1}}{2 \sum_{j=1}^n j^{-1}} \right). \quad (6.65)$$

Now,

$$\sum_{j=1}^n \left( j^2 - \frac{j}{2} \right)^{-1} \leq 2 \sum_{j=1}^n j^{-2} \leq \frac{\pi^2}{3} \quad \forall n \in \mathbb{N}. \quad (6.66)$$

Thus, we have

$$\phi \left( 0, \frac{1}{2} \right) = \phi \left( 0, r + \frac{1}{2} \right) = 1 \quad \forall r \in \mathbb{Z} \quad (6.67)$$

as required. □

### Proof of Lemma 6.3

The next step in the process is to construct a lower bound for  $\phi_n(0, x_3)$ . We have, as each region between the integers has a minimum at its halfway point,

$$\phi_n \left( 0, n - \frac{1}{2} \right) \leq \phi_n(0, x_3) \quad (6.68)$$

for any  $x_3 \in (-n, -n-1) \cup (-n-1, -n-2) \cup \dots \cup (n-1, n)$ ,  $\forall n \in \mathbb{N}$ . In the limit,

$$\phi(0, x_3) \geq \phi \left( 0, \frac{1}{2} \right) = 1 \quad \forall x_3 \in \mathbb{R}/\mathbb{Z} \quad (6.69)$$

□

**Proof of Lemma 6.4**

Finally, we construct an upper bound for  $\phi_n(0, x_3)$ . We have

$$\phi_n(0, x_3) = \frac{\sum_{j=-n}^n |x_3 - j|^{-1}}{2 \sum_{j=1}^n j^{-1}} \leq \frac{\pi |\cot(\pi x_3)|}{2(\ln(n) + \gamma)} + \phi_n\left(0, \frac{1}{2}\right) =: S_n, \quad (6.70)$$

where we use

$$H_n = \sum_{j=1}^n j^{-1} \geq \ln(n) + \gamma \quad \forall n \in \mathbb{N}. \quad (6.71)$$

The diagram (for  $n = 1$ ) shows that this is a sensible choice of bound. For  $x_3 \notin \mathbb{Z}$ ,

$$\phi(0, x_3) = \lim_{n \rightarrow \infty} \phi_n(0, x_3) \leq 0 + \phi\left(0, \frac{1}{2}\right) = 1 \quad (6.72)$$

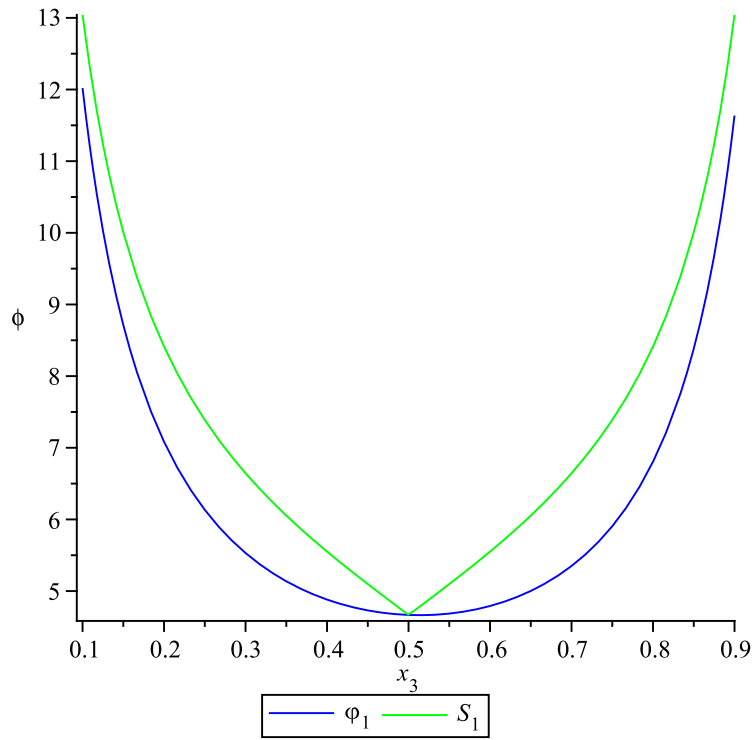


Figure 6.6: Plot illustrating the choice of upper bound for  $\phi$  in (6.70) for  $n = 1$  and  $x_3 \in [0, 1]$

Thus, we have proven that

$$\phi(0, x_3) = \lim_{n \rightarrow \infty} \phi_n(0, x_3) = \begin{cases} \infty & \text{if } x_3 \in \mathbb{Z}, \\ 1 & \text{if } x_3 \notin \mathbb{Z}. \end{cases} \quad (6.73)$$

□



### 6.4.2 The Case $\rho_2 > 0$

For  $\rho_2 > 0$ ,  $\phi_n$  is clearly non-singular everywhere as both terms in the denominator are always positive. Since  $\phi(\rho_2, x_3) = \phi(\rho_2, -x_3) \forall x_3 \in \mathbb{R}$ , we can study  $\phi$  for  $x_3 \geq 0$  without loss of generality.

**Theorem 6.5**  $\phi(\rho_2, x_3) = 1 \forall \rho_2 > 0, x_3 > 0.$

**Proof** Analytically, we see that

$$\begin{aligned} \left( \frac{\partial}{\partial x_3} \sum_{j=-n}^n (\rho_2^2 + (x_3 - j)^2)^{-\frac{1}{2}} \right) \Big|_{x_3=0} &= \left( \sum_{j=-n}^n (j - x_3) (\rho_2^2 + (x_3 - j)^2)^{-\frac{3}{2}} \right) \Big|_{x_3=0} \\ &= \sum_{j=-n}^n j (\rho_2^2 + j^2)^{-\frac{3}{2}} \\ &= 0. \end{aligned} \tag{6.74}$$

Thus, we have  $\phi_n(\rho_2, x_3) \leq \phi_n(\rho_2, 0)$ . Now,

$$\phi_n(\rho_2, 0) = \frac{\sum_{j=-n}^n (\rho_2^2 + j^2)^{-\frac{1}{2}}}{2 \sum_{j=1}^n j^{-1}} = \frac{\rho_2^{-1} + 2 \sum_{j=1}^n (\rho_2^2 + j^2)^{-\frac{1}{2}}}{2 \sum_{j=1}^n j^{-1}} \leq \frac{\rho_2^{-1} + 2 \sum_{j=1}^n j^{-1}}{2 \sum_{j=1}^n j^{-1}}. \tag{6.75}$$

Taking the limit as  $n \rightarrow \infty$  gives  $\phi(\rho_2, 0) \leq 1$  and thus  $\phi(\rho_2, x_3) \leq 1 \forall x_3 \geq 0$ . Finally, we show the reverse inequality. Using the fact that

$$\frac{1}{\sqrt{a^2 + b^2}} \geq \frac{1}{a + b} \forall a, b > 0, \tag{6.76}$$

we have

$$\begin{aligned} 2H_n \phi_n(\rho_2, x_3) &= \frac{1}{\sqrt{\rho_2^2 + x_3^2}} + \sum_{j=1}^n (\rho_2^2 + (x_3 - j)^2)^{-\frac{1}{2}} + \sum_{j=1}^n (\rho_2^2 + (x_3 + j)^2)^{-\frac{1}{2}} \\ &\geq \frac{1}{\sqrt{\rho_2^2 + x_3^2}} + \sum_{j=1}^n (\rho_2 + |x_3 - j|)^{-1} + \sum_{j=1}^n (\rho_2 + |x_3 + j|)^{-1}. \end{aligned} \tag{6.77}$$

Now,

$$\sum_{j=1}^n (\rho_2 + |x_3 - j|)^{-1} \geq \sum_{j=1}^n (\rho_2 + |x_3 + j|)^{-1} \tag{6.78}$$

and, as  $x_3 > 0$ ,

$$\begin{aligned}
 \sum_{j=1}^n j^{-1} - \sum_{j=1}^n (\rho_2 + |x_3 + j|)^{-1} &= (\rho_2 + x_3) \sum_{j=1}^n (j(\rho_2 + x_3) + j^2)^{-1} \\
 &\leq (\rho_2 + x_3) \sum_{j=1}^n j^{-2} \\
 &\leq (\rho_2 + x_3) \frac{\pi^2}{6}.
 \end{aligned} \tag{6.79}$$

Therefore,

$$\sum_{j=1}^n (\rho_2 + |x_3 - j|)^{-1} + \sum_{j=1}^n (\rho_2 + |x_3 + j|)^{-1} \geq 2 \left( H_n - \frac{\pi^2}{6} (\rho_2 + x_3) \right), \tag{6.80}$$

resulting in

$$\phi_n(\rho_2, x_3) \geq 1 + \frac{1}{2H_n \sqrt{\rho_2^2 + x_3^2}} - \frac{\pi^2}{12H_n} (\rho_2 + x_3). \tag{6.81}$$

Consequently,

$$\phi(\rho_2, x_3) = \lim_{n \rightarrow \infty} \phi_n(\rho_2, x_3) \geq 1, \tag{6.82}$$

yielding the result. □

### 6.4.3 Investigating the Spacetime

Recall that the metric is given by

$$\begin{aligned}
 ds^2 &= V^{-1} (d\tau + \vec{\omega} \cdot d\vec{r})^2 + V d\vec{r}^2, \\
 \vec{\nabla} V &= \vec{\nabla} \times \vec{\omega}.
 \end{aligned} \tag{6.83}$$

In order to investigate the behaviour of the metric for  $V$  given by

$$V(\rho_2, x_3) = \begin{cases} \infty & \text{if } \rho_2 = 0, x_3 \in \mathbb{Z}, \\ 1 & \text{if otherwise,} \end{cases} \tag{6.84}$$

we take  $V := c \in \mathbb{R}$ , a constant, so that  $\vec{\omega} = \vec{0}$ . We then have

$$ds^2 = V^{-1} d\tau^2 + V dx_1^2 + V dx_2^2 + V dx_3^2 \tag{6.85}$$

and the Riemann curvature  $[R]^2 = 0$ . Thus, in this case, the space is flat except at the location of the instantons, where delta singularities arise.

## Chapter 7

# Extreme Reissner-Nordström Black Holes

### 7.1 Introduction

In this chapter we shall apply the results obtained in previous chapters in a new context, that of Extreme Reissner-Nordström (ERN) black holes, generating new solutions with infinitely many of these black holes. As such, the structure of the chapter is as follows:

**Finitely many black holes:** We will outline the constructions of Hartle and Hawking [30] and Myers [50] in order to show how solutions with finitely many extreme black holes work in  $(D + 1)$ -dimensions for  $D \geq 3$ . We shall see that these metrics are regular at the event horizons. Solutions without naked singularities require point monopole sources and we shall see that using any other sources generates such singularities.

**Infinitely many black holes:** We will consider solutions in  $(D + 1)$ -dimensions for  $D \geq 3$  that have infinitely many identical ERN black holes. We demonstrated in chapter three the convergence of a periodic distribution of such black holes for  $D \geq 4$ . We examine the behaviour of a periodic distribution for  $D = 3$ , using an infinite constant to ensure convergence and exploring the resulting singularity structure. We then examine the cases of  $D = 4$  and  $D \geq 4$  and see that the Riemann curvature tensor is well-behaved. We can therefore infer that there are no unwanted singularities.

Lattice solutions will be constructed for  $D \geq 4$  and we shall see that these are also well-behaved. Finally, we shall modify the method of Anderson et al [1] to create solutions with

unevenly distributed black holes in several axes, which as we shall see in the section on dilaton theory, have well-behaved Riemann curvature scalars.

**Smoothness of event horizons:** We outline the work of Candlish and Reall [4] and see that if we have infinitely many identical black holes distributed along one (periodic) or many (lattice) of the axes in  $D = 4$  dimensions, then all the horizons are smooth. This is not the case if the black holes are unevenly distributed, where the horizon is  $C^2$  but not  $C^3$ . In higher dimensions, the horizon is  $C^0$  but not  $C^1$ .

**Einstein-Maxwell-Dilaton theory:** Finally in this chapter, we look at a modification of this ERN structure, allowing us to construct dilaton solutions. We will see that the metric is regular at the event horizon in some special cases, and construct periodic, lattice and non-periodic solutions in  $(D + 1)$ -dimensions. We also look briefly at how adding a cosmological constant affects the behaviour of the solution.

## 7.2 Finitely Many Black Holes

In this section we will first look at defining an Extreme Reissner-Nordström black hole and see that solutions with many black holes that balance the mass and charge can be constructed. We will then consider the behaviour of such multiple black hole solutions in  $(3+1)$  dimensions and their analytic extensions, as outlined in a 1977 paper by Hartle and Hawking [30]. Next, we consider the situation in  $(D + 1)$ -dimensions, where  $D > 3$ . The construction of such solutions is given by extending the method employed in the  $(3 + 1)$ -dimensional case into higher dimensions. In doing this we will follow the treatment given by Myers [50] (and note that similar results were found by Gibbons et al [19]). Finally, we will show that using sources other than point monopoles in these solutions results in the presence of naked singularities. These are singularities that are not hidden behind an event horizon, and so can be reached in a finite time by an observer at infinity. All these solutions are generalisations of the  $(D + 1)$ -dimensional **Majumdar-Papapetrou** metrics:

$$ds^2 = -V^{-2}dt^2 + V^{\left(\frac{2}{D-2}\right)}d\vec{r} \cdot d\vec{r}, \quad (7.1)$$

where  $V(x_i)$  is a harmonic function of the  $D$  spatial coordinates  $(x_1, \dots, x_D)$  and the electrostatic potential is  $A_0 = V^{-1}$ . The action is given by

$$\int d^{D+1}x \sqrt{-g} \left( R - \frac{D-1}{4(D-2)} F_{\mu\nu} F^{\mu\nu} \right). \quad (7.2)$$

### 7.2.1 What is an Extreme Reissner-Nordström Black Hole?

The Reissner-Nordström metric in  $(3 + 1)$  dimensions is given, in spherical coordinates, by [5]

$$ds^2 = -V dt^2 + V^{-1} dr^2 + r^2 d\Omega^2, \quad (7.3)$$

where we have

$$V := 1 - \frac{2Gm}{r} + \frac{GQ^2}{r^2}, \quad (7.4)$$

with  $m$  being the mass of the black hole,  $Q$  its electric charge,  $r$  its radius and  $G$  being the gravitational constant. It is a solution of the **Einstein-Maxwell equations**:

$$R_{\mu\nu} - \frac{1}{2} g_{\mu\nu} R = 2T_{\mu\nu},$$

$$\nabla_{[\mu} F_{\nu\rho]} = 0, \quad (7.5)$$

where

$$T_{\mu\nu} = F_{\mu\lambda} F_{\nu}^{\lambda} - \frac{1}{4} g_{\mu\nu} F_{\lambda\rho} F^{\lambda\rho}, \quad F_{\mu\nu} = \partial_{\mu} A_{\nu} - \partial_{\nu} A_{\mu}. \quad (7.6)$$

The metric has a curvature singularity at  $r = 0$ , which is obvious if we calculate the Riemann curvature scalar

$$[R]^2 = \frac{8G^2 (6m^2 r^2 - 12mQ^2 r + 7Q^4)}{r^8}. \quad (7.7)$$

It has event horizons when  $V(r) = 0$  and consequently at the radii

$$r_{\pm} = Gm \pm \sqrt{G^2 m^2 - GQ^2}, \quad (7.8)$$

leading to a number of possibilities. Of interest to us is the case where

$$Gm^2 = Q^2, \quad (7.9)$$

sometimes known as the **Extreme Reissner-Nordström (ERN) solution**. The potential in this case is given by

$$V = \left(1 - \frac{Gm}{r}\right)^2. \quad (7.10)$$

A curious property of such a solution is that the mass is, in some sense, balanced by the charge. Two or more ERN black holes with the same sign charge will attract each other gravitationally and repel each other electromagnetically such that the two effects cancel out. We can find solutions of the Einstein-Maxwell equations corresponding to any number of black holes in a stationary configuration. The metric in the ERN case is given by

$$ds^2 = - \left(1 - \frac{Gm}{r}\right)^2 dt^2 + \left(1 - \frac{Gm}{r}\right)^{-2} dr^2 + r^2 d\Omega^2. \quad (7.11)$$

A change of radial coordinate

$$\rho = r - Gm \quad (7.12)$$

yields the metric

$$ds^2 = -U^{-2}(\rho)dt^2 + U^2(\rho) (d\rho^2 + \rho^2 d\Omega^2), \quad (7.13)$$

where

$$U(\rho) := 1 + \frac{Gm}{\rho}. \quad (7.14)$$

In the original coordinate  $r$ , the electric field of the extremal solution can be written in terms of a vector potential  $A_\mu$  as

$$E_r = \partial_r A_0 = \frac{Q}{r^2}, \quad (7.15)$$

where the timelike component of the vector potential is given by

$$A_0 = -\frac{Q}{r} = -\frac{\sqrt{Gm}}{\rho + Gm}, \quad (7.16)$$

yielding

$$\sqrt{G}A_0 = U^{-1} - 1. \quad (7.17)$$

It can then be shown [5] that the Einstein-Maxwell equations (7.5) with (7.13), (7.17) can be satisfied by any time-independent solution of Laplace's equation

$$\nabla^2 U = 0, \quad (7.18)$$

and solutions that behave well at infinity will take the form

$$U = 1 + \sum_{j=1}^N \frac{Gm_j}{|\vec{r} - \vec{r}_j|}, \quad (7.19)$$

where the points  $\vec{r}_j$  are the locations of the black holes. We have therefore shown that it is possible to construct solutions in which many ERN black holes are in equilibrium. We now explore the resulting space-time in more detail.

### 7.2.2 Multiple Black Holes in (3 + 1) Dimensions

Hartle and Hawking [30] examine multiple ERN black hole solutions in detail as they explore analytic extensions of the (3 + 1)-dimensional **Majumdar-Papapetrou** metric

$$ds^2 = -V^{-2}dt^2 + V^2d\vec{r} \cdot d\vec{r}, \quad (7.20)$$

where  $\vec{r} = (x_1, x_2, x_3)$ . We will outline their construction and discuss the resulting space-time. From now on, we require that the units are such that  $c = G = 1$ . If we extend the solution so that  $V$  has  $N$  singularities, where the sources are point monopoles at  $\vec{r}_j$ , we have

$$V = 1 + \sum_{j=1}^N \frac{m_j}{|\vec{r} - \vec{r}_j|}, \quad (7.21)$$

where  $m_j > 0$  and  $m_j = e_j$  where  $m_j$  is the mass and  $e_j$  is the charge, for  $j = 1, \dots, N$ . If we allow  $V$  to run over a complete background space, then  $V$  is regular except when  $\vec{r} = 0$ . As we know from above, this solution corresponds to  $N$  stationary ERN black holes, but Hartle and Hawking demonstrate that the resulting spacetime is quite complicated.

Consider the case  $N = 2$ . We have the following potential:

$$V = 1 + \frac{m_1}{|\vec{r} - \vec{r}_1|} + \frac{m_2}{|\vec{r} - \vec{r}_2|} \quad (7.22)$$

A region of spacetime with this metric and coordinates ranging over a complete flat background space is a **Type I region**. It turns out that the metric is regular at  $\vec{r} = \vec{r}_1$ , and passing through it takes us into a region described by the same metric (7.20) but with potential

$$V'(\vec{r}') = 1 - \frac{m'_1}{|\vec{r}' - \vec{r}'_1|} + \frac{m'_2}{|\vec{r}' - \vec{r}'_2|} \quad (7.23)$$

with transformed coordinates

$$|\vec{r}' - \vec{r}'_1| = -|\vec{r} - \vec{r}_1| \quad \text{and} \quad |\vec{r}' - \vec{r}'_2| = \sqrt{|\vec{r} - \vec{r}_1|^2 + a^2 + 2a|\vec{r} - \vec{r}_1| \cos \theta}, \quad (7.24)$$

where  $a$  is the separation of the sources in the background coordinates. Such a region is called a **Type IIa region**. The metric is singular at the point where  $V' = 0$ , which we can see if we calculate the Maxwell field invariant

$$J = F_{\mu\nu}F^{\mu\nu} = -2 \left( \frac{\nabla V'}{V'^2} \right)^2 \rightarrow \infty \quad \text{as} \quad V' \rightarrow 0. \quad (7.25)$$

We can construct a region with similar properties by going through  $\vec{r} = \vec{r}_2$ , which we call a **Type IIb region**. We can pass between these regions, that is, from a Type I region into a Type II region and vice versa as we can extend the metric through  $\vec{r} = \vec{r}_1$  (or  $\vec{r} = \vec{r}_2$ ) in two different ways. However, the two null surfaces  $\vec{r} = \vec{r}_1$  and  $\vec{r} = \vec{r}_2$  represent two separate components of the event horizon. As the singularities are all contained between these surfaces, we must have two distinct black holes. This construction can be extended for more black holes (that is, for other values of  $N$ ).

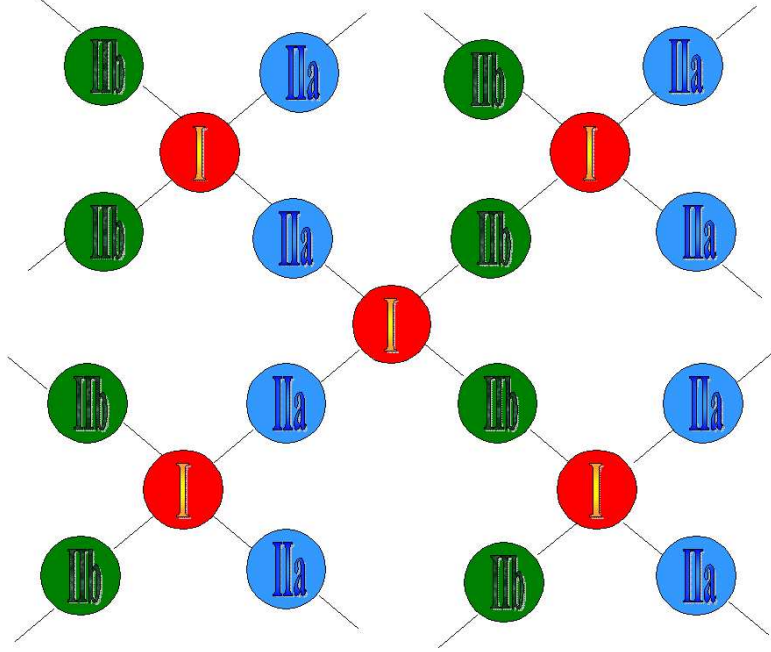


Figure 7.1: The most general extension of the two black hole Majumdar-Papapetrou metric

A Type IIa region is the interior region inside the event horizon at  $\vec{r} = \vec{r}_1$  and a Type IIb region is the interior region inside the event horizon at  $\vec{r} = \vec{r}_2$ .

### 7.2.3 Multiple Black Holes in $(D + 1)$ Dimensions

Myers [50] extends this multiple black hole construction to the case of  $D > 3$ . In this situation, we have the metric (7.1) with the potential



$$V = 1 + \sum_{j=1}^N \frac{m_j}{|\vec{r} - \vec{r}_j|^{D-2}}, \quad (7.26)$$

where  $\vec{r} = (x_1, \dots, x_D)$ . The Maxwell form in this case is given by

$$A_D = \pm \sqrt{\frac{D-1}{2(D-2)}} V^{-1}(\vec{r}), \quad (7.27)$$

and the mass to charge ratio is given by

$$\frac{|Q|}{m} = \sqrt{\frac{D-2}{D-1}}. \quad (7.28)$$

In the case of  $N = 1$ , the result is an ERN black hole in  $(D + 1)$ -dimensions. When  $N = 2$ , the potential takes the form

$$V = 1 + \frac{m_1}{|\vec{r} - \vec{r}_1|^{D-2}} + \frac{m_2}{|\vec{r} - \vec{r}_2|^{D-2}}. \quad (7.29)$$

As before, we will call this region a **Type I region**. It can be shown by a change of coordinates (we can introduce a new radial coordinate  $R := |\vec{r} - \vec{r}_1|^{D-2}$ ) that the metric is regular at  $\vec{r} = \vec{r}_1$  and we can pass through into a new region. Performing the coordinate transformation

$$|\vec{r}' - \vec{r}'_1| := |R|^{(D-2)^{-1}} \quad \text{and} \quad |\vec{r}' - \vec{r}'_2| := \sqrt{|\vec{r}' - \vec{r}'_1|^2 + a^2 + 2a|\vec{r}' - \vec{r}'_1| \cos \theta}, \quad (7.30)$$

where  $a$  is defined as above, gives a metric of the form of (7.1) but with potential

$$V'(\vec{r}') = 1 - \frac{m_1}{|\vec{r}' - \vec{r}'_1|^{D-2}} + \frac{m_2}{|\vec{r}' - \vec{r}'_2|^{D-2}}. \quad (7.31)$$

The resulting region will be called a **Type IIa region**. The metric is singular when  $V' = 0$ , which we can see by computing the Maxwell field invariant

$$J = F_{\mu\nu} F^{\mu\nu} = - \left( \frac{D-1}{D-2} \right) \left( \frac{\nabla V'}{V'^{\frac{D-1}{D-2}}} \right)^2 \rightarrow \infty \quad \text{as} \quad V' \rightarrow 0. \quad (7.32)$$

Therefore, the surface  $\vec{r} = \vec{r}_1$  is the event horizon surrounding that point. Consequently, we have a black hole. Passing through the surface  $\vec{r} = \vec{r}_2$  yields a second, separate black hole, and we can define a **Type IIb region** by similar logic to the above. We thus have different regions which we can pass between, yielding a configuration like that in the above diagram.

In the five-dimensional case, Gibbons et al [19] also produced multiple black hole solutions by looking at solitonic matter solutions that saturate the Bogomol'nyi bound and considering

the special case of no matter. They demonstrated that such solutions are supersymmetric, in the sense of admitting a Killing spinor.

#### 7.2.4 Sources Other Than Monopoles?

We can formulate Majumdar-Papapetrou metrics with sources other than discrete point sources. Suppose outside of a large sphere in the background space we have a solution  $V$  of Laplace's equation which approaches unity. This solution generates an asymptotically flat Majumdar-Papapetrou metric which we can analytically extend until it either vanishes or becomes infinite.

If  $V$  vanishes, then along some curve which approaches the point of vanishing, the field invariant  $J$ , which takes the same form as above, goes to infinity and indicates the presence of a naked singularity, which means that there is no event horizon around the singularity. If  $V$  approaches infinity at a point, then avoiding naked singularities requires  $|V|$  to be bounded below at the singularity and theorem from potential theory (See page 459 of [50]) necessitates  $V$  having the form

$$V(\vec{r}) = w(\vec{r}) + \frac{c}{\vec{r}^{(D-1)}}, \quad (7.33)$$

where  $c$  is a constant,  $\vec{r}$  is the distance from the singularity and  $w$  is regular there, but this is the same situation we've explored previously with point sources. To prevent naked singularities occurring in the case of having a singular curve,  $V$  must diverge no faster than logarithmically in order to prevent the equipotentials touching the singularity, but this still gives rise to a divergent  $J$ .

Therefore, the only way to avoid having naked singularities is to have  $V$  being generated by discrete point sources. We will now explore what happens when we try to construct Majumdar-Papapetrou metrics with infinitely many ERN black holes.

### 7.3 Infinitely Many Black Holes

In this section we will investigate Majumdar-Papapetrou metrics in different dimensions that have infinitely many black holes. In chapters three and six, we studied various ways of constructing gravitational instanton solutions with the Gibbons-Hawking metric whose potentials included infinitely many instantons, and here we will be looking at their parallel structures in this context. Thus, we will consider the following:

- **Periodic distributions of black holes** in the cases of both  $D = 3$  and  $D > 3$ . As in our earlier work, we will suppose the black hole sources to be periodically distributed along one of the axes and will discover that the validity of these constructions depends upon the convergence of  $V$ . For  $D > 3$ , the resulting constructions can be interpreted as behaving like black holes in a Kaluza-Klein background.
- **Lattices of black holes** will be constructed following the work of Myers [50]. These are extensions of his construction in the case  $D = 4$  into higher dimensions with more than one compact dimension.
- **Non-periodic distributions of black holes** following an analogous version in the Majumdar-Papapetrou context of the method of Anderson et al [1] for constructing a solution with infinitely many instantons unevenly distributed along one of the axes. We extend this to solutions with black holes unevenly distributed through several dimensions.

### 7.3.1 Periodic Distribution of Black Holes

Here, we will take the constructions of multiple black hole solutions given in the papers by Hartle and Hawking [30] for  $(3 + 1)$ -dimensions and by Myers [50] for  $(D + 1)$ -dimensions where  $D > 3$ , and will explore what happens when we allow the number identical of black holes to go to infinity and arrange them periodically along one of the axes. We will consider three cases:  $D = 3$ ,  $D = 4$  and  $D > 4$ .

In the first of these instances, we will see that the potential does not converge. This is not the case in higher dimensions and we can therefore write down solutions, which we can interpret in different ways. We can regard such solutions as representing an infinite string of black holes with a harmonic potential  $V$  such that in these particular coordinates, the event horizons of the black holes are “shrunk down to a point” (Rocek [56]). Alternatively, we can view such solutions as being charged black holes in a Kaluza-Klein background. We can therefore consider ourselves to have one periodic black hole, in analogy with a periodic Dirac monopole [62] or a Kaluza-Klein vortex [53].

Consider the  $(D + 1)$ -dimensional Majumdar-Papapetrou metric given by (7.1) with potential

$$V = 1 + \sum_{j=-\infty}^{\infty} \frac{m_j}{|\vec{r} - \vec{r}_j|^{D-2}}, \quad (7.34)$$

where  $\vec{r} = (x_1, \dots, x_D)$ . Suppose that the point sources in this case are identical and periodically distributed along the  $x_D$ -axis with period  $P$ , yielding

$$V = 1 + \sum_{j=-\infty}^{\infty} m (\rho_{D-1}^2 + (x_D - Pj)^2)^{(1-\frac{D}{2})}. \quad (7.35)$$

In the case of  $D = 4$ , we can simplify the potential to

$$V = 1 + \frac{\pi m}{P\rho_3} \left( \frac{\sinh(2\pi\rho_3 P^{-1})}{\cosh(2\pi\rho_3 P^{-1}) - \cos(2\pi x_4 P^{-1})} \right) \quad (7.36)$$

using contour integration (see Myers [50] and Rocek [56]). We have demonstrated in chapter two that this sum is convergent for all  $D > 4$ .

### The Case $D = 3$

In the case of  $D = 3$ , we hit a problem almost instantly. We have

$$V = 1 + \sum_{j=-\infty}^{\infty} m (\rho_2^2 + (x_3 - Pj)^2)^{-\frac{1}{2}}, \quad (7.37)$$

and we know that such a sum does not converge. Therefore, we cannot construct a compactified solution with infinitely many black holes in four dimensions simply by starting with the construction of Hartle and Hawking [30] for finitely many black holes and letting this number go to infinity.

We might be tempted to try to remedy the situation by subtracting an infinite constant from the potential in order to ensure convergence, yielding a potential

$$V = 1 + m \left( \sum_{j=-\infty}^{\infty} (\rho_2^2 + (x_3 - Pj)^2)^{-\frac{1}{2}} - 2 \sum_{j=1}^{\infty} (Pj)^{-1} \right). \quad (7.38)$$

We know that we can use a finite sum to obtain a good approximation of the above and thus can employ graphical methods to look at its shape. We can see from the diagram below the general shape of such a  $V$ , for  $m > 0$  as required in [30].  $V$  therefore has a zero strip and we know from our analysis earlier that for any given choice of  $x_3$  its behaviour can be successfully approximated near the zero by

$$V_{appx} = c - 2k \ln \rho_2, \quad (7.39)$$

where  $k$  and  $c$  are given by

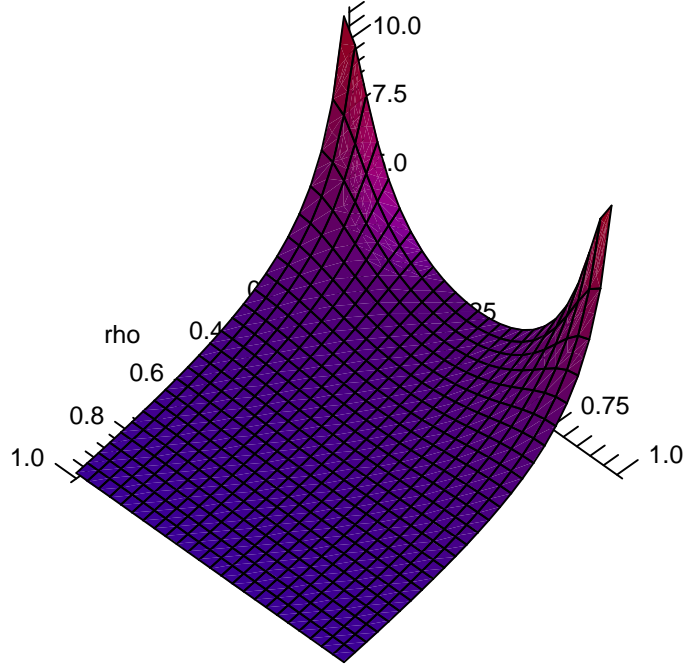


Figure 7.2: The periodic potential with an infinite constant (7.38) for ERN black holes in  $D = 3$  with  $\rho := \rho_2 \in [0, 1]$  and  $x_3 \in [0, 1]$

$$k = -\frac{\rho_{x_3}}{2} \frac{\partial V}{\partial \rho_2} \Big|_{\rho_{x_3}}, \quad c = -\rho_{x_3} \ln(\rho_{x_3}) \frac{\partial V}{\partial \rho_2} \Big|_{\rho_{x_3}}, \quad (7.40)$$

in which we have defined  $\rho_{x_3}$  to be the value of  $\rho_2$  such that  $V(\rho_2, x_3) = 0$ . We can then calculate the Riemann curvature scalar which gives us

$$R_{\mu\nu\rho\sigma} R^{\mu\nu\rho\sigma} = \frac{64k^2(V^2 - 6kV + 14k^2)}{V^8 \rho_2^4}, \quad (7.41)$$

and so when  $V$  is zero, we have a singularity which is not hidden from an observer by any of the black hole horizons and is thus a naked singularity. To demonstrate this, we follow the method outlined in [35] in the section on dilaton solutions, of which this is a special case.

#### The Case $D = 4$

In the case of  $D = 4$ , we follow the work of Myers [50] and therefore have potential

$$V = 1 + \sum_{j=-\infty}^{\infty} m (\rho_3^2 + (x_4 - P_j)^2)^{-1}. \quad (7.42)$$

The Maxwell vector potential is given by

$$A = \frac{\sqrt{3}}{2} V^{-1}. \quad (7.43)$$

We may regard this solution as a charged five-dimensional black hole in a Kaluza-Klein background  $\mathcal{M}^4 \times \mathbb{S}^1$ . To examine this solution further, we consider its short-range behaviour. If we take  $\rho_3, x_4 \ll P$ , we can simplify  $V$  to obtain an expression for a single monopole solution in five-dimensional asymptotically flat Minkowski space plus a constant:

$$V = 1 + \frac{m}{\rho_3^2 + x_4^2} + \underbrace{\frac{\pi^2 m}{3P^2}}_{\text{potential at } r_0 = 0} + \underbrace{O\left(\frac{\rho_3^2}{P^2}, \frac{x_4^2}{P^2}\right)}_{\text{terms that vanish as } r_0 \rightarrow 0}. \quad (7.44)$$

due to all the image sources

where

$$r_0 := \sqrt{x_1^2 + x_2^2 + x_3^2 + x_4^2}. \quad (7.45)$$

The topology of the region  $r_0 < P$  is similar to that of an ERN black hole and the topology, the area of the event horizon and the surface gravity (the acceleration needed to keep an object at the event horizon) are unaffected by the behaviour of the asymptotic exterior region ( $r_0 > P$ ), the topology of which differs as  $x_4$  is periodic. The potential in this case is given by

$$V \rightarrow 1 + \frac{\pi m}{P\rho_3} + \frac{2\pi m}{P\rho_3} \exp(-2\pi\rho_3 P^{-1}) \cos(2\pi x_4 P^{-1}) + \dots \quad \text{as } \rho_3 \rightarrow \infty. \quad (7.46)$$

We can think of the resulting solution as being a kind of electric Kaluza-Klein monopole solution, as opposed to the original Kaluza-Klein monopole which is purely magnetic. This interpretation arises from the fact that we have the magnetic field generated by the Kaluza-Klein field and also the electric (Maxwell) field. As the action contains this Maxwell field, the gauge field here is completely unrelated to that of the Kaluza-Klein case. The Einstein-Maxwell action compactified on  $\mathcal{M}^4 \times \mathbb{S}^1$  and restricted to massless fields as appropriate for the asymptotic region is given by

$$\int \exp(\phi) \left( \frac{P}{4} R^{(4)} - F^{(4)\mu\nu} F_{\mu\nu}^{(4)} \right) (-g^{(4)})^{\frac{1}{2}} d^4x, \quad (7.47)$$

where the gauge field is given by  $A^{(4)} = \sqrt{P}A$  and  $R^{(4)}$  is the Ricci scalar calculated over  $\mu, \nu = 0, 1, 2, 3$ . Note that  $\partial_{x_4}$  is only an asymptotic Killing vector and the dilaton  $\phi$  plays a non-trivial role as  $\exp(2\phi) = g_{x_4 x_4} = V$ .

### The Case $D > 4$

In this final case, the potential is given by,

$$V = 1 + \sum_{j=-\infty}^{\infty} m (\rho_{D-1}^2 + (x_D - Pj)^2)^{\left(1-\frac{D}{2}\right)}. \quad (7.48)$$

We may regard this solution as a charged  $(D + 1)$ -dimensional black hole in a Kaluza-Klein background  $\mathcal{M}^D \times \mathbb{S}^1$ . If we take  $\rho_{D-1}$ ,  $x_D \ll P$ . we can simplify  $V$  to obtain an expression for a single monopole solution in  $(D + 1)$ -dimensional asymptotically flat Minkowski space plus a constant:

$$V = 1 + m (\rho_{D-1}^2 + x_D^2)^{\left(1-\frac{D}{2}\right)} + \underbrace{\frac{2m}{P^2} \sum_{j=1}^{\infty} j^{(2-D)}}_{\text{potential at } r_0 = 0} + \underbrace{O\left(\left(\frac{\rho_{D-1}}{P}\right)^{(2-D)}, \left(\frac{x_D}{P}\right)^{(2-D)}\right)}_{\text{terms that vanish as } r_0 \rightarrow 0}.$$

due to all the image sources

(7.49)

Again, as  $x_D$  is periodic, the topology of the asymptotic exterior region ( $r_0 > P$ ) will differ.

### Singularities for $D \geq 4$ ?

We begin with the metric from the  $(D + 1)$ -dimensional Majumdar-Papapetrou case:

$$ds^2 = -V^{-2}dt^2 + V^{\left(\frac{2}{D-2}\right)}dr^2,$$

$$V = 1 + m \sum_{j=-\infty}^{\infty} (\rho_D^2 + (x_D + Pj)^2)^{\left(1-\frac{D}{2}\right)}, \quad (7.50)$$

which we know converges. For  $D \geq 4$ ,  $V \rightarrow 1$  as  $\rho_D \rightarrow \infty$  and that, as we are dealing with an infinite sum of positive terms,  $V$  is never zero and so we do not have to watch out for unwanted singularities as in the  $D = 3$  case. The Riemann curvature scalar, found as a special case of that for dilaton solutions in section 7.5, is well-behaved. Of course, examining the Riemann curvature tensor is not enough in of itself to show that there are no naked singularities present, but there is good reason to suspect from our analysis that there are indeed no such objects arising in this metric.

### 7.3.2 Black Hole Lattices

Myers [50] constructs a black hole lattice solution as a way of extending his solution with infinitely many black holes in  $(4 + 1)$ -dimensions into higher dimensions. We begin in a background space  $\mathbb{R}^D$  and insert identical monopole sources at points in a  $(D - 3)$ -dimensional

lattice. If we take the basis vectors for this lattice to be the standard basis vectors in  $\mathbb{R}^{(D-3)}$ ,  $\{\vec{e}_1, \dots, \vec{e}_{D-3}\}$  and  $\vec{\omega} = (\omega_1, \dots, \omega_{D-3})$  to be the position vector in the  $(D-3)$ -dimensional background subspace, the potential becomes

$$V = 1 + \sum_{j_i=-\infty}^{\infty} \frac{m}{|\vec{r} - \vec{r}_{j_i}|^{(D-2)}}, \quad (7.51)$$

where

$$|\vec{r} - \vec{r}_{j_i}| = \left( x_1^2 + x_2^2 + x_3^2 + |\vec{\omega} - j_i \vec{e}_i|^2 \right)^{\frac{1}{2}}. \quad (7.52)$$

If we sum over the lattice vertices, we obtain

$$V = 1 + \sum_{j_{D-3}=-\infty}^{\infty} \cdots \sum_{j_1=-\infty}^{\infty} m \left( \rho_3^2 + (\omega_1 + j_1)^2 + \cdots + (\omega_{D-3} + j_{D-3})^2 \right)^{(1-\frac{D}{2})}. \quad (7.53)$$

**Theorem 7.1** The potential (7.53) converges for  $D \geq 4$ .

**Proof** If  $D = 4$ , we have

$$V = 1 + \sum_{j_1=-\infty}^{\infty} m \left( \rho_3^2 + (\omega_1 + j_1)^2 \right)^{-1}, \quad (7.54)$$

which we know converges. In the case of  $D = 5$ , we have

$$\begin{aligned} V &= 1 + m \sum_{j_2=-\infty}^{\infty} \sum_{j_1=-\infty}^{\infty} \left( \rho_3^2 + (\omega_1 + j_1)^2 + (\omega_2 + j_2)^2 \right)^{-\frac{3}{2}} \\ &= 1 + m \lim_{N \rightarrow \infty} \left( \sum_{j_2=-N}^N \sum_{j_1=-\infty}^{\infty} \left( \rho_3^2 + (\omega_1 + j_1)^2 + (\omega_2 + j_2)^2 \right)^{-\frac{3}{2}} \right) \\ &\leq 1 + m \lim_{N \rightarrow \infty} \left( \sum_{j_2=-N}^N c_5(\rho_3) \left( \rho_3^2 + (\omega_2 + j_2)^2 \right)^{-1} \right) \\ &= 1 + m c_5(\rho_3) \sum_{j_2=-\infty}^{\infty} \left( \rho_3^2 + (\omega_2 + j_2)^2 \right)^{-1}, \end{aligned} \quad (7.55)$$

where we have defined

$$c_5(\rho_3) := \rho_3^2 \sum_{j_1=-\infty}^{\infty} \left( \rho_3^2 + (\omega_1 + j_1)^2 \right)^{-\frac{3}{2}}. \quad (7.56)$$

Thus,  $V$  converges by the comparison test.

□



We can see the sensibleness of the step between the second and third lines by considering the two functions

$$f(\rho_3, j_2) = \sum_{j_1=-\infty}^{\infty} \left( \rho_3^2 + (\omega_1 + j_1)^2 + (\omega_2 + j_2)^2 \right)^{-\frac{3}{2}}, \quad (7.57)$$

$$g(\rho_3, j_2) = \rho_3^2 \left( \rho_3^2 + (\omega_2 + j_2)^2 \right)^{-1} \sum_{j_1=-\infty}^{\infty} \left( \rho_3^2 + (\omega_1 + j_1)^2 \right)^{-\frac{3}{2}}, \quad (7.58)$$

and seeing that  $g$  is maximised when  $j_2 = -\omega_2$ , its location is determined by the choice of  $\omega_2$  and that the shape of the curves is dependent on  $\rho$ . When we compare the two functions, we see that  $f \leq g \forall \rho_3$ , as in the diagram below, in which plot  $g - f$  for different choices of  $\rho_3$  (We take  $\omega_1 = \omega_2 = 0$ ).

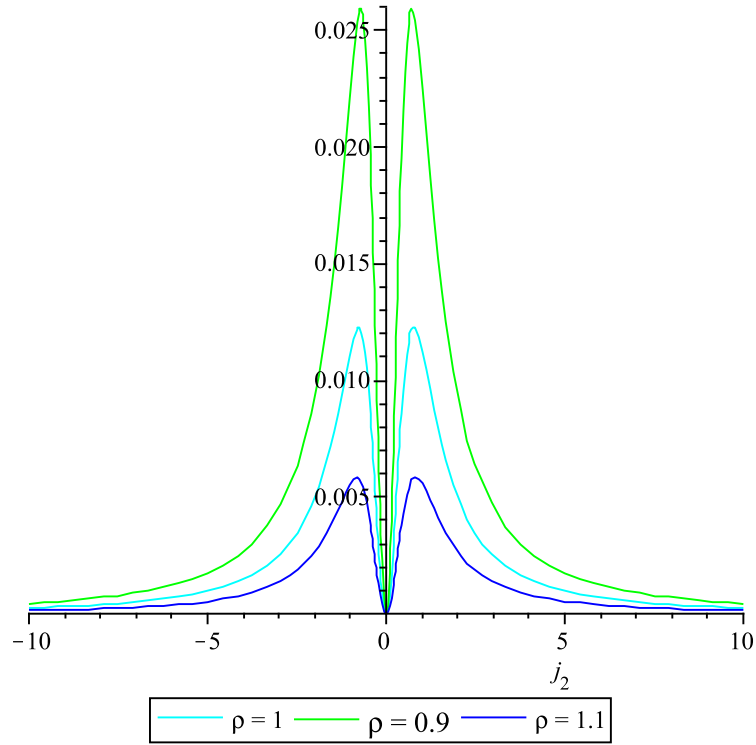


Figure 7.3: Plot of (7.58) - (7.57) for various  $\rho := \rho_3$ , with  $j_2 \in [-10, 10]$

In the case of  $D \geq 5$ , we can use the fact that

$$\begin{aligned} S &:= \sum_{k_1=-\infty}^{\infty} \left( \rho_3^2 + (\omega_1 + k_1)^2 + \cdots + (\omega_n + k_n)^2 \right)^{\left(1 - \frac{i}{2}\right)} \\ &\leq c_i \left( \rho_3^2 + (\omega_2 + k_2)^2 + \cdots + (\omega_n + k_n)^2 \right)^{\left(\frac{3}{2} - \frac{i}{2}\right)} \end{aligned} \quad (7.59)$$

for  $i \geq 5$ ,  $n \geq 2$ , where

$$c_i(\rho_3) := \rho_3^{(i-3)} \sum_{k_1=-\infty}^{\infty} (\rho_3^2 + (\omega_1 + k_1)^2)^{(1-\frac{i}{2})}, \quad (7.60)$$

to see that

$$\begin{aligned} V &\leq 1 + m \left( \prod_{i=5}^D c_i \right) \sum_{j_{D-3}=-\infty}^{\infty} (\rho_3^2 + (\omega_{D-3} + j_{D-3})^2)^{-1} \\ &= 1 + \left( \frac{\pi m}{\rho_3} \right) \left( \prod_{i=5}^D c_i \right) \left( \frac{\sinh(2\pi\rho_3)}{\cosh(2\pi\rho_3) - \cos(2\pi\omega_{D-3})} \right). \end{aligned} \quad (7.61)$$

Thus,  $V$  converges by the comparison test.

□

This yields a solution in a compactified background  $\mathcal{M}^4 \times T^{D-3}$  and we could straightforwardly modify the construction to give other solutions in a compactified background  $\mathcal{M}^{N+1} \times T^{D-N}$  for  $D-1 \geq N \geq 3$ .

In the region surrounding each of the lattice vertices, the black hole solution will look very similar to that of a single black hole in  $(D+1)$ -dimensions and quantities such as the surface gravity and the area of the event horizon are unchanged in the uncompactified space. However, the asymptotic region is more complicated because some of the dimensions are compact. We can get some idea of the long-range behaviour of the potential by replacing the discrete sums by an integral

$$V \approx 1 + \frac{m}{\kappa} \int \frac{d\vec{\omega}}{(\rho_3^2 + |\vec{\omega}|^2)^{(\frac{D}{2}-1)}} = 1 + \frac{m}{\kappa} \frac{\pi^{(\frac{D}{2}-1)}}{\Gamma(\frac{D}{2}-1)} \rho^{-1}, \quad (7.62)$$

where  $\kappa$  is the asymptotic volume of the compactified torus  $T^{D-3}$ . The ratio of mass and charge in this situation is given by

$$\frac{|Q|}{m} = \left( \left( \frac{N-2}{N-1} \right)^2 \frac{D-1}{D-2} \right)^{\frac{1}{2}}, \quad (7.63)$$

where the above is for the case when we reduce the  $(D+1)$ -dimensional theory to the background with  $(N+1)$  uncompactified dimensions.

### 7.3.3 Non-Periodic Distributions of Black Holes

Here we will construct a solution with infinitely many black holes distributed unevenly along one of the axes in a  $(D+1)$ -dimensional Majumdar-Papapetrou metric (7.1). In order to do

this, we will modify the construction of Anderson et al [1] which we looked at in the previous chapter, in which infinitely many instantons are unevenly distributed along one of the axes. This can be extended to generate solutions with black holes unevenly distributed through several dimensions.

### Uneven Distributions of Black Holes

We now generate a solution with infinitely many black holes distributed unevenly along one of the axes in a  $(D + 1)$ -dimensional Majumdar-Papapetrou metric (7.1). Each of our monopole sources will be identical, and have mass (charge)  $m > 0$ . Let  $\{\vec{r}_j\}_{j=0}^\infty \subset \mathbb{R}^D$  be a divergent sequence of points such that for some point  $\vec{r}_0 \in \mathbb{R}^D$ ,

$$1 + \sum_{j=1}^{\infty} \frac{m}{|\vec{r}_0 - \vec{r}_j|^{D-2}} < \infty. \quad (7.64)$$

We can then define a smooth function  $V : \mathbb{R}^D / \{\vec{r}_j\} \rightarrow \mathbb{R}$  by

$$V(r) := 1 + \sum_{j=1}^{\infty} \frac{m}{|\vec{r} - \vec{r}_j|^{D-2}}. \quad (7.65)$$

Clearly,  $V$  satisfies the Laplace equation on  $\mathbb{R}^D$ :

$$\nabla^2 V = \frac{\partial^2 V}{\partial(x_1)^2} + \cdots + \frac{\partial^2 V}{\partial(x_D)^2} = 0. \quad (7.66)$$

In Anderson et al's work, much attention needs to be given to the issue of smoothness at the points  $\vec{r}_j$ . However, in this context, we know that the metric (7.1) is regular at  $\vec{r} = \vec{r}_j$  and that these are the event horizons for the black holes, which enough to ensure that this construction makes sense.

As an example, suppose that the black holes are distributed along the  $x_D$  axis, so that the identical monopole sources are positioned at the points

$$\{\vec{r}_j = (0, \dots, 0, j^{1+\epsilon})\}_{j=1}^\infty \quad (7.67)$$

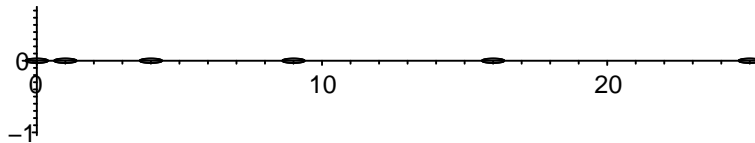


Figure 7.4: Non-periodic distribution (7.67) of black holes along  $x_D$ -axis

for some  $\epsilon > 0$ . Then we can define a function as above, such that at the point  $\vec{r}_0 := 0$ , we have

$$1 + \sum_{j=1}^{\infty} \frac{m}{\|\vec{r}_0 - \vec{r}_j\|^{D-2}} = 1 + \sum_{j=1}^{\infty} \frac{m}{(j^{1+\epsilon})^{D-2}} < \infty \quad (7.68)$$

for  $D \geq 3$ . We can then define a function  $V$  by (using the definition of  $\rho_n$  given in (1.3)),

$$V(r) := 1 + \sum_{j=1}^{\infty} \frac{m}{|\vec{r} - \vec{r}_j|^{D-2}} = 1 + \sum_{j=1}^{\infty} \frac{m}{\left(\rho_{D-1}^2 + (x_D - j^{1+\epsilon})^2\right)^{\left(\frac{D}{2}-1\right)}}, \quad (7.69)$$

which again converges for  $D \geq 3$ . If we were to take  $\epsilon = 0$ , then we would find ourselves back in the situation of having periodically distributed black holes, and thus no solution for  $D = 3$  due to the lack of convergence of  $V$ . We can extend this to construct a two-dimensional solution:

$$\left\{ \vec{r}_j = \left( 0, \dots, 0, j^{1+\epsilon} \cos\left(\frac{2\pi k}{n}\right), j^{1+\epsilon} \sin\left(\frac{2\pi k}{n}\right) \right) \right\}_{j=1}^{\infty} \quad (7.70)$$

for some  $\epsilon > 0$  and with  $k \in \{0, \dots, n-1\}$  and  $n \in \mathbb{N}$ . We then have, for  $\vec{r}_0 := 0$ ,

$$1 + \sum_{j=1}^{\infty} \frac{m}{\|\vec{r}_0 - \vec{r}_j\|^{D-2}} = 1 + \sum_{j=1}^{\infty} \frac{m}{\left(j^{2+2\epsilon} \left(\cos^2\left(\frac{2\pi k_1}{n}\right) + \sin^2\left(\frac{2\pi k_2}{n}\right)\right)\right)^{\left(\frac{D}{2}-1\right)}} = \sum_{j=1}^{\infty} \frac{m}{(j^{1+\epsilon})^{D-2}}, \quad (7.71)$$

which converges for  $D \geq 3$  as we fix  $n$  and always have  $k_1 = k_2$ . This is illustrated in the diagram below. We can then define a function  $V$  by

$$\begin{aligned} V &= 1 + \sum_{j=1}^{\infty} \frac{m}{\|\vec{r} - \vec{r}_j\|^{D-2}} \\ &= 1 + \sum_{j=1}^{\infty} \frac{m}{\left(\rho_{D-2}^2 + (x_{D-1} - j^{1+\epsilon} \cos\left(\frac{2\pi k}{n}\right))^2 + (x_D - j^{1+\epsilon} \sin\left(\frac{2\pi k}{n}\right))^2\right)^{\left(\frac{D}{2}-1\right)}}, \end{aligned} \quad (7.72)$$

which converges for  $D \geq 3$ . This could be further extended into higher dimensions, by having the black holes positioned on  $\mathbb{S}^n$  spheres with radii increasing in an  $r = j^{1+\epsilon}$  way. Note that the results in our section on dilaton theory for the Riemann curvature scalar for  $D \geq 4$  hold for these examples. We can see from these that the curvature is well-behaved and no singularities arise as  $V$  cannot become zero.

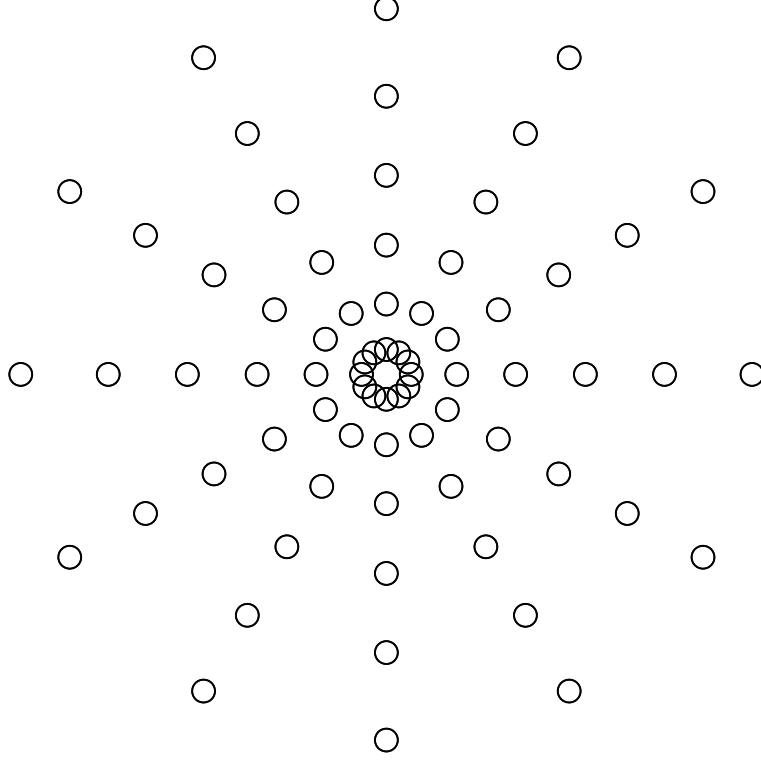


Figure 7.5: Non-periodic distribution (7.70) of black holes in two-dimensions

## 7.4 Smoothness of Event Horizons

In this section, we outline the work of Candlish and Reall [4], which looks at the smoothness of event horizons in multiple black hole solutions. We will see that in five dimensions, the horizons are smooth for all black holes in our infinite periodic solution, and otherwise are  $C^2$  but not  $C^3$ . In higher dimensions, the horizon is  $C^0$  but not  $C^1$ . To begin, we write the Majumdar-Papapetrou metric in spherical coordinates:

$$ds^2 = -V^{-2}dt^2 + V^{\left(\frac{2}{2-D}\right)} (dr^2 + r^2d\theta^2 + r^2 \sin^2 \theta d\Omega_{D-2}^2), \quad (7.73)$$

where  $d\Omega_{D-2}^2$  is the metric on the  $(D-2)$ -sphere. In these coordinates, the potential is given by

$$V = 1 + \frac{\mu_1}{r^{D-2}} + \sum_{j=2}^N \frac{\mu_j}{\left(r^2 + a_j^2 - 2a_j r \cos \theta\right)^{\left(\frac{D}{2}-1\right)}} = \frac{\mu_1}{r^{D-2}} + \sum_{n=0}^{\infty} h_n r^n Y_n(\cos \theta), \quad (7.74)$$

where the  $Y_n(\cos \theta)$  are the Gegenbauer polynomials,  $a_j$  gives the position along the axis of the  $j$ th black hole and the coefficients  $h_n$  are given by

$$h_n = \delta_{n,0} + \sum_{j=2}^N \frac{\mu_j}{|a_j|^{D-2} a_j^n}. \quad (7.75)$$

In order to look at the degree of smoothness of the event horizon, one must write both the exterior and interior metrics in **Gaussian null coordinates** and look at the order of magnitude up to which the two expressions agree.

#### 7.4.1 Gaussian Null Coordinates

In order to construct Gaussian null coordinates, we employ the following procedure. The intersection  $H^0$  of a hypersurface with a single component of the event horizon  $\mathcal{H}_0^+$  is topologically a sphere  $\mathbb{S}^{D-1}$ , onto which we introduce coordinates  $x^i$ . Define a coordinate  $v$  on  $\mathcal{H}_0^+$  to be the parameter distance from  $H_0$  along integral curves of  $U$ , which denotes the generator of time translations and is tangent to the null geodesic generators of  $\mathcal{H}_0^+$ . Now let  $W$  be the unique null vector satisfying

$$W \cdot U = 1 \quad \text{and} \quad W \cdot \frac{\partial}{\partial x^i} = 0 \quad (7.76)$$

on  $\mathcal{H}_0^+$ .  $\gamma(v, x^i)$  is defined to be the null geodesic that starts at  $(v, x^i)$  in  $\mathcal{H}_0^+$  and has tangent  $W$  there. We define Gaussian null coordinates in a neighbourhood of  $H_0$  by ascribing coordinates  $(v, \lambda, x^i)$  to the point which is a distance  $\lambda$  from  $\mathcal{H}_0^+$  along  $\gamma(v, x^i)$ . We can take  $x^i = (\Theta, \hat{\Omega}_{D-2})$ , which are the limiting values of  $(\theta, \Omega_{D-2})$  along  $\gamma$  as it approaches  $\mathcal{H}_0^+$ . The  $\text{SO}(D-1)$  symmetry implies that  $\Omega_{D-2} \equiv \hat{\Omega}_{D-2}$  but  $\Theta$  and  $\theta$  will not agree. In these coordinates, the metric has form

$$ds^2 = -V^{-2}dv^2 + 2dv d\lambda + \lambda f_1(\lambda, \Theta)dv d\Theta + f_2(\lambda, \Theta)d\Theta^2 + V^{\left(\frac{2}{D-2}\right)} r^2 \sin^2 \theta d\Omega_{D-2}, \quad (7.77)$$

where  $r = r(\lambda, \Theta)$  and  $\theta = \theta(\lambda, \Theta)$  are determined once we know  $\gamma$ . The problem then reduces to solving

$$0 = -V^2 + V^{\left(\frac{2}{D-2}\right)} \left( \dot{r}^2 + r^2 \dot{\theta}^2 \right), \quad (7.78)$$

$$\ddot{r} - V^{\left(\frac{D-4}{D-2}\right)} \partial_r V + \frac{V^{-1}}{D-2} \left( \dot{r}^2 \partial_r V - r^2 \dot{\theta}^2 \partial_r V + 2\dot{r}\dot{\theta} \partial_\theta V \right) - r \dot{\theta}^2 = 0 \quad (7.79)$$

with initial conditions

$$r(0, \Theta) = 0, \quad \theta(0, \Theta) = \Theta, \quad \left. \left( \frac{d\theta}{d\lambda} \right) \right|_{\lambda=0} = 0, \quad (7.80)$$

which yields

$$t = v - T(\lambda, \Theta), \quad T(\lambda, \Theta) \equiv \int V(\lambda, \Theta)^2 d\lambda. \quad (7.81)$$

In the case of  $D = 4$ , this means the horizon is  $C^2$  but can be shown not to be  $C^3$ ; in the case of  $D > 4$ , this means the horizon is  $C^0$  but can be shown not to be  $C^1$ . Let us explore the first of these cases, that of  $D = 4$ .

#### 7.4.2 Smoothness of Horizons for $D = 4$

We first note that solving the geodesic equations as described above and imposing the same initial conditions, we have the following expansions for  $r(\lambda, \Theta)$  and  $\theta(\lambda, \Theta)$ :

$$\begin{aligned} r &= \sqrt{2}\mu_1^{\frac{1}{4}}\lambda^{\frac{1}{2}} + \frac{h_0}{2\sqrt{2}\mu_1^{\frac{1}{4}}}\lambda^{\frac{3}{2}} + \mathcal{O}(\lambda^2), \\ \theta &= \Theta - \frac{2\sqrt{2}h_1 \sin \Theta}{\mu_1^{\frac{1}{4}}}\lambda^{\frac{3}{2}} + \mathcal{O}(\lambda^2). \end{aligned} \quad (7.82)$$

We consider the area of the 2-sphere orbits of the  $\text{SO}(3)$  symmetry present in the geometry, which is given by

$$A_2 = Vr^2 \sin^2 \theta. \quad (7.83)$$

We can see how  $A_2$  varies along  $\gamma$  as it approaches the horizon using our expressions for  $r$  and  $\theta$ . We have

$$\begin{aligned} A_2 &= \mu_1 \sin^2 \Theta + 2h_0\sqrt{\mu_1} \sin^2 \Theta \lambda + (h_0^2 - 4h_2\mu_1 \sin^2 \Theta) \sin^2 \Theta \lambda^2 \\ &\quad - \frac{128\sqrt{2}}{5}h_3\mu_1^{\frac{5}{4}} \sin^2 \Theta \cos \Theta \lambda^{\frac{5}{2}} + \mathcal{O}(\lambda^3). \end{aligned} \quad (7.84)$$

The presence of  $\mathcal{O}(\lambda^{\frac{5}{2}})$  terms indicates that  $A_2$  is not  $C^3$  at  $\lambda = 0$  as that would require  $h_3 = 0$  which (7.75) demonstrates is not the case for a multi-centre solution except in very rare circumstances. Hence the generic solution is not  $C^3$ . To show that it is  $C^2$  in a neighbourhood of the horizon, we compare the metric in the exterior and interior regions. In both cases, the metric will have the form of (7.73) but in the exterior region the potential will be  $V$  and in the interior region  $\hat{V}$ :

$$V = \frac{\mu_1}{r^2} + \sum_{n=0}^{\infty} h_n r^n Y_n(\cos \theta), \quad \hat{V} = \frac{\mu_1}{r^2} + \sum_{n=0}^{\infty} \hat{h}_n r^n Y_n(\cos \theta). \quad (7.85)$$

In the exterior region,  $\lambda > 0$  is the affine parameter along a past-directed geodesic  $\gamma$ . In the interior region,  $\hat{\lambda}$  is the affine parameter along a future-directed geodesic  $\hat{\gamma}$  with otherwise

the same properties as  $\gamma$ . We can then define Gaussian null coordinates as above, with  $v$  defined by

$$t = v + \hat{T}(\hat{\lambda}, \Theta), \quad \hat{T}(\hat{\lambda}, \Theta) \equiv \int \hat{V}(\hat{\lambda}, \Theta)^2 d\hat{\lambda}. \quad (7.86)$$

If we make the identification  $\lambda = -\hat{\lambda}$ , then comparing the interior and exterior metrics shows us that they match up in a  $C^2$  manner, which means up to  $\mathcal{O}(|\lambda|^{\frac{5}{2}})$ , provided that

$$\hat{h}_0 = -h_0, \quad \hat{h}_2 = h_2, \quad (7.87)$$

with the other coefficients unconstrained.

### 7.4.3 Reflection-Symmetric Solutions

In the case of  $D = 4$ , we can increase the differentiability in certain circumstances. Suppose the sources are **reflection-symmetric**, so we have  $N = 2M + 1$  black holes with parameters  $(\mu_1, 0), (\mu_j, \pm a_j), j = 2, \dots, M + 1$ . Then  $h_{2n+1} = 0$  for all  $n$  and we can write  $V$  as

$$V = V_0 + V_1, \quad V_0 = \frac{\mu_1}{r^2} + h_0, \quad V_1 = \sum_{n=1}^{\infty} h_{2n} r^{2n} Y_{2n}(\cos \theta), \quad (7.88)$$

so we just concentrate on the even terms. We now construct an analytic extension through  $r = 0$ . Define  $\lambda > 0$  by

$$\frac{dr}{d\lambda} = \sqrt{V_0}, \quad (7.89)$$

yielding

$$r = (2\sqrt{\mu_1}\lambda + h_0\lambda^2)^{\frac{1}{2}}. \quad (7.90)$$

We can then define the coordinate  $v$  by

$$dt = dv - V_0(\lambda)^2 d\lambda. \quad (7.91)$$

The solution in Gaussian null coordinates  $(v, \lambda, \theta)$  is analytic at  $\lambda = 0$  and thus can be extended into the region with  $\lambda < 0$ . We can define new coordinates in the interior of the black hole:

$$r = (-2\sqrt{\mu_1}\lambda - h_0\lambda^2)^{\frac{1}{2}} \quad (7.92)$$

and  $t$  as in the above equation. This puts the solution into a form like (7.73) with a new harmonic function



$$\tilde{V}(r, \theta) = -V(ir, \theta). \quad (7.93)$$

The analyticity of the solution determines not just  $\tilde{h}_0$  but the higher coefficients  $\tilde{h}_{2n}$  too. The solution is analytic at the horizon of the black hole at  $r = 0$ . To ensure this is the case for the rest of the black holes, we need an infinite string ( $N \rightarrow \infty$ ) of evenly spaced black holes.

#### 7.4.4 Consequences

Candlish and Reall argue in a later section of the paper that there is no higher dimensional analogue of the smoothness enhancement of the  $D = 4$  case. We therefore concentrate our attention on the  $D = 4$  case and look at our three solutions with infinitely many black holes thus far:

- In the periodic case, we have a solution with infinitely many black holes evenly distributed along one of the axes. This is the situation described in the smoothness enhancement case and so each of the black holes will have a smooth event horizon.
- In the lattice case, we are adapting the smoothness theory as Candlish and Reall's work assumes the black holes will lie on an axis. We can think of our lattice as containing a series of grids of black holes, with each grid containing rows of infinitely many black holes. In other words, we have a collection of reflection-symmetric structures and the overall structure will be reflection-symmetric. We should therefore expect all the black holes to have smooth horizons.
- In the non-periodic case, the central black hole will have a smooth horizon but because of the uneven spacing, this will not be the case for any of the other black holes.

## 7.5 Einstein-Maxwell-Dilaton Theory

In this section, we examine a generalisation of the Extreme Reissner-Nordström black holes by looking at **Einstein-Maxwell-dilaton theory**. The action in this case is given by, for  $(D + 1)$ -dimensions [59],

$$S = \int d^{D+1}x \frac{\sqrt{-g}}{16\pi} \left( R - \frac{4(\nabla\phi)^2}{D-1} - \exp\left(\frac{-4a\phi}{D-1}\right) F^2 \right), \quad (7.94)$$

where  $\phi$  denotes the dilaton field,  $F^{\mu\nu}$  the Maxwell field strength and  $a$  the dilaton coupling constant, which we can assume without loss of generality to be positive. The solutions we will consider will be extreme black holes, and the extremity condition here is that the ratio of mass to charge needs to be

$$\kappa := \frac{|Q|}{m} = \frac{4\pi\Gamma\left(\frac{D}{2}\right)}{\pi^{\frac{D}{2}}} \left(\frac{D-2+a^2}{2(D-1)}\right)^{\frac{1}{2}}. \quad (7.95)$$

### 7.5.1 Finitely Many Black Holes

We begin by looking in detail at the case of  $D = 3$  and have, for a single extreme black hole [18],

$$\begin{aligned} ds^2 &= -\left(1 - \frac{\mu}{r}\right)^{\left(\frac{2}{1+a^2}\right)} dt^2 + \left(1 - \frac{\mu}{r}\right)^{\left(\frac{-2}{1+a^2}\right)} dr^2 + \left(1 - \frac{\mu}{r}\right)^{\left(\frac{2a^2}{1+a^2}\right)} r^2 d\Omega^2, \\ \vec{A} &= \pm (1+a^2)^{-\frac{1}{2}} \left(1 - \frac{\mu}{r}\right)^{-1} dt, \\ \exp(-2a\phi) &= \left(1 - \frac{\mu}{r}\right)^{\left(\frac{2a^2}{1+a^2}\right)}, \end{aligned} \quad (7.96)$$

where the constant  $\mu$  is related to the mass and charge by

$$\mu = (1+a^2)m = (1+a^2)^{\frac{1}{2}}|Q|. \quad (7.97)$$

The electric repulsion is balanced out by the gravitational attraction and the attractive dilaton force, so we can regard this solution as an extension of the Majumdar-Papapetrou solutions.

If we calculate the Riemann curvature scalar

$$[R]^2 = \frac{4\mu^2 \left(12r^2 (a^2+1)^2 + 2\mu (\mu - 16ra^2) (a^2+1) + 7a^4\mu^2\right)}{(a^2+1)^4 r^4 (r-\mu)^4 \left(1 - \frac{\mu}{r}\right)^{\left(\frac{4}{1+a^2}\right)}}, \quad (7.98)$$

then we see that the metric is singular when  $r = 0$  and appears to be so when  $r = \mu$  if  $a \neq 0$ .

However, we can resolve the dilaton singularity in some cases by reinterpreting the solution as representing an extremal object in a higher-dimensional spacetime, following the method of Gibbons et al [18], meaning we can view (7.96) as the double-dimensional reduction of

$$ds^2 = \left(1 - \frac{\mu}{r}\right)^{\left(\frac{2}{1+p}\right)} (-dt^2 + d\vec{r}'^2) + \left(1 - \frac{\mu}{r}\right)^{-2} dr^2 + r^2 d\Omega^2, \quad (7.99)$$

where  $p \in \mathbb{Z}$  and  $\vec{r}' = (x_5, \dots, y_{4+p})$  are the additional coordinates. We begin with the  $(4+p)$ -dimensional Einstein-Maxwell action

$$S_{4+p} = \int d^{4+p}x \sqrt{-g} \{R - F_2^2\}, \quad (7.100)$$

where we have

$$\begin{aligned} ds_{4+p}^2 &= \exp(2\alpha\phi) d\vec{r}'^2 + \exp(2\beta\phi) g_{\mu\nu} dx^\mu dx^\nu, \\ F_2^{4+p} &= \frac{1}{2} F_{\mu\nu}(x) dx^\mu \wedge dx^\nu, \end{aligned} \quad (7.101)$$

with  $\mu, \nu = 0, 1, 2, 3$ . This action reduces to the four-dimensional action

$$S = (16\pi) \int d^4x \sqrt{-g} \left\{ R - \frac{1}{2} p(p+2) \alpha^2 (\nabla\phi)^2 - \exp(pa\phi) F_2^2 \right\}, \quad (7.102)$$

where we have  $2\beta + p\alpha = 0$  so that the metric has a canonical Einstein-Hilbert action. By choosing

$$\alpha = \frac{-2}{\sqrt{p(p+2)}}, \quad (7.103)$$

we recover the action (7.94) for  $D = 3$  with dilaton coupling constant

$$a = \beta = \sqrt{\frac{p}{p+2}}. \quad (7.104)$$

Thus, for these values of  $a$ , any solution of the Euler-Lagrange equations of (7.94) can be interpreted as a solution of the Euler-Lagrange equations of the  $(4+p)$ -dimensional action (7.100) with metric

$$ds^2 = \exp(2(a - a^{-1})\phi) d\vec{r}^2 + \exp(2a\phi) g_{\mu\nu} dx_\mu dx_\nu. \quad (7.105)$$

If  $p$  is even,  $r = \mu$  is an event horizon and we have a black hole. If  $p$  is odd, we have a non-singular space. In order to construct a multiple black hole solution, we follow a similar argument to that used for ERN black holes, using the coordinate transformation

$$r = \rho - \kappa m, \quad (7.106)$$

yielding

$$\begin{aligned} ds^2 &= -V^{-\left(\frac{2}{1+a^2}\right)} dt^2 + V^{\left(\frac{2}{1+a^2}\right)} d\vec{r}^2, \\ \vec{A} &= -(1+a^2)^{-\frac{1}{2}} V^{-1} dt, \\ \exp(-2a\phi) &= V^{\left(\frac{2a^2}{1+a^2}\right)}, \end{aligned} \quad (7.107)$$

where the potential  $V$  is given by [60]

$$V = 1 + \sum_{j=1}^N (1+a^2) m_j |\vec{r} - \vec{r}_j|^{-1}, \quad (7.108)$$

so the  $j$ -th static extreme black hole is located at  $\vec{r}_j$  and has mass  $m_j$ .

### Higher-Dimensional Solutions

Shiraishi [59] generalises this solution to  $(D + 1)$ -dimensions for  $D \geq 4$ . In this case, the metric is given by

$$\begin{aligned}
 ds^2 &= -U^{-2}dt^2 + U^{\left(\frac{2}{D-2}\right)}d\vec{r}^2, \\
 U &= V^{\left(\frac{D-2}{D-2+a^2}\right)} \quad \text{with} \quad V = 1 + (D-2)^{-1} \sum_{j=1}^N \mu_j |\vec{r} - \vec{r}_j|^{2-D}, \\
 A &= \pm \left( \frac{D-1}{2(D-2+a^2)} \right)^{\frac{1}{2}} V^{-1}dt \quad \text{and} \quad \exp\left(\frac{-4a\phi}{D-1}\right) = V^{\left(\frac{2a^2}{D-2+a^2}\right)}, \quad (7.109)
 \end{aligned}$$

where  $\mu_j$  is related to the mass and charge by

$$m_j = \frac{\pi^{\frac{D}{2}}(D-1)}{4\pi\Gamma\left(\frac{D}{2}\right)(D-2+a^2)}\mu_j, \quad |Q| = \left( \frac{D-1}{2(D-2+a^2)} \right)^{\frac{1}{2}} \mu_j. \quad (7.110)$$

The above argument concerning the re-interpretation of the dilaton singularities can be extended to higher dimensions [18].

### Special Cases

As we have noted, there are certain values of  $a$  for which the dilaton singularity is resolved, namely those for which  $a$  takes the form (7.104) for  $p \in \mathbb{Z}$ . We note some interesting cases:

- if  $a = 0$  then we obtain the  $(D + 1)$ -dimensional Majumdar-Papapetrou solutions of Hartle and Hawking [30] for  $D = 3$  and of Myers [50] for  $D \geq 4$ ;
- if  $a = 1$  we get a string theory solution in which the singularities and event horizons disappear in the extremal case [14];
- if  $a = \frac{1}{\sqrt{3}}$ , it corresponds to the reduction of five-dimensional Einstein-Maxwell or supergravity theory to four dimensions [60];
- if  $a = \sqrt{3}$ , we obtain five-dimensional Kaluza-Klein theory [18].

### 7.5.2 Infinitely Many Black Holes

We now move to consider what happens when we have infinitely many identical black holes. The potential becomes

$$V = 1 + \frac{4m\pi\Gamma\left(\frac{D}{2}\right)(D-2+a^2)}{(D-1)(D-2)} \sum_{j=-\infty}^{\infty} |\vec{r} - \vec{r}_j|^{2-D}. \quad (7.111)$$

We will investigate three cases. Firstly, a periodic distribution. This converges for  $D \geq 4$  and we have a well-behaved spacetime but does not converge for  $D = 3$  and using an infinite constant to ensure convergence gives rise to naked singularities. Secondly, a non-periodic distribution, adapting the method of Anderson et al [1] as before. Thirdly, we will construct a lattice of black holes. The latter two are trivial adaptations of the ERN case. Note that the event horizons will be smooth in the periodic and lattice cases and not in the non-periodic case.

### Periodic Distribution : $D = 3$

Suppose that the sources are periodically distributed along the  $x_3$ -axis

$$V = 1 + m \sum_{j=-\infty}^{\infty} (1 + a^2) (\rho_2^2 + (x_3 - Pj)^2)^{-\frac{1}{2}}, \quad (7.112)$$

This obviously does not converge and in order to make it converge, we subtract an infinite constant from the potential, yielding

$$V = 1 + m(1 + a^2) \left( \sum_{j=-\infty}^{\infty} (\rho_2^2 + (x_3 - Pj)^2)^{-\frac{1}{2}} - 2 \sum_{j=1}^{\infty} (Pj)^{-1} \right). \quad (7.113)$$

As  $m > 0$  and  $a \geq 0$ ,  $V$  has a zero strip and we know from our analysis in chapter three that for any given choice of  $x_3$  its behaviour can be successfully approximated near the zero by

$$V_{approx} = c - 2k \ln \rho_2, \quad (7.114)$$

where  $k$  and  $c$  are given by

$$k = - \left. \frac{\rho_{x_3}}{2} \frac{\partial V}{\partial \rho_2} \right|_{\rho_{x_3}}, \quad c = - \rho_{x_3} \ln(\rho_{x_3}) \left. \frac{\partial V}{\partial \rho_2} \right|_{\rho_{x_3}}, \quad (7.115)$$

in which we have defined  $\rho_{x_3}$  to be the value of  $\rho_2$  such that  $V(\rho_2, x_3) = 0$ . We can then calculate the Riemann curvature scalar which gives us

$$[R]^2 = \frac{64k^2 (V^2(a^2 + 1)^2 - 2kV(a^2 + 1)(a^2 + 3) + k^2(3a^4 + 10a^2 + 14))}{(1 + a^2)^4 \rho_2^4 V \left( \frac{4(2+a^2)}{1+a^2} \right)} \quad (7.116)$$

which, when  $a = 0$  reduces to the result for the ERN solution in  $(3 + 1)$ -dimensions,

$$[R]^2 = \frac{64k^2(V^2 - 6kV + 14k^2)}{V^8 \rho_2^4}. \quad (7.117)$$

Thus, when  $V$  is zero, we have a naked singularity. To demonstrate this, we begin by considering the external metric with  $V > 0$ :

$$ds^2 = -V^{-\left(\frac{2}{1+a^2}\right)} dt^2 + V^{\left(\frac{2}{1+a^2}\right)} dr^2. \quad (7.118)$$

We work with null radial geodesics, and thus have

$$t = t(s), \quad x := x_1(s), \quad x_2 = x_3 = x_4 = 0. \quad (7.119)$$

The metric then becomes

$$ds^2 = -V^{-\left(\frac{2}{1+a^2}\right)}(x) dt^2 + V^{\left(\frac{2}{1+a^2}\right)}(x) dx^2, \quad (7.120)$$

and therefore the Lagrangian is

$$\mathcal{L} = -V^{-\left(\frac{2}{1+a^2}\right)}(x) \dot{t}^2 + V^{\left(\frac{2}{1+a^2}\right)}(x) \dot{x}^2 = 0. \quad (7.121)$$

The geodesic equations, given by the Euler-Lagrange equations, are

$$\begin{aligned} \frac{d}{ds} \left( -2V^{-\left(\frac{2}{1+a^2}\right)}(x) \dot{t} \right) &= 0, \\ \frac{d}{ds} \left( 2V^{\left(\frac{2}{1+a^2}\right)}(x) \dot{x} \right) + \dot{t}^2 \frac{d}{dx} \left( V^{-\left(\frac{2}{1+a^2}\right)}(x) \right) - \dot{x}^2 \frac{d}{dx} \left( V^{\left(\frac{2}{1+a^2}\right)}(x) \right) &= 0. \end{aligned} \quad (7.122)$$

If we define

$$E := V^{-\left(\frac{2}{1+a^2}\right)} \dot{t}, \quad (7.123)$$

then we have

$$\dot{E} = 0 \quad \text{and} \quad \dot{x}^2 = E^2 \quad \Rightarrow \quad \frac{dt}{dx} = \frac{\dot{t}}{\dot{x}} = \pm V^{\left(\frac{2}{1+a^2}\right)}. \quad (7.124)$$

This gives us, if we employ our approximation to  $V$ ,  $V_{appx}$ ,

$$x = x_c \pm Es, \quad (7.125)$$

and

$$\begin{aligned} t &= \pm \int V^{\left(\frac{2}{1+a^2}\right)} dx \\ &= \pm \int (c - 2k \ln x)^{\left(\frac{2}{1+a^2}\right)} dx. \end{aligned} \quad (7.126)$$

We consider outgoing geodesics when we consider the positive case and for incoming geodesics the negative case. As  $x$  approaches  $x_0$ , which is the value of  $x$  such that  $V$  is zero, we see that this happens for a finite value of the parameter  $s$  and that  $t$  is finite. This means that

a photon can reach a large distance away from the singularity in a finite time and hence the singularity is naked. The same analysis applies to the interior metric as  $V < 0$  still yields a Lorentzian metric.

**Periodic Distribution :  $D \geq 4$**

We have the metric

$$ds^2 = -V^{\left(\frac{4-2D}{D-2+a^2}\right)} dt^2 + V^{\left(\frac{2}{D-2+a^2}\right)} d\tilde{r}^2, \quad (7.127)$$

$$V = 1 + \frac{4m\pi\Gamma\left(\frac{D}{2}\right)(D-2+a^2)}{(D-1)(D-2)} \sum_{j=-\infty}^{\infty} (\rho_{D-1}^2 + (x_D - Pj)^2)^{\left(1-\frac{D}{2}\right)},$$

which we know from earlier converges. As the coefficient before the sum is always positive as we assume  $m > 0$ , then as in the ERN case, we do not need to worry about singularities arising from  $V$  becoming zero. To understand the singularity structure, we proceed to calculate the Riemann curvature scalar by writing the metric in a generalised form of cylindrical coordinates:

$$ds^2 = -V^{\left(\frac{4-2D}{D-2+a^2}\right)} dt^2 + V^{\left(\frac{2}{D-2+a^2}\right)} (ds_{D-1}^2 + dx_D^2), \quad (7.128)$$

where  $\phi \in [0, 2\pi]$ ,  $\theta_i \in [0, \pi]$  and

$$\begin{aligned} x_1 &= \rho_n \cos \phi \sin \theta_1 \sin \theta_2 \cdots \sin \theta_{n-2}, \\ x_2 &= \rho_n \sin \phi \sin \theta_1 \sin \theta_2 \cdots \sin \theta_{n-2}, \\ x_3 &= \rho_n \cos \theta_1 \sin \theta_2 \cdots \sin \theta_{n-2}, \\ &\vdots \\ x_i &= \rho_n \cos \theta_{i-2} \sin \theta_{i-1} \cdots \sin \theta_{n-2}, \\ &\vdots \\ x_n &= \rho_n \cos \theta_{n-2}, \end{aligned} \quad (7.129)$$

yielding the part of the metric in  $n$ -dimensional polar coordinates

$$ds_n^2 = d\rho_n^2 + \rho_n^2 d\theta_{n-2}^2 + \rho_n^2 \sin^2 \theta_{n-2} d\theta_{n-3}^2 + \cdots + \rho_n^2 \sin^2 \theta_{n-2} \cdots \sin^2 \theta_1 d\phi^2. \quad (7.130)$$

We fix the value of  $x_D$  so that we can assume  $V = V(\rho)$ , which gives us

$$[R]^2 = \frac{4 \left( \tilde{a}\rho_{D-1}^2 + \tilde{b}\rho_{D-1} + \tilde{c} \right)}{(D-2+a^2)^4 \rho_{D-1}^2 V^{\left(\frac{4(D-1+a^2)}{D-2+a^2}\right)}}, \quad (7.131)$$

where

$$\begin{aligned}\tilde{a} &= a_1(\partial_{\rho_{D-1}}V)^4 + a_2V\partial_{\rho_{D-1}\rho_{D-1}}V(\partial_{\rho_{D-1}}V)^2 + a_3V^2(\partial_{\rho_{D-1}\rho_{D-1}}V)^2, \\ \tilde{b} &= 2(D-2)(D-2+a^2)^2V\partial_{\rho_{D-1}}V((D-2-a^2)(\partial_{\rho_{D-1}}V)^2 + V\partial_{\rho_{D-1}\rho_{D-1}}V), \\ \tilde{c} &= D(D-2)^2(D-2+a^2)^2V^2(\partial_{\rho_{D-1}}V)^2,\end{aligned}\tag{7.132}$$

with

$$\begin{aligned}a_1 &= (D^2 - 3D + 3)a^4 + 2(D-2)(2D^2 - 6D + 5)a^2 + \frac{124D^3 - 1305D^2 + 4965D - 6662}{2}, \\ a_2 &= -2\left((D^2 - 3D + 3)a^4 + (3D^3 - 15D^2 + 26D - 16)a^2 + (D-2)^2(2D^2 - 6D + 5)\right), \\ a_3 &= (D^2 - 3D + 3)(D-2+a^2)^2.\end{aligned}\tag{7.133}$$

We look at the first few cases. For  $D = 4$  we have

$$[R]^2 = \frac{4\left(\tilde{a}\rho_3^2 + \tilde{b}\rho_3 + \tilde{c}\right)}{(2+a^2)^4\rho_3^2V^{\left(\frac{4(3+a^2)}{2+a^2}\right)}},\tag{7.134}$$

where

$$\begin{aligned}\tilde{a} &= (7a^4 + 52a^2 + 127)(\partial_{\rho_3}V)^4 - 2(7a^4 + 40a^2 + 52)V\partial_{\rho_3\rho_3}V(\partial_{\rho_3}V)^2 + 7(a^2+2)^2V^2(\partial_{\rho_3\rho_3}V)^2, \\ \tilde{b} &= 4(a^2+2)^2V\partial_{\rho_3}V((2-a^2)(\partial_{\rho_3}V)^2 + V\partial_{\rho_3\rho_3}V), \\ \tilde{c} &= 16(a^2+2)^2V^2(\partial_{\rho_3}V)^2.\end{aligned}\tag{7.135}$$

For  $D = 5$ , we have

$$[R]^2 = \frac{4\left(\tilde{a}\rho^2 + \tilde{b}\rho + \tilde{c}\right)}{(3+a^2)^4\rho^2V^{\left(\frac{4(4+a^2)}{3+a^2}\right)}},\tag{7.136}$$

where

$$\begin{aligned}\tilde{a} &= (13a^4 + 150a^2 + 519)(\partial_{\rho_4}V)^4 - 2(13a^4 + 114a^2 + 225)V\partial_{\rho_4\rho_4}V(\partial_{\rho_4}V)^2 \\ &\quad + 13(a^2+3)^2V^2(\partial_{\rho_4\rho_4}V)^2, \\ \tilde{b} &= 6(a^2+3)^2V\partial_{\rho_4}V((3-a^2)(\partial_{\rho_4}V)^2 + V\partial_{\rho_4\rho_4}V), \\ \tilde{c} &= 45(a^2+3)^2V^2(\partial_{\rho_4}V)^2.\end{aligned}\tag{7.137}$$

For  $D = 6$ , we have

$$[R]^2 = \frac{4\left(\tilde{a}\rho_5^2 + \tilde{b}\rho_5 + \tilde{c}\right)}{(4+a^2)^4\rho_5^2V^{\left(\frac{4(5+a^2)}{4+a^2}\right)}},\tag{7.138}$$



where

$$\begin{aligned}
 \tilde{a} &= (21a^4 + 328a^2 + 1466) (\partial_{\rho_5} V)^4 - 2 (21a^4 + 248a^2 + 656) V \partial_{\rho_5 \rho_5} V (\partial_{\rho_5} V)^2 \\
 &\quad + 21(a^2 + 4)^2 V^2 (\partial_{\rho_5 \rho_5} V)^2, \\
 \tilde{b} &= 8(a^2 + 4)^2 V \partial_{\rho_5} V ((4 - a^2)(\partial_{\rho_5} V)^2 + V \partial_{\rho_5 \rho_5} V), \\
 \tilde{c} &= 96(a^2 + 4)^2 V^2 (\partial_{\rho_5} V)^2.
 \end{aligned} \tag{7.139}$$

For  $D = 7$ , we have

$$[R]^2 = \frac{4 (\tilde{a} \rho_6^2 + \tilde{b} \rho_6 + \tilde{c})}{(5 + a^2)^4 \rho_6^2 V^{\left(\frac{4(6+a^2)}{5+a^2}\right)}}, \tag{7.140}$$

where

$$\begin{aligned}
 \tilde{a} &= (31a^4 + 610a^2 + 3340) (\partial_{\rho_6} V)^4 - 2 (31a^4 + 460a^2 + 1525) V \partial_{\rho_6 \rho_6} V (\partial_{\rho_6} V)^2 \\
 &\quad + 31(a^2 + 5)^2 V^2 (\partial_{\rho_6 \rho_6} V)^2, \\
 \tilde{b} &= 10(a^2 + 5)^2 V \partial_{\rho_6} V ((5 - a^2)(\partial_{\rho_6} V)^2 + V \partial_{\rho_6 \rho_6} V), \\
 \tilde{c} &= 175(a^2 + 5)^2 V^2 (\partial_{\rho_6} V)^2.
 \end{aligned} \tag{7.141}$$

In terms of the special cases highlighted earlier, we can see that the metric is well-behaved everywhere, even at the event horizons (where they exist). Whilst again this is not definitive proof that these spacetimes do not contain any unwanted naked singularities, we can conclude that this is probably the reality.

### 7.5.3 Cosmological Black Holes

London [48] constructs a similar metric with a non-zero cosmological constant  $\Lambda \neq 0$  present, which we modify here by adding in the dilaton. We have infinitely many identical black holes with mass  $m$  and charge  $Q$ . The metric, potential and relevant relationships are given by, for  $D \geq 3$ ,

$$\begin{aligned}
 ds^2 &= -U^{-2} dt^2 + U^{\left(\frac{2}{D-2}\right)} d\vec{r}^2, \\
 U &= V^{\left(\frac{D-2}{D-2+a^2}\right)} \quad \text{with} \quad V = \lambda t + \frac{4m\pi\Gamma\left(\frac{D}{2}\right) (D-2+a^2)}{(D-1)(D-2)} \sum_{j=-\infty}^{\infty} |\vec{r} - \vec{r}_j|^{2-D}, \\
 \lambda^2 &= \frac{4(D-2+a^2)^2}{D(D-1)} \Lambda, \quad \vec{A} = \pm \left( \frac{D-1}{2(D-2+a^2)} \right)^{\frac{1}{2}} V^{-1} dt, \quad m = \left( \frac{D-1}{2(D-2+a^2)} \right)^{\frac{1}{2}} |Q|.
 \end{aligned} \tag{7.142}$$

### The Case $D = 3$

If  $D = 3$  and the black holes are periodically distributed along the  $x_3$ -axis then we have a non-convergent potential as before. If we subtract an infinite constant to make this converge, we have

$$V = \lambda t + m(1 + a^2) \left( \sum_{j=-\infty}^{\infty} (\rho_2^2 + (x_3 - Pj)^2)^{-\frac{1}{2}} - 2 \sum_{j=1}^{\infty} (Pj)^{-1} \right), \quad (7.143)$$

which for a fixed value of  $x_3$  can be approximated by

$$V_{appx} = \lambda t + c - 2k \ln \rho_2, \quad (7.144)$$

where the constants  $k$  and  $c$  are as in (7.115). In this case, the Riemann curvature scalar is given by

$$[R]^2 = \frac{4f}{\rho_2^2(1 + a^2)^4 V^4}, \quad (7.145)$$

where

$$\begin{aligned} f = & 16k^2 \rho_2^{-2} V^{-\left(\frac{4}{1+a^2}\right)} (V^2(a^2 + 1)^2 - 2kV(a^2 + 1)(a^2 + 3) + k^2(3a^4 + 10a^2 + 14)) \\ & + 3\lambda^4 \rho_2^2 V^{\left(\frac{4}{1+a^2}\right)} (a^4 - a^2 - 2) - 8k^2 a^2 \lambda^2 (2 - a^2). \end{aligned} \quad (7.146)$$

This reduces to (7.116) when  $\lambda$  is zero, and when  $V$  is zero we have a curvature singularity. If we try to show that this is a naked singularity, taking as before

$$t = t(s), \quad x := x_1(s), \quad x_2 = x_3 = x_4 = 0, \quad (7.147)$$

then the Lagrangian is given by

$$\mathcal{L} = -V^{-\left(\frac{2}{1+a^2}\right)}(t, x) \dot{t}^2 + V^{\left(\frac{2}{1+a^2}\right)}(x, t) \dot{x}^2 = 0. \quad (7.148)$$

Following the method above yields

$$\frac{dt}{dx} = \pm V^{\left(\frac{2}{1+a^2}\right)} \implies t = \pm \int (\lambda t + c - 2k \ln x)^{\left(\frac{2}{1+a^2}\right)}(t, x) dx, \quad (7.149)$$

and it is unclear how to resolve this integral, which we leave for further work.

**The Case  $D \geq 4$** 

We have

$$ds^2 = -V^{\left(\frac{4-2D}{D-2+a^2}\right)} dt^2 + V^{\left(\frac{2}{D-2+a^2}\right)} (ds_{D-1}^2 + dx_D^2),$$

$$V = \lambda t + \frac{4m\pi\Gamma\left(\frac{D}{2}\right)(D-2+a^2)}{(D-1)(D-2)} \sum_{j=-\infty}^{\infty} (\rho_{D-1}^2 + (x_D - Pj)^2)^{\left(1-\frac{D}{2}\right)}, \quad (7.150)$$

where  $ds_{D-1}^2$  is defined as in (7.130). Again, we do not have to worry about singularities being present as  $V$  converges and is always positive for  $D \geq 4$ . Calculating the Riemann curvature scalar for  $D = 4$  as an example gives

$$[R]^2 = \frac{4\left(\tilde{a}\rho_3^2 + \tilde{b}\rho_3 + \tilde{c}\right)}{\rho_3(2+a^2)^4 V^4\left(\frac{1+a^2}{2+a^2}\right)}, \quad (7.151)$$

where

$$\tilde{c} = 16V^2 V^{-\left(\frac{8}{2+a^2}\right)} (a^2 + 2)^2 (\partial_{\rho_3} V)^2,$$

$$\tilde{b} = 4(2+a^2) V^{-\left(\frac{4}{2+a^2}\right)} V \partial_{\rho_3} V \left( (2+a^2) V^{-\left(\frac{4}{2+a^2}\right)} \left( (4-a^2) (\partial_{\rho_3} V)^2 + V \partial_{\rho_3 \rho_3} V \right) - \lambda^2 (1+2a^2) V^{\left(\frac{2}{2+a^2}\right)} \right),$$

$$\tilde{a} = \tilde{a}_0 + \tilde{a}_2 a^2 + \tilde{a}_4 a^4, \quad (7.152)$$

with

$$\tilde{a}_0 = V^{-\left(\frac{8}{2+a^2}\right)} \left( 28V^2 (\partial_{\rho_3 \rho_3} V)^2 - 104V (\partial_{\rho_3} V)^2 \partial_{\rho_3 \rho_3} V + 127 (\partial_{\rho_3} V)^4 \right) - 2\lambda^2 V^{-\left(\frac{2}{2+a^2}\right)} \left( (\partial_{\rho_3} V)^2 + 2V \partial_{\rho_3 \rho_3} V \right) + 10\lambda^4 V^{\left(\frac{4}{2+a^2}\right)},$$

$$\tilde{a}_2 = V^{-\left(\frac{8}{2+a^2}\right)} \left( 7V^2 (\partial_{\rho_3 \rho_3} V)^2 - 14V (\partial_{\rho_3} V)^2 \partial_{\rho_3 \rho_3} V + 7 (\partial_{\rho_3} V)^4 \right) - 2\lambda^2 V^{-\left(\frac{2}{2+a^2}\right)} \left( (\partial_{\rho_3} V)^2 + 2V \partial_{\rho_3 \rho_3} V \right) + 4\lambda^4 V^{\left(\frac{4}{2+a^2}\right)},$$

$$\tilde{a}_4 = V^{-\left(\frac{8}{2+a^2}\right)} \left( 28V^2 (\partial_{\rho_3 \rho_3} V)^2 - 80V (\partial_{\rho_3} V)^2 \partial_{\rho_3 \rho_3} V + 52 (\partial_{\rho_3} V)^4 \right) + 10\lambda^2 V^{-\left(\frac{2}{2+a^2}\right)} \left( (\partial_{\rho_3} V)^2 - V \partial_{\rho_3 \rho_3} V \right) - 8\lambda^4 V^{\left(\frac{4}{2+a^2}\right)}. \quad (7.153)$$

This reduces to (7.134), (7.135) when we set  $\lambda$  to be zero, which provides a check of our calculation.

### 7.5.4 Lattice Solution

We modify our work in the ERN case to construct a lattice solution, beginning in a background space  $\mathbb{R}^D$  and inserting identical sources in a  $(D-3)$ -dimensional lattice. Taking the basis vectors for this lattice to be the standard basis vectors in  $\mathbb{R}^{(D-3)}$  and  $\vec{\omega} = (\omega_1, \dots, \omega_{D-3})$  to be the position vector in the  $(D-3)$ -dimensional background subspace gives us, summing over the lattice vertices,

$$\begin{aligned} V &= 1 + \sum_{j_{D-3}=-\infty}^{\infty} \cdots \sum_{j_1=-\infty}^{\infty} \lambda (\rho_3^2 + (\omega_1 + j_1)^2 + \cdots + (\omega_{D-3} + j_{D-3})^2)^{(1-\frac{D}{2})} \\ &\leq 1 + \frac{\pi\lambda}{\rho_3} \left( \prod_{i=5}^D c_i \right) \left( \frac{\sinh(2\pi\rho_3)}{\cosh(2\pi\rho_3) - \cos(2\pi\omega_{D-3})} \right), \end{aligned} \quad (7.154)$$

$$\lambda := \frac{4m\pi\Gamma\left(\frac{D}{2}\right)(D-2+a^2)}{(D-1)(D-2)}, \quad (7.155)$$

$$c_i(\rho_3) = \rho_3^{(i-3)} \sum_{k_1=-\infty}^{\infty} (\rho_3^2 + (\omega_1 + k_1)^2)^{(1-\frac{i}{2})}. \quad (7.156)$$

$V$  converges by the comparison test and we have a solution in a compactified background  $\mathcal{M}^4 \times T^{D-3}$ . To eliminate dilaton singularities,  $a$  takes values (7.104) for  $p \in \mathbb{Z}$ .

### 7.5.5 Non-Periodic Distribution

We can modify the method for the ERN case to construct solutions here with black holes unevenly distributed through several dimensions. Let  $\{\vec{r}_j\}_0^\infty \subset \mathbb{R}^D$  be a divergent sequence of points such that for some point  $\vec{r}_0 \in \mathbb{R}^D$ ,

$$1 + \frac{4m\pi\Gamma\left(\frac{D}{2}\right)(D-2+a^2)}{(D-1)(D-2)} \sum_{j=1}^{\infty} |\vec{r}_0 - \vec{r}_j|^{2-D} < \infty. \quad (7.157)$$

We define a smooth function  $V : \mathbb{R}^D / \{\vec{r}_j\} \rightarrow \mathbb{R}$  by

$$V = 1 + \frac{4m\pi\Gamma\left(\frac{D}{2}\right)(D-2+a^2)}{(D-1)(D-2)} \sum_{j=1}^{\infty} |\vec{r} - \vec{r}_j|^{2-D}, \quad (7.158)$$

which satisfies the Laplace equation on  $\mathbb{R}^D$ . We know that the metric is regular at the points  $\vec{r}_j$  for our special cases, when  $a$  takes the form (7.104) for  $p \in \mathbb{Z}$ . Thus, at these points, our construction makes sense and we have similar examples to the ERN case. The Riemann curvature scalar is given by (7.131), (7.132), (7.133), but this now holds for  $D \geq 3$ .

## Chapter 8

# Kaluza-Klein Black Holes

### 8.1 Introduction

In the previous chapter, we have considered solutions with metrics of the form

$$ds^2 = -V^{-2}dt^2 + V^{\left(\frac{2}{D-2}\right)}ds_{\mathbb{E}^D}^2, \quad (8.1)$$

where  $\mathbb{E}^D$  is the standard  $D$ -dimensional Euclidean space. This describes an arbitrary number of extreme Reissner-Nordström black holes in static equilibrium. We can also construct black hole solutions using the Gibbons-Hawking space instead of the Euclidean space. In five dimensions, these solutions have asymptotic structure given by a four-dimensional locally flat spacetime with a twisted  $\mathbb{S}^1$ . Their association with a compact dimension earns them the name **Kaluza-Klein black holes**.

In this chapter, we shall explore a variety of Kaluza-Klein black holes with different properties. We can write down the most general five-dimensional system we will work with, and consider various cases:

$$\begin{aligned} ds^2 &= -U^{-2} \left( d\tilde{t} + \alpha V^\beta (d\tau + \vec{\omega} \cdot d\vec{r}) \right)^2 + U \exp(\lambda\tilde{t}) ds_{GH}^2, \\ \vec{A} &= \frac{\sqrt{3}}{2} \exp(-\lambda\tilde{t}) \left( d\tilde{t} + \alpha V^\beta (d\tau + \vec{\omega} \cdot d\vec{r}) \right), \\ ds_{GH}^2 &= V^{-1} (d\tau + \vec{\omega} \cdot d\vec{r})^2 + V d\vec{r}^2, \\ U &= 1 + \sum_{j=1}^N m_j \exp(-\lambda\tilde{t}) |\vec{r} - \vec{r}_j|^{-1}, \quad V = \epsilon + \sum_{j=1}^N n_j |\vec{r} - \vec{r}_j|^{-1}, \quad \vec{\nabla}V = \vec{\nabla} \times \vec{\omega}. \end{aligned} \quad (8.2)$$

We introduce the coordinate transformation

$$t := \lambda^{-1} \exp(\lambda\tilde{t}) > 0, \quad (8.3)$$

yielding

$$\begin{aligned}
 ds^2 &= -U^2 \left( dt + \alpha V^\beta (d\tau + \vec{\omega} \cdot d\vec{r}) \right)^2 + U \left( V^{-1} (d\tau + \vec{\omega} \cdot d\vec{r})^2 + V d\vec{r}^2 \right), \\
 \vec{A} &= \frac{\sqrt{3}}{2} U^{-1} \left( dt + \alpha V^\beta (d\tau + \vec{\omega} \cdot d\vec{r}) \right), \\
 U &= \lambda t + \sum_{j=1}^N m_j |\vec{r} - \vec{r}_j|^{-1}, \quad V = \epsilon + \sum_{j=1}^N n_j |\vec{r} - \vec{r}_j|^{-1}, \quad \nabla \vec{V} = \vec{\nabla} \times \vec{\omega}. \quad (8.4)
 \end{aligned}$$

In order to avoid naked singularities being present, we require that  $m_j, n_j > 0 \forall j$ ,  $\beta = \pm 1$  and  $\alpha^2 \in [0, 1)$ .  $\lambda$  is related to a positive cosmological constant  $\Lambda$  by

$$\lambda = \pm \sqrt{\frac{4\Lambda}{3}}. \quad (8.5)$$

If  $\epsilon$  is zero then the base space is the Eguchi-Hanson space and if  $\epsilon$  is one then it is the Taub-NUT space. The coordinates in which we express the Gibbons-Hawking metric,  $(r, \theta, \phi, \tau)$  have ranges

$$-\infty < r < \infty, \quad 0 \leq \theta \leq \pi, \quad 0 \leq \phi \leq 2\pi, \quad 0 \leq \tau \leq 2\pi L \quad (8.6)$$

where the regularity of the metric requires that

$$n_j = \frac{h_j L}{2}, \quad (8.7)$$

where  $h_j \in \mathbb{N} \forall j$ . Such solutions are regular at the event horizons, as we will see later, and have the topology of the lens space  $L(h_j; 1) = \mathbb{S}^3 / \mathbb{Z}_{h_j}$ . The asymptotic behaviour of the solution is such that an observer at spatial infinity would observe a single Kaluza-Klein black hole with point source parameter  $m$  and nut charge  $n$  given by

$$m := \sum_{j=1}^N m_j, \quad n := \sum_{j=1}^N n_j. \quad (8.8)$$

There are four obvious categories of black holes which emerge:

- static, non-cosmological black holes ( $\alpha = 0, \lambda = 0$ ) explored in [37], denoted by SN;
- rotating, non-cosmological black holes ( $\lambda = 0, \alpha \neq 0$ ) explored in [51], denoted by RN;
- static, cosmological black holes ( $\alpha = 0, \lambda \neq 0$ ) explored in [36], [38], denoted by SC;
- rotating, cosmological black holes ( $\alpha \neq 0, \lambda \neq 0$ ) explored in [46], [49], denoted by RC.

We will investigate the situation where we have infinitely many black holes. As such, the structure of this chapter is as follows:

**Special cases:** We investigate the curvature of two special cases of the SN black holes, in order to act as checks for later calculations.

**Useful metrics:** We introduce the Klemm-Sabra and Reissner-Nordström (anti) de-Sitter metrics which will be useful in our work on SC and RC black holes. We show that these metrics are stationary.

**Regularity at the event horizons** We demonstrate that the RC black holes (of which the SC, RN and SN black holes will be treated as special cases) are regular at the event horizons.

**Asymptotic behaviour:** We look at the behaviour of the solutions at infinity to find their asymptotic structure, seeing that in the case of infinitely many black holes we have Kaluza-Klein type solutions. We consider the solutions with the Eguchi-Hanson and Taub-NUT base spaces separately. Further, we note that the result in [51] for the asymptotic form of the RN (and SN) metrics is incorrect.

**Periodic distributions:** We consider the behaviour of infinitely many black holes periodically distributed along one of the axes. We adapt the logarithmic approximation to  $U$  and  $V$  employed in chapter three to calculate the Riemann curvature scalar for both choices of  $\beta$  and show that the static black holes have naked singularities when either of the potentials is zero. The cosmological black holes also have singularities but, due to the difficulty of solving the Euler-Lagrange equations, it is not clear that they are naked. We give some useful examples in both cases and investigate the values of  $\alpha$  that give rise to closed timelike curves.

**Non-periodic and lattice distributions:** We follow the method of Anderson et al [1] to obtain solutions with the black holes unevenly distributed along one of the axes. We calculate the Riemann curvature scalar for both choices of  $\beta$ , give an example of a valid solution (one for which  $\vec{\omega}$  converges) and investigate the values of  $\alpha$  that give rise to closed timelike curves. We briefly discuss lattice solutions and see that they unfortunately do not offer any new possibilities.

**Examples:** Finally in this chapter, we consider the specific cases of SN, RN and SC black

holes, looking at the curvature for both periodic and non-periodic solutions, and in the case of RN black holes we also look at the ergoregions.

## 8.2 Special Cases

In this section we will introduce some special cases of SN black holes, the first of which we will use for checking some of our calculations later on and the second of which demonstrates a link with our earlier work in chapters two and three on Kaluza-Klein-type solutions.

Gauntlett et al [15] construct a class of Kaluza-Klein black holes by taking the four-dimensional Gibbons-Hawking space (3.2) and demonstrating that the triholomorphic Killing vector  $\partial_\tau$  of that metric is also a Killing vector of a class of five-dimensional spaces. They subsequently show that all timelike solutions of  $N = 2$ ,  $D = 3 + 1$  supergravity can be given by a reduction of this class of solutions to the Gibbons-Hawking space. The five-dimensional metric in this case is given by

$$ds^2 = -V^{-2}dt^2 + V^2 dr^2 + (d\tau + \vec{\omega} \cdot d\vec{r})^2 \quad (8.9)$$

with potential

$$V = 1 + \sum_{j=1}^N n_j |\vec{r} - \vec{r}_j|^{-1}, \quad (8.10)$$

giving the multi Taub-NUT solution for the four-dimensional part of the metric. This solution corresponds to the special case of SN black holes when  $V \equiv U$ . We take  $\rho := \rho_2$ . The Riemann curvature scalar is given by

$$[R]^2 = \frac{4d^2 (20V^2 - 132dV + 307d^2)}{\rho^4 V^8}, \quad (8.11)$$

for a periodic solution, where we calculated the above by taking  $V$  to be approximated by

$$V_{appx} = c - 2d \ln \rho; \quad (8.12)$$

for a non-periodic solution it is given by

$$[R]^2 = \frac{f(V)}{4\rho^2 V^8} \quad \text{with} \quad f(V) = \sum_{j=0}^4 v_j, \quad (8.13)$$

where the coefficients  $v_j$  are given by

$$v_0 = 127\rho^2 (\partial_\rho V)^4,$$



$$\begin{aligned}
 v_1 &= 4\rho (\partial_\rho V)^2 \left[ 15\rho (\partial_\rho V)^2 - 26\rho V \partial_{\rho\rho} V + 4V \partial_\rho V \right], \\
 v_2 &= 2 \left[ 2V^2 \left( 7(\partial_\rho V)^2 + 2\rho \partial_\rho V \partial_{\rho\rho} V + 7\rho^2 (\partial_{\rho\rho} V)^2 \right) \right. \\
 &\quad \left. + \rho (\partial_\rho V)^2 \left( 11\rho (\partial_\rho V)^2 + 8V (\partial_\rho V - 2\rho \partial_{\rho\rho} V) \right) \right], \\
 v_3 &= 4 \left[ 2V^2 (\partial_\rho V + \rho \partial_{\rho\rho} V)^2 + \rho^2 (\partial_\rho V)^2 \left( 2V \partial_{\rho\rho} V - 3(\partial_\rho V)^2 \right) \right], \\
 v_4 &= 27\rho^2 (\partial_\rho V)^4 + 12V^2 \left( \rho^2 (\partial_{\rho\rho} V)^2 + (\partial_\rho V)^2 \right) + 8\rho V \partial_\rho V \partial_{\rho\rho} V (V - 4\rho \partial_\rho V). \quad (8.14)
 \end{aligned}$$

If we take  $U \equiv 1$ , then we have the Kaluza-Klein multiple monopole solution with metric

$$ds^2 = -dt^2 + V d\vec{r}^2 + V^{-1} (d\tau + \vec{\omega} \cdot d\vec{r})^2. \quad (8.15)$$

The Riemann curvature scalar will be the same in the periodic case as it is in chapter three, and in the non-periodic case it is given by

$$[R]^2 = \frac{27\rho^2 (\partial_\rho V)^4 + 12V^2 \left( \rho^2 (\partial_{\rho\rho} V)^2 + (\partial_\rho V)^2 \right) + 8\rho V \partial_\rho V \partial_{\rho\rho} V (V - 4\rho \partial_\rho V)}{4\rho^2 V^6}, \quad (8.16)$$

which is the same result we obtained independently in chapter five for a non-periodic distribution of instantons (see (6.5)).

## 8.3 Useful Metrics

In this section we introduce three metrics that will be useful throughout this chapter when looking at cosmological black holes. We will look at the Eguchi-Hanson metric in different coordinates so as to make a link with the definition in chapter one, and at the Klemm-Sabra and Reissner-Nordström metrics, which will be horizon and asymptotic limits for cosmological black holes.

### 8.3.1 Eguchi-Hanson Metric

Ishihara et al [39] study the behaviour of black holes on the Eguchi-Hanson space in five-dimensional Einstein-Maxwell theory. The metric is given by

$$\begin{aligned}
 ds^2 &= -U^{-2} dt^2 + U \left( V^{-1} (d\tau + \vec{\omega} \cdot d\vec{r})^2 + V d\vec{r}^2 \right), \\
 U &= 1 + \sum_{j=1}^N m_j |\vec{r} - \vec{r}_j|^{-1}, \quad V = \sum_{j=1}^N n_j |\vec{r} - \vec{r}_j|^{-1}, \\
 \vec{\nabla} V &= \vec{\nabla} \times \vec{\omega}. \quad (8.17)
 \end{aligned}$$

The potential  $U$  converts NUT singularities (found when  $\vec{r} = \vec{r}_j$ ) into hyperspaces in the overall spacetime, each of these being a Killing horizon with respect to  $\partial_t$  and each cross-section of them with a  $t = \text{const}$  surface having a finite area, making them event horizons. In order to see the connection with the original form of the metric we gave in (2.17), we consider the case of two black holes and apply the coordinate transformation

$$r = a \left( \frac{\tilde{r}^4}{a^4} - \sin^2 \theta \right)^{\frac{1}{2}}, \quad \tan \theta = \left( 1 - \frac{a^4}{r^4} \right)^{\frac{1}{2}} \tan \tilde{\theta}, \quad \phi = \tilde{\tau}, \quad \tau = 2\tilde{\phi},$$

$$\tilde{m}_1 = \frac{m_1}{a}, \quad \tilde{m}_2 = \frac{m_2}{a}, \quad \tilde{n}_1 = \tilde{n}_2 = \frac{a}{8}, \quad (8.18)$$

giving us the metric

$$ds^2 = -U^{-2} dt^2 + U \left( \left( 1 - \frac{a^4}{\tilde{r}^4} \right)^{-1} d\tilde{r}^2 + \frac{\tilde{r}^2}{4} \left( 1 - \frac{a^4}{\tilde{r}^4} \right) (d\tilde{\tau} + \cos \tilde{\theta} d\tilde{\phi})^2 + \frac{\tilde{r}^2}{4} (d\tilde{\theta}^2 + \sin^2 \tilde{\theta} d\tilde{\phi}^2) \right). \quad (8.19)$$

### 8.3.2 The Klemm-Sabra Metric

Klemm and Sabra [46] construct a rotating, cosmological black hole solution by generalising the extreme Reissner-Nordström metric to give

$$ds^2 = - \left( \lambda t + \frac{m}{r^2} \right)^{-2} \left( dt + \frac{\sigma}{2r^2} (d\tau + \cos \theta d\phi) \right)^2$$

$$+ \left( \lambda t + \frac{m}{r^2} \right) \left( dr^2 + \frac{r^2}{4} (d\Omega^2 + (d\tau + \cos \theta d\phi)^2) \right), \quad (8.20)$$

where  $m$  is the mass and  $\sigma$  the angular momentum of the black hole and is proportional to  $\alpha$ . From hereon in we refer to this as the **Klemm-Sabra (KS) metric**.

### 8.3.3 The Reissner-Nordström de-Sitter Metric

We can generalise the Reissner-Nordström (anti) de-Sitter metric for rotating black holes, obtaining

$$ds^2 = - \left( \lambda t + \frac{m}{r^2} \right)^{-2} \left( dt + \frac{\sigma r^2}{4} (d\tau + \cos \theta d\phi) \right)^2$$

$$+ \left( \lambda t + \frac{m}{r^2} \right) \left( dr^2 + \frac{r^2}{4} (d\Omega^2 + (d\tau + \cos \theta d\phi)^2) \right). \quad (8.21)$$

From hereon in we refer to this as the **Reissner-Nordström (anti) de-Sitter (RNdS) metric**. Note that if  $\alpha$  (and hence  $\sigma$ ) is zero then we have

$$ds^2 = - \left( \lambda t + \frac{m}{r^2} \right)^{-2} dt^2 + \left( \lambda t + \frac{m}{r^2} \right) \left( dr^2 + \frac{r^2}{4} \left( d\Omega^2 + (d\tau + \cos\theta d\phi)^2 \right) \right). \quad (8.22)$$

### 8.3.4 Stationary Solutions

In order to see that these metrics yield stationary solutions, by which we mean there they have a timelike Killing vector, we apply **Eddington-Finkelstein** coordinates, letting

$$\tilde{r}^2 = \lambda t r^2 + m, \quad d\tilde{t} = (\lambda t)^{-1} dt - f(\tilde{r}) d\tilde{r}, \quad d\tilde{\tau} = d\tau - g(\tilde{r}) d\tilde{r}, \quad (8.23)$$

with

$$f_{KS}(\tilde{r}) := \frac{2\lambda\tilde{r}(\tilde{r}^6 - \sigma^2)(\tilde{r}^2 - m)^{-1}}{\lambda^2(\tilde{r}^6 - \sigma^2) - 4(\tilde{r}^2 - m)^2}, \quad g_{KS}(\tilde{r}) := \frac{4\lambda\sigma\tilde{r}}{\lambda^2(\tilde{r}^6 - \sigma^2) - 4(\tilde{r}^2 - m)^2}, \quad (8.24)$$

for the KS metric and

$$f_{RNdS}(\tilde{r}) := \frac{\lambda\tilde{r}^3}{2(\tilde{r}^2 - m)}, \quad g_{RNdS}(\tilde{r}) := \frac{\lambda\sigma\tilde{r}^3}{2(\tilde{r}^2 - m)}, \quad (8.25)$$

for the RNdS metric. The resulting metrics are given by

$$ds_{KS}^2 = \frac{\lambda^2\tilde{r}}{4} d\tilde{t}^2 - W_1^2 \left( d\tilde{t} + \frac{\sigma}{2\tilde{r}^2} W_1^{-1} (d\tilde{\tau} + \cos\theta d\phi) \right)^2 + W_2^{-1} d\tilde{r}^2 + \frac{\tilde{r}^2}{4} \left( d\Omega^2 + (d\tilde{\tau} + \cos\theta d\phi)^2 \right), \quad (8.26)$$

and

$$ds_{RNdS}^2 = \frac{\lambda^2\tilde{r}}{4} d\tilde{t}^2 - W_1^2 \left( d\tilde{t} + \frac{\sigma\tilde{r}^2}{4} W_1^{-1} (d\tilde{\tau} + \cos\theta d\phi) \right)^2 + W_2^{-1} d\tilde{r}^2 + \frac{\tilde{r}^2}{4} \left( d\Omega^2 + (d\tilde{\tau} + \cos\theta d\phi)^2 \right), \quad (8.27)$$

where

$$W_1 := 1 - \frac{m}{\tilde{r}^2}, \quad W_2 := \left( 1 - \frac{m}{\tilde{r}^2} \right)^2 - \frac{\lambda^2\tilde{r}^2}{4} + \frac{\lambda^2\sigma^2}{4\tilde{r}^4}. \quad (8.28)$$

Horizons occur at values of  $\tilde{r}$  such that  $W_2(\tilde{r}) = 0$ . If we define  $x := \lambda t \tilde{r}^2$ , then

$$\lambda^2 \left( (x + \tilde{m})^3 - \sigma^2 \right) - 4x^2 = 0, \quad (8.29)$$

so we have three horizons: an inner horizon ( $x_-$ ), an outer horizon ( $x_+$ ) and a cosmological horizon ( $x_c$ ) which are related by

$$x_- \leq 0 \leq x_+ \leq x_c. \quad (8.30)$$

In these coordinates, we can see that the metrics are stationary. If  $\sigma$  is zero, then we have

$$ds^2 = \left( \frac{\lambda^2 \tilde{r}}{4} - W_1^2 \right) d\tilde{t}^2 + W_2^{-1} d\tilde{r}^2 + \frac{\tilde{r}^2}{4} \left( d\Omega^2 + (d\tilde{\tau} + \cos\theta d\phi)^2 \right), \quad (8.31)$$

where

$$W_1 := 1 - \frac{m}{\tilde{r}^2}, \quad W_2 := \left( 1 - \frac{m}{\tilde{r}^2} \right)^2 - \frac{\lambda^2 \tilde{r}^2}{4}, \quad (8.32)$$

and so this metric is also stationary.

## 8.4 Regularity at the Event Horizons

In this section we will demonstrate that our black holes are regular at the event horizons. The argument is different for cosmological and non-cosmological black holes, so we discuss the two cases separately.

### 8.4.1 Non-Cosmological Black Holes

We study the behaviour of RN black holes (of which the SN black holes will be treated as a special case) near the event horizon. We have

$$ds^2 = -U^{-2} \left( dt + \alpha V^\beta (d\tau + \vec{\omega} \cdot d\vec{r}) \right)^2 + U \left( V^{-1} (d\tau + \vec{\omega} \cdot d\vec{r})^2 + V (dr^2 + r^2 d\Omega^2) \right), \quad (8.33)$$

where

$$U = 1 + \sum_{j=1}^N m_j |\vec{r} - \vec{r}_j|^{-1}, \quad V = \epsilon + \sum_{j=1}^N n_j |\vec{r} - \vec{r}_j|^{-1}, \quad (8.34)$$

$$\epsilon = 0, 1, \quad \alpha^2 \in [0, 1) \quad \text{and} \quad \beta = \pm 1. \quad (8.35)$$

Without loss of generality, we consider the case of two black holes positioned at

$$\vec{r}_1 = (0, 0, 0), \quad \vec{r}_2 = (0, 0, -a), \quad (8.36)$$

where  $a$  is the separation of the black holes. The potentials become

$$U = 1 + m_1 r^{-1} + m_2 (r^2 + a^2 + 2ar \cos\theta)^{-\frac{1}{2}},$$

$$\begin{aligned}
 V &= \epsilon + n_1 r^{-1} + n_2 (r^2 + a^2 + 2ar \cos \theta)^{-\frac{1}{2}}, \\
 \vec{\omega} \cdot d\vec{r} &= \left( n_1 \cos \theta + n_2 (a + r \cos \theta) (r^2 + a^2 + 2ar \cos \theta)^{-\frac{1}{2}} \right) d\phi.
 \end{aligned} \tag{8.37}$$

Note that, as  $r \rightarrow 0$ ,

$$\begin{aligned}
 U^{-2} &\rightarrow \frac{r^2}{m_1^2}, & U^{-2}V &\rightarrow 0, \\
 U^{-2}V^{-2} &\rightarrow 0, & U^{-2}V^2 &\rightarrow \frac{n_1^2}{m_1^2}, \\
 U^{-2}V^{-1} &\rightarrow 0, & UV^{-1} &\rightarrow \frac{m_1}{n_1}, \\
 UV &\rightarrow \frac{m_1 n_1}{r^2}, & r^2 UV d\Omega^2 &\rightarrow m_1 n_1 d\Omega^2,
 \end{aligned} \tag{8.38}$$

for both  $\epsilon = 0$  and  $\epsilon = 1$ . Then, under the coordinate transformation

$$\begin{aligned}
 d\tilde{\tau} &= d\tau + n_2 d\phi, \\
 dv &= dt - \left( \frac{F m_1^{\frac{1}{2}}}{n_1^{\frac{1}{2}} r} + \frac{m_1^{\frac{3}{2}} n_1^{\frac{1}{2}}}{r^2} \right) dr,
 \end{aligned} \tag{8.39}$$

where  $F$  is a constant, as  $r \rightarrow 0$  we see that

$$-U^{-2} dt^2 + UV dr^2 \simeq -2 \left( \frac{n_1}{m_1} \right)^{\frac{1}{2}} dv dr + \frac{F^2}{m_1 n_1} dr^2 + \mathcal{O}(r), \tag{8.40}$$

and the metric becomes

$$ds_{\beta=1}^2 \simeq -2 \left( \frac{n_1}{m_1} \right)^{\frac{1}{2}} dv dr + m_1 n_1 \left( d\Omega^2 + \left( 1 - \frac{\alpha^2 n_1^3}{m_1^3} \right) \left( \frac{d\tilde{\tau}}{n_1} + \cos \theta d\phi \right)^2 \right) + \frac{F^2}{m_1 n_1} dr^2 + \mathcal{O}(r) \tag{8.41}$$

when  $\beta = 1$  and

$$ds_{\beta=-1}^2 \simeq -2 \left( \frac{n_1}{m_1} \right)^{\frac{1}{2}} dv dr + m_1 n_1 \left( d\Omega^2 + \left( \frac{d\tilde{\tau}}{n_1} + \cos \theta d\phi \right)^2 \right) + \frac{F^2}{m_1 n_1} dr^2 + \mathcal{O}(r) \tag{8.42}$$

when  $\beta = -1$ . We note the following:

- In the SN case,  $\alpha = 0$  and so  $F = 0$ . The result does not depend on the choice of  $\beta$ ;
- In the RN case,  $\alpha \neq 0$  and so  $F \neq 0$ . The metric does depend on the choice of  $\beta$ .

Thus, in the SN case, the metric is given by

$$ds^2 \simeq -2 \left( \frac{n_1}{m_1} \right) dv dr + m_1 n_1 \left( d\Omega^2 + \left( \frac{d\tilde{\tau}}{n_1} + \cos \theta d\phi \right)^2 \right) + \mathcal{O}(r) \tag{8.43}$$

as  $r \rightarrow 0$ . We can see in both these cases that the metrics are regular at the event horizon. A similar argument shows that the event horizon of the second black hole is regular, and

this method can be generalised to any number of black holes. Now, from reference [51], the Killing vector field  $K := \partial_v$  becomes null at  $r = 0$  and is hypersurface orthogonal from  $K_\mu dx^\mu = g_{vr} dr$  at that place. Thus,  $r = 0$  is a Killing horizon. Each component of the metric is analytic in the region  $r = 0$  and therefore the spacetime has no curvature singularity on or outside the horizon. If we look at the intersection of the  $j$ -th event horizon with a static time-slice, the metric becomes

$$ds_{\beta=1}^2 \Big|_{r=0, v=const} = \frac{Lm_j h_j}{2} \left( d\Omega^2 + \left( 1 - \frac{\alpha^2 n_1^3}{m_1^3} \right) \left( \frac{d\psi}{n_1} + \cos \theta d\phi \right)^2 \right) \quad (8.44)$$

when  $\beta = 1$  and

$$ds_{\beta=-1}^2 \Big|_{r=0, v=const} = \frac{Lm_j h_j}{2} \left( d\Omega^2 + \left( \frac{d\tilde{\psi}}{n_1} + \cos \theta d\phi \right)^2 \right) \quad (8.45)$$

when  $\beta = -1$ , where  $0 \leq \psi = 2\tilde{\tau}L^{-1} \leq 4\pi$ . The horizon topology is consequently that of the lens space  $L(h_j; 1) = \mathbb{S}^3/\mathbb{Z}_{h_j}$ . Note that the value of  $\epsilon$  makes no difference to the result here.

### 8.4.2 Cosmological Black Holes

We now explore the behaviour of both RC and SC black holes near the event horizon, in the former situation looking at both choices of  $\beta$  separately. The metric is given in (8.4). If the two black holes are positioned as in (8.36) and the potentials are given by

$$\begin{aligned} U &= \lambda t + m_1 r^{-1} + m_2 (r^2 + a^2 + 2ar \cos \theta)^{-\frac{1}{2}}, \\ V &= \epsilon + n_1 r^{-1} + n_2 (r^2 + a^2 + 2ar \cos \theta)^{-\frac{1}{2}}, \\ \vec{\omega} \cdot d\vec{r} &= \left( n_1 \cos \theta + n_2 (a + r \cos \theta) (r^2 + a^2 + 2ar \cos \theta)^{-\frac{1}{2}} \right) d\phi, \end{aligned} \quad (8.46)$$

then near  $r \rightarrow 0$ , we have

$$U \rightarrow \lambda t + m_1 r^{-1}, \quad V \rightarrow n_1 r^{-1}, \quad \vec{\omega} \cdot d\vec{r} \rightarrow (n_1 \cos \theta + n_2) d\phi. \quad (8.47)$$

### 8.4.3 The Case $\beta = -1$

Ida et al [36] construct an SC solution which we adapt for the RC case. We employ the following coordinate transformations

$$\tilde{r}^2 = 4n_1 r, \quad n_1 d\tilde{\tau} = d\tau + n_2 d\phi, \quad \tilde{m}_1 = 4m_1 n_1, \quad \sigma = \alpha n_1^{-1}, \quad (8.48)$$

and thus

$$\begin{aligned}
 U &\rightarrow \lambda t + \tilde{m}_1 \tilde{r}^{-2}, & \alpha V^{-1} (d\tau + \vec{\omega} \cdot d\vec{r}) &\rightarrow \frac{\sigma \tilde{r}^2}{4} (d\tilde{r} + \cos \theta d\phi), \\
 V^{-1} (d\tau + \vec{\omega} \cdot d\vec{r})^2 + V d\tilde{r}^2 &\rightarrow d\tilde{r}^2 + \frac{\tilde{r}^2}{4} \left( d\Omega^2 + (d\tilde{r} + \cos \theta d\phi)^2 \right),
 \end{aligned} \tag{8.49}$$

which yields

$$\begin{aligned}
 ds^2 &\simeq - \left( \lambda t + \frac{\tilde{m}_1}{\tilde{r}^2} \right)^{-2} \left( dt + \frac{\sigma \tilde{r}^2}{4} (d\tilde{r} + \cos \theta d\phi) \right)^2 \\
 &\quad + \left( \lambda t + \frac{\tilde{m}_1}{\tilde{r}^2} \right) \left( d\tilde{r}^2 + \frac{\tilde{r}^2}{4} \left( d\Omega^2 + (d\tilde{r} + \cos \theta d\phi)^2 \right) \right),
 \end{aligned} \tag{8.50}$$

which is the same form as the RNdS metric (8.21).

#### 8.4.4 The Case $\beta = 1$

Matsuno et al [49] construct a solution with  $\beta = 1$  and we follow their method. We employ the following coordinate transformations

$$\tilde{r}^2 = 4n_1 r, \quad n_1 d\tilde{r} = d\tau + n_2 d\phi, \quad \tilde{m}_1 = 4m_1 n_1, \quad \sigma = 8\alpha n_1^3, \tag{8.51}$$

then we have

$$\begin{aligned}
 U &\rightarrow \lambda t + \tilde{m}_1 \tilde{r}^{-2}, & \alpha V (d\tau + \vec{\omega} \cdot d\vec{r}) &\rightarrow \frac{\sigma}{2\tilde{r}^2} (d\tilde{r} + \cos \theta d\phi), \\
 V^{-1} (d\tau + \vec{\omega} \cdot d\vec{r})^2 + V d\tilde{r}^2 &\rightarrow d\tilde{r}^2 + \frac{\tilde{r}^2}{4} \left( d\Omega^2 + (d\tilde{r} + \cos \theta d\phi)^2 \right),
 \end{aligned} \tag{8.52}$$

which yields

$$\begin{aligned}
 ds^2 &\simeq - \left( \lambda t + \frac{\tilde{m}_1}{\tilde{r}^2} \right)^{-2} \left( dt + \frac{\sigma}{2\tilde{r}^2} (d\tilde{r} + \cos \theta d\phi) \right)^2 \\
 &\quad + \left( \lambda t + \frac{\tilde{m}_1}{\tilde{r}^2} \right) \left( d\tilde{r}^2 + \frac{\tilde{r}^2}{4} \left( d\Omega^2 + (d\tilde{r} + \cos \theta d\phi)^2 \right) \right),
 \end{aligned} \tag{8.53}$$

which is the same form as the KS metric (8.20).

### 8.4.5 The SC Case

If we set  $\alpha$  (and hence  $\sigma$ ) to be zero, then with the black holes positioned as in (8.36) (see [38]), as  $r \rightarrow 0$ ,

$$ds^2 = - \left( \lambda t + \frac{m_1}{r} \right)^{-2} dt^2 + \left( \lambda t + \frac{m_1}{r} \right) \left( \frac{r}{n_1} (d\tau + \vec{\omega} \cdot d\vec{r})^2 + \frac{n_1}{r} d\vec{r}^2 \right),$$

$$\vec{A} = \frac{\sqrt{3}}{2} U^{-1} dt. \quad (8.54)$$

Applying the coordinate transformations

$$\tilde{r}^2 = 4n_1 r, \quad n_1 d\tilde{\tau} = d\tau + n_2 d\phi, \quad \tilde{m}_1 = 4m_1 n_1, \quad (8.55)$$

gives us

$$ds^2 \simeq - \left( \lambda t + \frac{\tilde{m}_1}{\tilde{r}^2} \right)^{-2} dt^2 + \left( \lambda t + \frac{\tilde{m}_1}{\tilde{r}^2} \right) \left( d\tilde{r}^2 + \frac{\tilde{r}^2}{4} (d\Omega^2 + (d\tilde{\tau} + \cos\theta d\phi)^2) \right), \quad (8.56)$$

which is the same form as (8.22). In all three cases, therefore, our metrics behave like stationary solutions at the event horizons as we can apply Eddington-Finkelstein coordinates as before.

## 8.5 Asymptotic Behaviour

In this section we will investigate the asymptotic behaviour of our black holes. We shall see that for both possible choices of  $\epsilon$ , many black holes will coalesce into a single black hole. We proceed by studying RC black holes, treating the other examples as special cases. We begin with a note on the paper of Nakagawa et al [51].

In this paper, the authors use the coordinate transformation given by (8.145) to obtain a formula for the asymptotic form of the metric. They take, in the single black hole case,

$$U \rightarrow 1, \quad V \rightarrow 1, \quad \vec{\omega} \cdot d\vec{r} \rightarrow n \cos\theta d\phi, \quad \tau \rightarrow \frac{L\tau}{2}, \quad (8.57)$$

and apply the coordinate transformation to give

$$ds^2 \simeq -d\tilde{t}^2 + 2\alpha^2 (1 - h^{-1}) d\tilde{t}^2 + n^2 (1 - \alpha^2) \left( \frac{\tilde{\tau}}{h} + \cos\theta d\phi \right)^2 + dr^2 + r^2 d\Omega^2. \quad (8.58)$$

Here, they appear to set  $h$  to be 1 in order to obtain the metric given in the paper:



$$ds^2 \simeq -d\tilde{t}^2 \frac{L^2}{4} (1 - \alpha^2) \left( \frac{\tilde{r}}{h} + \cos \theta d\phi \right)^2 + dr^2 + r^2 d\Omega^2. \quad (8.59)$$

This is not a problem in of itself, but in the case of multiple black holes, as each  $h_j \in \mathbb{N}$ , then we cannot do this and so their extension to many black holes is incorrect.

### 8.5.1 Asymptotic Behaviour for $\epsilon = 0$

If we again assume that we have two black holes positioned as in (8.36) so that the potentials are as in (8.46), then as  $r \rightarrow \infty$ , we have, if we let  $n := n_1 = n_2$ ,

$$U \rightarrow \lambda t + \frac{m_1 + m_2}{r}, \quad V \rightarrow \frac{n_1 + n_2}{r} = \frac{2n}{r}, \quad \vec{\omega} \cdot d\vec{r} \rightarrow (n_1 + n_2) \cos \theta d\phi = 2n \cos \theta d\phi. \quad (8.60)$$

#### The Case $\beta = -1$

Employing the following coordinate transformations

$$\tilde{r}^2 = 8nr, \quad nd\tilde{\tau} = d\tau, \quad \tilde{m}_j = 4m_j n, \quad \sigma = \alpha n^{-1}, \quad (8.61)$$

gives us

$$\begin{aligned} \lambda t + \frac{m_1 + m_2}{r} &\rightarrow \lambda t + \frac{2(\tilde{m}_1 + \tilde{m}_2)}{\tilde{r}^2}, \quad \alpha V^{-1} (d\tau + \vec{\omega} \cdot d\vec{r}) \rightarrow \frac{\sigma \tilde{r}^2}{4} \left( \frac{d\tilde{\tau}}{2} + \cos \theta d\phi \right), \\ V^{-1} (d\tau + \vec{\omega} \cdot d\vec{r})^2 + V d\tilde{r}^2 &\rightarrow d\tilde{r}^2 + \frac{\tilde{r}^2}{4} \left( d\Omega^2 + \left( \frac{d\tilde{\tau}}{2} + \cos \theta d\phi \right)^2 \right), \end{aligned} \quad (8.62)$$

and so the metric becomes

$$\begin{aligned} ds^2 \simeq & - \left( \lambda t + \frac{2(\tilde{m}_1 + \tilde{m}_2)}{\tilde{r}^2} \right)^{-2} \left( dt + \frac{\sigma \tilde{r}^2}{4} \left( \frac{d\tilde{\tau}}{2} + \cos \theta d\phi \right) \right)^2 \\ & + \left( \lambda t + \frac{2(\tilde{m}_1 + \tilde{m}_2)}{\tilde{r}^2} \right) \left( d\tilde{r}^2 + \frac{\tilde{r}^2}{4} \left( d\Omega^2 + \left( \frac{d\tilde{\tau}}{2} + \cos \theta d\phi \right)^2 \right) \right). \end{aligned} \quad (8.63)$$

#### The Case $\beta = 1$

Employing the following coordinate transformations

$$\tilde{r}^2 = 8nr, \quad nd\tilde{\tau} = d\tau, \quad \tilde{m}_j = 4m_j n, \quad \sigma = 8\alpha n^3, \quad (8.64)$$

gives us

$$\lambda t + \frac{m_1 + m_2}{r} \rightarrow \lambda t + \frac{2(\tilde{m}_1 + \tilde{m}_2)}{\tilde{r}^2}, \quad \alpha V (d\tau + \vec{\omega} \cdot d\vec{r}) \rightarrow \frac{4\sigma}{\tilde{r}^2} \left( \frac{d\tilde{\tau}}{2} + \cos\theta d\phi \right),$$

$$V^{-1} (d\tau + \vec{\omega} \cdot d\vec{r})^2 + V d\vec{r}^2 \rightarrow d\tilde{r}^2 + \frac{\tilde{r}^2}{4} \left( d\Omega^2 + \left( \frac{d\tilde{\tau}}{2} + \cos\theta d\phi \right)^2 \right), \quad (8.65)$$

and so the metric becomes

$$ds^2 \simeq - \left( \lambda t + \frac{2(\tilde{m}_1 + \tilde{m}_2)}{\tilde{r}^2} \right)^{-2} \left( dt + \frac{4\sigma}{\tilde{r}^2} \left( \frac{d\tilde{\tau}}{2} + \cos\theta d\phi \right) \right)^2$$

$$+ \left( \lambda t + \frac{2(\tilde{m}_1 + \tilde{m}_2)}{\tilde{r}^2} \right) \left( d\tilde{r}^2 + \frac{\tilde{r}^2}{4} \left( d\Omega^2 + \left( \frac{d\tilde{\tau}}{2} + \cos\theta d\phi \right)^2 \right) \right).$$
(8.66)

### Conclusion

These metrics are similar to the KS and RNdS metrics respectively with mass term  $2(\tilde{m}_1 + \tilde{m}_2)$  and angular momentum  $8\sigma$  for KS,  $\sigma$  for RNdS, but the topology of a  $\tilde{r} = \text{const}$  surface here has topology  $L(2; 1) = \mathbb{S}^3/\mathbb{Z}_2$  compared with  $\mathbb{S}^3$  in the aforementioned metrics, due to the presence of a  $\frac{d\tilde{\tau}}{2}$  term instead of a  $d\tilde{\tau}$  term. This means the black holes coalesce:

$$\text{Two black holes } (\tilde{m}_1, \sigma), (\tilde{m}_2, \sigma) \quad \longrightarrow \quad \text{One black hole } (2(\tilde{m}_1 + \tilde{m}_2), (8)\sigma). \quad (8.67)$$

For **SC black holes** (with  $\alpha$  and therefore  $\sigma$  being zero), we have

$$ds^2 \simeq - \left( \lambda t + \frac{2(\tilde{m}_1 + \tilde{m}_2)}{\tilde{r}^2} \right)^{-2} dt^2$$

$$+ \left( \lambda t + \frac{2(\tilde{m}_1 + \tilde{m}_2)}{\tilde{r}^2} \right) \left( d\tilde{r}^2 + \frac{\tilde{r}^2}{4} \left( d\Omega^2 + \left( \frac{d\tilde{\tau}}{2} + \cos\theta d\phi \right)^2 \right) \right).$$
(8.68)

For **RN black holes** (with  $\lambda t$  being replaced by 1), we have

$$ds^2 \simeq - \left( 1 + \frac{2(\tilde{m}_1 + \tilde{m}_2)}{\tilde{r}^2} \right)^{-2} \left( dt + \frac{4\sigma}{\tilde{r}^2} \left( \frac{d\tilde{\tau}}{2} + \cos\theta d\phi \right) \right)^2$$

$$+ \left( 1 + \frac{2(\tilde{m}_1 + \tilde{m}_2)}{\tilde{r}^2} \right) \left( d\tilde{r}^2 + \frac{\tilde{r}^2}{4} \left( d\Omega^2 + \left( \frac{d\tilde{\tau}}{2} + \cos\theta d\phi \right)^2 \right) \right).$$
(8.69)

For **SN black holes** (with  $\lambda t$  being replaced by 1 and  $\alpha$  being zero), we have

$$\begin{aligned}
 ds^2 \simeq & - \left( 1 + \frac{2(\tilde{m}_1 + \tilde{m}_2)}{\tilde{r}^2} \right)^{-2} dt^2 \\
 & + \left( 1 + \frac{2(\tilde{m}_1 + \tilde{m}_2)}{\tilde{r}^2} \right) \left( d\tilde{r}^2 + \frac{\tilde{r}^2}{4} \left( d\Omega^2 + \left( \frac{d\tilde{\tau}}{2} + \cos\theta d\phi \right)^2 \right) \right).
 \end{aligned} \tag{8.70}$$

### 8.5.2 Asymptotic behaviour for $\epsilon = 1$

The situation is more straightforward here. We temporarily revert to the form of the metric in (8.2). The asymptotic form of this metric is given by (see [36]):

$$\begin{aligned}
 ds^2 \simeq & \left( dt + \alpha V^\beta (d\tau + \vec{\omega} \cdot d\vec{r}) \right)^2 + \exp(\lambda t) \left( V^{-1} (d\tau + \vec{\omega} \cdot d\vec{r})^2 + V d\tilde{r}^2 \right), \\
 V = 1 + & \sum_{j=1}^N n_j |\vec{r} - \vec{r}_j|^{-1}, \quad \vec{\nabla} V = \vec{\nabla} \times \vec{\omega},
 \end{aligned} \tag{8.71}$$

which is the same metric as the Gross-Perry-Sorkin monopole we introduced in (2.35) but with a cosmological constant. If we have two black holes positioned once again as in (8.36) with  $V$  and  $\vec{\omega}$  as in (8.46), this metric becomes

$$\begin{aligned}
 ds^2 \simeq & \left( dt + \sigma \left( 1 + \frac{2n}{r} \right)^\beta \left( \frac{d\tilde{\tau}}{2} + \cos\theta d\phi \right) \right)^2 \\
 & + \exp(\lambda t) \left( n^2 \left( 1 + \frac{2n}{r} \right)^{-1} \left( \frac{d\tilde{\tau}}{2} + \cos\theta d\phi \right)^2 + \left( 1 + \frac{2n}{r} \right) d\tilde{r}^2 \right),
 \end{aligned} \tag{8.72}$$

if  $n := n_1 = n_2$ ,  $\sigma := n^2 \alpha$  and we use the coordinate transformation  $\tau = n\tilde{\tau}$ . As before, the black holes coalesce into one black hole with horizon topology  $L(2; 1) = \mathbb{S}^3/\mathbb{Z}_2$ .

For **SC black holes** we have

$$\begin{aligned}
 ds^2 \simeq & - \left( \lambda t + \frac{2(\tilde{m}_1 + \tilde{m}_2)}{\tilde{r}^2} \right)^{-2} dt^2 \\
 & + \left( \lambda t + \frac{2(\tilde{m}_1 + \tilde{m}_2)}{\tilde{r}^2} \right) \left( d\tilde{r}^2 + \frac{\tilde{r}^2}{4} \left( d\Omega^2 + \left( \frac{d\tilde{\tau}}{2} + \cos\theta d\phi \right)^2 \right) \right).
 \end{aligned} \tag{8.73}$$

For **RN black holes** we have

$$\begin{aligned}
 ds^2 \simeq & - \left( 1 + \frac{2(\tilde{m}_1 + \tilde{m}_2)}{\tilde{r}^2} \right)^{-2} \left( dt + \frac{\tilde{r}^2}{4} \left( \frac{d\tilde{r}}{2} + \cos\theta d\phi \right) \right)^2 \\
 & + \left( 1 + \frac{2(\tilde{m}_1 + \tilde{m}_2)}{\tilde{r}^2} \right) \left( d\tilde{r}^2 + \frac{\tilde{r}^2}{4} \left( d\Omega^2 + \left( \frac{d\tilde{r}}{2} + \cos\theta d\phi \right)^2 \right) \right).
 \end{aligned} \tag{8.74}$$

For **SN black holes** we have

$$\begin{aligned}
 ds^2 \simeq & - \left( 1 + \frac{2(\tilde{m}_1 + \tilde{m}_2)}{\tilde{r}^2} \right)^{-2} dt^2 \\
 & + \left( 1 + \frac{2(\tilde{m}_1 + \tilde{m}_2)}{\tilde{r}^2} \right) \left( d\tilde{r}^2 + \frac{\tilde{r}^2}{4} \left( d\Omega^2 + \left( \frac{d\tilde{r}}{2} + \cos\theta d\phi \right)^2 \right) \right).
 \end{aligned} \tag{8.75}$$

### 8.5.3 Conclusion

As we have seen, each of our RC metrics is asymptotic to a stationary metric that describes extreme rotating black holes with a cosmological constant, and similar results apply to our special cases. We could generalise these results for  $N$  black holes, as then we would have

$$U \simeq \lambda t + mr^{-1}, \quad V \simeq \epsilon + nr^{-1}, \quad \vec{\omega} \cdot d\vec{r} \simeq n \cos\theta d\phi, \tag{8.76}$$

where  $m$  and  $n$  are defined as in (8.8). Thus, the  $N$  black holes would coalesce into one black hole with horizon topology given by  $L(n; 1) = \mathbb{S}^3/\mathbb{Z}_n$ . This leaves us in an interesting situation in the case of having infinitely many identical black holes. We could interpret this as saying that, viewed from a distance, our five-dimensional space looks like a four-dimensional space, which is what one might expect in a Kaluza-Klein-type situation. Having looked at the asymptotic behaviour of our solutions and checked that the black holes are regular at the event horizons, we now move to looking at the specific situations that arise when we have infinitely many black holes, distributed in various ways.

## 8.6 Periodic Distributions

In this section, we let the number  $N$  of identical black holes go to infinity and distribute the black holes periodically along the  $x_3$ -axis. We will consider the most general (RC) case with the metric as in (8.4) and potentials given by

$$U = \lambda t + m \left( \sum_{j=-\infty}^{\infty} (\rho_2^2 + (x_3 + Pj)^2)^{-\frac{1}{2}} - 2 \sum_{j=1}^{\infty} (Pj)^{-1} \right),$$

$$V = 1 + n \left( \sum_{j=-\infty}^{\infty} (\rho_2^2 + (x_3 + Pj)^2)^{-\frac{1}{2}} - 2 \sum_{j=1}^{\infty} (Pj)^{-1} \right), \quad (8.77)$$

where we have subtracted an infinite constant in order to ensure convergence. Since we require that  $m > 0$  and  $n > 0$  in order to avoid singularities, both  $U$  and  $V$  will have zero strips (see figure 7.2 to get an idea of the general shape).

For a given choice of  $x_3$ , let  $\rho_U$  denote the value of  $\rho_2$  such that  $U(\rho_2, x_3) = 0$  when  $t$  is zero, and let  $\rho_V$  denote the value of  $\rho_2$  such that  $V(\rho_2, x_3) = 0$ . In order to investigate the singularity structure of the space, we need to approximate  $U$  and  $V$  near to where they become zero. We accomplish this by using logarithmic approximations

$$U_{approx} = \lambda t + a - 2b \ln \rho_2, \quad V_{approx} = c - 2d \ln \rho_2, \quad (8.78)$$

where

$$\begin{aligned} a &= -\rho_U \ln(\rho_U) \left( \frac{\partial}{\partial \rho_2} (U - \lambda t) \right) \Big|_{\rho_U}, & b &= -\frac{\rho_U}{2} \left( \frac{\partial}{\partial \rho_2} (U - \lambda t) \right) \Big|_{\rho_U}, \\ c &= -\rho_V \ln(\rho_V) \frac{\partial V}{\partial \rho_2} \Big|_{\rho_V}, & d &= -\frac{\rho_V}{2} \frac{\partial V}{\partial \rho_2} \Big|_{\rho_V}. \end{aligned} \quad (8.79)$$

We know from our work in previous chapters that this will provide a good approximation to  $U$  and  $V$  near to where they become zero.  $U_{approx}$  does satisfy the Laplace equation  $\nabla^2 U_{approx} = 0$  and for this choice of  $V_{approx}$ , we must have

$$\vec{\omega} = (0, 0, -2d\theta) \quad , \text{ where } \quad \theta = \arctan \left( \frac{x_1}{x_2} \right). \quad (8.80)$$

The metric then becomes, with cylindrical coordinates  $\vec{r} = (\rho, \theta, x_3)$ ,

$$ds^2 = -U^{-2} dt^2 + UV d\vec{r}^2 - 2\alpha V^\beta U^{-2} (d\tau - 2d\theta dx_3) dt + W (d\tau - 2d\theta dx_3)^2, \quad (8.81)$$

where

$$W := UV^{-1} - \alpha^2 U^{-2} V^{2\beta}. \quad (8.82)$$

We can then calculate the Riemann curvature tensor. We take  $\rho := \rho_2$ . There are two cases to consider.

### 8.6.1 The Case of $\beta = -1$

We have

$$[R]^2 = \frac{f}{4\rho^4 V^8 U^8} \quad \text{with} \quad f = \sum_{j=0}^8 u_j U^j, \quad (8.83)$$

where the coefficients  $u_j$  are given by

$$\begin{aligned} u_0 &= 544\alpha^4 d^4, & u_1 &= -904V^3 d^2 \alpha^2 \left(4b^2 + (\alpha\lambda\rho)^2\right), \\ u_2 &= 1152b\alpha^2 d^2 V^2 (V - 4d) + 127V^6 \left(16b^4 + 8(\alpha b\lambda\rho)^2 + (\alpha\lambda\rho)^4\right), \\ u_3 &= 240bV^5 \left(4b^2(d - V) + d(\alpha\lambda\rho)^2\right) - 128V\alpha^2 d^2 (V^2 - 9Vd + 24d^2), \\ u_4 &= 16V^4 \left(12b^2 (V^2 - 2dV + 2d^2) + (\alpha d\lambda\rho)^2\right), \\ u_5 &= -2V^7 \rho^2 \lambda^2 \left(4b^2 + (\alpha\lambda\rho)^2\right), \\ u_6 &= 128d^2 V^2 (V^2 - 6dV + 12d^2), & u_7 &= 0, \\ u_8 &= 10V^8 \rho^4 \lambda^4. \end{aligned} \quad (8.84)$$

We can see that  $f \rightarrow 544\alpha^4 d^4$  when either  $U$  or  $V$  tends to zero, and thus such points are singular.

### 8.6.2 The Case of $\beta = 1$

We have

$$[R]^2 = \frac{f}{4\rho^4 V^6 U^8} \quad \text{with} \quad f = \sum_{j=0}^8 u_j U^j, \quad (8.85)$$

where the coefficients  $u_j$  are given by

$$\begin{aligned} u_0 &= 544\alpha^4 d^4 V^6, & u_1 &= -904V^5 d^2 \alpha^2 \left(4b^2 + (\alpha\lambda\rho)^2 V^4\right), \\ u_2 &= 1152b\alpha^2 d^2 V^5 + 127V^4 \left(16b^4 + 8(\alpha b\lambda\rho)^2 V^4 + (\alpha\lambda\rho)^4 V^8\right), \\ u_3 &= 240bV^3 \left(4b^2(d - V) - 3d(\alpha\lambda\rho)^2 V^4\right) - 128V^5 \alpha^2 d^2, \\ u_4 &= 192V^2 b^2 (V^2 - 2dV + 2d^2) + 208(\alpha d\lambda\rho)^2 V^6, \\ u_5 &= -2V^5 \rho^2 \lambda^2 \left(4b^2 + (\alpha\lambda\rho)^2 V^4\right), \\ u_6 &= 128d^2 (V^2 - 6dV + 12d^2), & u_7 &= 0, \\ u_8 &= 10V^6 \rho^4 \lambda^4. \end{aligned} \quad (8.86)$$

We can see that  $f \rightarrow 544\alpha^4 d^4 V^6$  when  $U \rightarrow 0$  and  $f \rightarrow 1536d^4 U^6$  when  $V \rightarrow 0$ , and thus such points are singular.

### 8.6.3 Values of the Parameter $\alpha$

We now investigate how the fact that  $U$  and  $V$  can become negative in the periodic black hole solution affects the values that  $\alpha$  can take. Earlier, we insisted that  $\alpha \in [0, 1)$  in order to avoid the presence of **Closed Timelike Curves** (CTCs) in our solutions. Looking at the two-dimensional  $(\phi, \tau)$ -part of the metric, we see that

$$ds^2 \Big|_{(\phi, \tau)} = \left( UV^{-1} - \alpha^2 U^{-2} V^{2\beta} \right) (d\tau + \vec{\omega} \cdot d\vec{r}) + UV r^2 \sin^2 \theta d\phi^2. \quad (8.87)$$

The metric is positive definite, and thus CTCs are avoided if and only if

$$M = \begin{pmatrix} UV^{-1} - \alpha^2 U^{-2} V^{2\beta} & 0 \\ 0 & UV r^2 \sin^2 \theta \end{pmatrix} \quad (8.88)$$

is positive definite. We thus require that  $\det M > 0$  and  $W := UV^{-1} - \alpha^2 U^{-2} V^{2\beta} > 0$ . This means that

- if  $U > 0, V > 0$  or  $U < 0, V < 0$ , then  $UV > 0$ ; need  $W > 0$ ;
- if  $U > 0, V < 0$  or  $U < 0, V > 0$ , then  $UV < 0$  and so it is not possible to avoid having CTCs.

If  $\beta = -1$ , then  $W > 0$  if and only if  $U^3 V > \alpha^2$ . We can plot  $U^3 V$  for various examples (see (8.90), (8.91) and (8.92)) and find that

- if  $U \not\equiv V$ , then  $U^3 V \leq 0$  between  $\rho_U$  and  $\rho_V$ , and is otherwise positive;
- if  $U \equiv V$  then  $U^4 = 0$  at the point where  $U = 0$  (which is a turning point) and is otherwise positive.

If  $\beta = 1$ , then  $W > 0$  if and only if  $U^3 V^{-3} > \alpha^2$ . We see that

- if  $U \equiv V$ , then if  $\alpha^2 \in [0, 1)$  there will be no CTCs - they occur for  $\alpha \geq 1$ ;
- if  $U \not\equiv V$  then  $U^3 V^{-3} \leq 0$  between  $\rho_U$  and  $\rho_V$ , is zero when  $U$  is zero, is undefined when  $V$  is zero, and is otherwise positive.

From this, we can see that CTCs are inevitable in almost all circumstances, and always if we have two singularities. This is the case because we can always choose  $\alpha$  to be such that  $W \leq 0$  and so the matrix  $M$  is not positive definite. In particular, they will always arise in the region between the singularities, even in the simplest (SN) case.

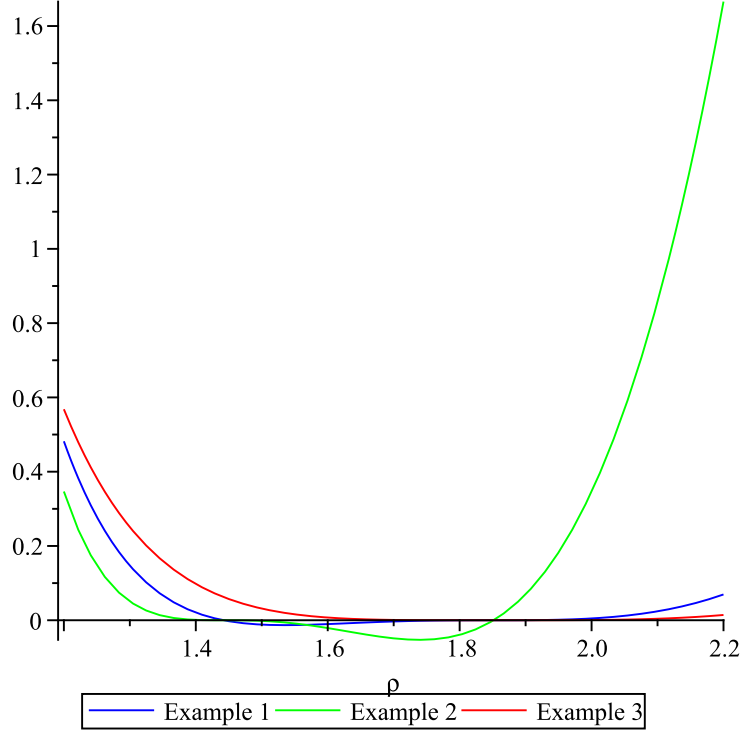


Figure 8.1: Presence of CTCs for non-cosmological black hole examples ((8.90), (8.91) and (8.92) are examples one, two and three respectively) and  $\beta = -1$ , with  $\rho := \rho_2 \in [1.3, 2.3]$

#### 8.6.4 Useful Examples

When we investigate periodic solutions, we will use standard examples. Let

$$\phi := \left( \sum_{j=-\infty}^{\infty} (\rho_2^2 + (x_3 + j)^2)^{-\frac{1}{2}} - 2 \sum_{j=1}^{\infty} j^{-1} \right), \quad (8.89)$$

then for RN and SN black holes, we have

$$U_1 = 1 + \phi, \quad V_1 = 1 + 2\phi, \quad (8.90)$$

$$U_2 = 1 + 2\phi, \quad V_2 = 1 + \phi, \quad (8.91)$$

$$U_3 = 1 + \phi = V_3; \quad (8.92)$$

for RC and SC black holes, we have

$$U_4 = \lambda t + \phi, \quad V_4 = 1 + 2\phi, \quad (8.93)$$

$$U_5 = \lambda t + 2\phi, \quad V_5 = 1 + \phi, \quad (8.94)$$

$$U_6 = \lambda t + \phi, \quad V_6 = 1 + \phi. \quad (8.95)$$

Note here we have taken  $\epsilon$  to be one, but similar results follow when  $\epsilon$  is zero.



## 8.7 Periodic Solutions - Singularity Properties

In this section, we look to see if the singularities at points where either  $U$  or  $V$  are zero, which arise with periodic distributions as above, are naked singularities. The situation is complicated by the fact that we have to look at two exterior and interior regions. Here, we can assume without loss of generality that  $\rho_V < \rho_U$  as the same argument applies in the other case. We can see from the diagram below that:

- for the exterior of  $V$ ,  $U > 0$  and  $V > 0$ ;
- for the interior of  $V$ ,  $U > 0$  and  $V < 0$  for  $\rho \in (\rho_V, \rho_U)$  and  $U < 0$  and  $V < 0$  for  $\rho > \rho_U$ ;
- for the exterior of  $U$ ,  $U > 0$  and  $V < 0$  for  $\rho \in (\rho_V, \rho_U)$  and  $U > 0$  and  $V > 0$  for  $\rho < \rho_V$ ;
- for the interior of  $U$ ,  $U < 0$  and  $V < 0$ .

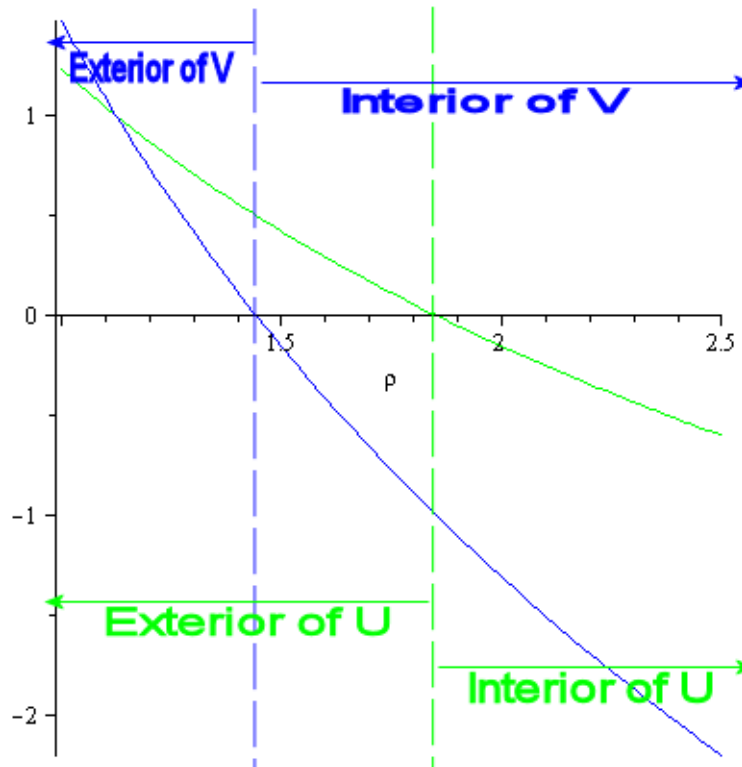


Figure 8.2: The interior and exterior regions for a Kaluza-Klein black hole

In order to ensure that the metric is Lorentzian throughout the spacetime, we see that

$$ds^2 = -U^{-2} \left( dt + \alpha V^\beta (d\tau + \vec{\omega} \cdot d\vec{r}) \right)^2 + U \left( V^{-1} (d\tau + \vec{\omega} \cdot d\vec{r})^2 + V d\vec{r}^2 \right) \quad (8.96)$$

in the regions where  $U > 0$  and  $V > 0$  or  $U < 0$  and  $V < 0$ , and

$$ds^2 = +U^{-2} \left( dt + \alpha V^\beta (d\tau + \vec{\omega} \cdot d\vec{r}) \right)^2 + U \left( V^{-1} (d\tau + \vec{\omega} \cdot d\vec{r})^2 + V d\vec{r}^2 \right) \quad (8.97)$$

in the region where  $U > 0$  and  $V < 0$ . Let us begin our analysis by considering radial null geodesics, giving us

$$t = t(s), \quad x := x_1(s), \quad x_2 = x_3 = \tau = 0, \quad (8.98)$$

yielding the metric

$$ds^2 = \pm U^{-2}(x, t) \left( dt + \alpha V^\beta(x) \omega_x dx \right)^2 + U(x, t) \left( V^{-1}(x) \omega_x^2 + V(x) \right) dx^2, \quad (8.99)$$

and thus the Lagrangian

$$\mathcal{L} = \pm U^{-2}(x, t) \left( \dot{t} + \alpha V^\beta(x) \omega_x \dot{x} \right)^2 + U(x, t) \left( V^{-1}(x) \omega_x^2 + V(x) \right) \dot{x}^2. \quad (8.100)$$

If we use our approximations for  $U$  and  $V$ ,

$$U_{appx} = \lambda t + a - 2b \ln x, \quad V_{appx} = c - 2d \ln x, \quad (8.101)$$

then  $\omega_x = 0$  and the Lagrangian becomes

$$\mathcal{L} = \pm U(x, t)^{-2} \dot{t}^2 + U(x, t) V(x) \dot{x}^2 = 0. \quad (8.102)$$

The geodesics are given by the Euler-Lagrange equations:

$$\begin{aligned} \frac{d}{ds} (\pm 2U^{-2} \dot{t}) - \frac{\partial U}{\partial t} (\mp 2U(x, t)^{-3} \dot{t}^2 + V \dot{x}^2) &= 0, \\ \frac{d}{ds} (2UV \dot{x}) \mp \dot{t}^2 \frac{\partial}{\partial x} (U^{-2}) - \left( U \frac{dV}{dx} + V \frac{\partial U}{\partial x} \right) \dot{x}^2 &= 0. \end{aligned} \quad (8.103)$$

At this point, we note that  $\alpha$  is not present and rotation does not play a part in these calculations; we now therefore consider two cases: non-cosmological and cosmological black holes.

### 8.7.1 Non-Cosmological Black Holes

We no longer have to consider  $U$  to be dependent on  $t$ , and so we have

$$U_{appx} = a - 2b \ln x, \quad V_{appx} = c - 2d \ln x,$$

$$\mathcal{L} = \pm U(x)^{-2} \dot{t}^2 + U(x) V(x) \dot{x}^2 = 0,$$

$$\begin{aligned} \frac{d}{ds} (\pm 2U^{-2}\dot{t}) &= 0, \\ \frac{d}{ds} (2UV\dot{x}) \mp \dot{t}^2 \frac{d}{dx} (U^{-2}) - \left( U \frac{dV}{dx} + V \frac{dU}{dx} \right) \dot{x}^2 &= 0. \end{aligned} \quad (8.104)$$

### ***U* and *V* have the Same Sign**

In this case of (8.96), if we have

$$\mathcal{L} = -U^{-2}\dot{t}^2 + UV\dot{x}^2 = 0, \quad (8.105)$$

then we can see that if we define

$$E := U^{-2}\dot{t}, \quad (8.106)$$

we have

$$\dot{E} = 0 \quad \text{and} \quad \dot{x}^2 = U^{-3}V^{-1}\dot{t}^2 \quad \Rightarrow \quad \frac{dt}{dx} = \frac{\dot{t}}{\dot{x}} = \pm U^{\frac{3}{2}}V^{\frac{1}{2}}. \quad (8.107)$$

We can therefore take

$$\begin{aligned} t &= \pm \int_{x_0}^{x_1} U^{\frac{3}{2}}V^{\frac{1}{2}} dx \\ &= \pm \int_{x_0}^{x_1} (a - 2b \ln x)^{\frac{3}{2}} (c - 2d \ln x)^{\frac{1}{2}} dx, \end{aligned} \quad (8.108)$$

where  $x_0$  is the position of either singularity and  $x_1$  is a finite but large distance from the singularity.

### ***U* and *V* have Opposite Signs**

The analysis in the case of (8.97) is similar. If we have

$$\mathcal{L} = U^{-2}\dot{t}^2 + UV\dot{x}^2 = 0, \quad (8.109)$$

then we see that if we define

$$E := U^{-2}\dot{t}, \quad (8.110)$$

we have

$$\dot{E} = 0 \quad \text{and} \quad \dot{x}^2 = -UV^{-1}E^2 \quad \Rightarrow \quad \frac{dt}{dx} = \frac{\dot{t}}{\dot{x}} = \pm U^2 (-UV^{-1})^{-\frac{1}{2}}. \quad (8.111)$$

We can therefore take

$$\begin{aligned}
 t &= \pm \int_{x_0}^{x_1} U^2 \left| UV^{-1} \right|^{-\frac{1}{2}} dx \\
 &= \pm \int_{x_0}^{x_1} (a - 2b \ln x)^2 \left| (a - 2b \ln x) (c - 2d \ln x)^{-1} \right|^{-\frac{1}{2}} dx
 \end{aligned} \tag{8.112}$$

throughout the whole spacetime. We can see that  $t$  is finite as we move away from either of the singularities in either direction and can therefore conclude that the singularities can be reached by an observer a significant distance away in a finite period of time and hence are naked singularities.

### 8.7.2 Cosmological Black Holes

The situation is more complicated here as the point where  $U$  is zero is not stationary; for a given  $t$ , the value of  $x$  such that  $U$  is zero is given by

$$x = \exp\left(\frac{a + \lambda t}{2b}\right), \tag{8.113}$$

so the singularity drifts through the spacetime! Rearranging the Lagrangian gives us

$$\frac{dt}{dx} = \pm U(x, t)^2 \left| U(x, t) V(x)^{-1} \right|^{-\frac{1}{2}}. \tag{8.114}$$

It is not clear how one might proceed in this situation and so we leave the question open for further work.

## 8.8 Non-Periodic and Lattice Distributions

As in previous chapters, we consider alternative methods of ensuring the convergence of the functions  $U$  and  $V$ , firstly by arranging the infinitely many identical black holes in a non-periodic pattern and secondly by using a three-dimensional lattice arrangement.

### 8.8.1 Non-Periodic Distributions of Black Holes

Firstly, we consider having a non-periodic distribution of black holes, modifying the method of Anderson et al [1]. Let  $\{\vec{r}_j\}_{j=0}^{\infty} \subset \mathbb{R}^3$  be a divergent sequence of points such that for some point  $\vec{r}_0 \in \mathbb{R}^3$ ,

$$\sum_{j=1}^{\infty} \frac{m}{|\vec{r}_0 - \vec{r}_j|} < \infty. \tag{8.115}$$

We can then define smooth functions  $U : \mathbb{R}^3 / \{\vec{r}_j\} \rightarrow \mathbb{R}$  and  $V : \mathbb{R}^3 / \{\vec{r}_j\} \rightarrow \mathbb{R}$  by

$$U(r, t) := \lambda t + \sum_{j=1}^{\infty} \frac{m}{|\vec{r} - \vec{r}_j|}, \quad V(r) := \epsilon + \sum_{j=1}^{\infty} \frac{n}{|\vec{r} - \vec{r}_j|}. \quad (8.116)$$

Clearly,  $U$  and  $V$  satisfy the Laplace equation on  $\mathbb{R}^3$ :

$$\nabla^2 U = \frac{\partial^2 U}{\partial t^2} + \frac{\partial^2 U}{\partial (x_1)^2} + \frac{\partial^2 U}{\partial (x_2)^2} + \frac{\partial^2 U}{\partial (x_3)^2} = 0 = \frac{\partial^2 V}{\partial (x_1)^2} + \frac{\partial^2 V}{\partial (x_2)^2} + \frac{\partial^2 V}{\partial (x_3)^2} = \nabla^2 V. \quad (8.117)$$

We know that the metric is regular at  $\vec{r} = \vec{r}_j$  and that these are the event horizons for the black holes, which is enough to ensure that this construction makes sense.

Recall from chapter six that if we use the example of having the black holes positioned at  $\vec{r}_j = (0, 0, j^{1+\kappa})$  for some  $\kappa > 0$ , then we have

$$\vec{\omega} \cdot d\vec{r} = \left( n \sum_{-\infty}^{\infty} \frac{x_3 - j^{1+\kappa}}{(\rho^2 + (x_3 - j^{1+\kappa})^2)^{-\frac{1}{2}}} \right) d\theta, \quad (8.118)$$

and fixing the value of  $x_3$  gives us a much simplified metric to work with. This converges if we take  $\kappa = 2$ , for instance.

### 8.8.2 The Case $\beta = -1$

We can calculate the Riemann curvature scalar, taking  $\rho := \rho_2$ , and see that

$$[R]^2 = \frac{f(U, V)}{4\rho^2 V^8 U^8} \quad \text{with} \quad f(U, V) = \sum_{j=0}^8 u_j U^j, \quad (8.119)$$

where the coefficients  $u_j$  are given by

$$\begin{aligned} u_0 &= 11\rho^2 \alpha^4 (\partial_\rho V)^4, \quad u_1 = -104\rho^2 \alpha^2 V^3 (\partial_\rho V)^2 \left( \alpha^2 \lambda^2 + (\partial_\rho U)^2 \right), \\ u_2 &= \rho V^2 \left[ 127\rho V^4 \left( \alpha^2 \lambda^2 + (\partial_\rho U)^2 \right)^2 - 20\rho \alpha^2 V (\partial_\rho V)^2 \partial_{\rho\rho} U \right. \\ &\quad \left. + 4\alpha^2 \partial_\rho U \partial_\rho V \left( 16\rho V \partial_{\rho\rho} V - 2V \partial_\rho V - 29\rho (\partial_\rho V)^2 \right) \right], \\ u_3 &= -4V \left[ \left( 26\rho^2 (\partial_\rho U)^2 \partial_{\rho\rho} U - 4\rho \partial_{\rho U} \left( \alpha^2 \lambda^2 + (\partial_\rho U)^2 \right) - 4\lambda^2 \alpha^2 \rho^2 \partial_{\rho\rho} U \right) V^5 \right. \\ &\quad \left. - 15\rho^2 V^4 \partial_\rho U \partial_\rho V \left( \alpha^2 \lambda^2 + (\partial_\rho U)^2 \right) + 2\alpha^2 V^2 \left( \rho^2 (\partial_{\rho\rho} V)^2 + (\partial_\rho V)^2 \right) \right. \\ &\quad \left. + \alpha^2 \rho V (\partial_\rho V)^2 (2\partial_\rho V - 11\rho \partial_{\rho\rho} V) + 15\alpha^2 \rho^2 (\partial_\rho V)^4 \right], \end{aligned}$$

$$\begin{aligned}
 u_4 &= 2V^4 \left[ 11\rho^2 (\partial_\rho U)^2 (\partial_\rho V)^2 + 14V^2 \left( \rho^2 (\partial_{\rho\rho} U)^2 + (\partial_\rho U)^2 \right) \right. \\
 &\quad \left. - 6\rho^2 \left( \alpha^2 \lambda^2 (\partial_\rho V)^2 + 2V \partial_\rho U \partial_\rho V \partial_{\rho\rho} U \right) \right. \\
 + \quad &4\rho V \left( V \partial_\rho U \partial_{\rho\rho} U + 2\partial_\rho V \left( \alpha^2 \lambda^2 + (\partial_\rho U)^2 \right) + \rho \partial_{\rho\rho} V \left( 2\alpha^2 \lambda^2 - (\partial_\rho U)^2 \right) \right) \left. \right], \\
 u_5 &= -2V^3 \left[ \rho^2 \lambda^2 V^4 \left( \alpha^2 \lambda^2 + (\partial_\rho U)^2 \right) - 4\rho^2 V \partial_\rho U \partial_\rho V \partial_{\rho\rho} V \right. \\
 &\quad \left. - 4V^2 (\partial_\rho V + \rho \partial_{\rho\rho} V) (\partial_\rho U + \rho \partial_{\rho\rho} U) + 6\rho^2 \partial_\rho U (\partial_\rho V)^3 \right], \\
 u_6 &= -V^2 \left[ 4\rho \lambda^2 V^5 (\partial_\rho U + \rho \partial_{\rho\rho} U) + \rho^2 (\partial_\rho V)^2 \left( 32V \partial_{\rho\rho} V - 27 (\partial_\rho V)^2 \right) \right. \\
 &\quad \left. - 4V^2 \left( 3\rho^2 (\partial_{\rho\rho} V)^2 + 2\rho \partial_\rho V \partial_{\rho\rho} V + 3 (\partial_\rho V)^2 \right) \right], \\
 u_7 &= -2\rho V^5 \left[ 2\lambda^2 V (\partial_\rho V + \rho \partial_{\rho\rho} V) - \rho \lambda^2 (\partial_\rho V)^2 \right], \quad u_8 = 10\rho^2 \lambda^4 V^8. \tag{8.120}
 \end{aligned}$$

### 8.8.3 The Case $\beta = 1$

We can calculate the Riemann curvature scalar to give

$$[R]^2 = \frac{f(U, V)}{4\rho^2 V^6 U^8} \quad \text{with} \quad f(U, V) = \sum_{j=0}^8 u_j U^j, \tag{8.121}$$

where the coefficients  $u_j$  are given by

$$\begin{aligned}
 u_0 &= 11\rho^2 \alpha^4 V^6 (\partial_\rho V)^4, \\
 u_1 &= -104\rho^2 \alpha^2 V^5 (\partial_\rho V)^2 \left( \alpha^2 \lambda^2 V^4 + (\partial_\rho U)^2 \right), \\
 u_2 &= -\rho V^4 \left[ -127\rho \left( \alpha^2 \lambda^2 V^4 + (\partial_\rho U)^2 \right)^2 + 20\rho \alpha^2 V (\partial_\rho V)^2 \partial_{\rho\rho} U \right. \\
 &\quad \left. + 4\alpha^2 \partial_\rho U \partial_\rho V \left( -16\rho V \partial_{\rho\rho} V + 2V \partial_\rho V - 3\rho (\partial_\rho V)^2 \right) \right], \\
 u_3 &= -4V^3 \left[ \rho^2 \partial_\rho V \left( 7\alpha^2 (\partial_\rho V)^3 - 15 (\partial_\rho U)^3 \right) - 4\rho \alpha^2 \lambda^2 V^5 (\partial_\rho U + \rho \partial_{\rho\rho} U) \right. \\
 &\quad \left. + 45\alpha^2 \rho^2 \lambda^2 V^4 \partial_\rho U \partial_\rho V + 2\alpha^2 V^2 \left( \rho^2 (\partial_{\rho\rho} V)^2 + (\partial_\rho V)^2 \right) \right. \\
 &\quad \left. + \left( 2\rho (\partial_\rho U)^2 (13\rho \partial_{\rho\rho} U - 2\partial_\rho U) + \alpha^2 \rho (\partial_\rho V)^2 (2\partial_\rho V - 3\rho \partial_{\rho\rho} V) \right) V \right], \\
 u_4 &= 2V^2 \left[ 11\rho^2 (\partial_\rho U)^2 (\partial_\rho V)^2 - 4\rho \partial_\rho U \left( 3\rho \partial_\rho V \partial_{\rho\rho} U - 2\partial_\rho U \partial_\rho V + \rho \partial_\rho U \partial_{\rho\rho} V \right) V \right. \\
 &\quad \left. + 8\rho \alpha^2 \lambda^2 (\rho \partial_{\rho\rho} V + \partial_\rho V) V^5 + 18\rho^2 \alpha^2 \lambda^2 V^4 (\partial_\rho V)^2 \right. \\
 &\quad \left. + 2 \left( 7\rho^2 (\partial_{\rho\rho} U)^2 + 2\rho \partial_\rho U \partial_{\rho\rho} U + 7 (\partial_\rho U)^2 \right) V^2 \right],
 \end{aligned}$$

$$\begin{aligned}
 u_5 &= -2V \left[ \rho^2 \alpha^2 \lambda^4 V^8 + \rho^2 \lambda^2 V^4 (\partial_\rho U)^2 + 2\rho^2 \partial_\rho U \partial_\rho V \left( 3(\partial_\rho V)^2 - 2V \partial_{\rho\rho} V \right) \right. \\
 &\quad \left. - 4V^2 (\partial_\rho U + \rho \partial_{\rho\rho} U) (\partial_\rho V + \rho \partial_{\rho\rho} V) \right], \\
 u_6 &= -4\rho V^5 \left( \lambda^2 (\rho \partial_{\rho\rho} U + \partial_\rho U) \right) - \rho^2 (\partial_\rho V)^2 \left( 32V \partial_{\rho\rho} V - 27(\partial_\rho V)^2 \right) \\
 &\quad + 4V^2 \left( 3\rho^2 (\partial_{\rho\rho} V)^2 + 2\rho \partial_\rho V \partial_{\rho\rho} V + 3(\partial_\rho V)^2 \right), \\
 u_7 &= -2\rho \lambda^2 V^3 \left[ 2V (\partial_\rho V + \rho \partial_{\rho\rho} V) - \rho (\partial_\rho V)^2 \right], \quad u_8 = 10\rho^2 \lambda^4 V^6. \tag{8.122}
 \end{aligned}$$

#### 8.8.4 Values of the Parameter $\alpha$

As in the periodic case, we need to investigate how having infinitely many black holes affects the values of  $\alpha$  we need in order to prevent CTCs arising. We know that we need the matrix  $M$  in (8.88) to be positive definite, and, as  $U$  and  $V$  will both be positive here to due to the absence of an infinite constant, this condition is equivalent to demanding that

$$W := UV^{-1} - \alpha^2 U^{-2} V^{2\beta} > 0 \iff \begin{cases} U^3 V > \alpha^2 & \text{if } \beta = -1, \\ U^3 V^{-3} > \alpha^2 & \text{if } \beta = 1. \end{cases} \tag{8.123}$$

If we define

$$\phi := \sum_{j=1}^{\infty} \frac{m}{|\vec{r} - \vec{r}_j|} \quad \text{and} \quad \psi := \sum_{j=1}^{\infty} \frac{n}{|\vec{r} - \vec{r}_j|}, \tag{8.124}$$

so that  $U = \lambda t + \phi$  and  $V = \epsilon + \psi$ , then

$$U^3 V = \begin{cases} \psi(\lambda t + \phi)^3 & \text{if } \epsilon = 0, \\ (1 + \psi)(\lambda t + \phi)^3 & \text{if } \epsilon = 1, \end{cases} \quad \text{and} \quad U^3 V^{-3} = \begin{cases} \psi^{-3}(\lambda t + \phi)^3 & \text{if } \epsilon = 0, \\ (1 + \psi)^{-3}(\lambda t + \phi)^3 & \text{if } \epsilon = 1. \end{cases} \tag{8.125}$$

For non-cosmological black holes, replace  $\lambda t$  in  $U$  with 1. As  $\phi$  and  $\psi$  will be positive functions everywhere, there will be values of  $\alpha$  for given examples such that CTCs can be avoided, but for some choices of  $\alpha$  they will still be present.

#### 8.8.5 Useful Example

We can use in later calculations (replacing  $\lambda t$  by 1 as necessary), the example we studied in chapter six, namely

$$U := \lambda t + m \sum_{j=-\infty}^{\infty} \left( \rho_2^2 + (x_3 - j^3)^2 \right)^{-\frac{1}{2}}, \quad V := \epsilon + n \sum_{j=-\infty}^{\infty} \left( \rho_2^2 + (x_3 - j^3)^2 \right)^{-\frac{1}{2}}. \tag{8.126}$$

### 8.8.6 Lattices of Black Holes

We can attempt to construct a lattice solution in the coordinates  $\{x_1, x_2, x_3\}$  by using the potential from the quasi-periodic instanton solution of chapter five, namely

$$V(\vec{r}) = r^{-1} + \sum_{\{\vec{q}\} \neq 0} \sum \psi(\vec{r}, \vec{q}), \quad (8.127)$$

where

$$\psi(\vec{r}, \vec{q}) := |\vec{r} - \vec{q}|^{-1} - |\vec{q}|^{-1} \left( 1 + \frac{\vec{q} \cdot \vec{r}}{q^2} + (2q^4)^{-1} \left( 3(\vec{q} \cdot \vec{r})^2 - q^2 r^2 \right) \right). \quad (8.128)$$

However, as we saw earlier, if we use the standard Euclidean basis then  $V$  will be zero in the regions around the black holes and at such points the Riemann curvature tensor goes to infinity, indicating the presence of singularities.

## 8.9 Static and Non-Cosmological Black Holes

Ishihara et al [37] construct static, non-cosmological (SN) black hole solutions on the Gibbons-Hawking multi-instanton space. They use the equations in (8.4) with  $\alpha = 0 = \lambda$ . In this setting, the action is given by

$$S = (16G\pi)^{-1} \int d^5x \sqrt{-g} (R - F_{\mu\nu} F^{\mu\nu}), \quad (8.129)$$

and the metric is given by

$$ds^2 = -U^{-2} dt^2 + U \left( V^{-1} (d\tau + \vec{\omega} \cdot d\vec{r})^2 + V d\vec{r}^2 \right). \quad (8.130)$$

It is easy to verify that we do indeed have a solution of the Einstein-Maxwell equations (7.5).

### 8.9.1 Periodic Solutions - Curvature

Using the logarithmic approximation given in (8.79) with  $\lambda = 0$ , we can calculate the Riemann curvature scalar and find that

$$[R]^2 = \frac{4f(U, V)}{\rho_2^4 V^6 U^6} \quad \text{with} \quad f(U, V) = \sum_{j=0}^4 u_j U^j, \quad (8.131)$$

where

$$\begin{aligned} u_0 &= 127b^4 V^4, & u_1 &= -60b^3 V^3 (V - d), \\ u_2 &= 12b^2 V^2 (V^2 - 2dV + 2d^2), & u_3 &= 0, & u_4 &= 8d^2 (V^2 - 6dV + 12d^2). \end{aligned} \quad (8.132)$$



Note that this is the result we get if we set  $\alpha = \lambda = 0$  for both the case of  $\beta = -1$  (see (8.83), (8.84)) and of  $\beta = 1$  (see (8.85), (8.86)), which provides a check of our earlier results. Moreover, if we set  $U \equiv V$ , so  $b \equiv d$ , then the result corresponds to that of (8.11) as required.

It remains to establish how the curvature behaves as  $U$  and  $V$  get close to zero, which we begin to do by looking at  $f$ :

$$\begin{aligned} f(0, V) &= 127b^4V^4, \\ f(U, 0) &= 96d^4U^4. \end{aligned} \tag{8.133}$$

In both cases, we then have

$$[R]^2 \begin{cases} < \infty & \text{at the points where both } U \neq 0, V \neq 0, \\ \infty & \text{at the points where either } U = 0 \text{ or } V = 0. \end{cases} \tag{8.134}$$

As we have seen, the resulting curvature singularities are naked.

### 8.9.2 Non-Periodic Solutions

The Riemann curvature scalar is given by considering both (8.119), (8.120) and (8.121), (8.122) with  $\alpha$  set to zero. We have (with  $\rho := \rho_2$ )

$$[R]^2 = \frac{f}{4\rho^2V^6U^6} \quad \text{with} \quad f = \sum_{j=0}^4 u_j U^j, \tag{8.135}$$

where the coefficients  $u_j$  are given by

$$\begin{aligned} u_0 &= 127\rho^2V^4 (\partial_\rho U)^4, \\ u_1 &= -4\rho V^3 (\partial_\rho U)^2 (26\rho V \partial_{\rho\rho} U - 15\rho \partial_\rho U \partial_\rho V - 4V \partial_\rho U), \\ u_2 &= 2V^2 \left( 4\rho V \partial_\rho U (2\partial_\rho U \partial_\rho V - \rho \partial_\rho U \partial_{\rho\rho} V + V \partial_{\rho\rho} U) + 14V^2 \left( \rho^2 (\partial_{\rho\rho} U)^2 + (\partial_\rho U)^2 \right) \right. \\ &\quad \left. + \rho^2 \partial_\rho U \partial_\rho V (11\partial_\rho U \partial_\rho V - 12V \partial_{\rho\rho} U) \right), \\ u_3 &= 4V \left( 2V^2 (\partial_\rho U + \rho \partial_{\rho\rho} U) (\partial_\rho V + \rho \partial_{\rho\rho} V) + \rho^2 \partial_\rho U \partial_\rho V \left( 2V \partial_{\rho\rho} V - 3(\partial_\rho V)^2 \right) \right), \\ u_4 &= 27\rho^2 (\partial_\rho V)^4 + 12V^2 \left( \rho^2 (\partial_{\rho\rho} V)^2 + (\partial_\rho V)^2 \right) + 8\rho V \partial_\rho V \partial_{\rho\rho} V (V - 4\rho \partial_\rho V). \end{aligned} \tag{8.136}$$

We can plot the curvature for the example given in (8.126) for  $m = n = 1$  and see that it is well-behaved.

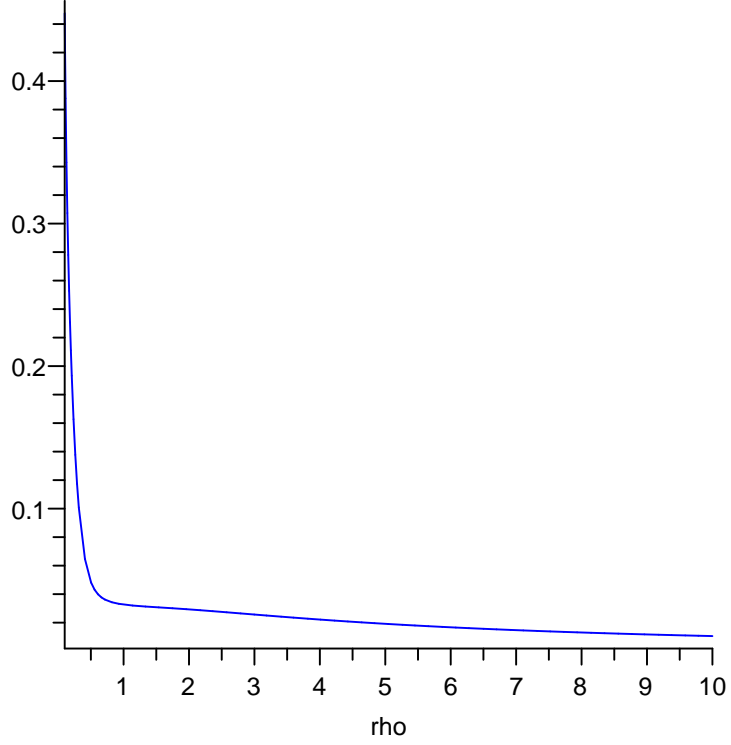


Figure 8.3: The Riemann curvature scalar (8.136) for non-periodic SN black holes using (8.126) with  $m = n = 1$  and  $\rho := \rho_2 \in [0, 10]$

## 8.10 Rotating, Non-Cosmological Black Holes

Nakagawa et al [51] construct rotating, non-cosmological (RN) black hole solutions, using (8.4) with  $\lambda = 0$ . In this setting, the action is given by

$$S = (16G\pi)^{-1} \int d^5x \sqrt{-g} \left( R - F_{\mu\nu} F^{\mu\nu} - \frac{2}{3\sqrt{3}} (\sqrt{-g})^{-1} \epsilon^{\mu\nu\rho\sigma\lambda} A_\mu F_{\nu\rho} F_{\sigma\lambda} \right), \quad (8.137)$$

where  $\vec{A}$  is the gauge potential one-form and  $\vec{F} = d\vec{A}$ , and the metric is given by

$$ds^2 = -U^{-2} \left( dt^2 + \alpha V^\beta (d\tau + \vec{\omega} \cdot d\vec{r}) \right)^2 + U \left( V^{-1} (d\tau + \vec{\omega} \cdot d\vec{r})^2 + V d\vec{r}^2 \right). \quad (8.138)$$

### 8.10.1 Periodic Solutions - Curvature

Using the logarithmic approximation, we can calculate the Riemann curvature scalar and we find, for  $\beta = -1$ ,

$$[R]^2 = \frac{f(U, V)}{\rho^4 V^8 U^8} \quad \text{with} \quad f(U, V) = \sum_{j=0}^6 u_j U^j, \quad (8.139)$$

where the coefficients  $u_j$  are given by

$$\begin{aligned}
 u_0 &= 136\alpha^4 d^4, & u_1 &= -904b^2 d^2 \alpha^2 V^3, \\
 u_2 &= 288b\alpha^2 d^2 V^2 (V - 4d) + 508b^4 V^6, \\
 u_3 &= 240b^3 V^5 (d - V) - 32\alpha^2 d^2 V (V^2 - 9Vd + 24d^2), \\
 u_4 &= 48b^2 V^4 (V^2 - 2dV + 2d^2), & u_5 &= 0, \\
 u_6 &= 32d^2 V^2 (V^2 - 6dV + 12d^2).
 \end{aligned} \tag{8.140}$$

For  $\beta = 1$ , we find that

$$[R]^2 = \frac{f(U, V)}{\rho^4 V^6 U^8} \quad \text{with} \quad f(U, V) = \sum_{j=0}^6 u_j U^j, \tag{8.141}$$

where the coefficients  $u_j$  are given by

$$\begin{aligned}
 u_0 &= 136\alpha^4 d^4 V^6, & u_1 &= -904b^2 d^2 \alpha^2 V^5, \\
 u_2 &= 288b\alpha^2 d^2 V^5 + 508b^4 V^4, \\
 u_3 &= 240b^3 V^3 (d - V) - 32\alpha^2 d^2 V^5, \\
 u_4 &= 48b^2 V^2 (V^2 - 2dV + 2d^2), & u_5 &= 0, \\
 u_6 &= 32d^2 (V^2 - 6dV + 12d^2).
 \end{aligned} \tag{8.142}$$

When  $U$  and  $V$  get close to zero, we have

$$\begin{aligned}
 f(U, 0) = f(0, V) &= 136\alpha^4 d^4 & \text{for} & \quad \beta = -1; \\
 f(U, 0) = 384d^2 U^6, f(0, V) &= 136\alpha^4 d^4 V^6 & \text{for} & \quad \beta = 1.
 \end{aligned} \tag{8.143}$$

Thus, at these points we have curvature singularities, which as we have seen are naked.

### 8.10.2 Periodic Solutions - Ergoregions

The **ergoregion** of a rotating black hole is an area around the event horizon inside of which an object will be dragged around in the direction of the black hole's rotation and so it is impossible to be stationary. The outer shell of the ergosphere is called the **stationary limit** and is given by

$$K^\mu K_\mu = \delta_0^\mu g_{\mu\nu} \delta_0^\nu = g_{00} = g_{tt} = 0. \tag{8.144}$$

Using the coordinate transformation

$$t = t' \sqrt{1 - \alpha^2}, \quad \tau = \tau' + \frac{\alpha t}{n(1 - \alpha^2)} = \tau' + \frac{\alpha t'}{n\sqrt{1 - \alpha^2}}, \quad (8.145)$$

where  $n$  is defined as in (8.8), we expand the relevant parts of the metric to see that

$$\begin{aligned} g_{t't'} &= -U^{-2} (1 - \alpha^2) - \frac{2\alpha^2 V^\beta U^{-2}}{n} + \frac{\alpha^2}{n^2 (1 - \alpha^2)} \left( UV^{-1} - \alpha^2 V^{2\beta} U^{-2} \right) \\ &= -U^{-2} \left( \sqrt{1 - \alpha^2} + \frac{\alpha^2}{n\sqrt{1 - \alpha^2}} V^\beta \right)^2 + \frac{\alpha^2}{n^2 (1 - \alpha^2)} UV^{-1} \\ &= 0. \end{aligned} \quad (8.146)$$

Now, as we assume without loss of generality that all the black holes are identical with horizon topology  $\mathbb{S}^3$  (so  $h_j = 1 \forall j$ ), we find that

$$\begin{aligned} g_{t't'} &= -U^{-2} \left( \sqrt{1 - \alpha^2} + \frac{2\alpha^2}{NL\sqrt{1 - \alpha^2}} V^\beta \right)^2 + \frac{4\alpha^2}{N^2 L^2 (1 - \alpha^2)} UV^{-1} \\ &\rightarrow \frac{\alpha^2 - 1}{U^2} \quad \text{as} \quad N \rightarrow \infty, \end{aligned} \quad (8.147)$$

and so the only way this can become zero is if  $\alpha = 1$ , which violates the condition we earlier placed on  $\alpha$  that  $\alpha \in [0, 1)$ . This would be an unusual spacetime in that remaining stationary would be impossible except at infinity. An observer would always be dragged along with the rotation of the black holes.

### 8.10.3 Periodic Solutions - Closed Timelike Curves

We now investigate if **closed timelike curves** (CTCs) do arise in this situation.

Following the method we discussed earlier, in order to avoid having CTCs, we require that

- if  $\beta = -1$  then  $U^3 V > 1$ ;
- if  $\beta = 1$  then  $U^3 V^{-3} > 1 \iff U > V$ .

In the first case, we need to investigate whether  $W := U^3 V - 1 > 0$  for all  $\rho_2$  and  $x_3$  such that  $U$  and  $V$  have the same sign.

We consider three examples:

For **example one** with  $U = U_1$ ,  $V = V_1$ ,  $U = 0$  when  $\rho_2 = 1.8514$ ,  $V = 0$  when  $\rho_2 = 1.442$  and  $W = 0$  when  $\rho_2 = 1.1233$  and  $\rho_2 = 2.6789$  for all  $x_3 \in [0, 1]$  and hence for all  $x_3 \in \mathbb{R}$ . Thus, in this spacetime, there are CTCs in the region  $\rho_2 \in [1.1233, 2.6789]$ .

For **example two** with  $U = U_2$ ,  $V = V_2$ ,  $U = 0$  when  $\rho_2 = 1.442$ ,  $V = 0$  when  $\rho_2 = 1.8514$  and  $W = 0$  when  $\rho_2 = 1.1238$  and  $\rho_2 = 2.1209$  for all  $x_3 \in [0, 1]$  and hence for all  $x_3 \in \mathbb{R}$ . Thus, in this spacetime, there are CTCs in the region  $\rho_2 \in [1.1238, 2.1209]$ .

For **example three** with  $U = U_3$ ,  $V = V_3$ ,  $U = V = 0$  when  $\rho_2 = 1.8514$  and  $W = 0$  when  $\rho_2 = 1.1238$  and  $\rho_2 = 3.0524$  for all  $x_3 \in [0, 1]$  and hence for all  $x_3 \in \mathbb{R}$ . Thus, in this spacetime, there are CTCs in the region  $\rho_2 \in [1.1238, 3.0524]$ .

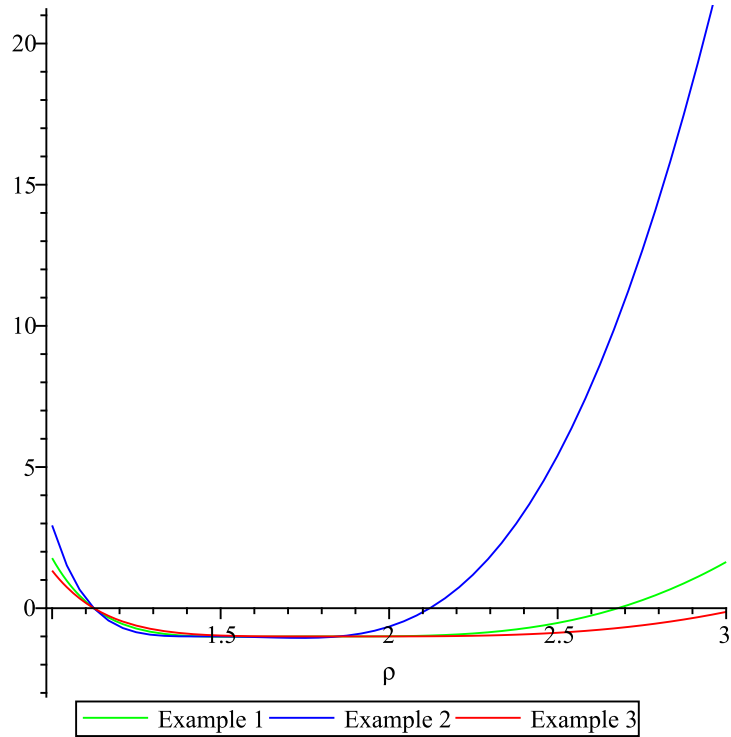


Figure 8.4: The regions of CTCs for three examples ((8.90), (8.91) and (8.92) are examples one, two and three respectively) of RN black holes with  $\rho := \rho_2 \in [1, 3]$

#### 8.10.4 Non-Periodic Solutions

The Riemann curvature scalar is given by (8.119), (8.120) for  $\beta = -1$  and (8.121), (8.122) for  $\beta = 1$ , where we assume that  $\lambda$  is zero and take  $\rho := \rho_2$ .

**The Case  $\beta = -1$** 

When  $\beta = -1$ , we have

$$[R]^2 = \frac{f}{4\rho^2 V^8 U^8} \quad \text{with} \quad f = \sum_{j=0}^6 u_j U^j, \quad (8.148)$$

where the coefficients  $u_j$  are given by

$$\begin{aligned} u_0 &= 11\rho^2 \alpha^4 (\partial_\rho V)^4, & u_1 &= -104\rho^2 \alpha^2 V^3 (\partial_\rho U)^2 (\partial_\rho V)^2, \\ u_2 &= -\rho V^2 \left[ -127\rho V^4 (\partial_\rho U)^4 + 4\alpha^2 \partial_\rho U (\partial_\rho V)^2 (29\rho \partial_\rho V + 2V) \right. \\ &\quad \left. + 4\rho \alpha^2 V \partial_\rho V (5\partial_\rho V \partial_{\rho\rho} U - 16\partial_\rho U \partial_{\rho\rho} V) \right], \\ u_3 &= -4V \left[ \alpha^2 \left( 2V \left( V (\partial_\rho V)^2 + \rho (\partial_\rho V)^3 + \rho^2 V (\partial_{\rho\rho} V)^2 \right) + \rho^2 (\partial_\rho V)^2 \left( 15 (\partial_\rho V)^2 - 11V \partial_{\rho\rho} V \right) \right) \right. \\ &\quad \left. + \rho V^4 (\partial_\rho U)^2 (26\rho V \partial_{\rho\rho} U - 15\rho \partial_\rho U \partial_\rho V - 4V \partial_\rho U) \right], \\ u_4 &= 2V^4 \left[ 4\rho V \partial_\rho U (2\partial_\rho U \partial_\rho V - \rho \partial_\rho U \partial_{\rho\rho} V + V \partial_{\rho\rho} U) + 14V^2 \left( \rho^2 (\partial_{\rho\rho} U)^2 + (\partial_\rho U)^2 \right) \right. \\ &\quad \left. + \rho^2 \partial_\rho U \partial_\rho V (11\partial_\rho U \partial_\rho V - 12V \partial_{\rho\rho} U) \right], \\ u_5 &= 4V^3 \left[ 2V^2 (\partial_\rho U + \rho \partial_{\rho\rho} U) (\partial_\rho V + \rho \partial_{\rho\rho} V) + \rho^2 \partial_\rho U \partial_\rho V \left( 2V \partial_{\rho\rho} V - 3(\partial_\rho V)^2 \right) \right], \\ u_6 &= V^2 \left[ 27\rho^2 (\partial_\rho V)^4 + 12V^2 \left( \rho^2 (\partial_{\rho\rho} V)^2 + (\partial_\rho V)^2 \right) + 8\rho V \partial_\rho V \partial_{\rho\rho} V (V - 4\rho \partial_\rho V) \right]. \end{aligned} \quad (8.149)$$

**The Case  $\beta = 1$** 

When  $\beta = 1$ , we have

$$[R]^2 = \frac{f}{4\rho^2 V^6 U^8} \quad \text{with} \quad f = \sum_{j=0}^6 u_j U^j, \quad (8.150)$$

where the coefficients  $u_j$  are given by

$$\begin{aligned} u_0 &= 11\rho^2 \alpha^4 V^6 (\partial_\rho V)^4, & u_1 &= -104\rho^2 \alpha^2 V^5 (\partial_\rho U)^2 (\partial_\rho V)^2, \\ u_2 &= -\rho V^4 \left[ -127\rho (\partial_\rho U)^4 + 4\alpha^2 \partial_\rho U (\partial_\rho V)^2 (2V - 3\rho \partial_\rho V) \right. \\ &\quad \left. + 4\rho \alpha^2 V \partial_\rho V (5\partial_\rho V \partial_{\rho\rho} U - 16\partial_\rho U \partial_{\rho\rho} V) \right], \\ u_3 &= -4V^3 \left[ \alpha^2 \left( 2V \left( V (\partial_\rho V)^2 + \rho (\partial_\rho V)^3 + \rho^2 V (\partial_{\rho\rho} V)^2 \right) + \rho^2 (\partial_\rho V)^2 \left( 7 (\partial_\rho V)^2 - 3V \partial_{\rho\rho} V \right) \right) \right. \\ &\quad \left. + \rho (\partial_\rho U)^2 (26\rho V \partial_{\rho\rho} U - 15\rho \partial_\rho U \partial_\rho V - 4V \partial_\rho U) \right], \end{aligned}$$

$$\begin{aligned}
 u_4 &= 2V^2 \left[ 4\rho V \partial_\rho U (2\partial_\rho U \partial_\rho V - \rho \partial_\rho U \partial_{\rho\rho} V + V \partial_{\rho\rho} U) + 14V^2 \left( \rho^2 (\partial_{\rho\rho} U)^2 + (\partial_\rho U)^2 \right) \right. \\
 &\quad \left. + \rho^2 \partial_\rho U \partial_\rho V (11\partial_\rho U \partial_\rho V - 12V \partial_{\rho\rho} U) \right], \\
 u_5 &= 4V \left[ 2V^2 (\partial_\rho U + \rho \partial_{\rho\rho} U) (\partial_\rho V + \rho \partial_{\rho\rho} V) + \rho^2 \partial_\rho U \partial_\rho V (2V \partial_{\rho\rho} V - 3(\partial_\rho V)^2) \right], \\
 u_6 &= 27\rho^2 (\partial_\rho V)^4 + 12V^2 \left( \rho^2 (\partial_{\rho\rho} V)^2 + (\partial_\rho V)^2 \right) + 8\rho V \partial_\rho V \partial_{\rho\rho} V (V - 4\rho \partial_\rho V). \quad (8.151)
 \end{aligned}$$

We can plot the curvature for the example given in (8.126) for  $m = n = 1$  and see that, for different choices of  $\alpha$ , it is well-behaved.

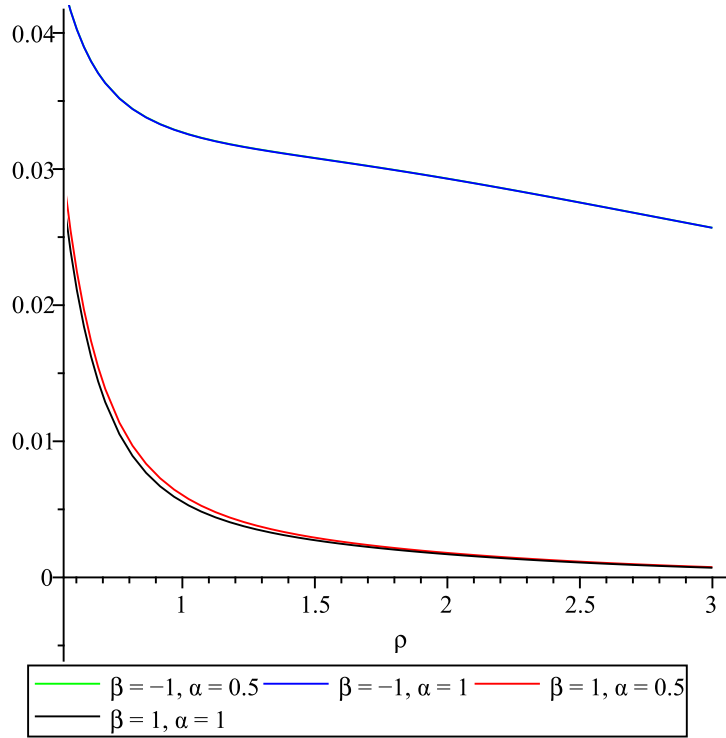


Figure 8.5: The Riemann curvature scalar (8.149) and (8.151) for non-periodic RN black holes using example (8.126) for  $m = n = 1$ , with  $\rho := \rho_2 \in [0, 3]$  and various  $\alpha, \beta$

## 8.11 Static, Cosmological Black Holes

Ishihara et al [38] construct static, cosmological black hole solutions using (8.4) with  $\alpha = 0$ . The action is given by

$$S = \frac{1}{16\pi G_5} \int dx^5 \sqrt{-g} (R + \Lambda - F_{\mu\nu} F^{\mu\nu}), \quad (8.152)$$

and the metric is

$$ds^2 = -U^{-2}dt^2 + U \left( V^{-1} (d\tau + \vec{\omega} \cdot d\vec{r})^2 + V d\vec{r}^2 \right). \quad (8.153)$$

### 8.11.1 Periodic Solutions - Curvature

Using the logarithmic approximation given in (8.79), we can calculate the Riemann curvature scalar and we find that

$$[R]^2 = \frac{f}{4\rho_2^4 V^6 U^6} \quad \text{with} \quad f = \sum_{j=0}^6 u_j U^j, \quad (8.154)$$

where the coefficients  $u_j$  are given by

$$\begin{aligned} u_0 &= 2032b^4V^4, & u_1 &= 960b^3V^3(d - V), & u_2 &= 192V^2b^2(V^2 - 2dV + 2d^2), \\ u_3 &= -8V^5b^2\rho_2^2\lambda^2, & u_4 &= 128d^2(V^2 - 6dV + 12d^2), & u_5 &= 0, & u_6 &= 10V^6\rho_2^4\lambda^4. \end{aligned} \quad (8.155)$$

When  $U$  and  $V$  get close to zero, we have  $f(U, 0) = 1536d^4U^4$  and  $f(0, V) = 2032b^4V^4$ . Thus, at these points we do indeed have curvature singularities.

### 8.11.2 Periodic Solutions - Closed Timelike Curves

We now investigate if closed timelike curves do arise in this situation. In order to avoid having CTCs, we require that

- if  $\beta = -1$  then  $W := U^3V > 1$ ;
- if  $\beta = 1$  then  $U^3V^{-3} > 1 \iff U > V$ .

In the first case, we need to investigate whether  $W > 0$  over a period in time, in this case  $t \in [0, 1]$ .

We consider three examples:

For **example four** with  $U = U_4$ ,  $V = V_4$ :

- When  $t = 0$ ,  $W = 0$  for  $\rho_2 = 0.7824$  and  $\rho_2 = 1.8514$ , for all  $x_3 \in [0, 1]$ ;
- When  $t = 0.5$ ,  $W = 0$  for  $\rho_2 = 0.9494$  and  $\rho_2 = 2.1954$ , for all  $x_3 \in [0, 1]$ ;
- When  $t = 1$ ,  $W = 0$  for  $\rho_2 = 1.1238$  and  $\rho_2 = 2.6790$ , for all  $x_3 \in [0, 1]$ .



For **example five** with  $U = U_5$ ,  $V = V_5$ :

- When  $t = 0$ ,  $W = 0$  for  $\rho_2 = 0.9032$  and  $\rho_2 = 1.9416$ , for all  $x_3 \in [0, 1]$ ;
- When  $t = 0.5$ ,  $W = 0$  for  $\rho_2 = 1.0086$  and  $\rho_2 = 2.0094$ , for all  $x_3 \in [0, 1]$ ;
- When  $t = 1$ ,  $W = 0$  for  $\rho_2 = 1.1238$  and  $\rho_2 = 2.1209$ , for all  $x_3 \in [0, 1]$ .

For **example six** with  $U = U_6$ ,  $V = V_6$ :

- When  $t = 0$ ,  $W = 0$  for  $\rho_2 = 0.6916$  and  $\rho_2 = 1.8514$ , for all  $x_3 \in [0, 1]$ ;
- When  $t = 0.5$ ,  $W = 0$  for  $\rho_2 = 0.8782$  and  $\rho_2 = 2.3772$ , for all  $x_3 \in [0, 1]$ ;
- When  $t = 1$ ,  $W = 0$  for  $\rho_2 = 1.1238$  and  $\rho_2 = 3.0524$ , for all  $x_3 \in [0, 1]$ .

For all these examples, CTCs are present.

### 8.11.3 Non-Periodic Solutions

Calculating the Riemann curvature scalar, taking  $\rho := \rho_2$ , we find

$$[R]^2 = \frac{f(U, V)}{4\rho^2 V^6 U^6} \quad \text{with} \quad f(U, V) = \sum_{j=0}^8 u_j U^j, \quad (8.156)$$

where the coefficients  $u_j$  are given by

$$\begin{aligned} u_0 &= 127\rho^2 V^4 (\partial_\rho U)^4, \\ u_1 &= 4\rho V^3 (\partial_\rho U)^2 \left[ 15\rho \partial_\rho U \partial_\rho V - 26\rho V \partial_{\rho\rho} U + 4V \partial_\rho U \right], \\ u_2 &= 2V^2 \left[ 11\rho^2 (\partial_\rho U)^2 (\partial_\rho V)^2 + 2 \left( 7\rho^2 (\partial_{\rho\rho} U)^2 + 2\rho \partial_\rho U \partial_{\rho\rho} U + 7 (\partial_\rho U)^2 \right) V^2 \right. \\ &\quad \left. - 4\rho \partial_\rho U \left( 3\rho \partial_\rho V \partial_{\rho\rho} U - 2\partial_\rho U \partial_\rho V + \rho \partial_\rho U \partial_{\rho\rho} V \right) V \right], \\ u_3 &= -2V \left[ \rho^2 V^4 \lambda^2 (\partial_\rho U)^2 + 2\rho^2 \partial_\rho U \partial_\rho V \left( 3 (\partial_\rho V)^2 - 2V \partial_{\rho\rho} V \right) \right. \\ &\quad \left. - 4V^2 (\partial_\rho U + \rho \partial_{\rho\rho} U) (\partial_\rho V + \rho \partial_{\rho\rho} V) \right], \\ u_4 &= -4\rho \lambda^2 V^5 (\rho \partial_{\rho\rho} U + \partial_\rho U) - \rho^2 (\partial_\rho V)^2 \left( 32V \partial_{\rho\rho} V - 27 (\partial_\rho V)^2 \right) \\ &\quad + 4V^2 \left( 3\rho^2 (\partial_{\rho\rho} V)^2 + 2\rho \partial_\rho V \partial_{\rho\rho} V + 3 (\partial_\rho V)^2 \right), \end{aligned}$$

$$\begin{aligned}
 u_5 &= -2\rho\lambda^2V \left[ 2V (\partial_\rho V + \rho\partial_{\rho\rho}V) - \rho (\partial_\rho V)^2 \right], \\
 u_6 &= 10\rho^2\lambda^4V^6.
 \end{aligned}
 \tag{8.157}$$

We can plot this for the example given in (8.126) with  $\lambda = 1$  and see that it is well-behaved.

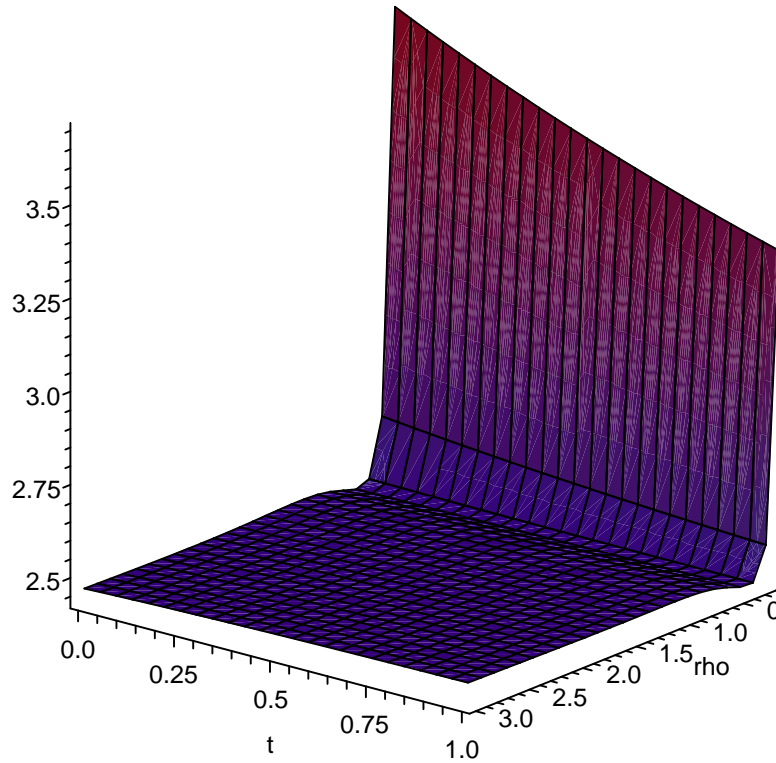


Figure 8.6: The Riemann curvature scalar (8.157) for non-periodic SC black holes using example (8.126) with  $\lambda = 1$ ,  $\rho := \rho_2 \in [0, 1]$ ,  $t \in [0, 1]$

## Chapter 9

# Conclusion and Bibliography

As a result of the fact that any hyperkähler four-metric with a triholomorphic Killing vector can be written in Gibbons-Hawking form for some choice of coordinates, infinite centre Gibbons-Hawking metrics appear in many contexts in mathematical physics, from gravitational instantons at the quantum end to black holes at the general relativistic end of the scale. Key to the behaviour of these Gibbons-Hawking metrics is the hyperkähler potential,  $V$ , which is related to the one-form  $\vec{\omega}$  by virtue of the metric being self-dual.

The problem that arises is that such a potential does not usually converge (only in contexts with  $D \geq 4$  spatial dimensions did we have a convergent potential). In this thesis, we have investigated four methods of ensuring convergence and studied the implications of the use of these methods in different contexts.

The standard method is to subtract an infinite constant from the potential, and this is found in much of the literature on gravitational instantons, monopoles, and constructions that incorporate hyperkähler four-metrics with a triholomorphic Killing vector.

We looked at Kaluza-Klein vortices (both with and without a cosmological constant), Dirichlet instantons (with single and multiple hypermultiplets) and gravitational calorons (and Euclidian Schwarzschild solutions with the same potential) in chapter four, extensions of these ideas to ALG instantons, seven-dimensional holonomy spaces and hyperbolic monopoles in chapter five, and ERN and Kaluza-Klein black holes in chapters seven and eight respectively.

As outlined in chapter three, subtracting an infinite constant results in points where the potential becomes zero, and the Riemann curvature scalar blows up to infinity. This means that

---

there are singularities, points of infinite density and spacetime curvature at which the laws of physics break down, that cannot be removed by a change of coordinates. In the contexts where it is appropriate to consider such a question (such as with monopoles and black holes), these points were actually naked singularities, something which is problematic because of the Cosmic Censorship principle; it renders the theory unphysical.

In chapter six, we explored different methods of ensuring the convergence of the potential. One alternative approach is to have a non-periodic distribution of sources, and we drew on the work of Anderson et al [1], creating new solutions for ERN, dilaton and Kaluza-Klein black holes. This approach worked well in its original instanton context, and we explored how it broke down in the periodic limit, yet in the black hole context, we encountered a new problem. Candlish and Reall showed [4] that only the central black hole in an infinite array arranged non-periodically along one or more axes would have a smooth event horizon, as such solutions are not reflection-symmetric.

We showed that lattices of instantons and Kaluza-Klein black holes had regions in which the potential became zero and so singularities were present, so this was not a helpful approach. We also tried using an infinite constant as a quotient to ensure convergence, but as we demonstrated, this gave rise to a flat spacetime with delta singularities arising at the positions of the instantons.

Overall, there is no one approach to the problem of ensuring the convergence of the periodic potential of an infinite-centre Gibbons-Hawking metric that is without problems across the range of contexts studied. We found that across the literature, the problem of the incompleteness of such metrics was acknowledged but the implications not fully appreciated. One would hope that this research would contribute to a greater awareness of the difficulties of working with such metrics in the range of varied contexts in which they occur, and stimulate a search for a universally applicable method of ensuring a convergent potential.

As this work is largely theoretical, one would be reluctant to talk too much about wider implications, except to say that the interconnectedness seen, with the range of contexts in which infinite-centre Gibbons-Hawking metrics may arise, is intriguing and worthy of further consideration.

In summary, we have looked at applications of infinite-centre Gibbons-Hawking metrics in

---

the contexts of

- Kaluza-Klein vortices, both without a cosmological constant and in AdS spacetime;
- Dirichlet instantons, with a single and multiple hypermultiplets;
- Gravitational calorons;
- ALG instantons, seven-dimensional holonomy spaces and hyperbolic monopoles;
- Majumdar-Papapetrou metrics, analytic extensions to ERN black holes and dilaton solutions;
- Kaluza-Klein black holes.

In terms of possible extensions of this work, we could explore the cosmological Kaluza-Klein black holes from chapter eight in more depth, looking at how we might show that the singularities that arise when either of the potentials becomes zero are naked, which we might do by numerical integration. The process of black hole coalescence for infinitely many Kaluza-Klein black holes would be interesting to study, particularly in the case of cosmological black holes with a Taub-NUT metric as while some work has been done in the Eguchi-Hanson case (see [43] and references therein), little seems to have been done to investigate the behaviour of these solutions.

Another possible context for investigation would be that of general relativity coupled with a Yang-Mills(-Higgs) field and a dilaton field, for which one might see [31], [19], [23]. It appears that similar issues may present themselves in that the potential is non-convergent and the use of the method of subtracting an infinite constant to ensure convergence gives rise to singularities. It would be worth exploring both if this is the case and if our alternative approach of having a non-periodic potential would be useful, hopefully leading to the finding of new solutions.

This would be a possible undertaking for the future.

# Bibliography

- [1] M. Anderson, P. Kronheimer, and C. LeBrun, *Complete Ricci-flat Kähler manifolds of infinite topological type*, *Comm. Math. Phys.* **125** (1989), 637–642.
- [2] M. Atiyah and N. Hitchin, *The geometry and dynamics of magnetic monopoles*, M. B. Porter Lectures, Princeton University Press, Princeton, NJ, 1988.
- [3] M Berger, *Sur les groupes d'holonomie des varités a connexion affine et des varités riemanniennes*, *Bull. Soc. Math. France* **83** (1953), 279–330.
- [4] G. Candlish and H. Reall, *On the smoothness of static multi-black hole solutions of higher-dimensional Einstein-Maxwell theory*, *Class. Quantum Grav.* **24** (2007), 6025–6039.
- [5] S. M. Carroll, *Spacetime and geometry: An introduction to general relativity*, Addison Wesley, 2004.
- [6] S. Cherkis and A. Kapustin, *Nahm transform for periodic monopoles and  $N = 2$  super Yang-Mills theory*, *Comm. Math. Phys.* **218** (2001), 333–371.
- [7] ———, *Hyperkähler metrics from periodic monopoles*, *Phys. Rev. D (3)* **65** (2002), 084015, 10.
- [8] ———, *Periodic monopoles with singularities and  $N = 2$  super-QCD*, *Comm. Math. Phys.* **234** (2003), 1–35.
- [9] M. Cvetič, G. W. Gibbons, H. Lu, and C. N. Pope, *Orientifolds and slumps in  $G_2$  and  $Spin(7)$  metrics*, *Ann. Physics* **310** (2004), 265–301.
- [10] M. J. Duff, *Kaluza-Klein theory in perspective*, (1994), hep-th/9410046.
- [11] G. Dunne and V. Khemani, *Numerical investigation of monopole chains*, *J. Phys. A* **38** (2005), 9359–9370.

- [12] T. Eguchi and A. Hanson, *Asymptotically flat self-dual solutions to Euclidean gravity*, Phys. Lett. B **74** (1978), 249.
- [13] K. Galicki, *Multi-centre metrics with negative cosmological constant*, Class. Quan. Grav. **8** (1991), 1529–1543.
- [14] D. Garfinkle, G. Horowitz, and A. Strominger, *Charged black holes in string theory*, Phys. Rev. D **43** (1991), 3140.
- [15] J. Gauntlett, J. Gutowski, C. Hull, S. Pakis, and H. Reall, *All supersymmetric solutions of minimal supergravity in five dimensions*, Class. Quantum Grav. **20** (2003), 4587–4634.
- [16] G. W. Gibbons and S. W. Hawking, *Gravitational multi - instantons*, Phys. Lett. B **78** (1978), 430.
- [17] ———, *Classification of gravitational instanton symmetries*, Comm. Math. Phys. **66** (1979), 291–310.
- [18] G. W. Gibbons, G. Horowitz, and P. K. Townsend, *Higher dimensional resolution of dilatonic black hole singularities*, Class. Quant. Grav. **12** (1995), 297–317.
- [19] G. W. Gibbons, D. Kastor, L. A. J. London, P. K. Townsend, and J. Traschen, *Supersymmetric self-gravitating solitons*, Nuc. Phys. B **416** (1994), 850–880.
- [20] G. W. Gibbons and N. Manton, *Classical and quantum dynamics of BPS monopoles*, Nuclear Phys. B **274** (1986), 183–224.
- [21] G. W. Gibbons and M. J. Perry, *New gravitational instantons and their interactions*, Proc. R. Soc. A **358** (1978), 467.
- [22] G. W. Gibbons and P. Ruback, *The hidden symmetries of multi-centre metrics*, Comm. Math. Phys. **115** (1988), 267–300.
- [23] G. W. Gibbons and P. K. Townsend, *Anti-gravitating BPS monopoles and dyons*, Phys. Lett. B **356** (1995), 472–478.
- [24] G. W. Gibbons and C. Warnick, *Hidden symmetry of hyperbolic monopole motion*, J. Geom. Phys. **57** (2007), 2286–2315.
- [25] D. Gilbarg and N. Trudinger, *Elliptic partial differential equations of second order*, Springer, 2001.
- [26] G. Giribet and O. Santillan, *Toric  $G_2$  and  $Spin(7)$  holonomy spaces from gravitational instantons and other examples*, Comm. Math. Phys. **275** (2007), 373–400.

- [27] D. Gross and M. Perry, *Magnetic monopoles in Kaluza-Klein theories*, Nuc. Phys. B **226** (1983), 29–48.
- [28] M. Gross and P. Wilson, *Large complex structure limits of K3 surfaces*, J. Differential Geom. **55** (2000), 475–546.
- [29] F. Gursey and H. C. Tze, *Complex and quaternionic analyticity in chiral and gauge theories*, Ann. Physics **128** (1980), 29–130.
- [30] J. B. Hartle and S. W. Hawking, *Solutions of the Einstein-Maxwell equations with many black holes*, Commun. Math. Phys. **26** (1972), 87–101.
- [31] J. A. Harvey and J. Liu, *Magnetic monopoles in  $n = 4$  supersymmetric low energy superstring theory*, Phys. Lett. B **268** (1991), 40–46.
- [32] S. W. Hawking, *Gravitational instantons*, Phys. Lett. A **60** (1977), 81–83.
- [33] S. W. Hawking and W. Israel, *General relativity: An Einstein centenary survey*, Cambridge University Press, 1979.
- [34] N. Hitchin, A. Karlhede, U. Lindstrom, and M. Roček, *Hyperkähler metrics and supersymmetry*, Comm. Math. Phys. **108** (1987), 535–589.
- [35] L. P. Hughston and K. P. Tod, *An introduction to general relativity*, Cambridge University Press, 1990.
- [36] D. Ida, H. Ishihara, M. Kimura, K. Matsuno, Y. Morisawa, and S. Tomizawa, *Cosmological black holes on Taub-NUT space in five-dimensional Einstein-Maxwell theory*, Class. Quantum Grav. **24** (2007), 3141–3149.
- [37] H. Ishihara, M. Kimura, K. Matsuno, and S. Tomizawa, *Kaluza-Klein multi-black holes in five-dimensional Einstein-Maxwell theory*, Class. Quantum Grav. **23** (2006), 6919–6925.
- [38] H. Ishihara, M. Kimura, and S. Tomizawa, *Topology change of coalescing black holes on Eguchi-Hanson space*, Class. Quant. Grav **23** (2006), L89.
- [39] H. Ishihara, M. Kiruma, K. Matsumo, and S. Tomizawa, *Black holes on Eguchi-Hanson space in five-dimensional Einstein-Maxwell theory*, Phys. Rev. D **74** (2006), 047501.
- [40] D. Joyce, *Compact manifolds with special holonomy*, Oxford Mathematical Monographs, Oxford University Press, 2000.



- [41] T. Kaluza, *Zum unitatsproblem der physik*, Sitzungsber. Preuss. Akad. Wiss., Phys. Math. **996** (1921).
- [42] S. Ketov, O. Santillan, and A. Zorin, *D-instanton sums for matter hypermultiplets*, Mod.Phys.Lett.A **19** (2004), 2645.
- [43] M. Kimura, H. Ishihara, S. Tomizawa, and C. Yoo, *Topology changing process of coalescing black holes on Eguchi-Hanson space*, Phys. Rev. D. **80** (2009), 064030.
- [44] O. Klein, *The atomicity of electricity as a quantum theory law*, Nature **118** (1926).
- [45] ———, *Quantentheorie und funfdimensionale relativit atstheorie.*, Z. Phys. **37** (1926).
- [46] D. Klemm and W. A. Sabra, *Charged rotating black holes in 5D Einstein-Maxwell (A)dS gravity*, Phys. Lett. B **503** (2001), 147.
- [47] C. LeBrun, *Explicit self-dual metrics on  $\mathbb{C}P_2 \# \dots \# \mathbb{C}P_2$* , J. Differential Geom. **34** (1991), 223–253.
- [48] L.A.J. London, *Arbitrary dimensional cosmological multi black holes*, Nucl. Phys. B **434** (1995), 709–735.
- [49] K. Matsuno, H. Ishihara, M. Kimura, and S. Tomizawa, *Coalescence of rotating black holes on Eguchi-Hanson space*, Phys. Rev. D **76** (2007), 104037.
- [50] R. C. Myers, *Higher-dimensional black holes in compactified spacetimes*, Phys. Rev. D **35** (1987), 455–466.
- [51] T. Nakagawa, K. Matsuno, H. Ishihara, and S. Tomizawa, *Rotating Kaluza-Klein multi-black holes with Gödel parameter*, Phys. Rev. D **78** (2008), 064016.
- [52] S. Nergiz and C. Saçlıoğlu, *A quasiperiodic Gibbons-Hawking metric and spacetime foam*, Phys. Rev. D (3) **53** (1996), 2240–2243.
- [53] V. Onemli and B. Tekin, *Kaluza-Klein vortices*, J. High Energy Phys. (2001), Paper 34, 7.
- [54] ———, *Kaluza-Klein monopole in ads spacetime*, Phys. Rev. D **68** (2003), 064017.
- [55] H. Ooguri and C. Vafa, *Summing up Dirichlet instantons*, Phys. Rev. Lett. **77** (1996), 3296–3298.
- [56] M. Rocek, *Does smoothing matter?*, (2006), arXiv:gr-qc/0603010.

- [57] P. Rossi, *Propagation functions in the field of a monopole*, Nuclear Phys. B **149** (1979), 170–188.
- [58] N. Sanchez, *Gravitational calorons*, Phys. Lett. B **125** (1983), 403–405.
- [59] K. Shiraishi, *Multicentred solution for maximally charged dilaton black holes in arbitrary dimensions*, J. Math. Phys. **34** (1992), 1480.
- [60] ———, *Many-body systems in Einstein-Maxwell-Dilaton theory*, (1995), arXiv:gr-qc/9507029.
- [61] J. van Dongen, *Einstein and the Kaluza-Klein particle*, Stud. Hist. Philos. Mod. Phys. **33** (2002), 185–210.
- [62] R. S. Ward, *Periodic monopoles*, Phys. Lett. B **619** (2005), 177–183.
- [63] ———, *A monopole wall*, Phys. Rev. D **75** (2007), 021701.
- [64] E. Weinberg and P. Yi, *Magnetic monopole dynamics, supersymmetry, and duality*, Phys. Rep. **438** (2007), 65–236.